# SONOCHEMICAL DEGRADATION OF TRICLOSAN, BENZOPHENONE-1 AND BENZOPHENONE -3 IN WATER

LINA PATRICIA VEGA GARZON

**UNIVERSITY OF ANTIOQUIA**

DOCTORAL THESIS

# SONOCHEMICAL DEGRADATION OF TRICLOSAN, BENZOPHENONE-1 AND BENZOPHENONE -3 IN WATER

*Author:*

Lina Patricia Vega Garzón

*Supervisor:*

Dr. Gustavo Peñuela

*A thesis submitted in fulfillment of the requirements for the degree of Philosophical Doctor*

*in the*

**Grupo Diagnóstico y Control de la Contaminación**
**Faculty of Engineering**
**University of Antioquia**

September, 2018

*To my daughter, a little, beautiful star that fell down from the sky and makes my life brighter every day*

# Contents

# List of Figures

# List of Tables

# List of Symbols

| | |
|---|---|
| $\Lambda$ | UV radiation wavelength |
| $[C]$ | Compound concentration |
| $[CPOH]$ | Chlorophenol concentration |
| $C_p$ | Heat Capacity |
| $D_{12}$ | Diffusivity of solute 1 in solvent 2 |
| $K_{COMP}$ | Ratio $k_1/k_{-1}$ for compound |
| $PE^*$ | Pulse Enhancement |
| $k_0$ | Constant for bulk solution degradation |
| $k_1$ | Constant rate for water decomposition by US |
| $k_2$ | Constant rate for OH-compound reaction |
| $k_2'$ | Constant for complex $OH^*Compound$ breakup |
| $k_3$ | Constant rate for $OH^*Compound$ reaction into P |
| $k_4$ | Constant rate for recombination of $OH^* + H^*$ |
| $k_5$ | Constant rate for reaction of $OH^*$ |
| $k_{a1}$ | Adsorption rate (according to Okitsu) |
| $k_{a-1}$ | Desorption rate (according to Okitsu) |
| $k_{COMP}$ | Pseudo first order rate constant for the reaction of the compound with OH radicals |
| $k_b$ | Ratio $k_b = \frac{k_1 k_2}{k_3'}$ |
| $\varphi_{ions}$ | % of the compound in anionic form |
| AOP | Advanced Oxidation Process |
| BP1 | Benzophenone 1 |
| BP3 | Benzophenone 3 |
| *CW* | Continuous Wave |
| $EC_{50}$ | Half Maximal Effective Concentration |
| GC-MS | Gas Chromatoghraphy – Mass Spectrometry |
| HPLC | High |
| $K_H$ | Henry Law's Constant |
| $K_{ow}$ | Octanol/Water partition Coefficient |
| $LC_{50}$ | Lethal Concentration 50% |
| LOEC | Lowest Observed Effect Concentration |
| *P* | Products |
| *PE* | Pulse Enhancement |
| $pK_a$ | Negative Logarithm of the acid dissociation constant |
| *PW* | Pulsed Wave |
| SPE | Solid Phase Extraction |
| TCS | Triclosan |

| | |
|---|---|
| TOC | Total Organic Carbon |
| TOX | Effect over luminosity according to Microtox test |
| US | Ultrasound |
| UVA | Ultraviolet A (Long Wavelengths) |
| UVC | Ultraviolet C (Short Wavelenghts) |
| WWTP | Wastewater Treatment Plant |
| $Deg$ | Degradation percent |
| $K'$ | Ratio $\frac{k_2}{k_3'}$ |
| $M$ | Mass |
| $PT$ | Pulse Time |
| $S$ | Synergy |
| $ST$ | Silent Time |
| $T$ | Temperature |
| $r$ | Overall rate of reaction |
| $t$ | Time |
| $v$ | Molar volume |
| $\theta$ | Ratio of the reaction sites in the bubble surface occupied by the solute (Okitsu et al. 2005) |
| $\mu$ | Viscosity |

# Acknowledgments

*One never notices what has been done; one can only see what remains to be done.*

*Marie Curie*

The author wish to thank NSERC the Colombian Administrative Department of Science, Technology and Innovation (COLCIENCIAS); and the University of Antioquia, especially GDCON research group and Dr. Gustavo Peñuela for financial and academic support of this research.

Also, to the Canadian Bureau for International Education (CBIE) and the ELAP program; the University of Saskatchewan, the department of Chemical and Biological Engineering and Dr Jafar Soltan for financial and academic support of the research made in Canada.

To all persons who contributed along these years to this work, all the analysts and researchers in the GDCON group, who shared with me invaluable knowledge that made this research possible and made me grow professionally and personally.

To my family who made me be what I am now, made me have love for knowledge and for giving a grain of sand to make this world a better place for all. Specially my mother, sister and niece who always have believed in me.

To Erik D. Taylor, Andrew Packham and Philip Pagnard who patiently read all papers and chapters helping with grammar correction.

To this beautiful planet that inspires us to think about the way of keeping it safe from our walking through it.

# Chapter 1

# 1 INTRODUCTION

## 1.1 Water treatment

Water pollution is a problem of primary concern from an economic, environmental and health perspective. One of the solutions includes wastewater treatment. It includes preliminary, primary, secondary and advanced treatment. Preliminary treatment removes materials that are easy to remove and prevents problems in subsequent treatment processes. Primary treatment separates solids, several of them insoluble in water, from liquid by settling using velocity reduction and chemical coagulation and flocculation. Secondary treatment removes dissolved and colloidal solids usually including a biological treatment that removes biodegradable compounds, and advanced treatment is used to remove nutrients and trace organics (Sharma and Sanghi 2012).

The treatment plants are not designed to remove emerging contaminants, which include personal care products and pharmaceuticals. These occur at trace levels in treated waste-water and the environment, and are of concern for human health and the aquatic ecosystem (Gogoi et al. 2018). Additionally, there are few health or environmental standards to provide guidelines for this treatment (Gogoi et al. 2018).

Advanced oxidation processes (AOPs) are technologies used for the treatment of wastewater with recalcitrant pollutants (Sharma and Sanghi 2012), and have shown good effectivity in its degradation (Babuponnusami and Muthukumar 2014a; Mahamuni and Adewuyi 2010; Malato et al. 2009; Marcelino et al. 2015; Oturan and Aaron 2014; Sathishkumar et al. 2016; Yang et al. 2014). Also, AOPs can be used in combination with biological treatments (Petrie et al. 2015).

## 1.2 Emerging pollutants

Emerging pollutants are products widely used in daily human activities such as pharmaceuticals, personal care products, surfactants, plasticizers, and chemical additives that are discharged to the environment mainly by wastewaters. These pollutants are unregulated and there is a consensus about their environmental concern (Petrovic 2003). Its presence has been widely reported in environmental

waters (Petrie et al. 2014). Their removal efficiencies were as high as 98% in plants with secondary treatments such as activated sludge, trickling filters, membrane bioreactors and nutrient removal (Petrie et al. 2014). Appreciable concentrations remain in effluents, as 7731 ng $L^{-1}$ for the analgesic tramadol have been found in river water (Petrie et al. 2014). Triclosan concentrations in river water in the US as high as 140 ng $L^{-1}$ (Kolpin et al. 2002). Benzophenone-1 has been found in concentrations of 37 ng $L^{-1}$ in river water in Spain (Negreira et al. 2009), and 47 ng $L^{-1}$ in river water in Korea (Jeon et al. 2006). Benzophenone-3 maximum concentration was 68 ng $L^{-1}$ in swiss rivers (Fent et al. 2010c), and 52 ng $L^{-1}$ in river water in Spain.

Conventional processes have shown to give form medium to good removal efficiencies for most of them. Influent wastewaters can contain antimicrobials, sunscreen agents and preservatives in concentrations >1000 ng $L^{-1}$. Triclosan has been found in influent wastewaters in the UK between 70 and 2500 ng $L^{-1}$; BP1 between 134 and 306 ng $L^{-1}$, and BP3 between 638 and 1195 ng $L^{-1}$ (Petrie et al. 2014).

### 1.2.1 Triclosan

Triclosan (5-chloro-2-{2,4-dichlorophenoxy}phenol) is an antibacterial agent used in personal care products, veterinarian, and industrial products. It has been detected in a number of aquatic species due to its persistence, concentration and bio accumulative nature. (Dann and Hontela 2011) proved that it is not toxic, mutagenic, or carcinogenic in mammals. But it has been shown that its acute toxic effect is more important in algae, invertebrates, and some fish species (Sabaliunas et al. 2003). For algal species such as *Scenedesmus subspicatus*, the 96h biomass $EC_{50}$ is 1.4 µg $L^{-1}$ (Orvos et al. 2002). The no-observed-effect concentration (NOEC) for algae is less than 1 µg $L^{-1}$ (Dann and Hontela 2011). For invertebrates such as Daphnia Magna, the 48h $EC_{50}$ is 390 µg $L^{-1}$ (Orvos et al. 2002). TCS toxicity over amphibian species was studied by (Palenske et al. 2010). Larval $LC_{50}$ values were reported as follows: 259–664 µg $L^{-1}$ (X. laevis), 367 µg $L^{-1}$ (A. crepitans blanchardii), 152 µg $L^{-1}$ (B. woodhousii woodhousii) and 562 µg $L^{-1}$ (R. sphenocephala). For freshwater crustacean *Thamnocephalus platyurus* and the fish *Orzyas latipes*, the 24h $LC_{50}$ values were 0.47 and 0.60 mg $L^{-1}$, respectively (Dann and Hontela 2011). The $LC_{50}$ (96 h) for embryo/larvae of the zebrafish (Danio rerio) is 0.42 mg $L^{-1}$ (Dann and Hontela 2011). It has also been proved, that TCS has teratogenic effects over this species, showing additional effects those related to acute toxicity. In the same way, TCS has shown negative impacts over hatching, embryonic development, enzyme activities and survival of Daphnia Magna. Its ability to disturb endocrine function in several

species such as Fish Medaka (Oryzias), North American bullfrog (Rana), South African clawed frog (Xenopus laevis) also has been widely demonstrated. In these species it showed weak androgenic and estrogenic activity (Dann and Hontela 2011).

The most important concern about the presence of triclosan in the environment is the generation of chlorodioxins, chlorinated phenols, polychlorinated biphenyl ethers, dihydroxy derivatives and bio accumulative species such as polychlorinated dibenzodioxins and methyltriclosan (Rule, Ebbett, and Vikesland 2005; Sirés et al. 2007; Wu et al. 2012; Song et al. 2012; Munoz et al. 2012). Polychlorinated dibenzo-*p*-dioxins are known toxic pollutants, being the acute toxicity of 2,3,7,8-tetrachlorodibenzo-*p*-dioxin one of the compound with the lowest LD50 values: 0.6μg/kg for male guinea pigs (Hites 2011). 2,7-dichlorodibenzo-*p*-dioxin, a known degradation TCS byprodyct produced a suppression of the antibody responses to both sheep erythrocytes, a T-dependent antigen, and dinitrophenyl-Ficoll, a T-independent antigen, similarly as 2,3,7,8-tetrachlorodibenzo-*p*-dioxin (Holsapple et al. 1986). This compound has been detected as TCS degradation byproducts by advanced oxidation processes such as photolytic degradation (Wong-Wah-Chung et al. 2007)(Lores et al. 2005)(Aranami and Readman 2007) , and in conventional wastewater treatments (Tohidi and Cai 2015)., but previous reports on TCS ultrasound degradation have not analyzed degradation byproduct

*Table 1. Triclosan Properties*

| | |
|---|---|
| Formula | $C_{12}H_7Cl_3O_2$ |
| Molecular Weight (g $mol^{-1}$) | 289.5 |
| Water solubility (mg $L^{-1}$) | 10 |
| Log $K_{ow}$ | 4.76 |
| Vapor pressure (mm Hg, 25$^oC$) | $4.65 * 10^{-6}$ |
| $K_H$ (Atm-$m^3$/mol) | $4.99 *10^{-9}$ |
| $pK_a$ | 7.9 |

### 1.2.2 Benzophenone-1

Benzophenone-1, (2,4-dihydroxybenzophenone) is an UV filter used to protect materials such as textiles, household products, agricultural chemicals, and cosmetics. UV filters reach the aquatic environment via wash-off from recreational activities or via sewage. Many of them are stable in the environment (Fent et al. 2008). BP1 has been found in rivers up to 47 ng $L^{-1}$, and in levels from 27 to 204 ng $L^{-1}$ in industrial drainage (Fent et al. 2008).

The BP1 has demonstrated effects over humans, fishes and rats. It exhibits multiple hormonal activities including estrogenicity and antiandrogenicity (Fent et al. 2008). Its anti-androgenic effects include the prevention of testosterone formation in humans. It has also xenoestrogenic effects such as the stimulation of the proliferation of BG-1 ovarian cancer (Park et al. 2013). Investigation of *in vivo* BP1 estrogenic activity in rainbow trout and madaka, by exposing juvenile fathead minows for 14 days, resulted in vitelogenin induction by BP1 at a LOEC of 4919 $\mu gL^{-1}$ (Fent et al. 2008). BP1 bioaccumulates in human and animal bodies, and also stimulates cell proliferation and metastasis on LNCaP prostate cancer cells in humans, acting as an exogenous factor to enhance prostate cancer progression (Kim et al. 2015). ((In et al. 2015) demonstrated the proliferation of MCF-7 human breast cancer cells

*Table 2. Benzophenone 1 Properties*

| | |
|---|---|
| Formula | $C_{13}H_{10}O_3$ |
| Molecular Weight (g mol-1) | 214.0 |
| Water solubility (mg L-1) | 413.4 |
| Log Kow | 3.0 |
| Vapor pressure (mm Hg, 25oC) | $1.41 * 10^{-7}$ |
| $K_H$ (Atm-$m^3$/mol) | $2.65 *10^{-11}$ |
| pKa | 7.53 |

### 1.2.3 Benzophenone-3

Benzophenone-3 (2-hydroxy-4-methoxybenzophenone, or oxybenzone) is an UV filter. It is used as a protection against solar UV radiation, and is found in cosmetics, personal care products, pharmaceuticals, and industrial commodities.

It is one of the most widely detected UV filters in the environment (Gago-Ferrero et al. 2012). It has been detected in river waters in concentrations up to 114 ng $L^{-1}$ in Slovenia and in sea water up to 269 ng $L^{-1}$ in Norway. In swimming pool waters it has been detected in higher concentrations up to 400 ng $L^{-1}$ in Slovenia. By the other hand, it has been found in raw wastewater at concentrations as high as 7800 ng $L^{-1}$ in Switzerland and in treated water as high as 7000 ng $L^{-1}$ (Fent et al. 2008).

BP3 has a low toxicity on water organisms. Acute toxicity on Daphnia magna expressed as 48 h-$EC_{50}$ values is 1.9 mg $L^{-1}$ (48 h acute immobilization assay) (Fent et al. 2010a). Additionally, BP3 is an endocrine disruptor. Its antiestrogenic and antiandrogenic activities in fishes has been demonstrated. (Blüthgen et al. 2012) confirmed the alteration of genes involved in steroidogenesis and hormonal pathways in zebrafish, at concentrations ranged from 2.4 to 312 µg $L^{-1}$. (Coronado et al. 2008) showed its effect over two fish species: Rainbow Trout and Japanese Medaka. The vitellogenin induction on rainbow trout resulted in a LOEC (14 d) of 0.75 mg/L, and on medaka, an LOEC (21 d) of 0.62 mg/L. BP3 also induced reduced the percentage of fertilized eggs at 0.62 mg/L. This shows its endocrine disruption effect, but it occurs at concentrations higher than those found in the environment.

BP3 has also shown harmful effects on mammals. (Schlumpf et al. 2004) found that BP3 increased uterine weight in immature rats. (Schlumpf et al. 2001) found that it increased the proliferation of MCF-7 breast cancer cells with a $EC_{50}$ of 3.73 µM.

*Table 3. Benzophenone 3 Properties*

| | |
|---|---|
| Formula | $C_{14}H_{12}O_3$ |
| Molecular Weight (g $mol^{-1}$) | 228.1 |
| Water solubility (mg $L^{-1}$) | 68.56 |
| Log $K_{ow}$ | 3.8 |
| Vapor pressure (mm Hg, 25°C) | $6.62 * 10^{-6}$ |

| | |
|---|---|
| $K_H$ (Atm-$m^3$/mol) | 1.5 *10 $^{-8}$ |
| $pK_a$ | 7.56 |

## 1.3 Advanced Oxidation Processes

In the AOPs occurs an attack of organic compounds by free radicals, between them, the most important, the radical hydroxyl ·OH, giving the transformation of the organic pollutants, and in some cases, total mineralization (Oturan and Aaron 2014). Conventional tertiary wastewater treatment processes have some disadvantages in degrading these compounds. Adsorption has high operational costs because the adsorbent needs to be recovered. Membrane technologies as ultrafiltration, nanofiltration and reverse osmosis processes have high costs and some operational problems, and many of them leave considerable amounts of persistent pollutants in the effluents (Muruganandham et al. 2014).

AOPs have demonstrated high degradation efficiencies for recalcitrant pollutants in low concentrations with easy operation conditions, and with low costs, including in many cases the possibility of using solar energy. Some AOPs include: ozonation, Fenton and photo-Fenton processes, ultrasound processes (US), and photocatalysis (Muruganandham et al. 2014).

Between them, US process has the advantage of generating OH radicals without adding chemicals or changing pH, and without the use of catalysts. US can degrade a wide variety of organic pollutants without the generation of sludge and the need of catalyst separation and recovery, or neutralization after the process. However, total mineralization cannot be achieved in most of the cases (Tijani et al. 2014).

Sonochemistry is based on the phenomenon called acoustic cavitation. Under the effect of US wave's creation and growth of bubbles occurs in water. After achieving the resonance size, these bubbles violently implode generating high pressures (1000 atm) and temperatures (>5000 K). Under this temperature and pressure conditions, water decomposes generating OH radicals. These radicals react with oxygen peroxide, solute or can recombine forming hydrogen peroxide (Henglein 1987). Solute degradation processes can take place inside the collapsing bubbles, in the bubble/liquid interphase, and in the bulk solution (Okitsu et al. 2006).

US has been effectively used for degrading pharmaceuticals as ciprofloxacin (De Bel et al. 2011), bisphenol A (Torres et al. 2008), α-ethynylestradiol (Frontistis and Mantzavinos 2012) and diclofenac (Hartmann et al. 2008). Pesticides such as atrazine

(Bianchi et al. 2006) and alachlor (Kidak and Dogan 2015). And also degrading additives and organic compounds such as carbon tetrachloride (Im et al. 2011; Pétrier and Francony 1997), alkylbenzen sulfonates (Dehghani et al. 2007), phenol (Kidak and Ince 2006; Pétrier and Francony 1997), and chloroaromatic derivatives (Petrier et al. 1998), among others.

US degradation process can be enhanced when combined with other advanced oxidation processes. Some hybrid process include: sonophotocatalysis, sono-Fenton, Sonophoto-Fenton, Sonoelectro-Fenton and sonolysis coupled with ozonolysis (Sathishkumar et al. 2016).

Fenton processes is based on hydrogen peroxide ($H_2O_2$) decomposition under the catalysis of ferrous ions ($Fe^{2+}$). In this way, $H_2O_2$ decomposes generating a large number of hydroxyl radicals, which degrade organic contaminants by a non-selective attack. The Fenton-based process must be conducted in a narrow range of working pH in order to maintain ferrous ions in solution (Sathishkumar et al. 2016). It has some advantages such as easy application on existent treatment process, the use of common and inexpensive chemicals, and no need of energy input (Oturan and Aaron 2014). Some disadvantages are the need of low working pH (2.8-3), accumulation of iron sludge that must be removed at the end of the treatment, and difficulties in $H_2O_2$ handling. Additionally, total mineralization cannot always be achieved because of the formation of $Fe^{(3+)}$-carboxylic acid complexes.

Fenton processes combined with sonication can result in enhanced degradation and the solution of some of these disadvantages because of enhanced solubility of iron ions. Also, reactions promoted by ultrasound produce more $Fe^{2+}$ ions, which are responsible for hydroxyl hydroperoxyl radical's formation. Additionally, Fenton process release OH radicals over the solution, opposed to the US were high OH radical concentration is achieved only over the bubble's surface, favoring its contact and reaction only with hydrophobic compounds. In this way, Fenton enhances mineralization efficiencies for US processes.

SonoFenton processes has been successfully applied to degradation of Reactive Blue 19 (Siddique et al. 2014); Reactive Red 2 (Wu et al. 2012a); Reactive Blue 181 (Basturk and Karatas 2014) and carbofuran (Ma et al. 2010). In all of these processes, degradation rates in the presence of US or the Fenton processes were enhanced, achieving total degradation in shorter times.

### 1.3.1 Triclosan removal by AOPs

TCS removal efficiencies in water treatment facilities in the United Kingdom ranged from 58 to 98% using rotating biological contactors, trickling filters and activated sludge between 2003 and 2004 (Thompson et al. 2014). And 97-98% of removal has been found in a constructed wetland in Texas (Waltman et al. 2006). Under anaerobic or anoxic conditions low removal rates are found (Chen et al. 2011). Several studies for TCS degradation by AOPs have been made. (Suarez et al. 2007) studied the aqueous ozone oxidation of TCS at neutral and high pH, and in wastewater matrix. Hydroxyl radicals were responsible for 35% of the TCS degradation, indicating that degradation takes place directly by triclosan reaction with ozone. (Chen et al. 2012) found 2,4-dichlorophenol, clorocatechol, mono-hydroxy-triclosan and di-hydroxy-triclosan as the reaction products for TCS degradation in aqueous ozone. (Munoz et al. 2012) studied Fenton like process for TCS oxidation. They found that degradation byproducts are less toxic than triclosan, and also that these byproducts are less toxic than those generated by another AOPs for TCS. (Song et al. 2012) used $BiFeO_3$ as heterogeneous catalyzer for $H_2O_2$ decomposition. In this way, they had good results for mineralization without using UV radiation that generates toxic byproducts. By the other hand, (Ren et al. 2014) found a synergistic effect for electrochemical and sonolysis processes in TCS degradation.

Two studies were found in the literature using sonochemical degradation of triclosan. Those studies carried out by (Naddeo et al. 2013) and (Sanchez-Prado et al. 2008) explore the extent, rate of degradation, kinetic rate constants for pseudo first order models, and the effect of matrix solution on degradation. Both studies were conducted at low frequencies (25, 45, and 80 kHz), and did not explore the effect of important variables such as frequency, pH and US mode. Additionally, they did not study byproducts and toxicity after US TCS degradation.

### 1.3.2 Benzophenone -1 removal by AOPs

Removal of BP1 in conventional treatment plants is not complete. Primary sedimentation and chemical coagulation/flocculation showed not to be effective in the removal of UV-filters like BP1 because of its low log $K_{OW}$ (Ramos et al. 2016). A 96% of removal for BP1 by a primary treatment followed by trickling filter beds was found by (Kasprzyk-Hordern et al. 2008). (Negreira et al. 2009) reported 83% removal of BP1 in WWTPs after activated sludge treatment. (Wu et al. 2018) reported a removal mean value of 97% in three WWTP in China. (Tsui et al. 2014a; b)

investigated five different wastewater treatment methods for 12 organic UV-filters in Hong-Kong, China. In them, BP1 was detected in all influent samples, with mean concentration of 163 ng $L^{-1}$. BP1 detection frequency in effluents was higher than 75% throughout the year in these treatment plants. The mean value concentration was 86 ng $L^{-1}$, and the maximum concentration was 155 ng $L^{-1}$. This indicates that BP1 is not totally degraded in conventional treatment plants. By the other hand, fungal treatment resulted in the degradation of more than 95% at 3 h for BP1 according to (Gago-Ferrero et al. 2012).

Few reports about BP1 degradation by AOP's have been issued. Only the study of (Gago-Ferrero et al. 2012) was found. They reported a 100% photodegradation after 24 h UV irradiation for BP1 in an initial concentration of 250 µg $L^{-1}$, using a SunTest apparatus equipped with a Xenon arc lamp providing a light intensity of 400 $W/m^2$.

### 1.3.3 Benzophenone-3 removal by AOPs

BP3 is removed partially in conventional wastewater treatment plants. During primary sedimentation, BP3 is removed in a very low extent in the sludge (<5%) because of its low Log Kow (3.8). This process is enhanced by the addition of chemical coagulation-flocculation resulting in a BP3 removal of 23 to 52% in dry season and 28 to 67% in wet season (Ramos et al. 2016). Secondary treatment has shown to be more effective in removing BP3, with efficiencies from 68 to 96% (Balmer et al. 2005); and up to 85% in a primary treatment followed by trickling filter beds (Kasprzyk-Hordern et al. 2008). (Negreira et al. 2009) reported a 90% of BP3 removal in WWTPs after activated sludge treatment. However, these conventional treatments do not totally achieve BP3 removal. (Tsui et al. 2014a; b) investigated five different wastewater treatment methods for 12 organic UV-filters. In these plants, BP3 was frequently detected in both influent and effluent, with mean concentration in the influent of 284 ng $L^{-1}$. But it was also detected in all effluent samples with a mean concentration of 111 ng $L^{-1}$, and maximum concentration of 541 ng $L^{-1}$.

Tertiary treatments have shown to have different efficiencies. During UV-disinfection, the BP3 removal efficiencies were lower than 30%. This is explained by the photo stability of this compound. Exposed to a radiation of a halogen lamp, with a wave- length spectrum between 290 and 800 nm, covering therefore the UVA and UVB ranges, and to natural light, BP3 showed a high stability (Santos et al. 2012). (Gago-Ferrero et al. 2012) found that BP3 remained unaltered after 24h of solar radiation treatment. (Vione et al. 2013) found similar results degrading BP3 by sunlight at an initial concentration of 20 µM, finding a half-life time of some weeks.

Ozonation and adsorption onto activated carbon are effective techniques to remove BP3 from aerobically treated grey water. (Hernández-Leal et al. 2011) reached removal efficiencies up to 83% using ozonation of BP3, in effluent waters from secondary and tertiary treatments in concentrations between 5 and 16.3 ng $L^{-1}$. (Gago-ferrero et al. 2013) achieved more than 95% of BP3 degradation in 40-50 minutes using ozonation for an initial BP3 concentration of 5.1 mg/L. (Hernández-Leal et al. 2011) obtained more than 99% of degradation in 15 min of ozonation of 285 ng/L of BP3. (Hernández-Leal et al. 2011) reported BP3 removals up to 93% using activated carbon. By the other hand, BP3 is very susceptible to chlorination (Santos et al. 2012). It was shown by (Negreira et al. 2008) that halogenated forms of 3-methoxy phenol, and halogenated forms of BP3 were formed. Trichloro-methoxyphenol was the most abundant of the BP3 cleavage byproducts.

Advanced Oxidation Processes (AOP's) have been used for BP3 degradation using ozonation, oxidation with Fe(VI), photocatalysis, UVC/$H_2O_2$, photo Fenton-like, and ultrasound (US) degradation at low frequencies. (Celeiro et al. 2018) degraded BP3 (91%) in synthetic swimming pool waters using $TiO_2$-P25. They obtained its total degradation after 30 min of irradiation UVA (λ= 360 nm). The addition of $H_2O_2$ to the $TiO_2$-P25/UVA improved substantially the reaction rate. The same authors reported for UVC/$H_2O_2$ system, an optimal $H_2O_2$ concentration of 0.59 mM, and a BP3 removal efficiency of 95% after 6 min of irradiation. (Yang and Ying 2014) treated BP3 by oxidation with Fe (VI) obtaining a half-life of 167.8 s of Fe (VI) concentration of 10 mg/l, and pH 8.

## 1.4 Objectives

### 1.4.1 General

To study the ultrasound degradation process of triclosan, benzophenone-1 and benzophenone-3, evaluating the variables affecting it.

### 1.4.2 Specific

- To study the effect of the following variables on US degradation: Frequency, power, pH, radical scavenger presence, and US mode.
- To determine the degradation kinetics of US process

- To identify the degradation products of US degradation processes and propose possible degradation routes
- To study the mineralization by US degradation
- To evaluate the synergistic effects between US and Fenton processes for degradation of these compounds
- To study the toxicity evolution by the studied processes

# Chapter 2

# 2 FUNDAMENTALS OF SONOCHEMISTRY, UV/$H_2O_2$ AND FENTON PROCESSES

## 2.1 Sonochemistry

### 2.1.1 General

Sonochemistry is the result of acoustic cavitation, that is, creation, expansion, and implosive collapse of gas bubbles in liquids under ultrasound irradiation (Apfel 1981). This phenomenon occurs only if radiation intensity is high enough to produce cavitation, and if there is a dissolved gas in the liquid (Fitzgerald et al., 1956). This ultrasound irradiation can be generated by the piezoelectric effect, or by mechanical cavitation. Most of the modern ultrasonic devices use piezoelectric materials that convert electrical energy into mechanical (ultrasound waves) energy (Mahvi 2009).

Reactions occur because of the high temperatures induced by cavitation, because ultrasound intensities of 5-10 W/$cm^2$ can make a small gas bubble reduce its volume generating temperatures of hundreds of degrees centigrade. This bubble compression generates large amounts of heat, which in turn generates a short duration Hot Spot because heat transfer to the surroundings is very low (Suslick et al. 1999). These hot spots produce temperatures of 5000K and pressures up to 1000 atm. Acoustic cavitation can be of two types: transient and stable. Transient cavitation is responsible for sonochemistry. Transient cavities exist just for a few cycles flowed by a violent implosion (Mahvi 2009).

Nowadays, it is well known not only hot spots are responsible for chemical reactions, but three kind of reactions occur during sonolysis: pyrolysis, ·OH and ·H

radical reactions, and supercritical water oxidation (Makino et al., 1983)(Hua et al. 1995). Kinetic studies have shown sonochemical reactions take place in two locations: inside the bubbles and in the liquid. The last is because of heating of surrounding liquid; liquid drops injection in the hot spot due to wave surface distortions, or because of jets from the collapsing bubble (Suslick et al. 1999). Sonochemistry is also accompanied by light emission. This sonoluminiscence is a useful proof of the conditions created during bubble collapse, measured by spectroscopy (Suslick et al. 1999).

The reactions of radical generation are described by the following expressions:

$$H_2O \overset{)))}{\rightarrow} \dot{H} + \dot{O}H \tag{1}$$

$$O_2 \overset{)))}{\rightarrow} 2\dot{O} \tag{2}$$

$$\dot{O} + H_2O \longrightarrow 2\,\dot{O}H \tag{3}$$

$$\dot{H} + O_2 \longrightarrow H\dot{O}_2 \longrightarrow \dot{O}H + \frac{1}{2}O_2 \tag{4}$$

Oxygen could suffer thermolysis according to (Hua and Hoffmann 1997):

$$O_2 \rightarrow 2\dot{O} \tag{5}$$

Riesz et al., 1985, used spin trapping and electronic spin resonance to confirm free hydroxyl radicals formation. Reaction with pollutants occur at rates only limited by a molecule's diffusion and is well established. Nowadays, its formation has been probed, but not for direct effect of the radiation, but by thermic decomposition of water in the gas bubbles implosion phase (Henglein, 1987).

Radical recombination is described by the following reactions:

$$\dot{H} + \dot{H} \longrightarrow H_2 \tag{6}$$

$$\dot{H} + \dot{O}H \longrightarrow H_2O \tag{7}$$

$$2\dot{O}H \longrightarrow H_2O_2 \tag{8}$$

$$2H\dot{O}_2 \longrightarrow H_2O_2 + O_2 \tag{9}$$

Free radicals $\dot{H}$ and $\dot{OH}$ react with oxygen molecules, between them, or with the pollutants. Hydrogen peroxide generation occurs mainly in the bulk and at the cool interface of the bubble. Both hydrogen peroxide and OH radicals are responsible for oxidation reactions (Pétrier 2015a).

Reaction conditions depend on the characteristics of the ultrasound radiation (frequency, power density) and on dissolved gas properties. First studies about ultrasound nature indicated frequency, power and physicochemical properties of the gas influenced $H_2O_2$ and $\dot{OH}$ generation, because they influenced the collapse temperatures and pressures (Hua and Hoffmann 1997).

Cavitation bubbles contain dissolved gas and vaporized water. Equilibration of the pressure inside the bubble leads to the entry of liquid vapor and entry of dissolved gas in the period of lower pressures. When pressure increases, gas from the bubble dissolves in the liquid and the liquid vapor liquefies in the compression step (Pétrier 2015a). This mass transfer process is related to the bubble surface. Subsequently, bubble size increases with the matter entering but this growth is not limitless. There is a critical size in which the bubble collapses. For ultrasound between 20 kHz and 1 MHz, the duration of the collapse is in microseconds. Under these conditions, collapse is adiabatic, generating the high temperatures and pressures previously mentioned (Pétrier 2015a).

Reaction mechanisms of the organic compounds depend mainly on the compound properties. Hydrophobic and volatile compounds suffer thermic decomposition inside collapsing bubbles as long as hydrophilic and low volatility compounds degrade by reaction with hydroxyl radicals coming from cavitation bubbles. For this kind of compounds, high frequencies are more effective than low (De Bel et al., 2011).

### 2.1.2 Variables influencing compounds degradation by Ultrasound

***Frequency***

Frequency influence on sonochemical degradation rates has been reported in several studies (Rayaroth et al. 2015a) (De Bel et al. 2011)(Torres et al. 2008)(Petrier et al. 1994)(Pétrier and Francony 1997). Ultrasound frequency influences the kind of processes occurring in solution. At low frequencies, physical effects predominate and the number of cavitation events are less than those at higher frequencies (Thangavadivel et al. 2012). Also, higher bubble volumes make leads to higher vapor content in collapsing bubbles. This effect generates less energetic implosion of bubbles resulting in lower OH radical generation. Conversely, at high frequencies,

bubble lives and sizes are smaller, resulting in a lower vapor content at the collapse moment, generating more energetic bubbles implosion. In general, frequency influences the rate of hydroxyl radicals generated (Hua and Hoffmann 1997).

Another important fact for explaining dependency of degradation efficiency from US frequency is at high frequencies, the resonant radius for bubbles is smaller than at low frequencies; therefore, fewer acoustic cycles are required before the bubble reaches resonant size. This results in more frequent collapse of bubbles and consequently, a higher hydroxyl radicals generation rate (Hua and Hoffmann 1997). Also, it has been suggested at high frequencies, hydroxyl radicals are ejected out of the bubble before they can recombine in the gas phase because the collapse time at higher frequencies is shorter (Hua and Hoffmann 1997). Additionally, it has been observed - differences in the distribution of cavitational activity over the reactors depending on frequency. For low frequencies, maximum energy gets dissipated near the irradiating surface in a cone like structure. This generates a wide variation in sonochemical activity along the fluid for low frequencies and a more uniform distribution for higher frequencies (Sutkar and Gogate 2009). It has been shown that optimal frequency is mainly a function of properties of the substance (Adewuyi and Oyenekan 2007).

***Power***

The importance of power density on ultrasound degradation rates is very high. As power density of US radiation increases, acoustic amplitude increases generating more violent collapse of the bubbles (Adewuyi and Oyenekan 2007).

There is a lower and upper limit values for the ultrasound amplitude inducing cavitation which generates an optimized oxidation yield for each reactor design under defined experimental conditions (Pétrier 2015a). The lower limit corresponds to the threshold value for wave amplitude that generates cavitation. Under this value there are no oxidation reactions. Degradation rates start increasing with power densities from this value to an optimum. Above this value, further power increases cause a decrease in degradation rates (Sivakumar and Pandit 2001). At higher power intensities, a cloud of bubbles is formed close to the transducer. This cloud prevents the ultrasound waves of propagation because of the scattering phenomena. Several studies have analyzed the optimum power level for different sonochemical systems finding it depends on the reacting volume, operating pressure, physicochemical properties of bulk liquid, area of irradiating element and frequency of operation (Beckett and Hua 2001).

Another factor to take into account is ultrasound intensity is not uniform, but variates along the bulk fluid. It decreases with an increase in the distance from transducer, a phenomenon known as attenuation of sound wave. It occurs due to refraction, reflection, and absorption of the wound waves. This could generate the possibility of passive zones in the reactor (Sutkar and Gogate 2009).

The amount of power dissipated in the liquid medium is usually determined by the calorimetric method. This method consists of the measurement of the initial rate of the fluid temperature rise when irradiated by ultrasound, and assumes all the mechanical energy released from the generator in the form of ultrasound waves is converted in heat, and the system is adiabatic, ignoring possible heat loses to the fluid surroundings (Kimura et al. 1996).

The equation expressing power for calorimetric method is:

$$Power = C_p \frac{dT}{dt} M \tag{10}$$

Where: $C_p$ is the heat capacity of water, $\frac{dT}{dt}$ is the initial temperature change in water for a time interval *t*; and $M$ is the mass of water used.

Another but less used way of determining power intensity is measuring the chemical yield of the Weissler reaction. This is based on water containing $CCl_4$ generates molecular chlorine under US radiation. This chlorine reacts with iodine ions liberating molecular iodine that is measured by titrating with sodium thiosulfate solutions adding starch solution (Kimura et al. 1996); or measuring the absorbance of $I_3^-$ ions formed by the reaction of $I_2$ with $I^-$ in excess (Koda et al. 2003).

***Ultrasound Mode***

US radiation can be emitted in pulses, which influences the possibility of pollutant molecules to migrate towards the bubble surface and the effectivity of the formation, growing and imploding of the bubbles; having a positive effect on degradation rates in many cases, especially when reaction with OH radicals is taking place on the bubble surface.

According to (Xiao et al. 2013c), the silent times in pulsed US allows time for pollutant molecules to diffuse toward bubble interface, where OH radicals concentration is higher. This is certain when molecules have a high diffusivity in the reaction fluid, and it depends mainly on molecule size.

Diffusivity can be calculated according to the following expression (Hayduk and Laudie 2015):

$$D_{12} = \frac{14.0 * 10^{-5}}{\mu_2^{1.1} v_1^{0.6}} \quad (11)$$

Where $D_{12}$is the diffusivity ($cm^2\ s^{-1}$) of solute (1) in solvent (2); $\mu_2$ is solvent viscosity (cps); and $v_1$is the solute molar volume at normal boiling point ($cm^3\ gmol^{-1}$).

This is why pulsed mode has a more intense effect on small molecules with molar volumes less than 130 ml/mol can diffuse more readily to bubble interface (Xiao et al. 2014). This effect is also higher for compounds high octanol/water partition coefficient ($K_{ow}$).

A way of measuring the effect of pulsed model ultrasound is calculating the difference in initial degradation rates or degradation percentage between pulsed wave mode US (PW) and continuous wave model US (CW) by Pulse Enhancement (PE*), which is defined as:

$$PE^*(\%) = \frac{(Deg)_{PW} - (Deg)_{CW}}{(Deg)_{CW}} \times 100\% \quad (12)$$

Where $(Deg)_{PW}$ is the degradation percent for PW mode US, and $(Deg)_{CW}$ is the degradation percent for PW mode US.

Total reaction time for PW mode US is calculated according to the following equation (Yang et al. 2005):

$$t_{total} = t_{sonication}\left(1 + \frac{ST}{PT}\right) \quad (13)$$

Where $t_{total}$ is the total reaction time; $t_{sonication}$ is the real sonication time; $ST$ is the time between pulses (Silent Time); and $PT$ is the Pulse Time.

The other important effect of pulsed ultrasound is the effectiveness in the bubble's creation, expansion and implosion. During continuous wave ultrasound, bubble clusters could appear. Due to the proximity of the bubbles, they cannot absorb enough energy to get the threshold size and their proximity increases bubble coalescence, generating bubbles larger than the resonant ratio, being sonochemically

inactive. Pulsed model US can make this effect diminish because it lets time for the clusters to disperse and reduces coalescence allowing a higher number of bubbles to become sonochemically active (Deojay et al. 2011).

For nonvolatile compounds has been demonstrated there is a dependence on the degradation rates on the pulse length and silent times. (Yang et al. 2005) showed short pulses generated insufficient activation for cavitation bubbles and long pulses favored surfactant accumulation over the bubble surface.

Although pulsed model ultrasound seems to have this positive effect on US degradation rates for pollutants with these properties, a clear relationship between pulse time and silent time duration or with the ratio of both have not been established. Some authors have proposed the ability of ultrasound to generate chemically active bubbles could be dependent on the ratio of the US pulse length and pulse interval (Deojay et al. 2011) and enhancement of ultrasound during pulsed ultrasound depends on the frequency (Yang et al. 2008).

However, studies dealing with pulsed mode ultrasound have been made under a limited range of pulsing conditions and a straightforward relationship has not been established.

(Deojay et al. 2011) conducted a study varying conditions for pulse length and pulse interval in a wide range for octyl benzene sulfonate ultrasound degradation trying to find the relationship of degradation rates with these two variables. They did not find a clear trend for the degradation rate as a function of ultrasound frequency and pulse mode, despite having found there was an effect of these two variables.

***pH***

The pH does not have an influence on the phenomenon of ultrasound cavitation; however, compounds that present a change in their molecular form because of a pH change have different degradation rates by ultrasound depending on its ionic form according to the pH value. The reason for this is that molecular or ionic form for certain compounds have different hydrophobicities. The ionic form will usually degrade less rapidly than the molecular form because it is more hydrophilic, and consequently, more soluble tending to accumulate less over the bubble surface where hydroxyl radical's concentration is higher and most of the reaction is occurring (Pétrier 2015a).

### 2.1.3 Kinetic models for Ultrasound reactions

There have been a number of approaches to understand the mechanism of ultrasound degradation reactions and kinetic models derived from these mechanisms. Okitsu et al. (2006), proposed a non-heterogeneous kinetic model for azo dyes ultrasound degradation in water. The model was similar to a Langmuir–Hinshelwood mechanism or Eley–Rideal mechanism occurring in the bubble-solution interface. In this model, a nonlinear expression for the rate of reaction of degradation was used. The reaction rate depends on the pollutant concentration in the bulk solution, the rate constant of reaction between OH radicals and the pollutant, and the ratio of the rate constants of adsorption and desorption of the pollutant over the bubble interface. Some studies - such as that of Chiha et al. (2010) for phenol, 4-isopropylphenol and Rhodamine B, and Chiha et al. (2011) for 4-cumilphenol - concluded that the reaction occurs on the bubble surface after kinetic data fitted well with this expression. This model is based on the assumption that before collapsing of the bubble a pseudo-equilibrium of adsorption and desorption of pollutant at the gas/liquid interface exists. They also assumed that after the bubble collapses, adsorbed pollutant molecules react with OH radicals which are assumed to be at a high concentration in this region once collapse occurs. They argued that such assumptions are valid at low frequencies because bubble lifetime is larger than that at high frequencies, and resonance bubble radius is larger (Okitsu et al. 2006). In their study, they proposed the rate of adsorption of the solute, $r$, from the bulk solution to the reaction site, is proportional to its concentration in the bulk solution and to $(1-\theta)$, where $\theta$ is the ratio of the reaction sites in the bubble surface occupied by the solute (Okitsu et al. 2005). This results in a general model (equation (*14*)):

$$r = k\theta = \frac{kK[C]}{1+K[C]} \tag{14}$$

Where $K = {k_{a1}}/{k_{a-1}}$, $k_{a1}$ and $k_{a-1}$ are the adsorption and desorption rate constants on the bubble surface, and $k$ is the pseudo first order rate constant for the reaction of the solute with OH radicals. Although this is a widely used model, taking into account that growing and explosion of bubbles is a process that takes less than 2 μs, an equilibrium such as that proposed by Okitsu et al. (2006) could hardly be established.

On the other hand, Serpone et al. (1994) proposed a general reaction mechanism for chlorophenol degradation by ultrasound where reactions can occur in the bulk solution or in the interface, reaching a general expression similar to that of Okitsu. However, in this model, if the reaction is taking place in the bubble interface, where

OH concentration is high and pollutant concentration is low, the rate expression becomes of first order in the concentration of the pollutant, as we will show later. They found the following expression for the overall rate of sonochemical decomposition of 4-chlorophenol in air equilibrated aqueous media for high initial concentrations of chlorophenol (CPOH) (>75μ$M$):

$$r = k_0 + \frac{kK[CPOH]_0}{1 + K[CPOH]_0} \tag{15}$$

This is a particular rate equation for the ultrasound degradation of chlorophenol at high concentrations. It can be noted that without the constant term it is the same expression developed by (Okitsu et al. 2005), but constants have different meanings. In this expression, $k_0$ is the bulk solution degradation, which is a constant because of the particular value that parameters for chlorophenol had in the general expression they developed. The second term is the rate expression for degradation taking place on the bubble interface. Overall rate is the sum of degradation in both, the bulk solution, and the bubble surface.

For the contaminants degradation based on the reaction mechanisms proposed by Serpone et al. (1994), we have the following: Initially, water molecules decompose by the effect of ultrasound cavitation according to equation (*16*):

$$H_2O + ))) \overset{k_1}{\rightarrow} OH^* + H^* \tag{16}$$

Compounds (C) and OH* radicals encounter at the bubble/solution interface, according to this reaction:

$$OH^* + C \overset{k_2}{\rightarrow} OH^*C \tag{17}$$

In this expression, $k_2$ is determined by diffusional characteristics of OH radicals and solute in aqueous media. The complex $OH^*C$ can breakup according to:

$$OH^*C \overset{k_2'}{\rightarrow} OH^* + C \tag{18}$$

Or can form the products (P) as in equation (*19*):

$$OH^*C \overset{k_3}{\rightarrow} P \tag{19}$$

An assumption is made that reaction in equation (*19*) follows a first order reaction and that there is pseudo-steady state condition, which is, the $[OH^*C]$ concentration is constant. Also, the rate of separation of the unreacted complex $[OH^*C]$ is much lower than the rate at which products form, that is: $k_3 \gg k_2'$, which is a plausible assumption for reactions with OH radicals (Buxton et al. 1988). Thus, the reaction rate for the formation of products in (*19*) can be expressed as:

$$\frac{d[P]}{dt} = -\frac{d[C]}{dt} = k_2[OH^*][C] \tag{20}$$

Thus, the controlling step in the formation of products is the interaction of hydroxyl free radicals with compound molecules. The reaction rate constant in (*20*), $k_2$, depends on the diffusivity of the pollutant and of the OH radicals in solution.

It should be taken into account that other reactions occur simultaneously in solution. Recombination of radicals and formation of hydrogen peroxide can occur mainly at the interface, but it could also occur in the bulk solution at very low rates (Serpone et al. 1994):

$$OH^* + H^* \overset{k_4}{\rightarrow} H_2O \tag{21}$$

$$2OH^* \overset{k_5}{\rightarrow} H_2O_2 \tag{22}$$

Where $k_4$ $and$ $k_5$ are the reaction rate constants for reactions between the radicals. Using equations (*20*), (*21*) and (*22*), and following the same procedure used by Serpone et al. (1994), the following expression is obtained:

$$\left(\frac{d[C]}{dt}\right) = \frac{k_1 k_2 [C]}{(k_4[H^*] + k_5[OH^*] + k_2[C]\ )} \tag{23}$$

Simplifying for $[H^*]$ and $[OH^*]$ as constants:

$$\left(\frac{d[C]}{dt}\right) = \frac{k_1 k_2 [C]}{(k_3' + k_2[C]\ )} = \frac{k_1 K[C]}{(1 + K[C]\ )} \tag{24}$$

Where $K' = \frac{k_2}{k_3'} = \frac{k_2}{k_4[H^*]+k_5[OH^*]}$

This kinetic expression developed for degradation of the compounds analized based on the model proposed by Serpone et al. (1994) has the same form of kinetic expression as proposed by Okitsu et al.(2006). But this expression was derived without the assumption of a steady state of adsorption and desorption of molecules

over the bubble surfaces. Constants have different meanings too. Here, $k_1$ is the constant for radical generation which depends on many variables, principally those of the ultrasound generator system, such as frequency and power. $K'$ value depends on $k_2$, the rate constant for the C-OH complex conversion into products. $K'$ value also depends on $k_3'$. This constant depends on radical concentrations and rate constants of recombination.

On the other hand, rate expression of (Serpone et al. 1994) is applicable to reaction in both bulk solution and in bubble surface not only to reactions taking place in the bubble interface as assumed by (Okitsu et al. 2006).

Half-life of an OH radical is around $10^{-3}$ μs as shown by x-ray diffraction analysis (Pryor 1986), and in liquid medium it has been found that molecules migrate the distance of molecular diameter in a time range of $10^{-4}$ to $10^{-2}$ μs. Because of its short life, it could be expected that OH radicals have a low molecular mobility in water. Then, high OH radicals concentration could mainly be found in the bubble surface. In expression (23), condition $k_4[H^*] + k_5[OH^*] \gg k_2[C]$ is fulfilled for low C concentrations over bubble surface. This is expressed as:

$$\left(\frac{d[C]}{dt}\right) = k_b[C] \tag{25}$$

Where $k_b = \frac{k_1 k_2}{k_3'}$

This is a pseudo first order reaction kinetics rate expression.

## 2.2 $H_2O_2$/UV/US processes

UV light might degrade organic pollutants by electron transfer from the excited state of the carbon by radiation to ground state molecular oxygen with subsequent recombination of the radical ions by hydrolysis of the radical cation or by hemolysis to form radicals (Legrini et al. 1993).

UV radiation between 200 and 300 nm can photolyse $H_2O_2$ breaking the O-O bond and leasing to the generation of OH radicals, which can also decompose other $H_2O_2$ molecules. Initiation reaction is the following (Oturan and Aaron 2014):

$$H_2O_2 + hv \rightarrow 2HO^* \tag{26}$$

Propagation steps are:

$$HO^* + H_2O_2 \rightarrow H_2O + HO_2^* \quad (27)$$

$$H_2O_2 + HO_2^* \rightarrow HO^* + H_2O + O_2 \quad (28)$$

$$HO^* + HO_2^- \rightarrow HO_2^* + OH^- \quad (29)$$

And termination steps are:

$$2HO_2^* \rightarrow H_2O_2 + O_2 \quad (30)$$

$$HO^* + HO_2^* \rightarrow H_2O + O_2 \quad (31)$$

$$2HO^* \rightarrow H_2O_2 \quad (32)$$

The initiation step, that is, generation of OH radicals depends on the characteristics of the radiation source such as power and wave length range and on the properties of the medium related with radiation transmission (Oturan and Aaron 2014).

Additions of $H_2O_2$ to sonochemical reactions usually has a limited activating effect, mainly because $H_2O_2$ does not go towards bubble surface where the OH radicals concentration is high. However, combination of $H_2O_2$/UV/US has shown good results giving complete oxidation and mineralization in processes where it was not obtained by UV or US alone. $H_2O_2$ dissociation occurs in the bulk solution, opposed to the US effect which takes place only on the bubble's surface. This synergistic effect has been showed to be important for high frequency US (>300 kHz)(Pétrier 2015a).

Additionally, US can enhance $H_2O_2$ decomposition according to this reaction:

$$H_2O_2 + ))) \rightarrow 2HO^* \quad (33)$$

## 2.3 Fenton Processes

Fenton processes consist of the generation of OH radicals by the reaction between iron ions and $H_2O_2$ (García et al. 2015). $Fe^{2+}$ is oxidized to $Fe^{3+}$ and $H_2O_2$ is reduced generating OH, according to (Machulek Jr. et al. 2013) (Bagal and Gogate 2014; Ince and Ziylan 2015):

$$Fe^{2+} + H_2O_2 + H^+ \rightarrow Fe^{3+} + HO^* + H_2O \quad (34)$$

The Fe (III) can be reduced to Fe (II) by a $H_2O_2$ molecule, but at a much slower rate than Fe(II) oxidation (Machulek Jr. et al. 2013):

$$Fe^{3+} + H_2O_2 \rightarrow Fe^{2+} + OH_2^* + H^+ \quad (35)$$

A low pH (2.8-3.0) is necessary for the catalytic effect of $Fe^{3+}/Fe^{2+}$ to enhance the propagation of Fenton's reaction. Stoichiometric and under-stoichiometric amounts of $Fe^{3+}$ can effectively be used because of the regeneration of $Fe^{2+}$ according to equation (*36*) (Oturan and Aaron 2014).

$$Fe^{3+} + H_2O \rightarrow FeOH^{2+} + H^+ \quad (36)$$

$OH_2^*$ radical is much less reactive than $HO^*$ radical, and therefore, less efficient degrading organic compounds. Also, regeneration of $Fe^{2+}$can take place more effectively by the following reactions:

$$Fe^{3+} + OH_2^* \rightarrow Fe^{2+} + O_2 + H^+ \quad (37)$$

$$Fe^{3+} + R^* \rightarrow Fe^{2+} + R^+ \quad (38)$$

$$Fe^{3+} + O_2^{*-} \rightarrow Fe^{2+} + O_2 \quad (39)$$

In this way, $Fe^{3+}$ can be reduced by perhydroxyl radicals, organic radicals, and superoxide ions (Oturan and Aaron 2014). Recycling of the catalyst depends on the redox potential of the solution. Intermediates formed on the oxidative degradation may impact Fe speciation by redox processes and by complex reactions (García et al. 2015)

The Fenton process is effective in degrading a diverse amount of chemical compounds. Its efficiency depends on variables such as pH, $H_2O_2$ and catalyst concentrations (Oturan and Aaron 2014). However, some disadvantages for this oxidation process includes the slow rate of the Fe(II) regeneration process and also the formation of recalcitrant compounds that inhibit total mineralization (García et al. 2015; Machulek Jr. et al. 2013).

### 2.3.1 Variables influencing compounds degradation by Fenton Processes

***$Fe^{2+}$ concentration***

Degradation rate usually increases with the concentration of the ferrous ion. However, this increase becomes marginal after certain concentration (Babuponnusami and Muthukumar 2014b). Also, a big amount of iron salts will result in a big proportion of unused salts, contributing to the final value of total dissolved solids in the treatment effluent. A stoichiometric amount of $Fe^{2+}$ is generally used in Fenton reactions (Bagal and Gogate 2014a).

***$H_2O_2$ concentration***

$H_2O_2$ concentration is an important variable determining degradation rates and mineralization efficiency. Enough $H_2O_2$ must be present in solution to degrade the main compound and the intermediates if mineralization is the goal. However, high $H_2O_2$ concentrations can decrease oxidation rates due to OH trapping by $H_2O_2$ (Machulek Jr. et al. 2013) . This is why some Fenton processes are made continuously adding $H_2O_2$ during the process. Scavenging reaction is as follows (Wu et al. 2012a):

$$OH^{\cdot} + H_2O_2 \rightarrow HO_2^{\cdot} + H_2O \quad (40)$$

$$2OH^{\cdot} \rightarrow H_2O_2 \quad (41)$$

***pH***

Optimum pH for Fenton processes has been found to be around 3. At higher pH values, iron complexes such as iron oxohydroxides and precipitates as ferric hydroxide results in a lower hydroxyl radical's generation. The reason for this is there are less free iron ions that react more easily with hydrogen peroxide. Additionally, hydrogen peroxide gets solvated at very low pH values when there is a high presence of $H^+$ ions, forming the stable oxonium ion (Babuponnusami and Muthukumar 2014b). This is why an adequate pH control for solution is necessary for getting good efficiencies.

## 2.4 SonoFenton processes

The Fenton process has some disadvantages such as the need for using low pH levels for adequate release of iron ions. SonoFenton processes overcome this problem mainly by $Fe^{2+}$ regeneration and HOO radicals production (Ince and Ziylan 2015):

$$Fe - O_2H^{2+}+))) \rightarrow Fe^{2+} + HOO^* \quad (42)$$

Added to the effect of $Fe^{2+}$ decomposing $H_2O_2$ in Fenton reactions, Fenton process can be enhanced by US by the generation of additional OH radicals from $H_2O$ decomposition (equation*(33)*) and by improving iron ions solubility.

US also provides additional reaction mechanisms by pyrolysis, degrading some compounds that are refractory to the Fenton process. US enhances mass transfer rates due to the turbulence it generates in the reactor (Bagal and Gogate 2014b). This results in better overall reaction rates by favoring contact between radicals and compounds, and between $H_2O_2$ and iron ions.

## 2.5 Process optimization by Response Surface Methodology

Response Surface Methodology (RSM) is a collection of mathematic and statistic tools useful for modelling and analyzing systems in which a response variable is influenced by several variables. The goal of this methodology is its optimization. In order to achieve this, the relationship between independent variables and the response variable has to be determined. Usually a low order polynomial equation is suitable in a small region. The function can usually be expressed by a first-order or second order model (Montgomery 2012).

The steepest ascend method is the most common approach used for optimizing the response variable. It is based on moving towards its fastest growing direction. The path of steepest ascend is usually the line that goes through the center of the interest area and normal to the fitted response surface.

In this approach, the optimization process is as follows:

Initially, there is a screening step in which a $2^k$ design is used in search of the variables having effect on the response variable using few experiments. k is the number of variables, and the design is $2^k$ because each variable takes two values for the analysis.

Once it has been defined which variables have a significant influence on the response variable by statistical methods, the experimenter must move on these variables towards the optimum by the path of steepest ascend, until no further increase in response variable is observed, and a lack of fit of the first-order model is observed. In that moment, the experimental design can be enhanced looking for a surface curvature. One way of doing this is adding central points, using an approach as the central composite design, or just adding another level to each variable. These additional points are added to adjust a quadratic model. With this quadratic model, the stationary points can be found. They are those in which first derivatives for the function on each variable equals zero. Drawing contour plots for the response surface, it can be determined if the stationary point is a maximum, a minimum, or a saddle point (Montgomery 2012).

# Chapter 3

# 3 METHODOLOGY

## 3.1 Chemicals

Solutions for all the experiments were prepared using Millipore water (18MΩ cm). Triclosan (>99%), from Sigma Aldrich (St 13Louis, MO, USA), benzophenone 3 (>98%) from Alfa Aesar, and benzophenone 1 (>99%) from Alfa Aesar were used in liquid chromatography and in ultrasonic degradation experiments.

For Liquid chromatography HPLC grade acetonitrile was obtained from Fisher Chemicals (NJ, USA); methanol HPLC grade (>99.98%), J.T. Baker was obtained from Avantor Performance Materials, Inc. (Center valley, PA, USA).

For solid phase extraction, dichloromethane for analysis EMSURE (>99.8%) from Merck KGaA (Darmstadt, Germany), methanol Baker analyzed LC-MS reagent (99.9%) from Avantor (PA, US), and Nitrogen 5.0 (>99.9999%) from Linde were used. Strata Phenyl (200 mg/3 mL), Strata-X-C (200 mg/3 mL) and Agilent PS DVB (500 mg/6 mL) cartridges were used for extraction.

The pH was adjusted, with 1.0 M NaOH from Sigma Aldrich (St Louis, MO, USA). Iron(II) Sulphate heptahydrate (>99%) from Sigma Aldrich (Germany) was used as catalyst, hydrogen peroxide, 35% w/w aq. soln., stab from Alfa Aesar, and Sodium tiosulphate pentahydrate for analysis (>99.5%) from Merck (Darmstad, Germany) was used for quenching in Fenton reactions.

As radical scavengers methanol, pure ethyl alcohol HPLC/spectrophotometric grade from Sigma Aldrich (St Louis, MO, USA), 2-propanol USP grade from Panreac (99.5%) (Barcelona, Spain), and sodium acetate anhydrous (>99%) from Carlo Erba (Cornaredo, Italy) were used.

For ecotoxicity assays Microtox Acute reagent, reconstitution solution, diluent and adjusting osmotic solution, from Modern Water (New Castle, DE, USA) were used.

He 5.0 (>99.9999%) from Linde was used for GC-MS.

## 3.2 Experimental Set ups

### 3.2.1 Probe Tip Ultrasound Reactor

An Ultrasonic VCX-500 (Sonics and Materials, USA) with probe tip system (Figure 1. Scheme of Probe Tip ReactorFigure 1 and Figure 2) was used as an US low frequency (40 kHz) generator for kinetic analysis for Triclosan degradation. A solid probe (tip diameter: 13 mm, length: 136 mm, material: titanium alloy) was used to generate ultrasonic waves. The probe was immersed in the reaction solution, leaving a distance of 4 cm from the reactor bottom. Solution temperature was maintained at 25±2$^{o}$C using a water cooling bath. Ultrasonic energy density calculated by the calorimetric method was 76W/L (amplitude: 40%). A volume of 250 mL of reaction solution was used in every experiment and samples of 1.5 mL were withdrawn at different time intervals for TCS analysis.

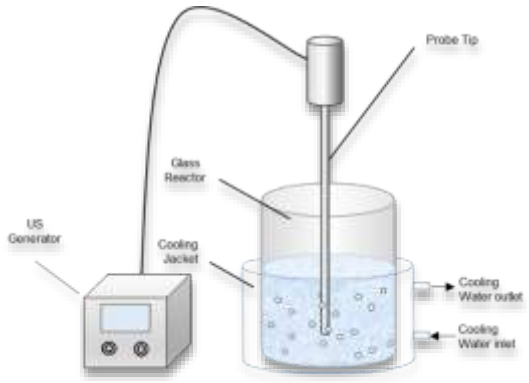


*Figure 1. Scheme of Probe Tip Reactor*

*Figure 2. Probe Tip Reactor*

### 3.2.2 Bath Multifrequency Ultrasound Reactor

A Meinhardt Ultrasonics with a Power multifrequency Generator MG was used (Figure 3, Figure 4 and Figure 5). This generator has a digital display where the following operational parameters can be changed: Power amplitude from 0 to 100%, frequency according to the values for each transducer, and mode as pulsed or continuous. For pulsed mode silent time and pulse time can be changed from 1 to 10000 ms continuously. And it has a timer for establishing the total time for operation after which the generator turns off (Figure 3)

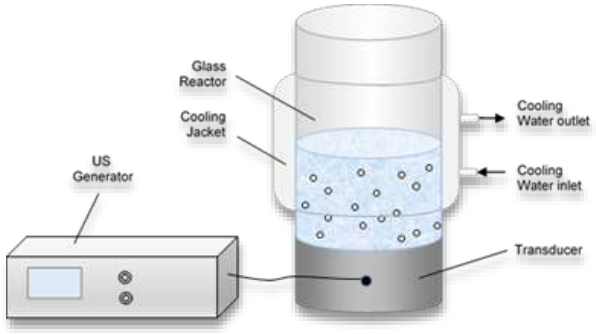


*Figure 3. Scheme of the Bath Multifrequency US Reactor*


*Figure 4. Multifrequency Ultrasound Generator*


*Figure 5. Multifrequency Ultrasound Generator Display*

Two transducers were used to generate ultrasonic wave: One for frequencies: 215 and 373 kHz and another one for frequencies: 574, 856 and 1134 kHz. A cylindrical glass reactor with a capacity of 500 mL coupled to the transducer was used for the reactions. Solution temperature was kept at 25±2°C using cooling water flowing through the reactor jacket (Figure 6).


*Figure 6. Glass reactor with Cooling Jacket*

Ultrasonic energy density for this reactor calculated by the calorimetric method (Kimura et al. 1996), is shown in Figure 7. Reactor was half filled using a solution volume of 300 mL for each experiment. Different sample volumes were withdrawn at different time intervals depending on the variable to be measured.

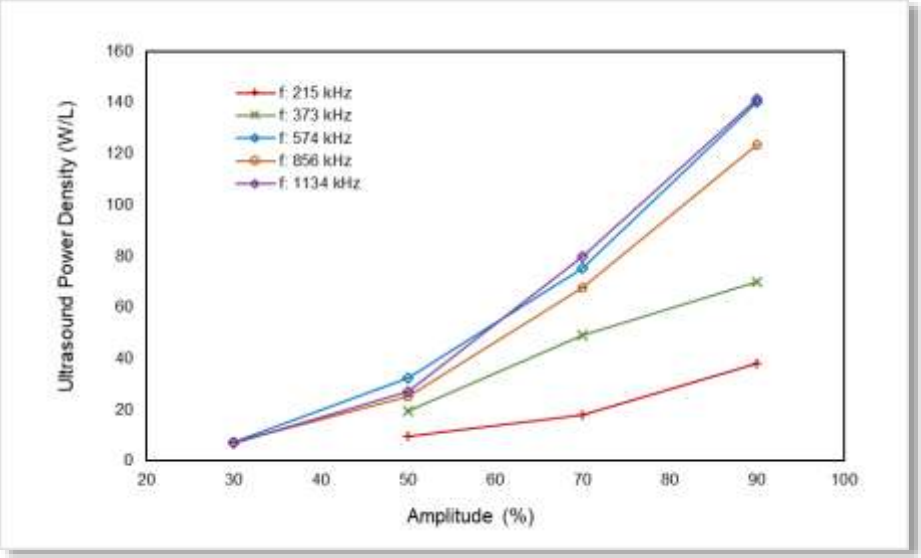


*Figure 7. Ultrasonic energy density for Multifrequency reactor*

### 3.2.3 Bath Low Frequency Ultrasound Reactor

A Meinhardt Ultrasonics with a Power Generator for low frequency (40 kHz) ultrasound was used (Figure 8). Transducer and reactor setup are the same as the bath multifrequency reactor (Figure 6), just changing the transducer for the one for 40 kHz. This generator has an amplitude adjustment knob for changing power amplitude with the following positions: 0.2, 0.4, 0.6, 0.8 and 1.0. This indicates the percentage of the total power amplitude. One transducer was used to generate ultrasonic waves at 40 kHz. A cylindrical glass reactor with a capacity of 500 mL coupled to the transducer was used for the reactions. Solution temperature was kept at 25±2$^{o}$C using a water cooling flowing through the reactor jacket. Ultrasonic energy density calculated by the calorimetric method was 36.9 W/L (amplitude: 50%). The reactor was half filled using a solution volume of 300 mL for each experiment. Sample volumes were withdrawn at different time intervals for the analysis to be made.

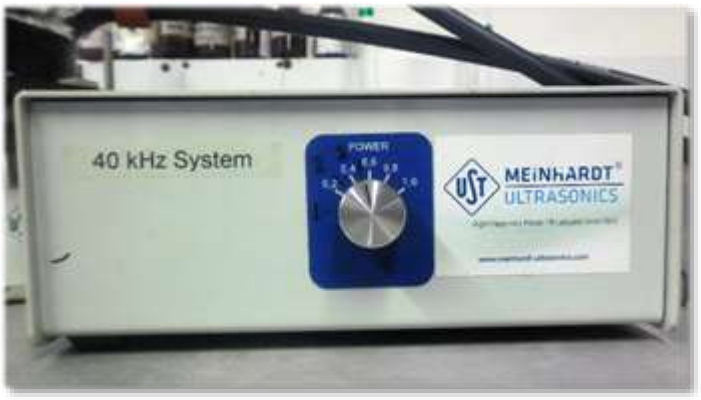


*Figure 8. US Generator for 40 kHz*

### 3.2.4 Fenton/Ultrasound/UV Reactor

The Meinhardt Ultrasonics with a Power multifrequency Generator MG with the transducer for frequency at 574 kHz, was used for UV/US/$H_2O_2$ reactions. A cylindrical glass reactor with a capacity of 500 mL coupled to the transducers was used for the reactions. A flat blade agitator was used for keeping the solution mixed throughout the experiments. A mercury lamp, reference OSRAM Germicidal Puritec HNS G5 6W, was used for generating UV radiation. Wave length was 254 nm. The lamp was located inside the reactor, inside a quartz tube, as shown in Figure 9. Solution temperature was kept at 25±2$^{o}$C using a water cooling flowing through the reactor jacket. Ultrasonic energy density calculated by the calorimetric method was 36.9 W/L (amplitude: 50%) for low frequency generator and 30 W/L for high frequency generator. For UV reactions, the lamp was turned on at time 0. The reactor was covered with an aluminum foil to avoid radiation loses. The reactor was half filled using a solution volume of 300 mL for each experiment. Sample volumes were withdrawn at different time intervals for the analysis to be made. Reactions were stopped using sodium thiosulfate solution.

*Figure 9. Fenton/Ultrasound/UV reactor Setup*

## 3.1 Chemical and Biological Analysis

### 3.1.1 HPLC Analysis

***Triclosan***

TCS concentration for kinetic analysis in the probe type reactor was determined by reverse phase chromatography using a Thermo Scientific Dionex UltiMate 3000 Series HPLC system (Figure 10), with auto sampler, an Acclaim 120 C18 column (silica with a 120 A$^{o}$ pore diameter, 5 µm, 4.6 x 250 mm) and a Diode Array Detector set at 254 nm. The mobile phase was a mixture of acetonitrile and mili Q water (70:30, v/v); flow rate was 1.0 mL/min, injection volume was 80µL and column temperature was 40$^{o}$C. This analytical procedure showed good linearity in the range of 0.1 to 10ppm ($R^2$=0.9997). For other experiments, TCS concentration was determined using Agilent 1200 Series HPLC system with auto sampler, a Zorbax SB-C18 column (porous silica with 80 A$^{o}$ pore diameter, 3.5 µm, 4.6 x 150 mm), and a Diode Array Detector set to 205 nm. The mobile phase was a mixture of acetonitrile/mili Q water (55:45, v/v), flow rate was 1.2 mL/min, injection volume was 80µL, and column temperature was 30$^{o}$C. This analytical procedure showed good linearity in the range of 0.02 to 2 ppm ($R^2$=0.999). The detection limit was 0.0028

ppm, and quantification limit was 0.009 ppm. Repeatability was 1.6% for the measurement range.

*Figure 10. HPLC*

***Benzophenone-3***

BP-3 concentration in water was determined for all the experiments by reverse phase chromatography using an Agilent 1200 Series HPLC system with auto sampler, a Zorbax SB-C18 column (porous silica with 80 $A^o$ pore diameter, 3.5 µm, 4.6 x 150 mm), and a Diode Array Detector set at 288 nm. The mobile phase was a mixture of acetonitrile and mili Q water (70:30, v/v), flow rate was 0.8 mL/min, injection volume was 100µL and column temperature was 30$^o$C. This analytical procedure showed good linearity in the range of 0.02 to 2 ppm ($R^2$=0.9999). The detection limit was 0.0015 ppm, and quantification limit was 0.005 ppm. Repeatability was 1.3 % for the measurement range.

***Benzophenone-1***

BP-1 concentration was determined by reverse phase chromatography using an Agilent 1200 Series HPLC system with auto sampler, a Kinetex column C8 phase (core-shell silica with 100 $A^o$ pore diameter, 2.6 µm, 4.6 x 150 mm), and a Diode Array Detector set at 288 nm. The mobile phase was a mixture of methanol and mili Q water (60:40 v/v), flow rate was 0.5 mL/min, injection volume was 80µL and column temperature was 30$^o$C. This analytical procedure showed good linearity in the range of 0.02 to 2 ppm ($R^2$=1). The detection limit was 0.0019 ppm, and

quantification limit was 0.006 ppm. Repeatability was 1.7 % for the measurement range.

### 3.1.2 TOC Analysis

For this study, a TOC analyzer Apollo 9000 was used, with autosampler STS 8000 (Figure 11). High temperature combustion method was used according to Standard Methods 5310B. Samples are homogenized and diluted if necessary, and a portion is injected in the reaction chamber. This chamber is filled with an oxidant catalyzer as cobalt oxide. Water is vaporized and organic carbon is oxidized to $CO_2$ and $H_2O$ at 680°C. $CO_2$ is passed through a nondispersive infrared (NDIR) detector which generates a non-linear signal that is proportional to the instantaneous concentration of $CO_2$ in the carrier gas. Inorganic carbon is converted in $CO_2$ by acidifying and sparge of the sample previous to injection. And to avoid the corrosives scrubber removes halogens from the carbon dioxide before it enters the detector. The corrosives scrubber is a glass tube filled with Pyrex wool and tin and copper granules (Teledyne Tekmar Co 2003). This analytical procedure showed good linearity in the range of 0.2 to 20 ppm of C ($R^2$=0.99). The detection limit was 0.5 ppm.

*Figure 11. TOC Analyzer*

### 3.1.3 GC-MS Analysis

Analytes from degraded solutions were extracted by SPE as described in section 3.4.3. Subsequently, extracted samples were analyzed in a gas chromatograph Agilent 7890A coupled to a mass spectrometer Agilent 5975C (Figure 12). This has a programmed temperature Vaporizing Multi Mode Inlet (MMI), in mode pulsed Splitless. An Agilent 19091S-433UI HP-5ms Ultra Inert 30 m x 250 µm x 0.25 µm column was used for compounds separation. Oven temperature was set at 50 °C for 3 min, and then it was rated at 10 °C/min to 310 °C, and held for 5 minutes. Injector temperature was set at 150 °C for 0.1 min, rated at 600 °C/min to 325 °C, held by 5 min, then rated 5 °C/min to 290°C and held for 10 minutes. Interphase temperature was 250 °C. Mass spectrum was obtained by electronic impact at 70 eV using full scan mode. Injection volume was 5 µL. Masshunter software was used for quantification, detection and identification of degradation byproducts using NIST 14 Mass Spectral Library.

*Figure 12. GC - MS Spectrometer*

### 3.1.4 Toxicity Analysis

A Microtox Model 500 Analyzer was used for measuring toxicity. Reduction in the bioluminescence of marine bacteria Vibrio Fischeri, when exposed to the pollutants, was measured. This assay is widely used because of its high sensitivity, reproducibility, easy application to organic and inorganic pollutants, and because it is internationally standardized (La Farre et al. 2001)

In this test, a solution of known concentration is mixed with the bacteria in suspension. Luminescence is measured in this solution and in a saline control solution, detecting the bioluminescence inhibition, defined as in (La Farre et al. 2001).

$$\% I = \left[1 - \left(\frac{Dilution\ light}{Control\ light}\right)\right] * 100 \quad (43)$$

Where dilution light is the measured luminescence for the diluted sample, and Control light is the luminescence for the control solution.

With the system Microtox® Model 500 Analyzer (Figure 13) this inhibition is measured in experiments made by duplicate, at a temperature of 15ºC, generally after 5 or 15 minutes of bacteria exposure to the solution. Software for Microtox ®, collects necessary data for calculating $EC_{50}$; that is, the pollutant concentration reducing 50 % of the initial luminescence. This software generates a graph of concentration vs effect %, and estimates the concentration corresponding to the 50 % of effect. The software uses the equation that best fits the data ($R^2$>0.95)

*Figure 13. Microtox Analyzer*

81.9 % Basic Test was used for determining this value. It is used for water samples of low toxicity making successive dilutions of the sample, and measuring the luminescence of the reconstituted bacteria in the diluted reagent (without pollutant), and after adding 900 µL of the sample diluted in different percentages, in such a way that the higher percentage measured corresponds to the 81.9% of the initial concentration for the sample.

For measuring toxicity evolution through degradation processes, the 81.9% Screening Test is used. This test is designed for use with samples of low toxicity. It compares the effect % for the diluted reagent or saline control with the sample from the reaction at time t, in a dilution of 81.9 %. A control sample is used in which only diluent is used. Results are presented as $TOX/TOX_0$, indicating the ratio between the inhibition % at time t, and at time 0.

Vibrio Fischeri bacteria must be kept frozen before the assays. For toxicity analysis, the vial containing the lyophilized bacteria must be retired from the freezer, and agitated for settling bacteria at the bottom. The reconstitution solution is then added to the vial, which is mixed thoroughly, dispensing by a pipette at least 10 times. This reconstituted bacteria must be used within 3 hours after reconstitution.

### 3.1.5 Solid Phase Extraction Procedures

The concentration of reaction byproducts in treated samples are very low. That is why pre-concentration techniques are needed. Solid Phase Extraction is a good technique for purifying and concentrating without contaminating the samples (Figure 14) (Martinez and Peñuela 2012).

Three SPE columns were used: Strata Phenyl (55 µm, 70 A, 200mg/3mL), Strata X-C (33 µm, 200 mg/3 mL) and PS DVB (500mg/6 mL). Conditioning of the columns was made by filling the columns with methanol twice, followed by one time with mili Q water. Then, 100-200 mL of reaction solution was passed through the columns at a rate of 5 mL/min. After that, analytes were eluted with a mix of 6 mL of dichloromethane-methanol (80/20), and the resulting extract was dried with nitrogen to a volume of 700 µL. The extract was washed from the walls of the recipient with pure methanol and transferred in a total volume of 1 mL to vials for being analyzed by GC-MS.

*Figure 14. Solid Phase Extraction Setup*

# Chapter 4

# 4 SONOCHEMICAL DEGRADATION OF TRICLOSAN IN WATER IN A MULTIFREQUENCY REACTOR

## 4.1 Abstract

Degradation of triclosan (TCS) by multifrequency ultrasound (US) was studied at high and low frequencies. Frequency effect on initial degradation rates was analyzed and an optimum frequency was found. Power density always has a positive effect on degradation rates over the whole equipment work range. A reaction mechanism similar to that proposed by Serpone resulted in a pseudo-linear model that fitted statistically better than the nonlinear model proposed by Okitsu. Pulsed US showed a positive effect on degradation rates; however, simultaneous analysis of the effect of power, frequency, pulse time, and silent time did not show a clear trend for degradation as a function of pulse US variables. According to these results and those for degradation in the presence of radical scavengers, it was concluded that US TCS degradation was taking place in the bubble/liquid interface. A toxicity test was conducted by Microtox®, showing a decrease in toxicity as TCS concentration decreased; and increase in toxicity after total depletion of TCS. Eight possible degradation byproducts were identified by GC-MS analysis, and a degradation pathway was proposed.

## 4.2 Introduction

Triclosan (5-chloro-2-{2,4-dichlorophenoxy}phenol) is commonly used as an antiseptic agent in personal care and consumer products (Petrovic 2003). Detection frequency of TCS has been as high as 57.6% in the United States surface waters where it had an average concentration of 0.14µg/L between 1999 and 2000 (Kolpin et al. 2002). In spite of TCS being a non-persistent chemical and not being toxic for humans and some mammals, it has negative effects on aquatic ecosystems, such as changes in capacity of nutrient assimilation and in the structure of the food chain in water bodies (Sabaliunas et al. 2003). But, the most important aspect in environmental pollution caused by TCS is the generation of toxic compounds such as clorodioxins, chlorinated phenols, polychlorinated biphenyl ethers, dihydroxy derivatives and bioaccumulative species such as polychlorinated dibenzodioxins and methyltriclosan (Rule, Ebbett, and Vikesland 2005; Sirés et al. 2007; Wu et al. 2012; Song et al. 2012; Munoz et al. 2012).

A number of reports about TCS degradation by common oxidation processes have been published. These methods include chlorination (Rule et al. 2005) and oxidation with permanganate (Wu et al. 2012b). Advanced oxidation processes have also been applied for degradation of TCS. Those include electroFenton (Sirés et al. 2007), Fenton like (Munoz et al. 2012; Song et al. 2012), and photocatalytic processes (Son et al. 2009; Stamatis et al. 2014).

Sonochemical degradation is an advanced oxidation process extensively studied for removal of recalcitrant organic pollutants at low concentrations (Son, Ko, and Zoh 2009; Stamatis et al. 2014). Sonochemical degradation is caused by acoustic cavitation, that is, the creation, expansion, and implosive collapse of gas bubbles in liquids irradiated by US waves (Apfel 1981). Thermal decomposition of water in the compression of oscillating bubbles produces mainly hydroxyl free radicals (Henglein 1987). These radicals react with hydrogen molecules, oxygen peroxide, pollutants, or they can recombine forming hydrogen peroxide, mainly in the bubble interface (Henglein 1987). Solute degradation processes can take place in different sites; inside collapsing bubbles, in the bubble/liquid interface, and in bulk solution (Okitsu et al. 2006).

Ultrasound has the advantage over other advanced oxidation processes in that it can be used in very complex matrices. It does not need visible light radiation, does not use additional reactants, does not need to change solution pH, does not generate sludge, and does not require catalysts. However, it is a high cost process due to the high amount of energy needed for operation (Mahamuni and Adewuyi 2010). Understanding of the mechanism of the reaction and the effect of ultrasound system is useful in the search for process optimization. Many variables such as US power, frequency, reactor geometry, mode of US (pulsed or continuous), pH, among others influence the extent of a pollutant degradation by US. Two studies have reported on low frequency sonochemical degradation of TCS exploring the extent, rate of degradation, general rate values (Naddeo et al. 2013) and the effect of solution matrix on the rate of degradation (Sanchez-Prado et al. 2008). However, these studies besides being made at low-medium frequencies (20 and 80 kHz) (Pétrier 2015b) did not analyze the effect of variables such as frequency, US mode, pH and radical scavengers, the same as toxicity evolution and generated byproducts. Those variables are analyzed in this study looking for a broader understanding of this process. Some interesting effects such as the use of dual frequencies for further augmentation of ultrasound intensity (Khanna et al. 2013), and of solution toxicity after TCS depletion should be considered for future studies.

## 4.3 Results and Discussion

### 4.3.1 Effect of Frequency

Ultrasound frequency is an important variable that influences the kind of processes occurring in solution. At low frequencies, physical effects predominate and the number of cavitation events are less than those at higher frequencies (Thangavadivel et al. 2012). Also, higher bubble volumes make leads to higher vapor content in collapsing bubbles. This effect generates less energetic implosion of bubbles resulting in lower OH radical generation. On the other hand, at high frequencies, bubble lives and sizes are smaller, resulting in a lower vapor content at the collapse moment, generating more energetic bubbles implosion. It has been shown that optimal frequency is mainly a function of properties of the substance (Adewuyi and Oyenekan 2007). For analyzing this effect on US degradation of TCS, experiments at the same power density were conducted, and degradation pattern was established for different frequencies. In Figure 15, TCS degradation profiles for frequencies from 215 kHz to 1134 kHz at power density of 40 W/L is shown. In Figure 16, profiles are shown for 574, 856 and 1134 kHz and a power density of 140 W/L.

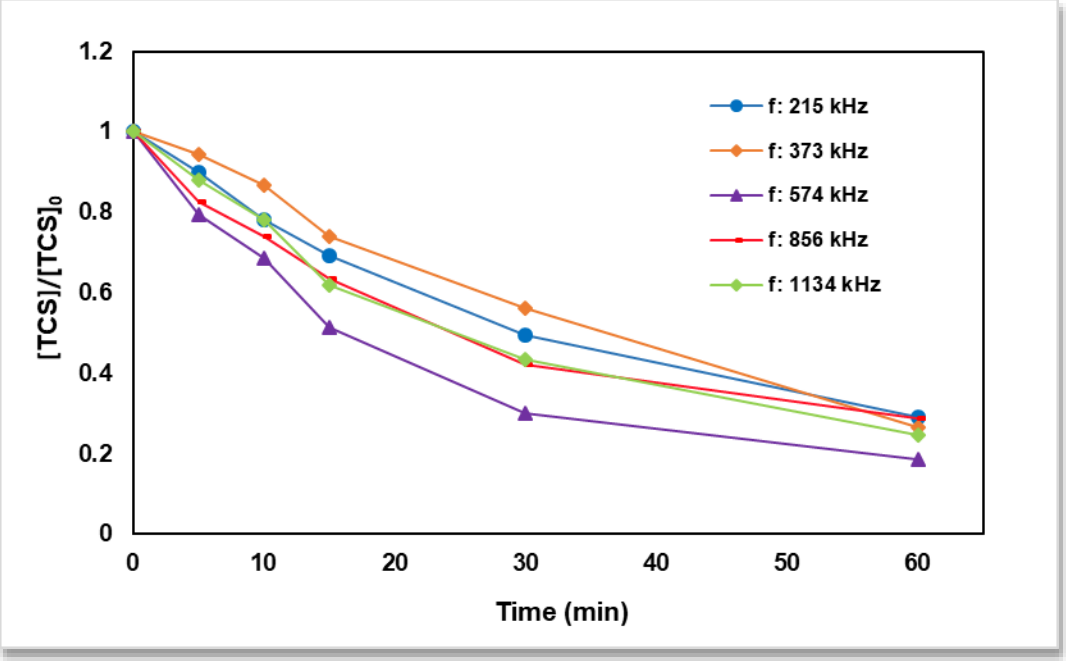


*Figure 15. Effect of frequency on TCS degradation. Power density: 40W/L, Solution volume: 300 mL, initial TCS concentration: 1 mg/L, T: 25°C±2°C*

For both power density levels, the frequency of 574 kHz had the highest degradation rates. At 40 W/L, 88% of TCS was degraded in 60 minutes, while at 140 W/L TCS

was completely degraded in less than 25 minutes. This time is equal to or less than 20% of those found in previous studies for US degradation of TCS. (Sanchez-Prado et al. 2008) used 80 kHz US, nominal power= 135 W, ($C_0$=5µg/L) obtaining almost 100% TCS degradation in 120 minutes. Conversely, (Naddeo et al. 2013) used 45 kHz US, power density=100W/L, ($C_0$=1 µg/L) and obtained 95% TCS degradation at 180 minutes, in a mixture of 23 contaminants. At higher frequencies of 856 and 1134 kHz, shorter rarefaction cycles generate molecules that could not be sufficiently stretched to generate the bubble. Also overall bubble surfaces are smaller, and mass transfer of the pollutants towards the bubble surface dominate the overall rate, resulting in lower degradation rates.

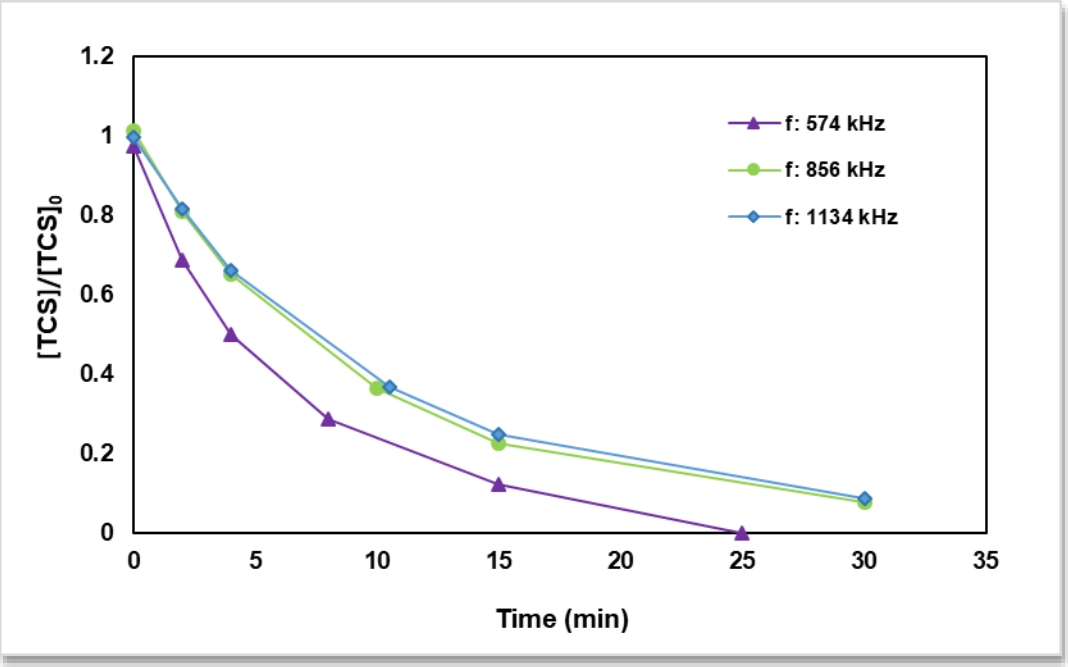


*Figure 16. Effect of frequency on TCS degradation. Power density: 140W/L, Solution volume: 300 mL, initial TCS concentration: 1 mg/L, T: 25°C±2°C*

### 4.3.2 Effect of Power Density

Power density has an important impact on ultrasound degradation rates. As power density of US radiation increases, acoustic amplitude increases generating more violent collapse of the bubbles (Adewuyi and Oyenekan 2007). It has been widely demonstrated that power density has an optimum value in which maximum pressure and temperature during collapse generates an optimal degradation rate. This occurs because at high densities bubble shielding occurs attenuating the effect of the US radiation. At power intensities higher than the optimum, a dense cloud of

bubbles forms close to the transducer. This cloud prevents the ultrasound waves propagation due to scattering and absorption. Although some studies report that electrical energy loss is higher as power increases due to decoupling effect (van Iersel et al. 2008), at the conditions used in this study (reactor geometry, liquid height, frequency level) this effect is not occurring.

Experiments were conducted at the optimum frequency of 574 kHz varying power densities. Figure 17 shows the profile of concentration with reaction time.

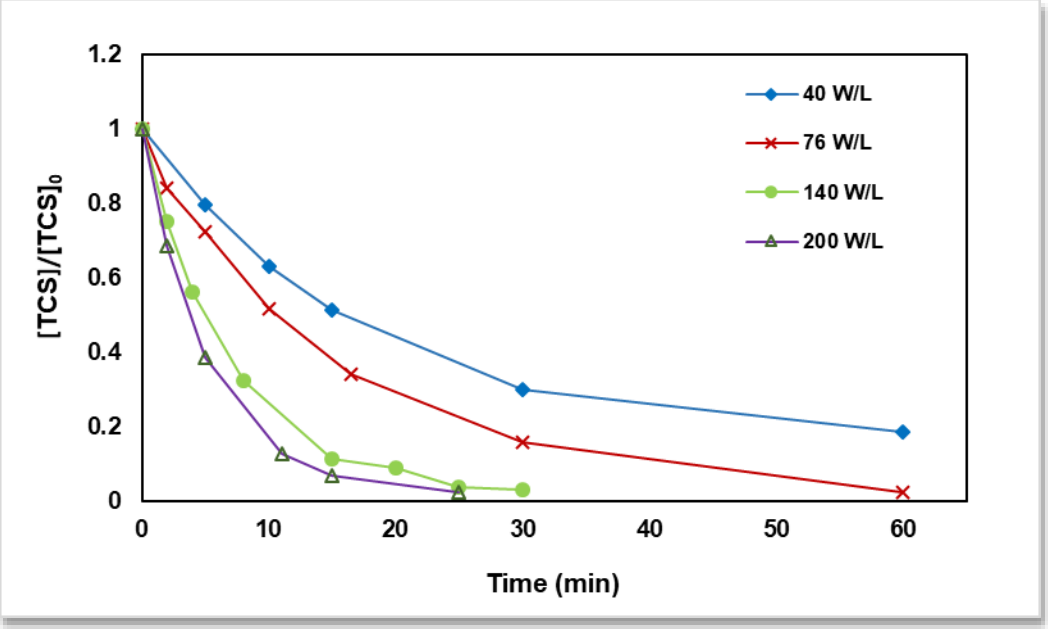


*Figure 17. Effect of power density on TCS degradation. Frequency: 574 kHz, Solution volume: 300 mL, initial concentration: 1 mg/L, T: 25°C±2°C*

As can be seen in this figure, for this reactor and under the conditions mentioned, the highest TCS degradation rate was obtained at the highest power density level of the equipment, 200 W/L. There was no optimum power value after which degradation rates started to decrease. Although some studies report that electrical energy loss is higher as power increases due to decoupling effect (van Iersel et al. 2008), at the conditions (reactor geometry, liquid height, frequency level) this effect is not occurring.

### 4.3.3 Pulsed Ultrasound Effect

Pulsed wave (PW) is US radiation in intermittent pulses of specific duration. Various studies have found that under certain optimal conditions, PW US enhances the

degradation of the compound when a reaction is taking place in the bubble interface. Pulsed wave US allows time for diffusion of the molecules to the interface, where the reaction is taking place (Xiao et al. 2013c). Xiao et al. (2014) showed that in PW mode US, small sized and highly diffusing molecules diffuse more quickly to the cavitation bubbles, contrary to the effect for large molecules. This effect is more important for small compounds with molar volumes less than 130 ml/mol that can diffuse more readily to bubble interface. The authors also concluded PW enhancement is higher for compounds with high diffusivity and high octanol/water partition coefficient ($K_{ow}$). TCS is expected to degrade at bubble surface, because of its hydrophobic and nonvolatile character (Log $K_{ow}$=4.76, $K_H$ = 4.99 *10 $^{-9}$ Atm-$m^3$/mol). Thus, a PW mode US enhancement was expected for its US degradation.

In Figure 18, results are shown for Pulse Enhancement (PE*). PE is defined as:

$$PE^*(\%) = \frac{(Deg)_{PW} - (Deg)_{CW}}{(Deg)_{CW}} \times 100\% \quad (44)$$

Where $(Deg)_{PW}$ is degradation percent for PW mode US, and $(Deg)_{CW}$ is degradation percent for CW mode US, after 10 minutes of sonication, and for the corresponding frequency and power density levels. Total reaction time for PW mode US was calculated according to the following equation (Yang et al. 2005):

$$t_{total} = t_{sonication}\left(1 + \frac{ST}{PT}\right) \quad (45)$$

Where $t_{total}$ is the total reaction time; $t_{sonication}$ is the real sonication time (10 minutes); $ST$ is the time between pulses (Silent Time); and $PT$ is the Pulse Time. For this equipment $ST$ and $PT$ could be varied in a range from 0 to 10000 ms continuously. Pulse time and silent times of 10 and 50 ms were used.

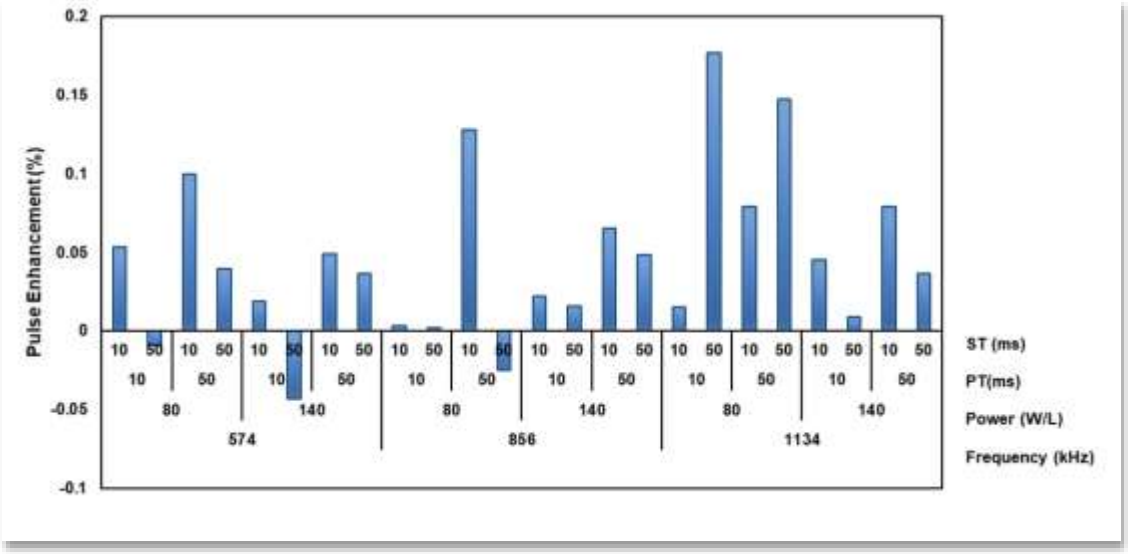


*Figure 18. Pulse Enhancement for PW mode US. Reaction Vol: 300 mL, T: 25°C±2°C*

From this set of experiments, an experimental design $2^3$ with four central points was devised along with an ANOVA analysis. This showed the only variable that had a statistical significance and effect over degradation after 10 minutes of degradation was the power density. That is, there was not a clear trend for degradation percent as a response to variations in PT, ST, or PT/ST. However, from Figure 18 it could be seen that PW enhancement was positive in almost all the experiments, and its values were higher for the low power density level used (80 W/L). Figure 19 shows the degradation profiles for continuous and PW mode US. It shows that degradation is slightly faster for PW mode US. In order to compare the initial degradation rates for the reaction using pulsed wave ultrasound with those using continuous wave ultrasound, an ANOVA analysis was conducted. Models without the effect of pulsed wave mode, and those taking into account the effect of the pulsed ultrasound mode as a dummy variable were compared. Because of the low Pr value for the F statistic in the ANOVA analysis, it was concluded that pulsed wave mode has a positive effect on the initial degradation rate of triclosan. Initial reaction rates for PW US were 15.3 % higher for the batch reactor, 574 kHz, initial concentration: 1 mg/L and power density 140W/L. For the probe type reactor at a lower frequency (20 kHz), initial concentration 1.9 mg/L, power density 76W/L, and volume 250 mL, initial reaction rate was 17% higher for PW US.

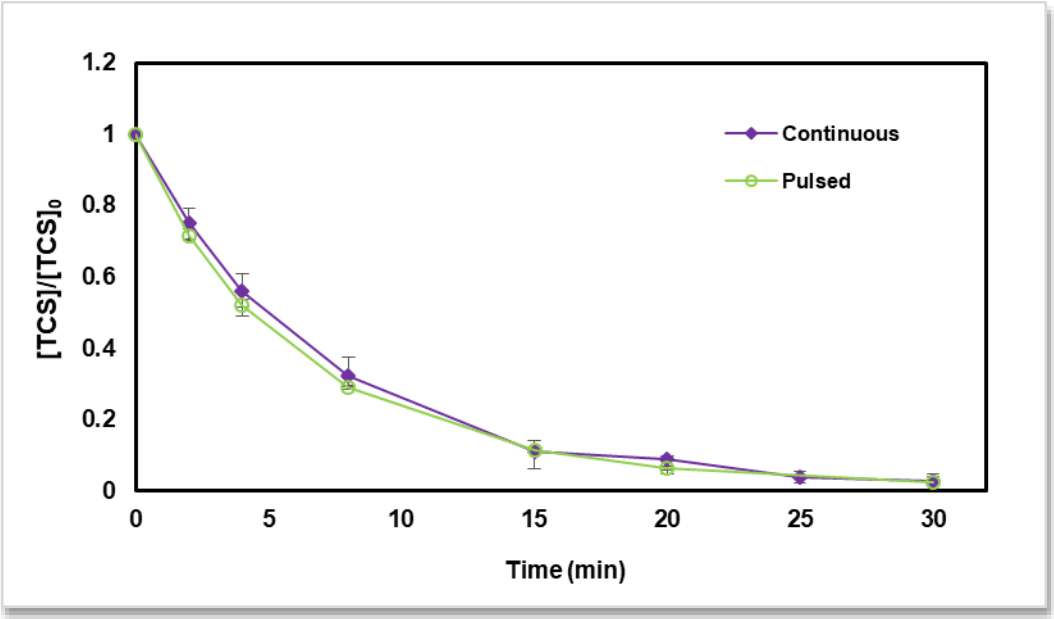


*Figure 19. TCS degradation profiles for continuous and PW mode US. Frequency: 574 kHz, power density: 140 W/L, initial TCS concentration: 1 mg/L, solution volume: 300 mL, T: 25°C±2°C*

Higher initial reaction rates for PW US mode for low and high frequencies and for different reactor types confirm TCS is degraded at the interfacial region. For periods without US radiation, TCS molecules diffuse from the bulk solution to the bubble interface. However, enhancement was not high because of TCS molar volume (194.3 mL/mol) and diffusivity ($5{,}9*10^{-6}$) as calculated according to (Hayduk and Laudie 2015). In general, pulse enhancement is higher for low molar volumes (<130 ml/mol) and high diffusivity molecules. This is because in the silent times for pulsed ultrasound, small molecules diffuse faster towards the molecule surface, being more available to react with OH radicals in this site. (Xiao et al. 2013c).

### 4.3.4 Effect of Radical Scavengers

Recent studies recognize that sonochemical decomposition of organic compounds in water can proceed in three regions (Okitsu et al. 2005): Inside bubbles; At the interface between the cavitation bubbles and the bulk solution; and in the bulk solution

In regions 1 and 2 mainly pyrolysis and radical reactions occur, and in region 3, reactions with OH radicals are the most prevalent.

Xiao et al. (2013) studied the ability of various radical scavengers to interact with cavitation bubbles reporting that acetic acid/acetate appears to scavenge OH free radicals only in the solution, without any interaction with the bubble interface. Other

studies have found some alcohols such as tertbutanol, ethanol, methanol, isopropyl alcohol (Ince et al. 2009)(Serna-Galvis et al. 2015)(Zúñiga-Benítez et al. 2016) (Latch et al. 2005a; De Bel et al. 2011) scavenge OH radicals in the bubble surface and bulk solution. Since TCS is not a volatile compound and is hydrophobic (Log $K_{ow}$ = 4.76), it is expected that it tends to accumulate mostly in the interface region of the cavitation bubbles.

Experiments were made using methanol, ethanol and 2-propanol as radical scavengers using a radical scavenger: TCS molar ratio of 500:1. The resulting degradation profiles are shown in Figure 20.

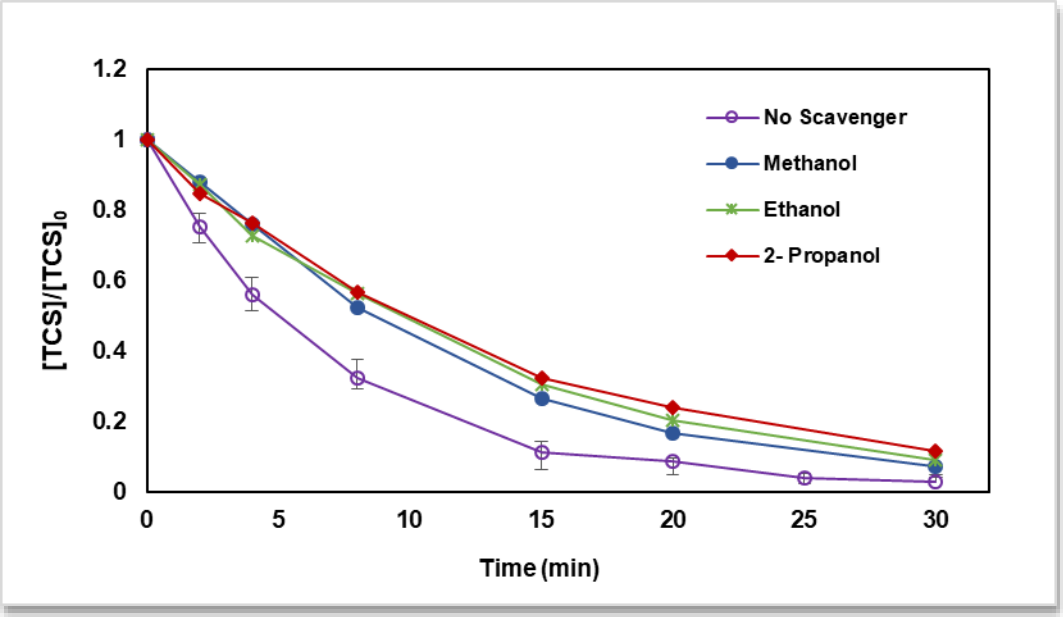


*Figure 20. Effect of radical scavengers ethanol, methanol and 2-propanol in TCS degradation by US in bath reactor. Frequency: 574 kHz, power density: 140 W/L, initial TCS concentration: 1 mg/L, solution volume: 300 mL, T: 25°C±2°C*

Comparing the initial TCS degradation rates for US degradation at 574 kHz, with scavenger, inhibition was 51.4% for methanol, 47.4% for ethanol, and 42.0% for 2-propanol. Henry's law constant for TCS ($K_{H\text{-}TCS}$ is 4.99 *10 $^{-9}$ atm-m$^3$/mol) is much lower than those for radical scavengers used ($K_{H\text{-}Methanol}$ is 4.55 *10$^{-6}$ atm-m$^3$/mol , $K_{H\text{-}ethanol}$ is 5 *10$^{-6}$ atm-m$^3$/mol, and $K_{H\text{-}propanol}$ is 7.5 *10$^{-6}$ atm-m$^3$/mol). Thus, TCS degradation inhibition in the presence of the scavengers is explained by the scavenger's accumulation at bubble interface due to their higher volatility. This generates higher reaction rates of scavengers with OH radicals than those of TCS.

### 4.3.5 Kinetics of Sonochemical Degradation

US degradation reactions are modeled usually as a pseudo first order kinetics expression. However Okitsu et al. (2006), proposed a non-heterogeneous kinetic model similar to a Langmuir–Hinshelwood or Eley–Rideal mechanism occurring in the bubble-solution interface. This model is based on the assumption that before collapsing of the bubble a pseudo-equilibrium of adsorption and desorption of pollutant at the gas/liquid interface exists. This results in the general model:

$$r = k_{TCS}\theta = \frac{k_{TCS}K_{TCS}[TCS]}{1 + K_{TCS}[TCS]} \quad (46)$$

Where $K_{TCS} = {}^{k_{a1}}/_{k_{a-1}}$, $k_{a1}$ and $k_{a-1}$ are the sorption and desorption rate constants in the bubble surface, and $k$ is the pseudo first order rate constant for the reaction of TCS with OH radicals.

On the other hand, Serpone et al. (1994) proposed a general reaction mechanism for chlorophenol degradation by US where reactions can occur in the bulk solution or in the interface, reaching a general expression similar to that of Okitsu. However, in this model, considering that the reaction is taking place in the bubble interface, where OH concentration is high and pollutant concentration is low, the rate expression becomes of first order in the concentration of TCS. Details of these models are provided in Section 2.1.3.

$$\left(\frac{d[TCS]}{dt}\right) = k_{b-TCS}[TCS] \quad (47)$$

Equations (*46*) and (*47*) were evaluated to determine the goodness of fit of the experimental data to the expressions. Several experiments were conducted measuring initial TCS degradation rates for various TCS initial concentrations. Two different conditions were used for this purpose: One, using the probe tip reactor for low frequency: 20 kHz, power density: 76W/L, pH: 6.9, volume: 250 mL, temperature: 25±2˚C. The other, with the ultrasonic bath with planar transducer, high frequencies: 574 kHz, power density: 140W/L, pH: 6.9, volume: 300 mL, temperature: 25±2˚C. Concentrations varied from 1.7 to 11 μM. Data for 25 minutes of reaction for probe tip reactor, and two minutes of reaction for reactor with planar transducer was used. In this time, less than 20% of TCS degradation was achieved in both cases. The use of these initial rates avoid the interference of the reaction byproducts.

Nonlinear regression analysis was used for testing the goodness of the fit of the model for equation (*46*) by an algorithm in R Software version 3.1.3 using the instruction nls. This approach generated nonlinear (weighted) least-squares estimates of the parameters. On the other hand, ordinary least squares analysis was used for testing the pseudo first order model (equation (*47*)). Results for regression parameters, t statistic probabilities (p), coefficient of determination ($R^2$), and Sum of Squared errors (SSE) are shown in Table 4 and Table 5 . Experimental values and predicted curves by the two models are shown in Figure 21.

*Table 4. Parameters of the kinetic models for triclosan degradation. Probe Tip reactor*

| **Model** | **Parameters** | **$R^2$** | **SSE** |
|---|---|---|---|
| Equation **(46)** | $k_{TCS}K_{TCS}$: 0.0058181 *(t value:12.786, p= 4.48e-07)* | | |
| | $K_{TCS}$: 0.0026467 *(t value: 0.375, **p= 0.717**)* | | 0.00012399 |
| Equation **(47)** | $k_{b-TCS}$: 0.0054015 *(t value: 18.419, p= 1.87e-08)* | 0.9742 | 0.00011442 |

*Table 5. Parameters of the kinetic models for triclosan degradation. Batch Reactor*

| **Model** | **Parameters** | **$R^2$** | **SSE** |
|---|---|---|---|
| Equation **(46)** | $k_{TCS}K_{TCS}$: 0.132667 *(t value: 14.745, p= 7.44e-12)* | | |
| | $K_{TCS}$: 0.011051 *(t value: 1.354 , **p= 0.192**)* | | 0.06942 |
| Equation **(47)** | $k_{b-TCS}$: 0.110441*(t value: 26.083 p= 2.43e-16)* | 0.9728 | 0.0618 |

According to the squared sum of residues (SSE) with similar values a good fit for both models was achieved. Pseudo first order model (equation (*47*)) had a good correlation coefficient, a good p value for t statistics for equation parameters, and an F-statistic value of 339.3 and 680.3 for the probe tip reactor and bath reactor, respectively. This proves the goodness of fit for this model. However, the model in equation (*46*) gives a low value for the t value of the parameter $K_{TCS}$ in the denominator, for both reactors. There is no statistical evidence for the validity of this parameter, and consequently of this model.

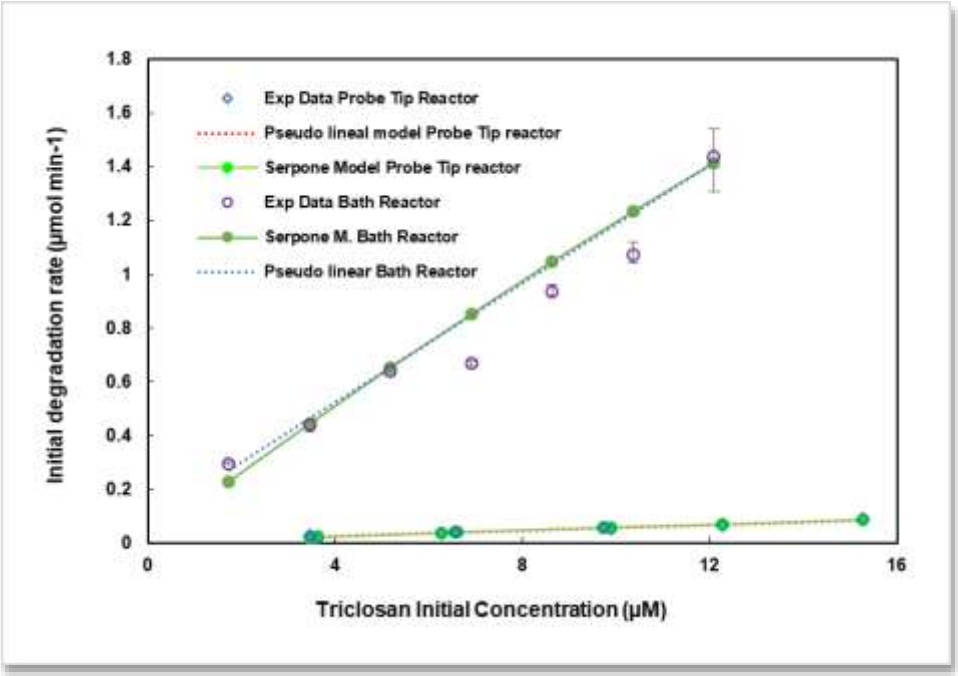


*Figure 21. Initial degradation rate vs TCS initial concentration. Probe tip reactor: Frequency: 20 kHz, power density: 76W/L, pH: 6.9, volume: 250 mL, temperature: 25±2˚C. Bath reactor: Frequency: 574 kHz, power density: 140 W/L, pH: 6.9, volume: 300 mL, temperature: 25±2˚C. Predicted curves for the linear model (dotted line), and the Serpone et al. (1994) model (continuous line)*

Based on this analysis, pseudo first order model better explained TCS degradation for both reactors and at low and high frequencies. Conditions used to obtain equation (*47*) are applicable, and match with the fact that TCS degrades mainly at bubble surface, according to the proposed mechanism by Serpone et al. (1994). Rate constant for the batch reactor was 20.4 times higher than for probe tip reactor. Many variables may explain this, but especially, frequency and power density values, that were higher for the batch reactor can be mentioned. (Sanchez-Prado et al. 2008) found a rate constant of 0.0272 $min^{-1}$ for the linear model for TCS degradation in deionized water, for a frequency of 85kHz and nominal power of 135 W. This value is four times less than that found in this study. In their study, Sanchez-Prado et al. used data for 120 minutes reaction time. The approach used in this study is a more accurate representation of the initial reaction rates.

### 4.3.6 Effect of pH

Depending on its $pK_a$ value, at certain pH levels, a compound can be in its molecular or in its ionic form with different proportions. An ionic form of a compound has

different hydrophobicity than its molecular form and hydrophobic compounds in their molecular form accumulate more readily in the interfacial area than in their ionic form. TCS has a $pK_a$=7.9, and at a pH of 6.9 it is almost completely in its molecular form. At higher pH values TCS is in its deprotonated form and tends to accumulate less in the bubble interface where radical OH concentration is higher. US experiments at pH 10 were conducted to examine the effect of pH on initial rate for TCS degradation. At pH 10 about 99% of TCS is in anionic form, according to the following expression (Chiha et al. 2011):

$$\varphi_{ions} = \frac{1}{1 + 10^{(pK_a - pH)}} \tag{48}$$

Comparing the results for pH 10 with those obtained at natural pH at optimal frequency and high power density level, it can be seen in Figure 22 that there is no difference in degradation rates. At this pH value, TCS is still highly hydrophobic (Log $K_{ow}$ = 3) (Behera et al. 2010). Because of this, reducing TCS hydrophobicity at pH 10 could generate a lower mobility of the molecules towards the bubble surface, but also, in the phenolate form, TCS is more reactive with OH radicals than in the phenolic form, because $O^-$ is better in activating the aromatic ring as has been found in studies of chlorine mediated oxidation (Rule et al. 2005). As can be seen from these experiments, the net effect is null. Therefore there is no reduction in the total degradation rate at higher pH values.

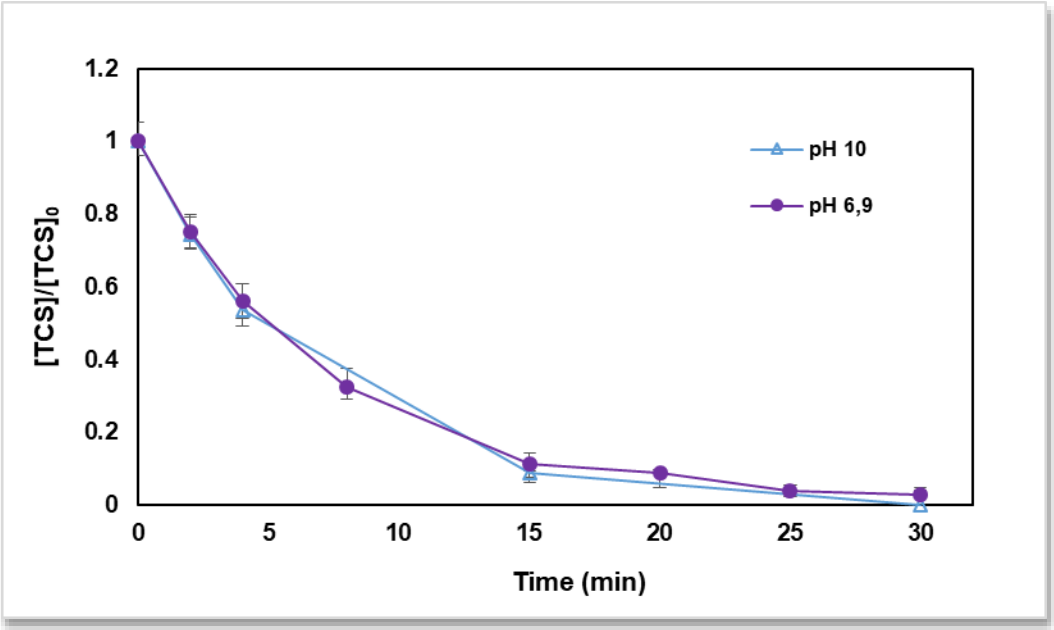


*Figure 22. Effect of pH on TCS degradation by US. Frequency: 574 kHz, power density: 140 W/L, initial TCS concentration: 1 mg/L, solution volume: 300 mL, T: 25°C±2°C*

### 4.3.7 Toxicity

An ecotoxicity assay was conducted using Microtox® equipment that measures the decrease in the natural luminescence of the marine bacteria *Vibrio Fischeri* in the presence of TCS in aqueous solution. Diminishing bioluminescence indicates diminishing cellular respiration. Toxic substances change the percentage of protein and lipid synthesis, thus changing the light emission level. The toxicity is expressed as effective concentration $EC_{50}$: pollutant concentration producing a 50% reduction in light emission (Onorati and Mecozzi 2004).

The 81.9% Basic Test was used as shown in the Guide to Microtox M500 procedure for acute toxicity. Initial TCS concentration was 0.68 mg/L in deionized water and response was measured at 5 and 15 minutes. There was not a significant difference in the response for 15 minutes to that of 5 minutes. $EC_{50}$ was 0.164 mg/L. This result is similar to that obtained by (Farré et al. 2008) who found a $EC_{50}$ value of 0.28 mg/L using Microtox procedure for TCS in concentrations ranging from 0.0375 to 2 mg/L.

Toxicity path as US degradation occurred was measured for a TCS solution with an initial concentration of 0.68 mg/L, treated at 574 kHz and 140 W/L for 90 minutes. 3 mL samples were withdrawn at different times, and analyzed using Microtox by the 81.9% Screening Test. Results are shown in Figure 23.

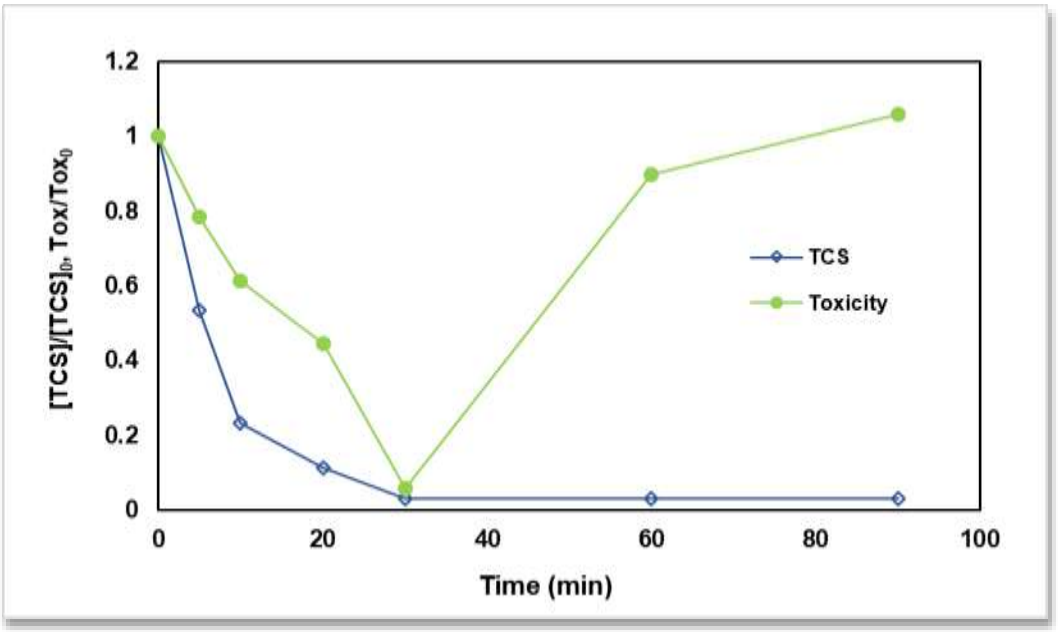


*Figure 23. Toxicity evolution for TCS degradation by US. Initial concentration: 0.68 mg/L, frequency: 574 kHz, power density: 140W/L, volume: 300 mL, T: 25°C±2°C*

Toxicity profile shows that toxicity decreases as TCS concentration decreases, increasing afterwards. (Farré et al. 2008) found that methyl TCS, a possible TCS degradation byproduct had an $EC_{50}$ of 0.21 mg/L (Microtox acute toxicity method), slightly lower than that of TCS. 2,7/2,8-dichlorodibenzo-p-dioxin (2,8-DCDD) has been detected as a TCS degradation byproduct when degraded by photolysis (Zhang et al. 2015)(Son et al. 2009)(Wong-Wah-Chung et al. 2007)(Latch et al. 2005b), $TiO_2$ photocatalysis (Son et al. 2009), and oxidation with ferrate (Yang et al. 2011); however, it has been reported that its acute toxicity is low (Blair 1971). In general, according to other studies on TCS degradation by advanced oxidation processes, remaining TCS has been found as the main responsible for toxicity in treated solutions (Yang et al. 2011). However, no information about byproducts after total TCS depletion was found, and this study focused only on US byproducts until TCS was totally depleted. This is the reason why further study must be done about generated byproducts after triclosan is depleted, in order to understand the cause of this toxic effect. This will help to determine if stopping degradation before total mineralization is the best option for US triclosan degradation.

However, it can be expected that other polychlorinated dibenzo-p-dioxins (PCDDs) and polychlorinated dibenzofurans (PCDFs) are being generated. One of them, the tetrachloro dibenzo-p-dioxin has one of the lowest known LD50 (Hites 2011). Trichloro and tetrachloro phenol, possible TCS degradation byproducts could be transformed in this highly toxic chemical, and other similar.
However, further research is needed to fully understand the reason behind toxicity increase after TCS depletion.

### 4.3.8 Degradation Products

Deionized water spiked at 10 mg/L with TCS was sonicated and aliquots of the solution were taken at 40 and 90% of TCS degradation. Compounds were isolated from the water samples by solid-phase extraction. Separation and detection of degradation products was carried out by gas-chromatography-mass spectrometry. Eight possible compounds were detected, based on the presence of the molecular ion, interpretation of their fragment ions in the mass spectra was conducted using Masshunter Software and NIST 14 Mass Spectral Library.

2,7/2,8-dibenzodichloro-p-dioxin was identified at 40 and 90% of TCS degradation, for the three SPE columns used. This is a very well-known TCS degradation product. It has been reported as produced by the direct effect of UV radiation at basic and neutral pH (Mezcua et al. 2004)(Latch et al. 2005a)(Wong-Wah-Chung et al. 2007)(Lores et al. 2005)(Aranami and Readman 2007), and in municipal wastewater

treatment plants (WWTPs) (Tohidi and Cai 2015). The reaction mechanism that we proposed for its production by ultrasound degradation includes hydrogen abstraction from the phenolic moiety by OH radicals and posterior cyclization (Fig 24). Previous studies of TCS photodegradation have shown that this reaction is caused by the effect of direct UV radiation on TCS and depends on UV wavelength (Aranami and Readman 2007) (Stamatis et al. 2014). However, the results obtained in this study show that this reaction can occur due to the direct attack of OH radicals. The peak area found at 40 and 90% of TCS degradation is very similar, showing that this is a persistent byproduct.

Naphtalene was detected at 40% of TCS degradation with SPE extraction with PS DVB column. This compound has been reported by (Summoogum et al. 2012) in the oxidation of dibenzo-p-dioxin with $O_2/N_2$ mixture at temperatures between 400-800°C. In this case, it is proposed that in US degradation it is produced by the attack of OH radicals over dibenzo-p-dioxin as shown in Figure 24.

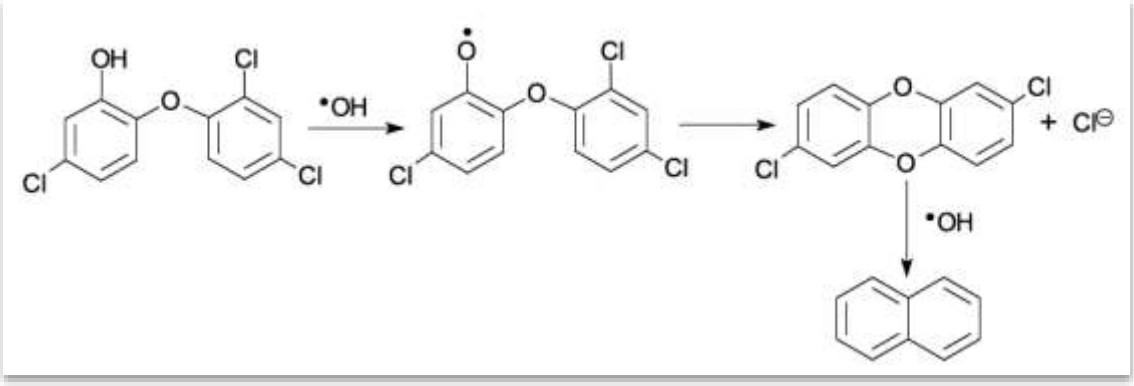


*Figure 24. Reaction mechanism for dibenzodichloro-p-dioxin formation*

2,4 dichlorophenol was also identified at both reaction times, for the three SPE columns. This compound has been previously reported as a TCS photolysis (Latch et al. 2003) (Latch et al. 2005a), photocatalytic (Yu et al. 2006) and permanganate oxidation byproduct (Wu et al. 2012b). For US treatment, we propose that it is produced by reductive chlorination via electron attack and cleavage of the ether bond.

4-chloro-3-(4 chlorophenoxy)phenol was detected at both reaction times with Phenyl and XC columns. 2-phenoxyphenol and 2'-chloro[1,1'-biphenyl]-2,5-diol were also detected as possible degradation products at both reaction times, and were extracted by XC column. These are hydroxyl-TCS derivatives formed by the electrophilic attack of OH radicals over dichloro benzene or chlorophenol rings of TCS molecule or its hydroxylated derivatives, followed by dechlorination.

Acetic acid was detected in samples at 60 and 90 minutes of reaction extracted by SP DVB column. Oxalic acid was also detected in sample at 60 minutes of reaction extracted by Strata Phenyl Column. After cleavage of the benzene ring, further oxidation of intermediates could lead to ring opening generating these carboxylic acids before mineralization. Carboxylic acids such as oxalic, formic, and acetic have been previously detected as final products of TCS degradation (Sirés et al. 2007). The total mechanism proposed is shown in Figure 25.

## 4.4 Conclusions

Optimum frequency for TCS degradation was 574 kHz and optimum power value was 200 W/L - the highest achievable power value for US reactor. For these values, total TCS degradation was achieved in 25 minutes. Two different kinetic models for TCS degradation at natural pH were proposed based on the models found in other studies for US degradation of organic pollutants. These models considered that reaction with OH radicals takes place at the bubble's surface. But their reaction mechanisms were different. One was based on a saturation type reaction over the bubble surface while the other took into account that radical reactions could take place over the bubble surface or in the bulk solution. A pseudo-linear kinetic model resulting from the application of the second mechanism had the best statistical fit for this system. The kinetic constant had a value 0.110441 $min^{-1}$ (574kHz, 140 W/L), four times higher than those found in other studies for US TCS degradation at lower frequencies. TCS degradation at natural pH takes place over the bubble surface and its degradation rate depends on TCS bulk concentration, the rate of generation and recombination of radicals, and the rate of reaction between TCS and OH radicals.

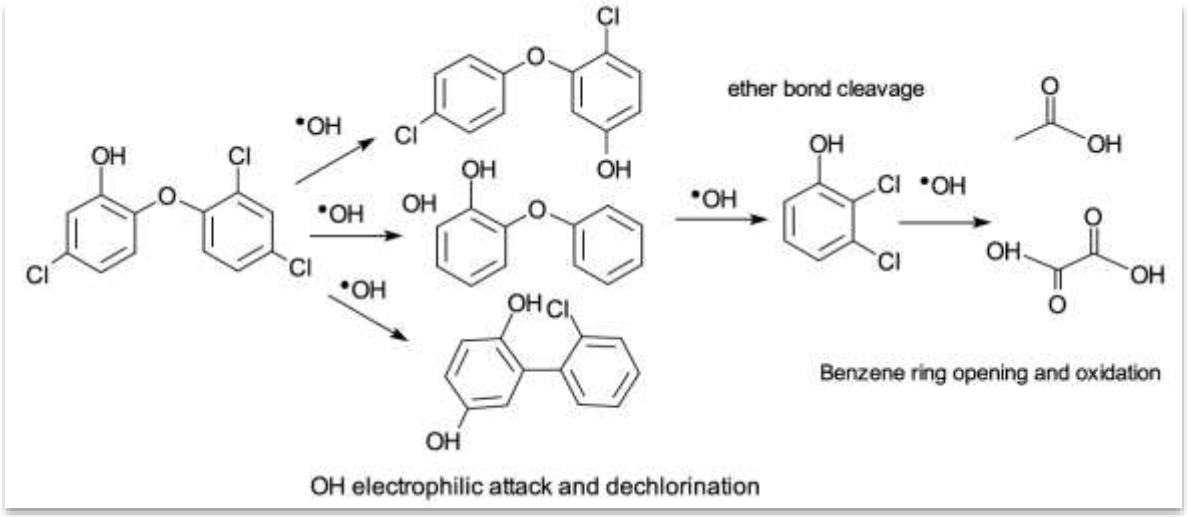


*Figure 25. Reaction mechanism for TCS degradation by US*

Initial reaction rates for PW US were 15.3 % higher than those for continuous US and inhibition was between 42.0-51.4% for different alcohols as radical scavengers in the bulk fluid and bubble surface. These results confirmed TCS is being degraded at the bubble's surface. Toxicity EC50 value measured in the Microtox® toxicity test was 0.164 mg/L. Toxicity decreased continuously with TCS depletion. After TCS total degradation toxicity increased showing that toxic by-products are being generated.

Eight possible degradation byproducts were found, among them 2,7/2,8-dibenzodichloro-p-dioxin and 2,4 dichlorophenol, showing that OH radicals could generate this toxic byproducts at neutral pH, and that further research is needed to understand their fate in US processes.

# Chapter 5

# 5 HIGH FREQUENCY SONOCHEMICAL DEGRADATION OF BENZOPHENONE-3 IN WATER

## 5.1 Abstract

Degradation by high frequency ultrasound of benzophenone-3 (BP-3) is a promising treatment process as it does not need additives and does not generate waste. In this chapter the variables affecting this process were studied. The frequency effect on initial degradation rates was analyzed for various frequencies between 215 and 1134 kHz, and an optimum frequency of 574 kHz was found in this range. Power density had a positive effect on degradation rates over the whole work range. Kinetics adjusted statistically well to a pseudo-linear kinetic model. According to these results and those for degradation in presence of radical scavengers, a conclusion was made that BP-3 degradation was taking place in the bubble/liquid interphase. Toxicity test was conducted by Microtox methods, finding an $EC_{50}$ for 5 minutes of 1.7 mg/L, and for 15 minutes of 2.07 mg/L. Toxicity profile along degradation path showed a decrease at the beginning growing after 30 % of BP-3 degradation. Four possible degradation byproducts were found by Gas Chromatography-Mass Spectrometry (GC-MS) analysis, and a degradation path was proposed.

## 5.2 Introduction

Benzophenone-3 (2-hydroxy-4-methoxybenzophenone, or oxybenzone) (BP-3) is a UVA filter used in personal care products (Blüthgen et al. 2012). This emergent pollutant reaches superficial waters by run off or via wastewater (Fent et al. 2010c)(Li et al. 2007). In the environment it is a persistent and bio-accumulative compound (Gago-ferrero et al. 2013). It has been demonstrated it is an endocrine disruptor. It alters genes responsible for the production of sexual hormones; effect that has been probed in fish and rats (Blüthgen et al. 2012) (Schlumpf et al. 2004). Also, alterations in kidney, liver and reproductive organs have been demonstrated in rats when dermally and orally administrated (Calafat et al. 2008).

Advanced Oxidation Processes (AOP's) have been used for BP-3 degradation including, ozonation, oxidation with Fe(VI), photodegradation, and ultrasound (US) degradation at low frequencies. (Gago-ferrero et al. 2013) achieved more than 95 %

of BP-3 degradation in 40-50 minutes using ozonation for an initial BP-3 concentration of 5.1 mg/L, and an ozone inlet concentration of 85.7 μmol/$L_{gas}$, and gas flow rate of 120 mL/min. (Hernández-Leal et al. 2011) obtained more than 99 % of degradation in 15 min of ozonation of water containing 285 ng/L of BP-3. (Yang and Ying 2014) treated BP-3 by oxidation with Fe (VI) obtaining a half-life of 167.8 s of Fe(VI) concentration of 10 mg/l, and pH 8. However, photodegradation has not resulted in good degradation efficiencies. (Gago-Ferrero et al. 2012) found that BP-3 remained unaltered after 24h of solar radiation treatment. (Vione et al. 2013) found similar results degrading BP-3 by sunlight at an initial concentration of 20 μM, finding a half-life time of some weeks.

US degradation of compounds in water is caused by the creation, expansion, and implosive collapse of gas bubbles in liquids irradiated by US waves (Apfel 1981). Thermal decomposition of water by the compression of oscillating bubbles produces hydroxyl free radicals responsible for degradation (Henglein 1987). US has advantages over other AOP's the absence of added chemicals, of visible light radiation, of change of solution pH, of generated sludge, and of catalysts.

(Zúñiga-Benítez et al. 2016) used ultrasound for degrading BP-3 in a probe-tip reactor for low frequency US (20 kHz). They studied the effect of ultrasonic applied power, pollutant initial concentration, solution pH, presence of gases, and of radical scavengers. However, it has been shown that US degradation at high frequency levels generally results in higher degradation rates mainly for hydrophobic compounds (Navarro et al. 2011)(Kidak and Ince, 2006). This study analyzes BP-3 degradation at frequencies between 215-1134 kHz and the main variables affecting this process. This includes power, frequency, concentration, scavenger's presence and pH. Toxicity evolution and some degradation products were also analyzed.

## 5.3 Results and Discussion

### 5.3.1 Effect of frequency

One of the most important variables influencing ultrasound degradation processes is frequency. At low frequencies higher temperatures (5000K) and pressures (1000 atm) are obtained, predominating the physical effects on reaction (Thangavadivel et al. 2012). At low frequencies higher bubble volumes are obtained. This produces a high vapor content inside the bubble. Consequently the energetic implode of bubbles generates a lower number of OH radicals. Also, at low frequencies the number of cavitation events is less than at higher frequencies.

High frequencies give smaller bubble lives and sizes, and in consequence, there is a lower vapor content within. This generates a more energetic bubble implosion and a high OH radical's production. However, a detrimental effect at higher frequencies can be caused because the shorter rarefaction cycles could generate that molecules do not get sufficiently stretched to generate a bubble (Rayaroth et al. 2015b). This is, the cavitation efficiency decreases, but occurs more frequently (Pétrier and Francony 1997). Also, overall rates can be dominated by mass transfer due to lower bubble's surfaces at higher frequencies (Adewuyi and Oyenekan 2007). Because of this, an optimum frequency exists. This optimum depends on the substance properties related to the vapor pressure that influences the energy of bubbles implosion, the hydrophobicity and volatility that determines the place were reaction is taking place, and the mass transfer towards the bubble that depends mainly on the molecule size (Pétrier and Francony 1997). Several studies have found that US degradation of nonvolatile–hydrophobic compounds occur at higher rates at high frequencies, or have an optimum in the high frequency range(Yang et al. 2008)(Yang et al. 2008)(Yang et al. 2008) (Yang et al. 2008). (Petrier et al. 1998) showed that chlorobenzene degrades more readily at an US frequency of 500 kHz than at one of 20 kHz. The same effect was found for atrazine and pentachlorophenol degradation at 20 and 500 kHz (Petrier et al. 1996). (Pétrier and Francony 1997) degraded phenol and carbon tetrachloride at 20, 200, 500 and 800 kHz, finding that 200 kHz was the optimum frequency. 4-cumylphenol was degraded by US at 80, 300 and 600 kHz, being 300 kHz the optimum frequency (Chiha et al. 2011).

In Figure 26 and Figure 27, BP-3 degradation profiles for frequencies from 215 kHz to 1134 kHz at power densities of 40 W/L and 140 W/L are shown.

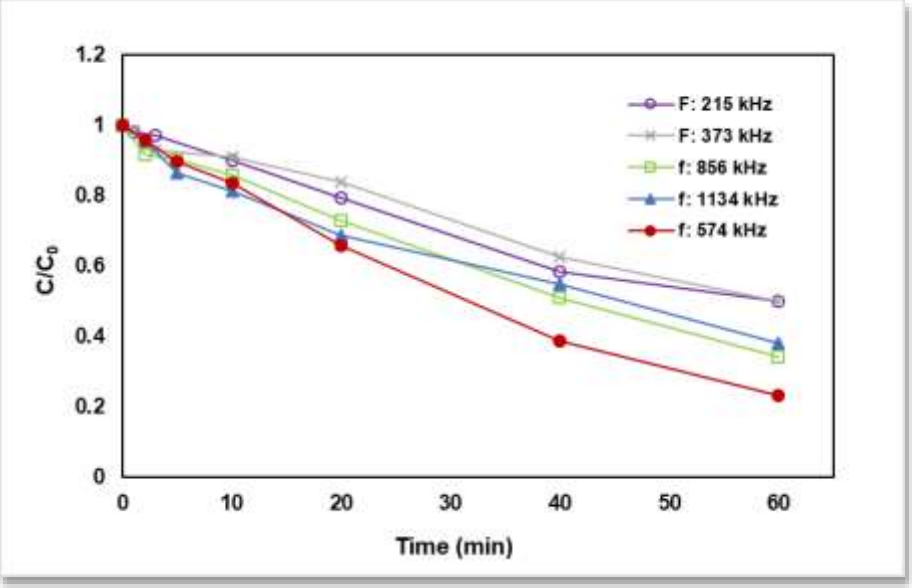

*Figure 26. Effect of frequency on BP-3 degradation. Power density: 40W/L, Solution volume: 300 mL, $C_0$: 1 mg/L, T: 25±2°C*

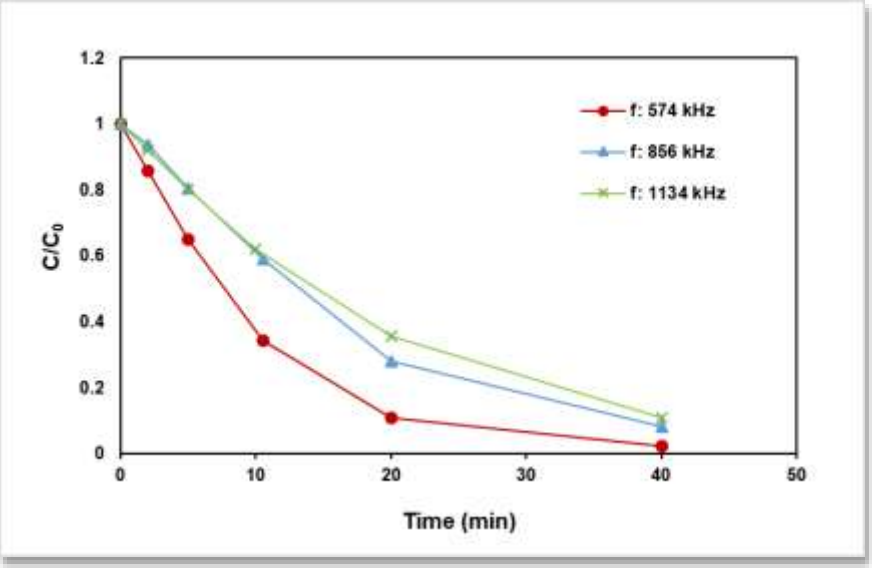


*Figure 27. Effect of frequency on BP-3 degradation. Power density: 140W/L, Solution volume: 300 mL, $C_0$: 1 mg/L, T: 25±2°C*

In this study, for both power density levels analyzed, the optimum frequency was 574 kHz. At this frequency the highest degradation rates were obtained. At a power density of 40 W/L, 77 % of BP-3 ($C_0$= 1mg/L), was degraded in 60 minutes, and at a higher value of 140 W/L, BP-3 was completely degraded in 40 minutes. In (Zúñiga-Benítez et al. 2016) for a higher value of power density (200 W/L), but for a low frequency of 20 kHz, only 50 % of degradation was achieved in 60 minutes of reaction. This shows that for the same levels of power intensity, high ultrasound frequencies are better until an optimum after which degradation rates start declining.

### 5.3.2 Effect of power density

In Figure 28, the effect of power density on BP-3 degradation is shown. Power intensity has an important influence in ultrasound degradation rates. As power intensity of ultrasound radiation increases, acoustic wave amplitude increases generating more violent collapse of the bubbles and high OH radicals generation (Adewuyi and Oyenekan 2007). It has been widely demonstrated that power intensity has an optimum value in which pressure and temperature during collapse generates an optimal degradation rate. At higher intensities bubble shielding occurs

attenuating the effect of the ultrasound radiation (Cheng et al. 2012). In this study, the shielding effect is observed in that an increase in the power density does not result in a proportional increase in the degradation rate (van Iersel et al. 2008). In Figure 28, degradation curves for 140 and 200W/L are closer than those for 40 and 90 W/L. However, degradation rates continue being higher for higher power densities.

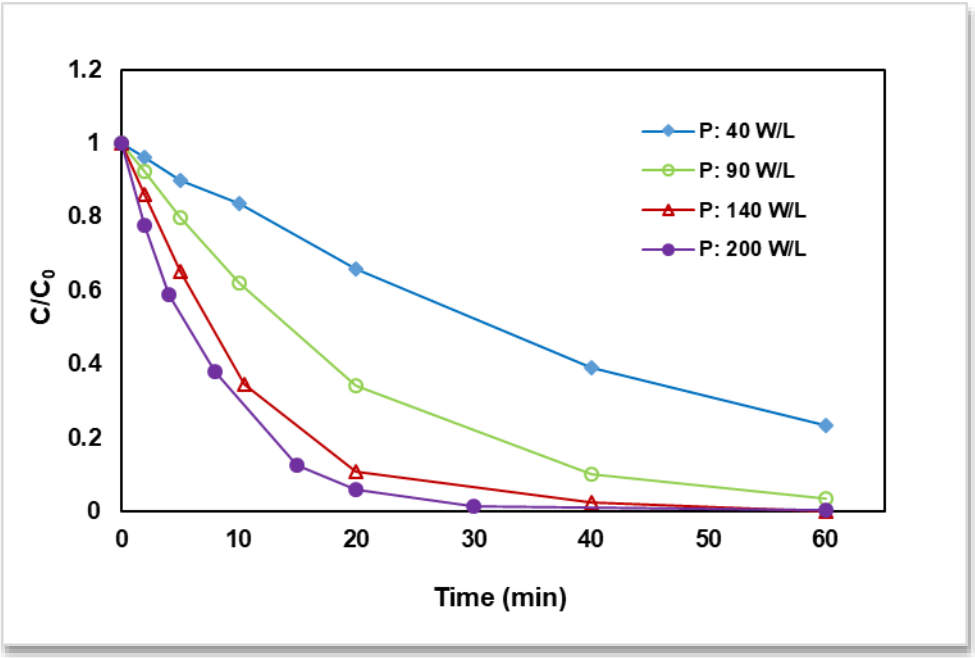


*Figure 28. Effect of power density on BP-3 degradation. Frequency: 574 kHz, Solution volume: 300 mL. $C_0$: 1 mg/L, T: 25 ±2oC*

Degradation rates grew continuously with power density, having its maximum value at 200 W/L, the maximum allowable power for the equipment. At this level 98 % degradation was achieved in 30 minutes. This is half the time obtained in the previous study made in a probe tip reactor at the same power density level, but at low frequency (20 kHz) and higher BP-3 initial concentration (3.9 mg/L). (Zúñiga-Benítez et al. 2016).

### 5.3.3 Radical scavengers effect

Sonochemical decomposition of organic compounds in water can proceed inside the bubbles, at the interphase between the cavitation bubbles and the bulk solution, and at the bulk solution (Okitsu et al. 2005). Inside the bubbles and at the bubble surface mainly pyrolysis and radical reactions occur, and at bulk solution reactions with OH radicals are the most important.

Volatility is measured by Henry's law constant ($K_H$), which relates partial pressure of BP-3 above the liquid, with its concentration in the solution. Since BP-3 is not a volatile compound, it is expected that it does not pyrolyze in cavitation bubbles, because the effect of volatility on degradation rates becomes pronounced at $K_H$ values above $2.4*10^{-5}$ atm-$m^3$/mol (Nanzai et al. 2008). BP-3 $K_{H\text{-}BP\text{-}3}$ is $1.5*10^{-8}$ atm-$m^3$/mol. On the other hand, as BP-3 is hydrophobic (Log $K_{ow}$ = 3.8), it is expected that it tends to accumulate mostly in the interphase region of the cavitation bubbles.

Studies made by (Ince et al. 2009)(Serna-Galvis et al. 2015)(Zúñiga-Benítez et al. 2016) (Latch et al. 2005a; De Bel et al. 2011) show that some alcohols like tertbutanol, ethanol, methanol, and isopropyl alcohol scavenge OH radicals at bubble surface and bulk solution. At the other hand, acetic acid/acetate appears to scavenge OH radicals only in the solution, without any interaction with the bubble interphase (Xiao et al, 2013).

To check where reaction of BP-3 is taking place, and to probe OH radicals are the responsible for its degradation, experiments were made using ethanol, 2-propanol and sodium acetate as radical scavengers. Radical scavenger concentration of 4.3 mM was used. BP-3 initial concentration was 4.3 µM, so radical scavenger was always in excess. Resulting degradation profiles are shown in Figure 29.

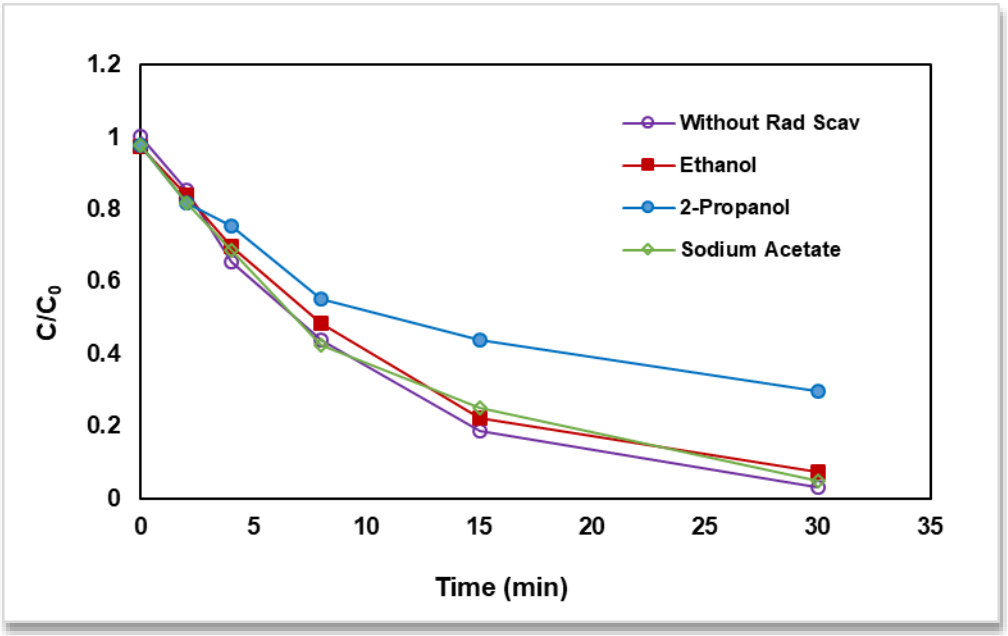


*Figure 29. Effect of radical scavengers on BP-3 degradation. Frequency: 574 kHz, power density: 200W/L, solution volume: 300 mL. $C_0$: 1 mg/L, T: 25 ±2°C*

Comparing initial BP-3 degradation rates for US degradation at 574 kHz, with scavenger, inhibition was 11.5 % for ethanol, 28.5 % for 2-propanol, and it has no

statistical difference for sodium acetate. Henry's law constant for BP-3 ($K_{H\text{-}BP\text{-}3}$ is $1.5*10^{-8}$ atm-$m^3$/mol) is much lower than those for radical scavengers used ($K_{H\text{-}ethanol}$ is $5*10^{-6}$ atm-$m^3$/mol, and $K_{H\text{-}2\text{-}propanol}$ is $7.5*10^{-6}$ atm-$m^3$/mol). Thus, BP-3 degradation inhibition in presence of the scavengers is explained by the scavengers' quenching of OH radicals in the bubble, interphase, and bulk solution, and to a diminished available energy for $H_2O$ thermolyisis (Xiao et al. 2013b). This generates higher reaction rates of scavengers with OH radicals than those of BP-3. At the other hand, sodium acetate did not have any effect on initial degradation rates because it scavenge OH radicals in the bulk solution, showing that under this conditions BP-3 degradation is taking place only at the bubble surface.

### 5.3.4 Kinetics of sonochemical degradation

Different models have been proposed for explaining ultrasound reactions kinetics. Okitsu et al. (2006) proposed a non-heterogeneous kinetic model similar to a Langmuir–Hinshelwood or Eley–Rideal mechanism. In this approach assumption is made that reaction is occurring in the bubble-solution interphase. There, a pseudo-equilibrium of adsorption and desorption of pollutant exists before collapsing of the bubble at the gas/liquid interphase. This results in a general model that is summarized in tye following equation:

$$r = k_{BP3}\theta = \frac{k_{BP3}K_{BP3}[BP3]}{1 + K_{BP3}[BP3]} \tag{49}$$

Where $K_{BP3} = {k_{a1}}/{k_{a-1}}$, $k_{a1}$ and $k_{a-1}$ are the sorption and desorption rate constants in the bubble surface, and $k$ is the pseudo first order rate constant for the reaction of BP-3 with OH radicals.

The general reaction mechanism for chlorophenol degradation by ultrasound by Serpone et al. (1994) proposed reactions could take place in the bulk solution or in the interphase. The resulting general expression was similar to that of Okitsu. But in this model, when reaction is taking place in the bubble interphase, where OH concentration is high and pollutant concentration is low, the rate expression becomes of first order in the concentration of benzophenone 3:

$$\left(\frac{d[BP3]}{dt}\right) = -k_{b-BP3}[BP3] \tag{50}$$

Detailed explanation of these models is presented in section 2.1.3. Rate equations (*49*) and (*50*) were evaluated to check the goodness of fit of the experimental data to

these expressions. Statistical methods were used for correlating BP-3 initial concentration and initial degradation rates for various initial BP-3 initial concentration levels. Degradation rates were calculated for the first two reaction minutes. In this time, less than 20 % of BP-3 degradation was achieved. Thus the interaction of reaction products with OH radicals was minimized and mainly the interaction of BP-3 and these radicals was analyzed. Experiments were made at 574 kHz and 140 W/L. BP-3 initial concentrations were in the range from 2.3 to 21.6 µM.

The goodness of fit of the model for equation (*49*) was analyzed by nonlinear regression by an algorithm in R using the instruction nls. Nonlinear (weighted) least-squares estimates of the parameters were found. The pseudo first order model (equation (*50*)) was analyzed by ordinary least squares analysis by an algorithm in R for linear regressions. Regression parameters, t statistic probabilities (p), coefficient of determination ($R^2$), and Sum of Squared errors (SSE) for both are shown in Table 6. Figure 30 presents the experimental values and predicted curves for both models.

*Table 6. Parameters of the kinetic models for BP-3 degradation*

| Model | Parameters | $R^2$ | SSE |
|---|---|---|---|
| **Equation (*49*)** | $k_{BP3}K_{BP3}$: 0.0402448 *(t value:5.599, p= 1.48e-05)* | | 0.05038 |
| | $K_{BP3}$:-0.0001664 *(t value:* -0.022, ***p= 0.982****)* | | |
| **Equation (*50*)** | $k_{b-BP3}$: 0.040402 *(t value: 25.353, p= 2e-16)* | 0.9669 | 0.04922 |

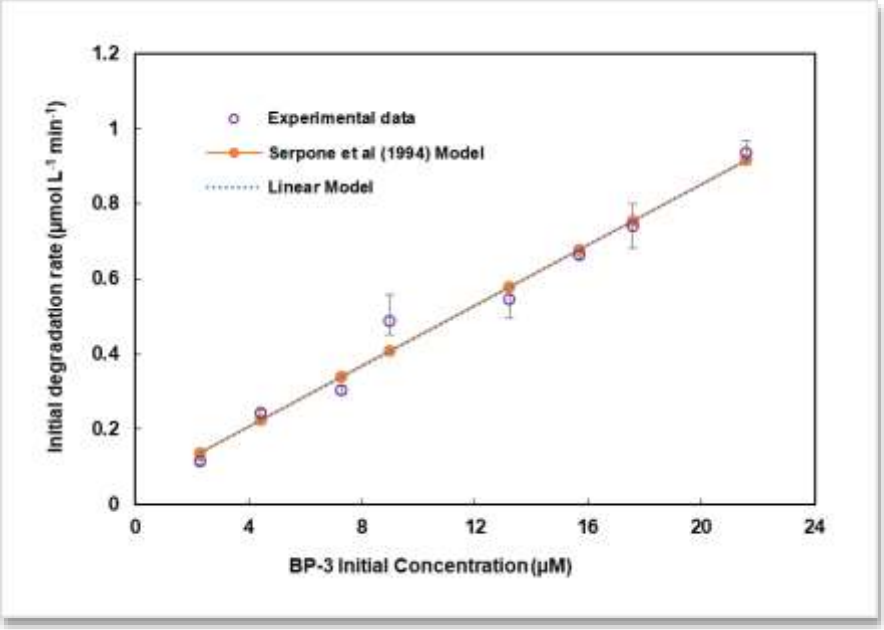


*Figure 30. Initial degradation rate vs BP-3 initial concentration. Frequency: 574 kHz, power density by calorimetric method: 200 W/L, pH: 6.9, volume: 300 mL, temperature: 25±2˚C).*

The squared sum of residues (SSE) had similar values for both models showing a goof fit of the data. Pseudo first order model (equation (*50*)) had a good correlation coefficient and a good p value for t statistics for equation parameter. The nonlinear model presented in equation (*49*) gives a low value for the t value of the parameter $K_{BP3}$ in the denominator. Consequently there is no statistical evidence for the validity of this parameter and consequently of this model.

On the other hand, pseudo first order model explained adequately BP-3 degradation having good p values for t statistic and a good $R^2$ and SSE. Therefore conclusion can be made that BP-3 degrades mainly at bubble surface according to the approach proposed by Serpone et al. (1994). Rate constant was 0.0404 $min^{-1}$. The linear model does not go through the origin having a slight deviation that could be attributed to a small part of the reaction taking place on the bulk solution and experimental errors. This result was different to that of (Zúñiga-Benítez et al. 2016) who obtained that kinetics followed a nonlinear model as that presented in equation (*49*). Difference can be attributed to that this kinetic analysis was made at a higher frequency level (574 kHz). At this frequency there are different conditions for OH radical concentrations and for the diffusivity could have a different effect, affecting in a different way overall degradation rates.

### 5.3.5 Effect of pH

A compound can be in its molecular or in its ionic form with different proportions depending on its $pK_a$ value. Hydrophobic compounds in their molecular form accumulate more readily in the interfacial area than in their ionic form. BP-3 has a $pK_a$=7.56, and at a natural pH of 6.9 it is almost completely in its molecular form. At higher pH values than 7.56, BP-3 is in its deprotonated or phenolate form, and tends to accumulate less in the bubble interphase where radical OH concentration is higher. Ultrasound experiments at pH 10 were conducted to examine this effect on initial rate for BP-3 degradation. At this pH value more than 99 % of BP-3 is in anionic form, according to the following expression (Chiha et al. 2011):

$$\varphi_{ions} = \frac{1}{1 + 10^{(pK_a - pH)}} \tag{51}$$

Comparing degradation for pH 10 with those obtained at natural pH, it can be seen in Figure 31 that there is no difference in degradation rates. However, it is known that for phenolic compounds, the deprotonated form, or phenolate is more reactive with OH radicals because it undergoes one-electron oxidation much more readily than phenolic form (Greenberg 2009). However, OH radical reaction rates are

usually limited by mass transfer. Therefore a possible reason for the nule effect of the pH over degradation rates is that both species have similar diffusivities in water.

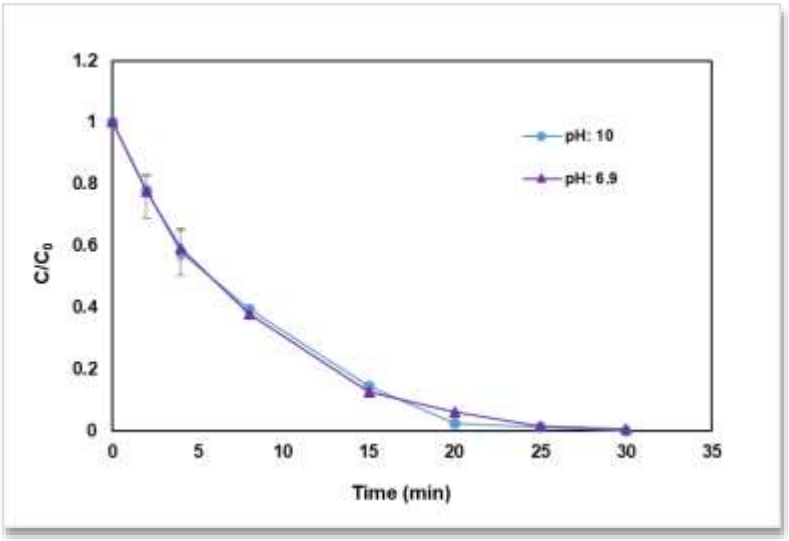


*Figure 31. Effect of pH on BP-3 degradation by ultrasound. Power density: 200W/L, frequency: 574 kHz, solution volume: 300 mL, $C_0$: 1 mg/L, T: 25±2°C*

### 5.3.6 Toxicity

A Microtox® equipment was used for conducting ecotoxicity essays. It measures the decrease in the natural luminescence of the marine bacteria *Vibrio Fischeri* in the presence of BP-3 in aqueous solution. A diminishing in the bioluminescence indicates the diminishing in their cellular respiration. When exposed to the toxic substances, there is a change in the percentage of protein and lipid synthesis, and this changes the light emission level. Toxicity is expressed as effective concentration $EC_{50}$: pollutant concentration generating a 50 % reduction in light emission (Onorati and Mecozzi 2004).

For determining BP-3 acute toxicity, 81.9 % Basic test was used according to the Guide to Microtox M500 procedure. A BP-3 solution in deionized water with a concentration of 4.93 mg/L was used, response was measured for several dilutions at 5 and 15 minutes. Resulting $EC_{50}$ for 5 minutes was 1.7 mg/L, and for 15 minutes was 2.07 mg/L. Microtox procedures are widely used because its results are generally correlated with those for acute toxicity analysis made on *Daphnia Magna* (La Farre et al. 2001). For BP-3, (Fent et al. 2010b) reported a value for acute toxicity $LC_{50}$ value on *Daphnia Magnia* of 1.9 g/L, very close to this result found using *Vibrio Fischeri* bacteria.

Toxicity path as US degradation occurred was measured for a treated BP-3 solution with an initial concentration of 1 mg/L, irradiated at 574 kHz and 200 W/L for 90 minutes. 3 mL samples were withdrawn at different times, and analyzed in Microtox equipment by the 81.9 % Screening Test. Results are shown in Figure 32.

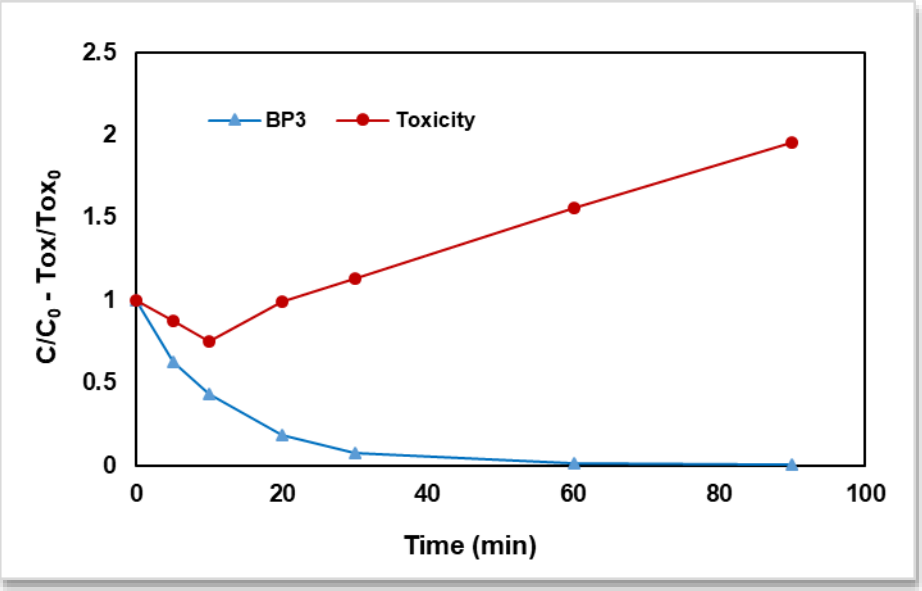


*Figure 32. Toxicity evolution for Benzophenone-3 degradation by ultrasound. Power density: 140 W/L, frequency: 574 kHz, solution volume: 300 mL, $C_0$: 4.93 mg/L, T: 25±2°C*

There are few reports about BP-3 byproducts by OH reaction. (Gago-Ferrero et al. 2012) found dihydroxybenzophenone (BP-1) as one of the byproducts of BP-3 photodegradation, being 200 times more strogenic than BP-3. Another possible compound such as 2,2′-dihydroxy-4-methoxybenzophenone found in BP-3 ozonation (Gago-ferrero et al. 2013) and other similar possible hydroxylated byproducts could have more harmful effects than BP-3 (Jeon et al. 2008), but their presence as US byproducts were not confirmed. Byproducts found in this study are less toxic than BP-3: Benzoic acid has an $EC_{50}$ (48 h, Daphnia Magna) of 9.93 mg/L; acetic acid of 300.82 mg/L; and formic acid of 34 mg/L; while BP3 has an $EC_{50}$ (Daphnia Magna, 48 h) of 1.09 (Zhao et al. 1998)(Du et al. 2017). These byproducts were found at the beginning of the degradation and could partly explain the diminishing in toxicity. However, further research beyond that made in this study is needed to understand the reason of the toxicity increase as BP-3 after this degradation extent.

### 5.3.7 Degradation byproducts

Four possible degradation byproducts were found. Deionized water spiked at 10 mg/L with BP-3 was sonicated and aliquots of the solution were taken when 30 % of degradation was achieved. Compounds were isolated by SPE according to procedure described in 2.3.2 section. Separation and detection of degradation products was accomplished by gas-chromatography-mass spectrometry (Section 2.3.3). Possible compounds were detected, based on the presence of the molecular ion, interpretation of their fragment ions in the mass spectra using an identification program of NIST 14 Mass Spectral Library. Spectrums are shown in Figure 63, Figure 64 and Figure 65 in the Appendix 1.

1-(2-Hydroxy-4-methoyphenyl) propan-1-one was identified in the extract made with Phenyl Column, at 22.235 min. The mechanism proposed for its generation is the hydroxylation by OH radicals attack over the non-substituted benzene moiety, leading to posterior ring opening.

Benzoic acid was identified in the extract made with XC Column at 10.154 min. This compound was found by (Vione et al. 2013) in their study of BP-3 photo transformation. This byproduct can be generated after bond cleavage between the carbonyl group and the aromatic ring with hydroxyl and methoxy functions (Vione et al. 2013). Other similarly generated byproducts found in this study were acetic acid and formic acid obtained in the extract made with DVB (4.093 min) and XC columns (3.26 min). These acids can be generated by non-specific OH attack over oxidized BP-3 intermediates after bond cleavage between the two benzene rings and its opening. A general proposed mechanism is shown in Figure 33.

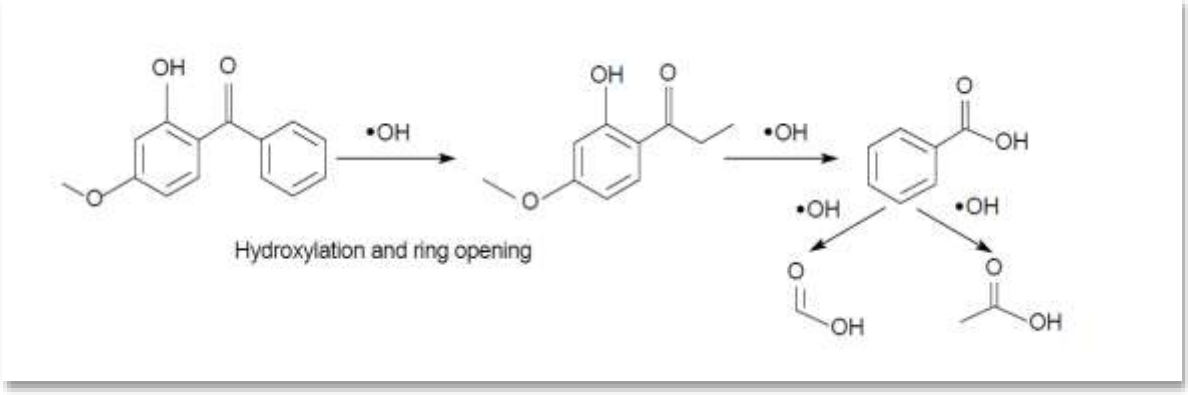


*Figure 33. BP-3 proposed degradation mechanism*

## 5.4 Conclusions

Optimum frequency for benzophenone-3 degradation was 574 kHz and optimum power value was 200 W/L. For these values, 98 % BP-3 degradation was achieved in 30 minutes. Two different kinetic models for BP-3 degradation at natural pH were proposed. One was based on a saturation type reaction over the bubble surface while the other took into account radical reactions could take place over the bubble surface or in the bulk solution. A pseudo-linear kinetic model resulting from the application of the second mechanism had the best fit for this system. The kinetic constant had a value of 0.040402 $min^{-1}$, (574kHz, 140 W/L), four times higher than those found in other studies for US BP-3 degradation at lower frequencies. BP-3 degradation at natural pH takes place over the bubble surface and its degradation rate depends on its bulk concentration, the rate of generation and recombination of radicals, and the rate of reaction between BP-3 and OH radicals.

Inhibition with radical scavengers was 11.5 % for ethanol, 28.5 % for 2-propanol, and it has no statistical difference for sodium acetate. These results confirmed BP-3 is being degraded only at the bubble's surface. Toxicity $EC_{50}$ value measured in the Microtox® toxicity test was 1.7 mg/L after 5 minutes. Toxicity decreased with BP-3 depletion until 30 % degradation, increasing afterwards, showing that more toxic by-products are being generated.

Four possible degradation byproducts were found: 1-(2-Hydroxy-4-methoxyphenyl) propan-1-one, benzoic acid, acetic acid, and formic acid.

# Chapter 6

# 6 HIGH FREQUENCY SONOCHEMICAL DEGRADATION OF BENZOPHENONE-1 IN WATER

## 6.1 Abstract

Ultrasound (US) degradation of the endocrine disruptor BP1 was studied. Optimum frequency of 856 kHz and optimum power density value of 30 W/L was found using a multifrequency bath reactor degrading an aqueous solution of BP1 at 2 mg/L. Kinetic models proposed by Serpone and Okitsu were proposed as possible for BP1 degradation, and experimental data adjusted adequately to the model proposed by Serpone for degradation over the bubble surface, resulted in a pseudo lineal relation. Experiments made with radical scavengers and pulsed US mode showed that BP1 degrades over the bubble surface and a small fraction in the bulk fluid, having an important enhancement effect by pulsed US. Five possible degradation byproducts were found, and a general degradation mechanism was proposed. Toxicity profile along the treatment was made using the Microtox procedure with *Vibrio Fischeri* luminescent bacteria.

## 6.2 Introduction

Benzophenone-1, (2, 4- dihydroxybenzophenone) (BP1) is an UV filter used to protect materials such as textiles, household products, agricultural chemicals, and cosmetics. BP1 is an endocrine disrupter with demonstrated effects over humans, fishes and rats. Its hormonal activities include estrogenicity and antiandrogenicity (Fent et al. 2008). Among its effects are the prevention of testosterone formation in humans, the stimulation of the proliferation of BG-1 ovarian cancer (Park et al. 2013), the enhancement of prostate cancer progression (Kim et al. 2015), and promotion of the proliferation of MCF-7 human breast cancer cells (In et al. 2015).

BP1 bioaccumulates in human and animal bodies, and reaches the aquatic environment via wash-off from recreational activities or via sewage. It has been found in rivers up to 47 ng $L^{-1}$, and in levels from 27 to 204 ng $L^{-1}$ in industrial drainage (Fent et al. 2008).

BP1 is not completely removed in conventional treatment plant processes. Primary sedimentation and chemical coagulation/flocculation have shown not to be effective in the removal of UV-filters like BP1 because of its low log $K_{OW}$ (Ramos et al. 2016). A 96% of removal for BP1 by a primary treatment followed by trickling filter beds

was found by (Kasprzyk-Hordern et al. 2008). (Negreira et al. 2009) reported 83% removal of BP1 in WWTPs after activated sludge treatment. (Wu et al. 2018) reported a removal mean value of 97% in three WWTP in China, (Tsui et al. 2014a; b) investigated five different wastewater treatment methods for 12 organic UV-filters in Hong-Kong, China. In them, BP1 was detected in all influent samples, with mean concentration of 163 ng $L^{-1}$. BP1 detection frequency in effluents was higher than 75% throughout the year in these treatment plants. The mean value concentration was 86 ng $L^{-1}$, and the maximum concentration was 155 ng $L^{-1}$. This indicates that BP1 is not totally degraded in conventional treatment plants. On the other hand, fungal treatment resulted in the degradation of more than 95% at 3 h for BP1 according to (Gago-Ferrero et al. 2012).

Few reports about BP1 degradation by AOP's have been issued. Only the study of (Gago-Ferrero et al. 2012) was found. They reported a 100% photodegradation after 24 h UV irradiation for BP1 in an initial concentration of 250 µg $L^{-1}$, using a SunTest apparatus equipped with a Xenon arc lamp providing a light intensity of 400 $W/m^2$.

US degradation of compounds in water is caused by the cavitation phenomenon, that is, the creation, expansion, and implosive collapse of gas bubbles in liquids irradiated by US waves (Apfel 1981). This collapse generates pressures up to 10.000 atm and temperatures up to 5000°K. At these extreme conditions, water dissociates generating hydroxyl and Hydrogen radicals. These radicals oxidize dissolved organic compounds in solution (Doosti et al. 2012).

It has been shown that US degradation at high frequency levels results in higher degradation rates for hydrophobic compounds (Navarro et al. 2011)(Kidak and Ince, 2006). This study analyzes BP-1 degradation at frequencies between 215 and 1134 kHz and the variables affecting this process. This includes power and frequency levels, initial BP-1 concentration, scavenger's presence and pH. Toxicity evolution and degradation products were also analyzed.

## 6.3 Results and Discussion

### 6.3.1 Effect of frequency

Frequency is a very important variable influencing ultrasound degradation of organic compounds. At low frequencies, cavitation events are less than those at high frequencies, and physical effects are predominant in the degradation mechanism (Thangavadivel et al. 2012). At low frequencies, bubble longevity and sizes are larger. This higher bubble volumes and lives make bubbles to content more water

vapor and therefore less energetic bubbles implosion. Thus, there is less OH radical production at low frequencies. This would imply that at higher frequency, there is greater degradation by radical oxidation. However, the beneficial effects of high frequencies start diminishing after an optimal value depending on the properties of the substance (Adewuyi and Oyenekan 2007). At higher frequencies, shorter rarefaction cycles could lead to molecules that do not get stretched enough to generate a bubble (Rayaroth et al. 2015b). Additionally, at high frequencies, the smaller bubble surfaces make that overall rates are highly influenced by mass transfer (Adewuyi and Oyenekan 2007).

Figure 34 shows the frequency effect over BP1 degradation percent after 30 minutes of reaction, and over initial degradation rates for a power density of 30 W/L. Frequencies analyzed were 373, 574, 856 and 1134 kHz.

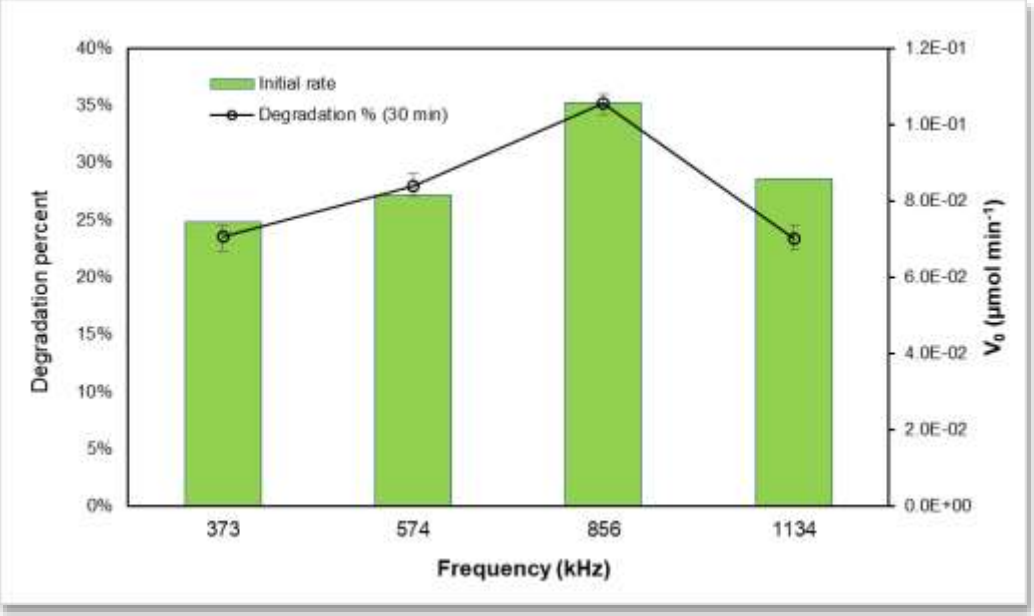


*Figure 34. Effect of frequency on BP1 degradation. Power density: 40W/L, Solution volume: 300 mL, initial BP1 concentration: 2 mg/L, T: 25°C±2°C*

It can be noticed that the optimum frequency for BP1 degradation in water at a power density of 40 W/L is 856 kHz. For this frequency value, the initial rate was 0.105 µmol/L min, and a 35.2% of BP1 degradation was achieved after 30 minutes.

### 6.3.2 Effect of power density

Power density is another important variable influencing degradation rates. Acoustic wave amplitudes are higher at higher power densities, and generate more violent collapse of the bubbles, and consequently an increase in OH radicals generation

(Adewuyi and Oyenekan 2007). However, the same as with frequency, power density has a positive effect until a certain value is reached, after which an effect called bubble shielding occurs. This effect occurs when the presence of a high quantity of bubbles does not let the proper propagation of the ultrasound irradiation attenuating its effect (Cheng et al. 2012).

From the Figure 35, it can be noticed that optimum power density for BP1 degradation in water at 856 kHz is 40 W/L. For this frequency value, initial rate was 0.105 µmol/min, and a 35.2% of BP1 degradation was achieved after 30 minutes.

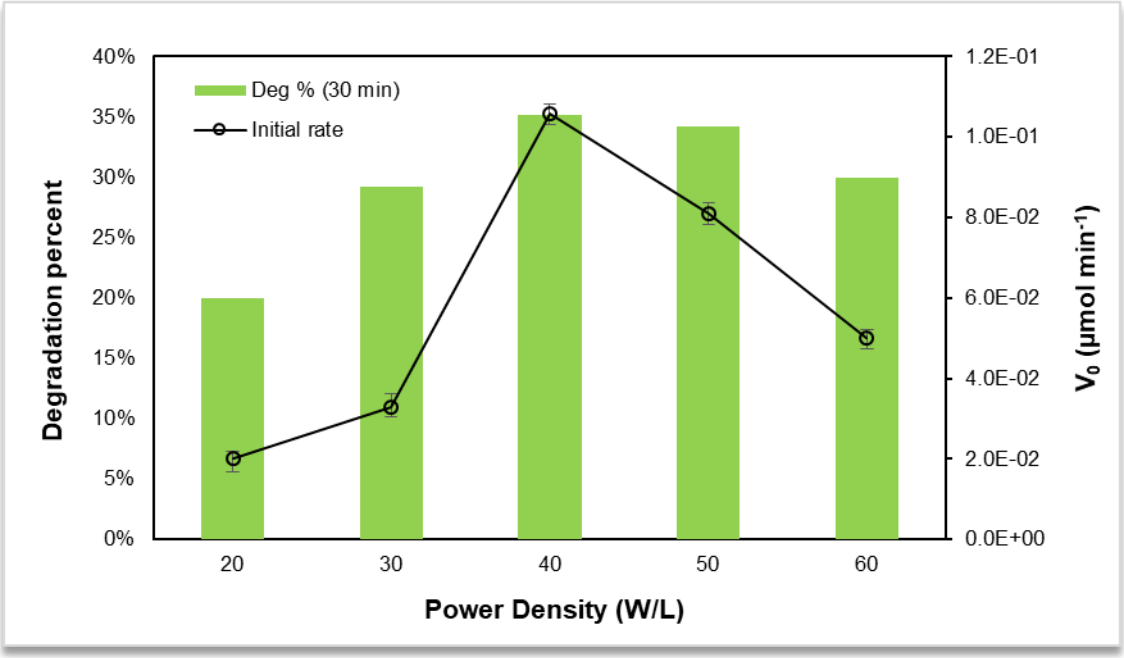


*Figure 35. Effect of Power Density on BP1 degradation. Frequency: 856 kHz, Solution volume: 300 mL, initial BP1 concentration: 2 mg/L, T: 25°C±2°C*

### 6.3.3 Radical scavengers and Pulsed Mode US effect

It is known that US decomposition of organic molecules can take place in three different places: inside the bubbles by pyrolysis; bubble surface by radical reaction and some pyrolisis, and in the bulk solution, by radicals reaction (Okitsu et al. 2005). Volatile compounds tend to get in vapor phase inside the bubbles degrading by pyrolysis. BP1 has a Henry's law constant ($K_H$) of 2.65 *10 $^{-11}$ atm-m$^3$/mol. $K_H$ relates the partial pressure of BP1 above the liquid, with its concentration in the solution. Taking into account that compounds with a $K_H$ above 2.4*10$^{-5}$ atm-m$^3$/mol are the ones which degrade mostly by this mechanism (Nanzai et al. 2008), it is expected

that BP1 does not accumulate in the vapor phase and therefore does not suffer pyrolysis. Additionally, BP1 is relatively hydrophobic Log Kow= 3.0, hence it is expected to accumulate in the interphase reaction for the cavitation bubbles.

Comparing initial BP1 initial degradation rates for US degradation for an initial concentration of 9.34µmol/L, at 856 kHz and power density of 30 W/L, with a ratio 1000:1 for scavenger: BP1, inhibition was 41% for methanol, and 9.7% for sodium acetate. Alcohols like methanol scavenge OH radicals both over the bubble surface and in the bulk solution (Serna-Galvis et al. 2015) (Zúñiga-Benítez et al. 2016); while acetic acid/acetate scavenge radicals only in the bulk solution, having no interaction at the bubble surface (Xiao et al, 2013). Thus, a conclusion can be made that BP1 can be degraded mainly over the bubble surface and a small proportion on the bulk solution. In the same way, the presence of methanol in the vapor phase decreases the available energy for water thermolysis with the consequent decrease in the production of OH radicals. (Xiao et al. 2013b). In a previous study, we found that, for a similar compound such as BP3, US degradation was not inhibited by sodium acetate. BP1 Log $K_{ow}$ is 3.0 and BP3 Log $K_{ow}$ is 3.8. BP1 is less hydrophobic than BP3 and migrates more slowly to the bubble surface, having the possibility of reacting in a small proportion in the bulk liquid.

Pulse Enhancement (PE*). PE is defined as:

$$PE^{*}(\%) = \frac{(v_0)_{PW} - (v_0)_{CW}}{(v_0)_{CW}} \times 100\% \quad (52)$$

Where $(v_0)_{PW}$ is initial rate for PW mode US, and $(v_0)_{CW}$ is initial rate for PW mode US. Total reaction time for PW mode US was calculated according to the following equation (Yang et al. 2005):

$$t_{total} = t_{sonication}\left(1 + \frac{ST}{PT}\right) \quad (53)$$

Where $t_{total}$ is the total reaction time; $t_{sonication}$ is the real sonication time (10 minutes); $ST$ is the time between pulses (Silent Time); and $PT$ is the Pulse Time. For this equipment could be varied in the range 0-10000 ms continuously. Pulse time and silent times of 50 and 50 ms were used. PE under this conditions was 56.7%. This shows that as BP1 is relatively hydrophobic, and is a molecule of middle size favoring the diffusion of the molecules from the bulk solution to the bubble interface during silent times. Enhancement was high because BP1 has a relatively low molar volume (164.4 mL/mol) and high diffusivity ($6.5*10^{-6}$) as calculated according to (Hayduk and Laudie 2015).

### 6.3.4 Kinetics of sonochemical degradation

Ultrasound reaction kinetics have been explained by two different models: The one proposed by (Okitsu et al. 2005), and the one by Serpone et al. (1994). The first one is based on the assumption that US degradation occurs in the bubble-solution interphase, and therefore it is modeled as a pseudo-equilibrium of adsorption and desorption of the pollutant in that surface before the collapse of the bubble. This model is summarized in equation (*54*):

$$r = k_{BP1}\theta = \frac{k_{BP1}K_{BP1}[BP1]}{1 + K_{BP1}[BP1]} \tag{54}$$

Where $\theta$ is the ratio of pollutant molecules occupied in the reaction site $K_{BP1} = {k_{\mathrm{a1}}}/{k_{\mathrm{a-1}}}$, $k_{\mathrm{a1}}$ and $k_{\mathrm{a-1}}$ are the adsorption and desorption rate constants on the bubble surface, and $k$ is the pseudo first order rate constant for the reaction of the solute with OH radicals. This model also assumes that after the bubble collapses, adsorbed pollutant molecules react with OH radicals which are assumed to be at a high concentration in this region once a collapse occurs. They argued that such assumptions are valid at low frequencies because bubble lifetime is larger than at high frequencies, and resonance bubble radius is larger

By the other hand, (Serpone et al. 1994) proposed a general reaction mechanism for US degradation taking place in the bulk solution or in the interphase. Following reactions are occurring throughout US degradation:

$$H_2O + ))) \overset{k_1}{\rightarrow} OH^* + H^* \tag{55}$$

BP1 and OH* radicals encounter at the bubble/solution interphase, according to this reaction:

$$OH^* + BP1 \xrightarrow{k_{2-\mathrm{BP1}}} OH^*BP1 \tag{56}$$

In this expression, $k_{2-\mathrm{BP1}}$ is determined by diffusional characteristics of OH radicals and BP1 in aqueous media. The complex can breakup according to:

$$OH^*BP1 \xrightarrow{k'_{2-\mathrm{BP1}}} OH^* + BP1 \tag{57}$$

Or can form the products (P) as in equation (*58*):

$$OH^*BP1 \xrightarrow{k_{3-\mathrm{BP1}}} P \tag{58}$$

Recombination of radicals and formation of hydrogen peroxide can occur mainly at the interphase, but it could also occur in the bulk solution at very low rates (Serpone et al. 1994):

$$OH^* + H^* \overset{k_4}{\rightarrow} H_2O \tag{59}$$

$$2OH^* \overset{k_5}{\rightarrow} H_2O_2 \tag{60}$$

As explained before, in section 2.1.3, the following expression was found for the overall rate of sonochemical decomposition of BP1:

$$\left(\frac{d[BP1]}{dt}\right) = \frac{k_1 k_{2-BP1} BP1}{(k_4[H^*] + k_5[OH^*] + k_{2-BP1}[BP1])} \tag{61}$$

Simplifying for $k_4[H^*]$ and $k_5[OH^*]$ as constants:

$$\left(\frac{d[BP1]}{dt}\right) = \frac{k_1 k_{2-BP1}[BP1]}{(k'_{3-BP1} + k_{2-BP1}[BP1])} = \frac{k_1 K_{Serp-BP1}[BP1]}{(1 + K_{Serp-BP1}[BP1])} \tag{62}$$

Where $K_{Serp-BP1} = \frac{k_{2-\mathrm{BP1}}}{k'_{3-\mathrm{BP1}}} = \frac{k_{2-\mathrm{BP1}}}{k_4[H^*]+k_5[OH^*]}$

Half-life of an OH radical is around $10^{-3}$ μs as shown by x-ray diffraction analysis (Pryor 1986), and in liquid medium it has been found that molecules migrate the distance of molecular diameter in a time range of $10^{-4}$ to $10^{-2}$ μs. Because of its short life, it could be expected that OH radicals have a low molecular mobility in water. Therefore, high OH radical concentrations could mainly be found in and close to the bubble surface. In expression (60), condition is fulfilled for low BP1 in this place.

This is expressed as:

$$\left(\frac{d[BP1]}{dt}\right) = k_{b-BP1}[BP1] \tag{63}$$

Where $k_b = \frac{k_1 k_2}{k'_3}$

This is a pseudo first order reaction kinetics rate expression.

The goodness of fit of the experimental data was evaluated for rate equations (*54*) and (*63*). Statistical methods were used for correlating BP1 initial concentrations and initial degradation rates for various initial BP1 concentration levels. Degradation rates were calculated for the first 15 reaction minutes. In this time, less than 20 % of BP1 degradation was achieved. Thus, the interaction of reaction products with OH radicals was minimized and mainly the interaction of BP1 and these radicals was analyzed. For (*54*) a nonlinear (weighted) least-squares estimates of the parameters were found. For (*63*), ordinary least squares estimates were found. An algorithm in R using instruction nls (nonlinear least squares) was used for the former, and instruction lm (linear model) for the last expression. Experiments were made at 856 kHz and 30 W/L. BP1 initial concentrations were in the range 5.01 - 75.05 µM. Results are shown in Figure 36.

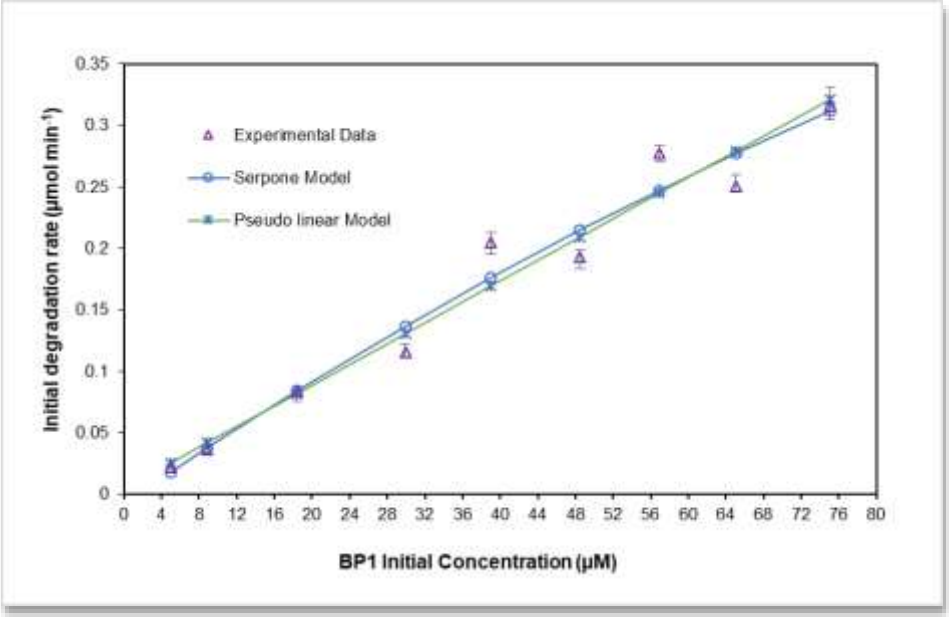


*Figure 36. Kinetic models for BP1 degradation. Experiments made at frequency: 856 kHz, power density: 30 W/L Solution volume: 300 mL, T: 25°C±2°C.*

Regression parameters, t statistic probabilities (p), coefficient of determination ($R^2$), and Sum of Squared errors (SSE) for estimated parameters are shown in Table 7.

*Table 7. Parameters of the Kinetic Models for BP1 degradation*

| Model | Parameters | $R^2$ | SSE |
|---|---|---|---|
| **Equation (54)** | $k_{BP1}K_{BP1}$: 0.005356 (t value: 2.985, p= 0.0245)<br>$K_{BP1}$: 0.003382 (t value: 0.656, p= 0.5359) | | 0.023 |
| **Equation (63)** | $k_{b-BP1}$: 0.0042214 (t value: 13.33, p= 3.13e-6) | 0.9621 | 0.0223 |

The squared sum of residues (SSE) had similar values for both models showing a good fit of the data. Pseudo first order model (equation (*63*)) had a good correlation coefficient and a good p value for t statistics for equation parameter. The nonlinear model presented in equation (*54*) had a low value for the t value of the parameter in the denominator. This show there is no statistical evidence for the validity of this parameter and consequently of this model.

Consequently, a conclusion can be made that BP1 degradation kinetics by US follows a pseudo first order model, and that reaction mechanisms can be explained according to the approach proposed by Serpone et al. (1994)

### 6.3.5 Degradation byproducts

To find possible degradation byproducts, reaction was made at a frequency of 574 kHz, a power density of 30 W/L, and pulsed mode with ST/PT: 10 ms/10 ms, for an initial BP1 concentration of 19.2 mg/L. 200 mL form the reactor were withdrawn and Solid Phase extraction was made according to the procedure specified in Materials and Methods Section.

In this way, benzaldehyde was obtained in the extract made for solutions after 30 and 120 radiation minutes being its abundance 3 times at 120 minutes than at 30 minutes. Its formation can be explained by the cleavage between the aromatic ring with carbonyl group and the aromatic ring containing the hydroxyl groups as shown in Figure 37. Thus, benzaldehyde can be generated by non-specific OH attack over oxidized BP1 intermediates after this cleavage. Further oxidation generates benzoic acid, which was identified in the extract made for the solution after 120 radiation minutes. (Vione et al. 2013) also found benzoic acid as a degradation byproduct in their study for BP3 nitrate photolysis, (•OH as reactive species) and with nitrate + bicarbonate (involving •OH and/or $CO_3^{-\bullet}$)(Vione et al. 2013).

Hydroxyl groups make the benzene ring very reactive. Conversely, the CO group is a deactivator of the benzene ring. In this way, the aromatic ring containing the hydroxyl groups is highly reactive, and its opening can be carried out after or before the benzene's ring cleavage. Acetophenone was identified in the extract made of the solution after 30 and 120 radiation minutes, being its abundance according to the peak area 2.5 times at 120 than at 30 minutes. Its origin can be explained by the direct attack of OH radicals on the hydroxylated aromatic ring which suffers opening by this attack, or by reaction between the aromatic ring with CO group and methyl radicals coming from the decomposition of the hydroxylated ring. A similar mechanism can generate 1 phenyl-2 buten-1-one, which was found at 30 and 120

minutes of reaction, with very similar areas at both times. And also can generate 1-phenyl, 1-butanone, found at 30 and 120 reaction minutes with similar areas.

A general proposed mechanism is shown in Figure 37. GC-MS spectrums are presented in Figure 66 in Appendix 1.

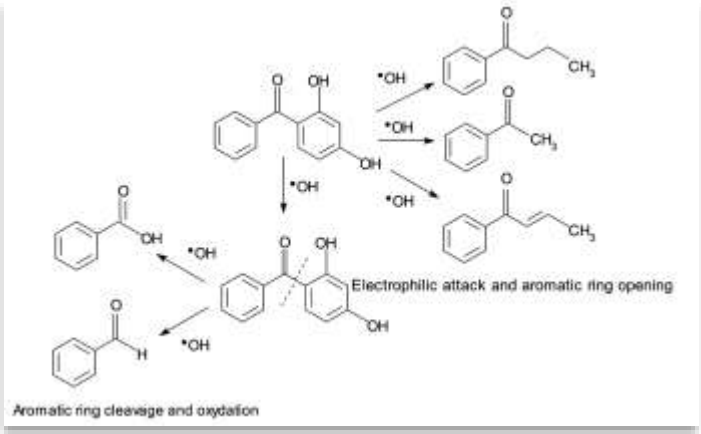


*Figure 37. General proposed mechanism for BP1 degradation by US*

### 6.3.6 Toxicity

Microtox® equipment was used for making ecotoxicity assays in the presence of BP1 in aqueous solution. The toxic substances affect cellular respiration of this bacteria diminishing bioluminescence. The 81.9% Basic Test was used as shown in the Guide to Microtox M500 procedure for acute toxicity, and toxicity was expressed as EC50: the effective concentration of pollutant concentration producing a 50% reduction in light emission. (Onorati and Mecozzi 2004)

For this assay, initial BP1 concentration used was 25 mg/L in deionized water and effect % over luminescence was measured after five and 15 minutes of bacteria exposition to the pollutant solution. There was not a significant difference in the response for 15 minutes to that of five minutes. Measured $EC_{50}$ was 11.5 mg/L.

For analyzing toxicity path as US degradation occurred, a Microtox 81.9% Screening Test was used. For a BP1 solution with an initial concentration of 25 mg/L, treated at 574 kHz, 30 W/L, pulsed mode (PT/ST: 10/10) during 120 minutes. 3 mL samples were withdrawn at different times and analyzed. Results for relative effect % after 15 minutes are shown in Figure 38**¡Error! No se encuentra el origen de la referencia.**. Toxicity profile shows that toxicity slightly increases as BP1 concentration decreases, having a maximum at 90 minutes of reaction, being 30% more toxic than BP1 solution, after 80% of BP1 depletion. Afterwards, toxicity decreases, achieving a final

Toxicity 13.8% higher than initial when BP1 is totally depleted. Acetophenone, and benzaldehyde, two of the persistent degradation byproducts, have a $EC_{50}$ for this assay of 883 and 24 mg/L respectively (Jennings et al. 2001). Their toxicity values are much lower than that of BP1. Benzoic acid has a slightly higher toxicity than BP1 ($EC_{50}$: 9.93 mg/L)(Zhao et al. 1998), and toxicity values by this assay for 1 phenyl-2 buten-1-one, and 1-phenyl, 1-butanone were not found in the literature. Therefore, taking into account that BP1 is not very toxic, the fact that toxicity does not change or decrease during the treatment process is not an important factor to consider for determining its relevance for BP1 treatment. However, further research about degradation byproducts is needed.

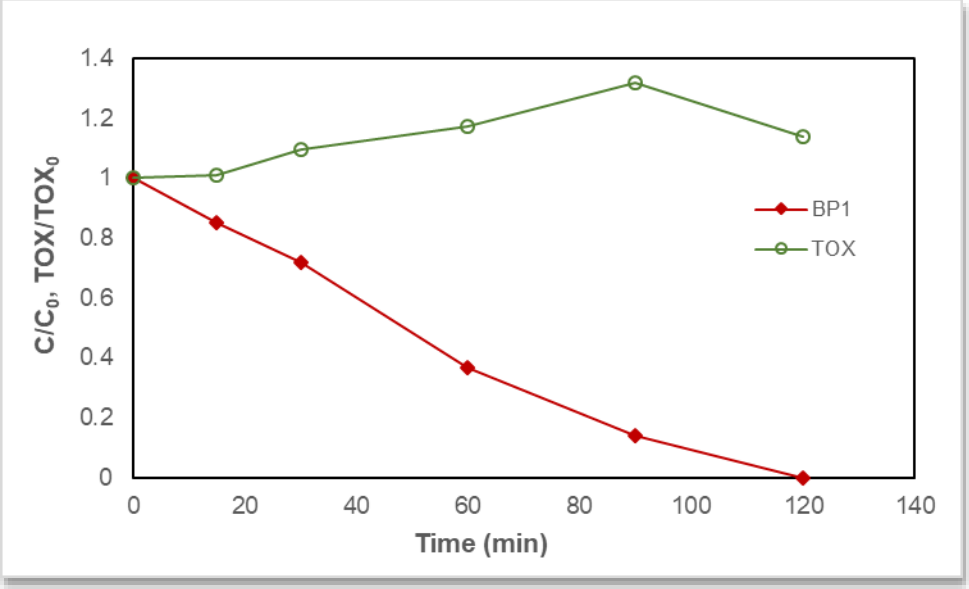


*Figure 38. Toxicity profile for BP1 degradation. Experiments made at frequency: 856 kHz, power density: 30 W/L. Initial BP1 concentration: 25 mg/L. Solution volume: 300 mL, T: 25°C±2°C.*

## 6.4 Conclusions

Optimum frequency for BP1 degradation was 854 kHz and optimum power value was 40 W/L. For these values, initial degradation rate was 0.105 µmol/L min. Two different kinetic models for BP1 degradation at natural pH were proposed based on the models found in other studies for US degradation of organic pollutants. These models considered that reaction with OH radicals takes place at the bubble's surface. One was based on a saturation type reaction over the bubble surface while the other took into account that radical reactions could take place over the bubble surface or in the bulk solution. A pseudo-linear kinetic model resulting from the application of

the second mechanism had the best statistical fit for this system. The kinetic constant had a value of 0.00422 $min^{-1}$, (854kHz, 40 W/L). Initial reaction rates for PW US was 56.7% higher than those for continuous US, and inhibition was 41% for methanol, and 9.7% for sodium acetate, when used as radical scavengers. Thus, the conclusion is made that degradation takes place over the bubble surface, and a small fraction in the bulk fluid surrounding the bubble surface. In the same way, its degradation rate depends on BP1 bulk concentration, the rate of generation and recombination of radicals, and the rate of reaction between TCS and OH radicals.

Toxicity $EC_{50}$ value measured in the Microtox® toxicity test was 11.5 mg/L. Toxicity increased continuously with BP1 depletion. After BP1 total degradation toxicity increased until a value 30% higher than initial, achieving a final Toxicity 13.8% higher than initial when BP1 is totally depleted, and showing that by-products with similar and higher toxicity than BP1 are being generated.

Five possible degradation byproducts were found, among them, benzaldehyde, acetophenone, benzoic acid, 1 phenyl-2 buten-1-one and 1-phenyl, 1-butanone.

# Chapter 7

# 7 COMPARATIVE STUDY OF TRICLOSAN, BENZOPHENONE 1 AND BENZOPHENONE 3 DEGRADATION IN WATER BY UV/$H_2O_2$/US PROCESSES

## 7.1 Abstract

Comparison of initial degradation rates after 15 minutes of reaction was made for UV, $H_2O_2$, US, and their combinations for the three compounds analyzed in this research. An UV lamp at 254 nm, and high frequency ultrasound (574kHz) were used. Pollutant initial concentration for all the experiments was 5.18 µmol/L, hydrogen peroxide/compound ratio was 20. For these compounds it was found that US was more effective degrading the most hydrophobic compound, in this case, triclosan. For this compound the addition of UV radiation and hydrogen peroxide had just marginal effects. For BP1, the less hydrophobic compound, interesting synergies were found with peroxide and UV radiation. The highest synergies were found, for $H_2O_2$/UV and $H_2O_2$/UV/US BP1 degradation, with values of 7.5 and 6 respectively. Methodology and experimental setup are described in section 3.2.4, runs were repeated three times.

## 7.2 Results and Discussion

### 7.2.1 Triclosan Degradation by combined processes

Figure 39 shows initial rates and degradation percent after 15 minutes of reaction for the processes used.

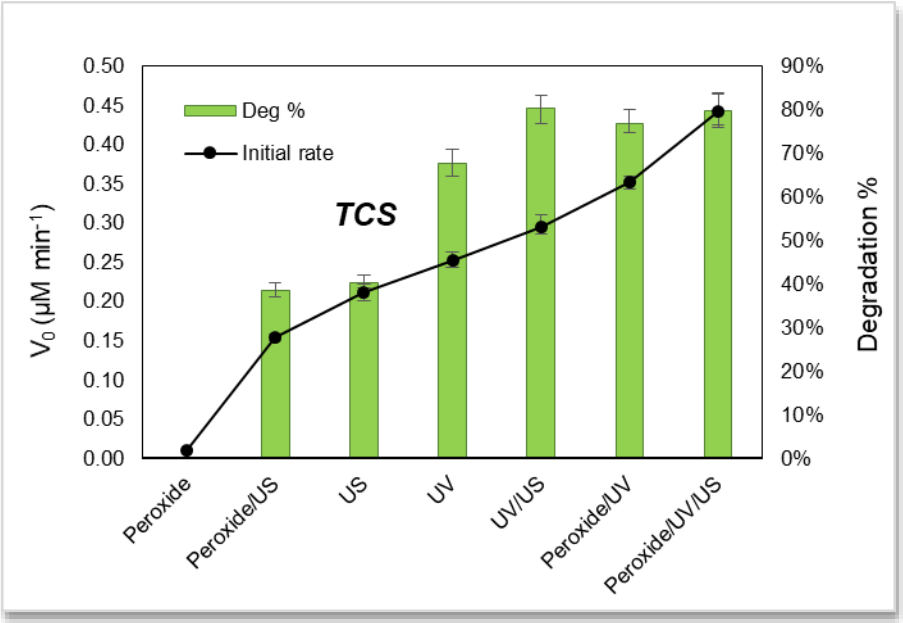


*Figure 39. Initial rate and degradation percent after 15 mins of reaction. Solution volume: 300 mL, $C_0$: 5.18µmol/L, T: 25°C±2°C UV: λ: 254 nm; US: 574 kHz, 30 W/L, PT/ST: 20/20; $H_2O_2$/$TCS_0$: 20*

The processes analyzed were: ultrasound alone, hydrogen peroxide, UV radiation and their combinations. For triclosan, peroxide treatment alone did not have any effect, followed by $H_2O_2$/US as the processes with the lowest efficiency. US degradation rate was in third place. This is according to previous studies that showed TCS is very susceptible for US degradation because of its hydrophobicity and diffusivity, and readily degrades at high frequency US values (Vega et al. 2018). That study showed that TCS degradation occurred by OH radicals attack, mainly over the US formed bubble surface. (Rozas et al. 2016), also used $H_2O_2$/UV treatment for TCS degradation, and found very similar efficiencies using UV alone and $H_2O_2$.

UV radiation had the fourth fastest initial degradation rate. Several studies have been made about photolytic degradation of Triclosan, showing that it is easily degraded by light radiation. UV radiation at 254 nm (Wong-Wah-Chung et al. 2007) has shown to be more effective for degrading Triclosan than UV radiation at 365 nm (Yu et al. 2006). In the environment, photodegradation is one of the main mechanisms of TCS elimination. Its degradation has been observed in freshwater and seawater samples, with a half-life relatively short (4-8 days), and with the formation of toxic byproducts such as dichlorodibenzodioxin and thrichlorodibenzodioxin (Latch et al. 2005a)(Sanchez-Prado et al. 2006)(Aranami and Readman 2007)(Son et al. 2009)(Zhang et al. 2015).

However, these results cannot be conclusive by themselves, to know what process is the most efficient for degrading TCS, because the extent of degradation depends on the power level for US, and on the characteristics of the radiation for UV and $H_2O_2$ concentration.

A good comparative analysis can be made for hybrid process using the concept of synergy. It was calculated according to the following equation:

$$S = \frac{Initial\ rate\ _{US+perox}}{Initial\ rate_{US} + Initial\ rate_{perox}} \quad (64)$$

This equation applies for initial rates, but synergies were calculated also using degradation percent rather than initial rates. Synergies are shown in Figure 40. In this figure, it can be noticed that the only two process that have a synergistic effect when combined are peroxide and UV (S > 1). Peroxide alone that does not have any effect on TCS molecules; but, when exposed to UV radiation, it is converted to OH radicals that degrade TCS. UV also degrades TCS molecules directly, having an overall effect that is greater than the UV radiation effect alone.

Interestingly, a combination of peroxide and US does not have a synergistic effect; that is, the sum of their combined effects is less than the sum of their separate effects. US treatment alone has a slightly higher rate than in combination. This can be explained because TCS is highly hydrophobic and tends to accumulate on the bubble surface, while $H_2O_2$ and OH radicals generated by US effect over it, are mainly in the bulk fluid. This means that OH radicals coming from a peroxide decomposition do not have effect over TCS molecules. In addition, a scavenger effect could be occurring on the OH radicals generated by hydrogen peroxide, according to (Babuponnusami and Muthukumar 2014a).

Similarly, UV/US treatment did not have synergy. Scavenging reactions could be the responsible, but further research is needed to fully understand this effect.

Mineralization results could be very different due to the fact that hydrogen peroxide dissociation occurs mainly in the bulk of the solution (Pétrier 2015a), where most of degradation byproducts are, because of their higher hydrophobicity than that of TCS.

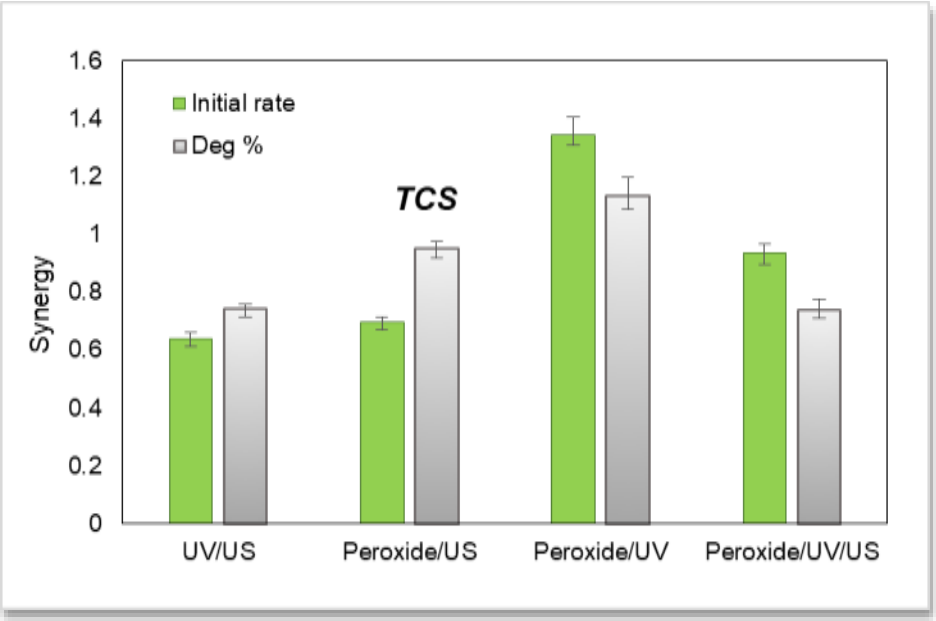


*Figure 40. Synergy values for initial rate and degradation percent after 15 mins of reaction. Solution volume: 300 mL, $C_0$: 5.18µmol/L, T: 25°C±2°C UV: λ: 254 nm; US: 574 kHz, 30 W/L, PT/ST: 20/20; $H_2O_2/TCS_0$: 20*

### 7.2.2 Benzophenone 1 Degradation by combined processes

Figure 41 shows initial rates and degradation percent after 15 minutes of reaction for benzophenone 1 degradation. UV and peroxide processes did not have an appreciable degradation in 15 treatment minutes.

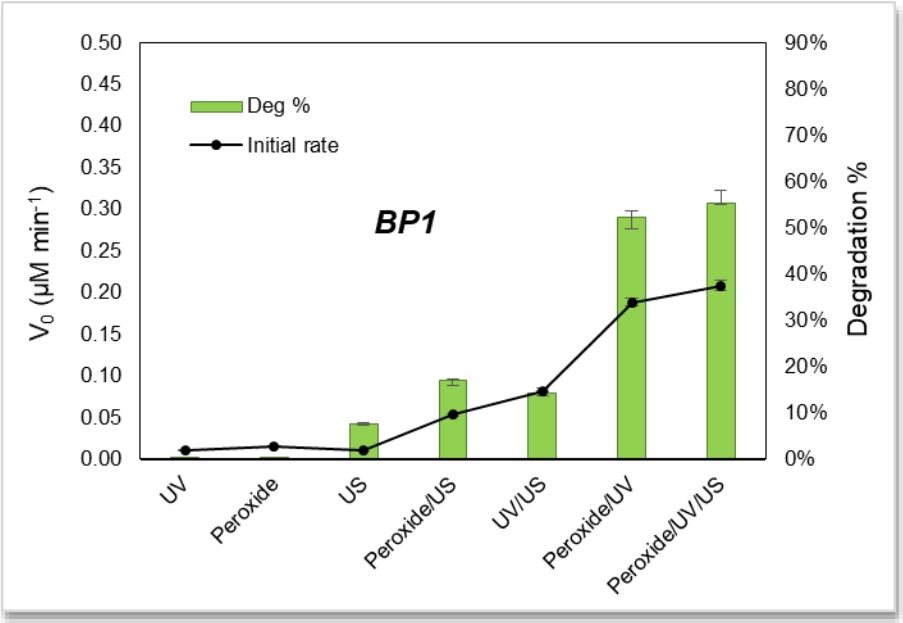


*Figure 41. Initial rate and degradation percent after 15 mins of reaction. Solution volume: 300 mL, $C_0$: 5.18µmol/L, T: 25°C±2°C UV: λ: 254 nm; US: 574 kHz, 30 W/L, PT/ST: 20/20; $H_2O_2$/$BP1_0$:20*

From Figure 42, it can be noticed that the three compounds have low absorption of UV radiation at 254 nm. (Gago-Ferrero et al. 2012) used a SunTest apparatus from Heraeus (Hanan, Germany) equipped with a Xenon arc lamp providing a light intensity of 400 W/m², and obtained a degradation for a BP1 solution at low concentration (250 µg/L) in 24 h, showing UV radiation has an effect, but degradation rates are low for this compound.

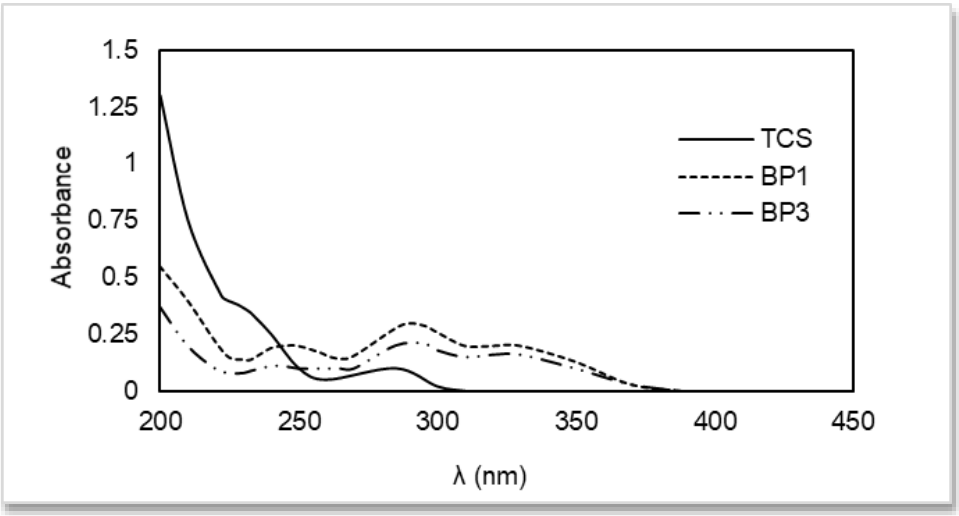


*Figure 42. Absorbance for TCS, BP1 and BP3*

Conversely, a combination of peroxide and US; and also peroxide and UV, showed an important enhancement for BP1 degradation efficiency. For peroxide/US, with an S value of 2 (Figure 43), enhancement can be explained by the peroxide conversion to OH radicals under the effect of US radiation. Opposite to TCS, that is more hydrophobic, BP1 could have an advantage of the OH radical's presence in the bubble in the bulk fluid, coming from peroxide reaction by US.

As shown in Figure 43, a synergy value of 6-7 was found by combining peroxide and UV treatments. A high conversion rate of $H_2O_2$ to OH radicals by UV radiation (254 nm) is expected to be the main reason. The combination of UV and US also had a positive synergistic effect (~2), showing that mass transfer could be a limiting step in UV radiation degradation, but $H_2O_2$ decomposition by UV radiation could have an improved effect over US radiation alone. Synergistic index for the three combined processes is slightly smaller than that for the peroxide/UV process. This means that using US, no additional enhancement is achieved. A probable reason is that the effect of OH radicals generation enhancement due to the UV effect over peroxide is much higher than that of mass transfer improvement due to turbulence generated by US. Also, it could be that a scavenging effect of OH radicals by peroxide. Conclusion was made that under experimental conditions of this study, the best process for degrading BP1 is peroxide/UV.

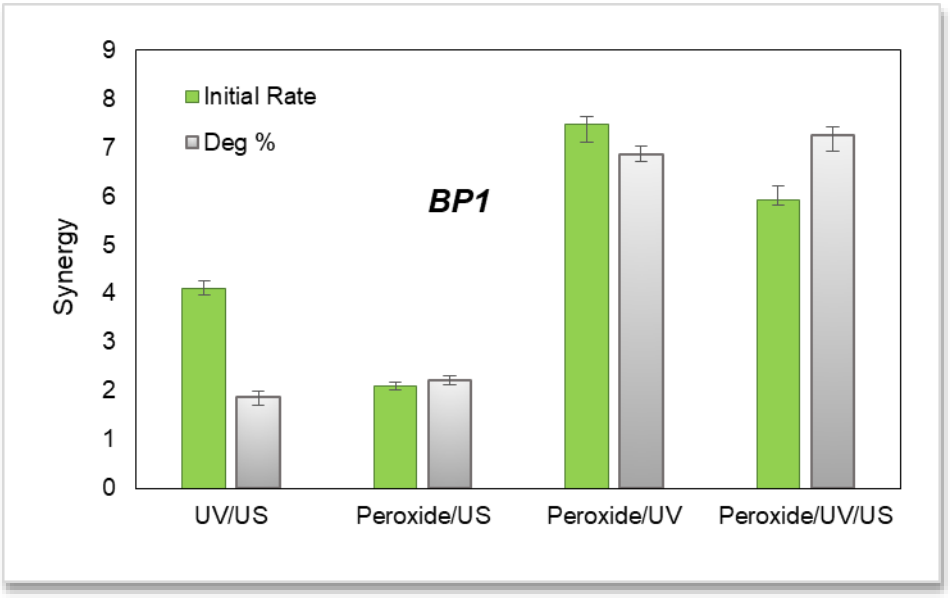


*Figure 43. Synergy values for initial rate and degradation percent after 15 mins of reaction. Solution volume: 300 mL, $C_0$: 5.18µmol/L, T: 25°C±2°C UV: λ: 254 nm; US: 574 kHz, 30 W/L, PT/ST: 20/20; $H_2O_2/BP1_0$: 20*

### 7.2.3 Benzophenone 3 degradation by combined processes

Figure 44 show results for the processes used for Benzophenone 3.

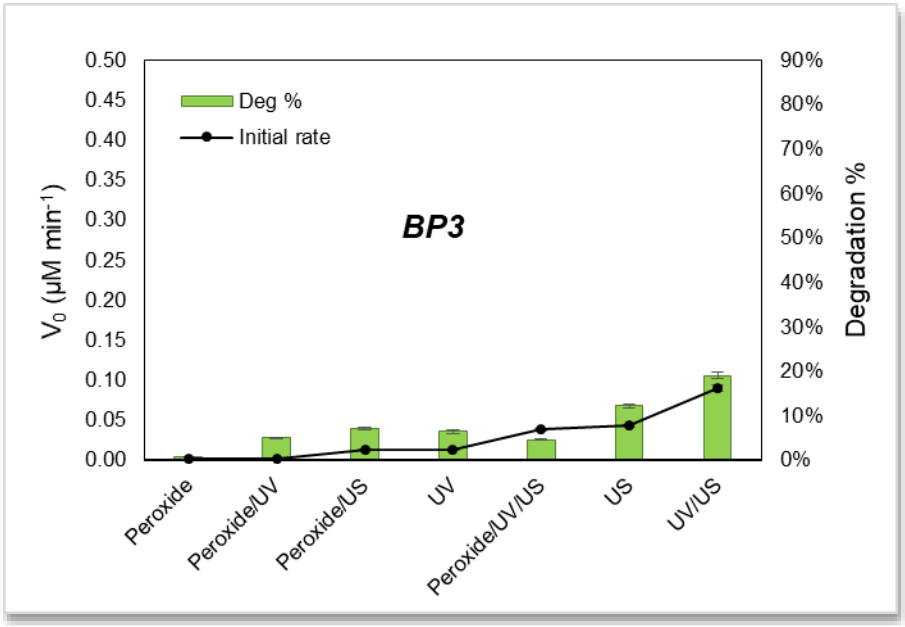


*Figure 44. Initial rate and degradation percent after 15 mins of reaction. Solution volume: 300 mL, $C_0$: 5.18µmol/L, T: 25°C±2°C UV: λ: 254 nm; US: 574 kHz, 30 W/L, PT/ST: 20/20; $H_2O_2$/$BP3_0$: 20*

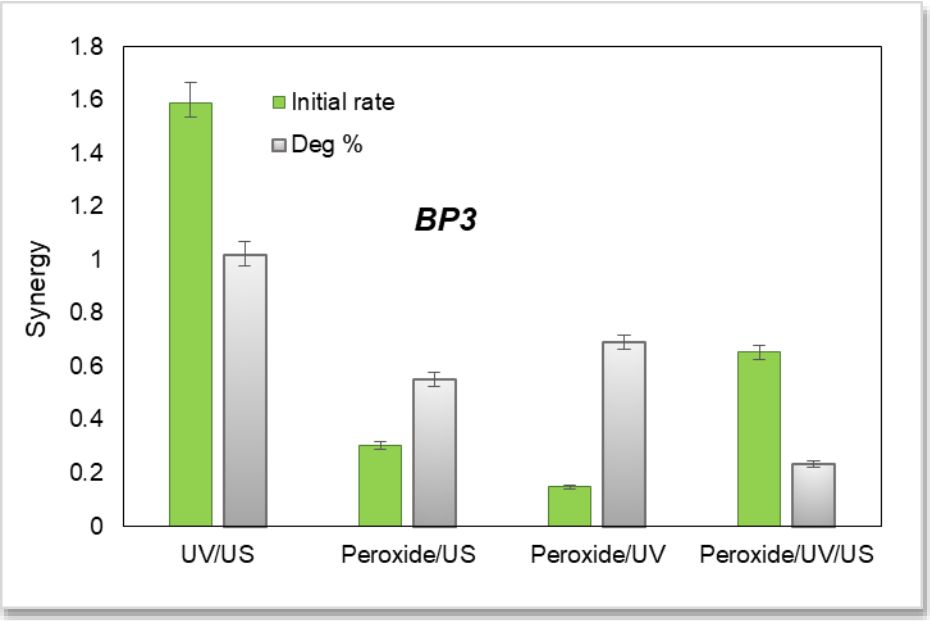


*Figure 45. Synergy values for initial rate and degradation percent after 15 mins of reaction. Solution volume: 300 mL, $C_0$: 5.18µmol/L, T: 25°C±2°C UV: λ: 254 nm; US: 574 kHz, 30 W/L, PT/ST: 20/20; $H_2O_2/BP3_0$: 20*

Peroxide alone, and its combination with US and UV, showed the lowest degradation rates. UV radiation was in the middle of the range for degradation rates, followed by US and UV/US. In general, degradation rates for BP3 were the lowest for the three compounds under analysis. But, opposite to the others, peroxide combined with US and UV did not give the best results. BP3 has shown to be photostable under UV and solar radiation (Liu et al. 2011)(Semones et al. 2017), and for US treatment, its degradation rate is higher than that for BP1 but lower than that for TCS. Its hydrophobicity and diffusivity is in the middle of the other compounds. In this case, the results found for the process with peroxide, in which degradation rates are lower than those for UV and US alone, do not have a straightforward explanation. The reason for these results could be related with the consumption of OH radicals by subproducts generated. The reason why US and US/UV process are the best for this compound could be indicating that BP3 is preferentially degraded over the bubble surface by US generated OH radicals. Also, that it is being degraded by UV radiation directly, more than the generated byproducts. Further research is recommended to clearly stablish the reason for these results.

## 7.3 Conclusions

Treatment under US, UV, $H_2O_2$ and their possible combinations was made for three emerging pollutants: TCS, BP1 and BP3. The same conditions for US power,

frequency, UV radiation, initial molar concentration, and $H_2O_2$/compound molar ratio were used, to compare between treatments and between compounds.

Initial degradation rates for US treatment were in this order: TCS: 0.212 > BP3: 0.043 > BP1: 0.022 µmol/L min. Degradation rate for TCS was 4.9 times that for BP3, and 9.6 times that for BP1. For the three compounds, octanol partition coefficient, Log $K_{OW}$, related to hydrophobicity is in the following order: TCS: 4.76 > BP3: 3.8 > BP1: 3.0. And diffusivity in the following order: BP1: $6.5*10^{-6}$ > BP3:$6.0*10^{-6}$ > TCS: $5,9*10^{-6}$ $cm^2/s$, calculated according to (Hayduk and Laudie 2015). Although a general conclusion cannot be made based on these values, it can be noticed that hydrophobicity plays a very important role in US degradation efficiency in this case.

Previous studies have shown the importance of the octanol/water partition coefficients ($K_{ow}$) on US degradation efficiency of a compound; this is because highly hydrophobic molecules migrate more readily to bubble interphase where OH radical concentrations are the highest. By the other hand, (Xiao et al. 2014) showed the diffusion effect is important for small compounds with molar volumes less than 130 ml/mol. In this study, molecules have molar volumes of 194.3, 190, and 164.4 for TCS, BP3 and BP1 respectively. Therefore, according to (Xiao et al. 2014), diffusivity did not have an important influence over US degradation rates for these high molecule sizes.

Similarly, degradation rate by UV (for TCS), was with a rate 19 times that for BP3, and 73 times that for BP1. This is confirmed by the result in literature where direct photolytic degradation is an important mechanism identified for TCS degradation, while BP1 and BP3 are photostable. To our knowledge, only one study deals with photo degradation of BP1, and it has a total degradation time of 24 hours. That study also found that BP3 was more stable to UV light than BP1, contrary to our results; but there is not a consensus in the literature about BP3 stability to UV and sunlight radiation, as shown in the discussion of this chapter.

The hybrid processes peroxide/UV showed the best synergy value for TCS and BP1. This combination was the only hybrid process with a positive synergy for TCS, with a S value for BP1 close to 7. Surprisingly, for BP3 results for hybrid process, peroxide gave the worst results. As there is not a clear explanation for this from the analysis of its degradation mechanism, the conclusion can be made that analytic interferences from degradation byproducts can be masking the results, and further research is needed to clarify the results for BP3.

For BP1, in all the processes, lower degradation rates, but higher synergy values for hybrid process, were obtained, in comparison to those for TCS. UV alone and US alone are comparatively less efficient degrading BP1 than TCS. The reason is that

BP1 is photostable, and for US, its low comparative mobility towards the bubble surface makes it more stable towards US radiation. The addition of $H_2O_2$ for degrading BP1 is very effective because OH radicals produced using this method locate in the bulk solution; whereas US is not having effect and BP1 is present. In the same way, UV decomposes very effectively $H_2O_2$ and OH radicals do have the degradation effect that UV alone does not have over BP1.

In general, for highly hydrophobic compounds, US is a very effective degradation option, and the addition of UV and $H_2O_2$ only has a marginal beneficial effect. However, for less hydrophobic compounds, important synergic effects can be obtained from the addition of $H_2O_2$ because of the generation of OH radical degrading in the bulk fluid. UV effect will depend on the compound's photostability.

# Chapter 8

# 8 COMPARATIVE STUDY OF TRICLOSAN DEGRADATION IN WATER BY ENHANCED FENTON PROCESSES

## 8.1 Abstract

Fenton combined with low frequency ultrasound (US) processes are studied and the effect of variables such as $Fe^{2+}$ concentration, $H_2O_2$ concentration and pH were analyzed. For both $Fe^{2+}$ and $H_2O_2$ concentration, a maximum concentration was found after which scavenging effects were important. However, these inhibition effects were considerably more important when US was not present. The best conditions found in a wide range of these variables were: $Fe^{2+}$/TCS: 1.25; $H_2O_2$/TCS: 25, pH: 4; a sonoFenton TCS degradation of 80.4% in 10 reaction minutes. SonoFenton had a considerably higher effect on TOC and toxicity decrease than Fenton and US alone; however, mineralization was only 30% after 30 reaction minutes and total TCS depletion for the sonoFenton process. Toxicity decreased with TCS concentration confirming results of previous studies that US and Fenton-like process generate less toxic by-products. SonoFenton showed a synergy up to 1.63 under certain conditions, showing combining both processes is a very effective way for TCS degradation.

## 8.2 Introduction

(Munoz et al. 2012) studied a Fenton-like ($H_2O_2/Fe^{3+}$) process for TCS oxidation. Song et al, (2012) (Song et al. 2012) also used a Fenton-like process for TCS oxidation, looking for reaction conditions to avoid the use of UV radiation because it generates toxic byproducts. They used $BiFeO_3$ as the heterogeneous catalyzer for $H_2O_2$ decomposition and found degradation products that were less toxic than TCS and byproducts from other advanced oxidation degradation processes. Conversely, US has been studied for TCS degradation by Sanchez-Prado et al (2008) (Sanchez-Prado et al. 2008). They analyzed the effect of water matrix over degradation rate constants using a US frequency of 80 kHz in a probe tip reactor. Naddeo et al, 2013 (Naddeo et al. 2013), used the same kind of reactor for exploring the degradation rates and extent of the reaction for low frequency US (20 kHz). Vega et al (2018)(Vega et al.

2018) studied TCS degradation by high frequency US, analyzing frequency, density power, pH, scavenger effect, and finding a reaction mechanism.

Fenton process consists in the activation of $H_2O_2$ by ferrous ions to form active oxygen species such as OH radicals that readily oxidize organic and inorganic compounds (Babuponnusami and Muthukumar 2014b). Ferrous ions oxidize to ferric ions decomposing $H_2O_2$ into OH radicals according to equation *(34)*. The ferric ions get reduced again to form ferrous ions by reaction with excess hydrogen peroxide in a reaction called Fenton-like (equation *(35)*). This reaction allows $Fe^{2+}$ regeneration giving rise to a cyclic mechanism in which ferrous ions act as the catalyzer (Babuponnusami and Muthukumar 2014b).

Sonochemical degradation is being extensively studied for removal of emerging organic pollutants in low concentrations (Rooze et al. 2013)(Goel et al. 2004). This degradation is caused by the acoustic cavitation, that is, the creation, expansion and implosive collapse of gas bubble in liquids irradiated by US waves generating OH radicals that readily react with them (Apfel 1981).

Fenton processes can be enhanced by US by the output of additional OH radicals by US cavitation and by improving the solubility of iron ions. Also, US promotes the generation of more $Fe^{2+}$ ions, raising hydroxyl radical generation, according to reaction in equation (*42*) (Ince and Ziylan 2015). Additionally, mass transfer is enhanced due to turbulent conditions created by US (Bagal and Gogate 2014a). In this work, a comparative study of TCS US degradation combined with Fenton and photoFenton process is made trying to find the suitability of using the combined processes. Synergies between these oxidation processes are studied; toxicity and byproducts generation are analyzed giving special attention to its persistence in each process. With these data, the best process in terms of degradation, mineralization rates, and eco-toxicity behavior is chosen. The effect of variables such as pH, $H_2O_2$, and $Fe^{3+}$ concentration in degradation and mineralization rates are also analyzed.

## 8.3 Results and Discussion

### 8.3.1 $Fe^{2+}$ concentration effect

Fenton processes consists mainly in the reaction of $H_2O_2$ by the oxidation of ferrous ions to ferric ions generating hydroxyl radicals as described in equation (*34*)(Babuponnusami and Muthukumar 2014a). In this process, ferric ions reduce to ferrous ions by the action of excess $H_2O_2$ shown in equation (*35*). This iron reduction

is slower than oxidation reaction, but both processes together generate a cyclic process in which ferrous ions act as catalyzers.

In Fenton reactions OH radicals are the main responsible for degradation. However, these radicals can be scavenged by ferrous ions, according to the following reaction:

$$Fe^{2+} + HO^{*} \rightarrow Fe^{3+} + OH^{-} \quad (65)$$

This is the reason why although at high ferrous ion concentrations, high degradation rates are usually found, some authors report a marginal increase after certain ferrous ion concentration levels. Additionally, this high concentration generates an increase in the content of total dissolved solids and increases the possibility of iron precipitation. $Fe^{2+}$/compound ratios from 0.01 to 1 have been used in previous studies for Fenton degradation of phenol, 2-chlorophenol and 2,4-dichlorophenol (Chamarro et al. 2001; Siedlecka and Stepnowski 2005). In this research the analyzed range for $Fe^{2+}$/compound ratio was between 0.058 and 1.154.

Results for initial degradation rates and degradation percent after 10 minutes are shown in Figure 46**¡Error! No se encuentra el origen de la referencia.**.

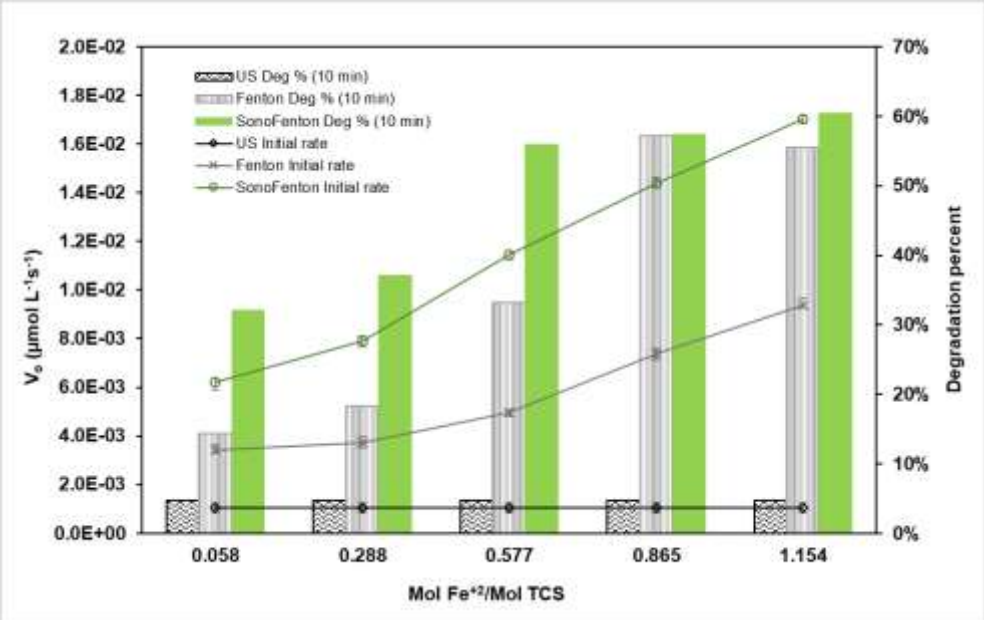


*Figure 46. TCS degradation results varying Fe $^{2+}$/TCS ratio. Reaction vol: 300 mL, $[TCS]_0$: 4.5 µmol/L, Mol $H_2O_2$:Mol TCS: 11.5, pH: 3, Temp: 25±2°C, US frequency: 40 kHz, US power density: 36.9 W/L*

Initial TCS concentration was 4.5 µmol/L, and reaction pH was 3. The highest initial degradation rate found was 7.66 x $10^{-3}$ µmol $L^{-1}$ $s^{-1}$, and highest degradation percent

after 10 minutes of reaction was 60.4%. This occurred for sonoFenton process made at a $Fe^{2+}$/TCS ratio of 1.154. In this study, the inhibitory effect of high $Fe^{2+}$ concentrations was observed after a $Fe^{2+}$/TCS ratio of 0,856.

Additionally, synergy for the combined processes was calculated according to the following equation:

$$S = \frac{Initial\ rate\ _{US+Fenton}}{Initial\ rate_{US} + Initial\ rate_{Fenton}} \quad (66)$$

This equation applies for initial rates, but synergies were calculated also using degradation percent rather than initial rates. For all the $Fe^{2+}$/TCS ratios calculated, synergies were around or more than 1 as shown in Figure 47. For $Fe^{2+}$/TCS ratios below 0.577, the initial degradation rate and degradation percent of the combined process is more than the sum of the rates of each process made separately. From this, it was concluded there is a synergic effect when combining US and Fenton for TCS degradation for low ferrous ions concentrations.

Degradation efficiencies were in the order: SonoFenton>Fenton>US, for all the $Fe^{2+}$/TCS ratios used. It can be concluded that US enhances the Fenton process, and additionally there is an interesting synergy between both processes.

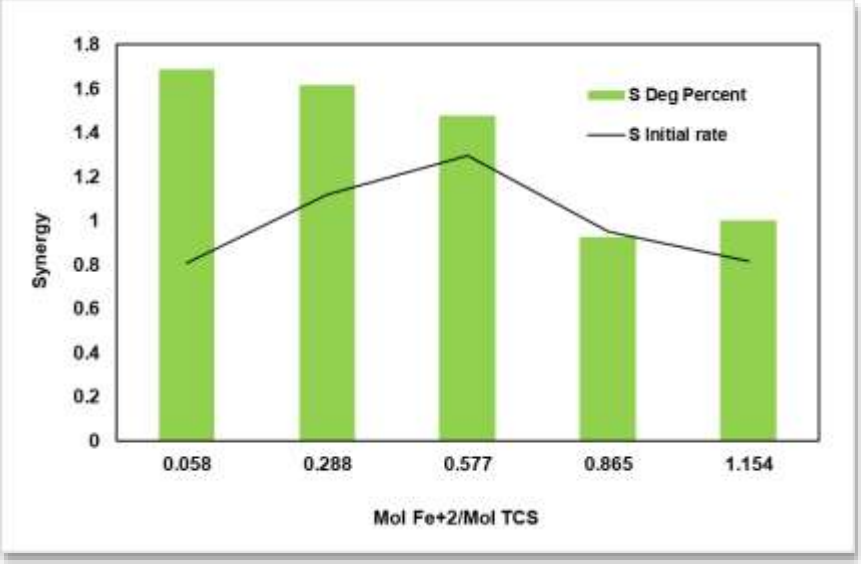


*Figure 47. Synergy varying Fe 2+/TCS ratio. Reaction vol: 300 mL, [TCS]0: 4.5 µmol/L, Mol H2O2:Mol TCS: 11.5, pH: 3, Temp: 25±2oC, US frequency: 40 kHz, US power density: 36.9 W/L*

The effect of $H_2O_2$ concentration is very important for the efficiency of the Fenton reaction. In general, an increase in the amount of hydrogen peroxide will result in an increase in the pollutant degradation yield. However, at very high concentrations, $H_2O_2$ could act as an OH radical scavenger according to(Babuponnusami and Muthukumar 2014a):

$$HO^* + H_2O_2 \rightarrow HOO^* + H_2O \quad (67)$$

In this study, a range for $H_2O_2$/TCS ratio between 5.8 and 46.1 was used to analyze this effect. Results for initial degradation rates and degradation percent after 10 minutes of degradation are shown in Figure 48.

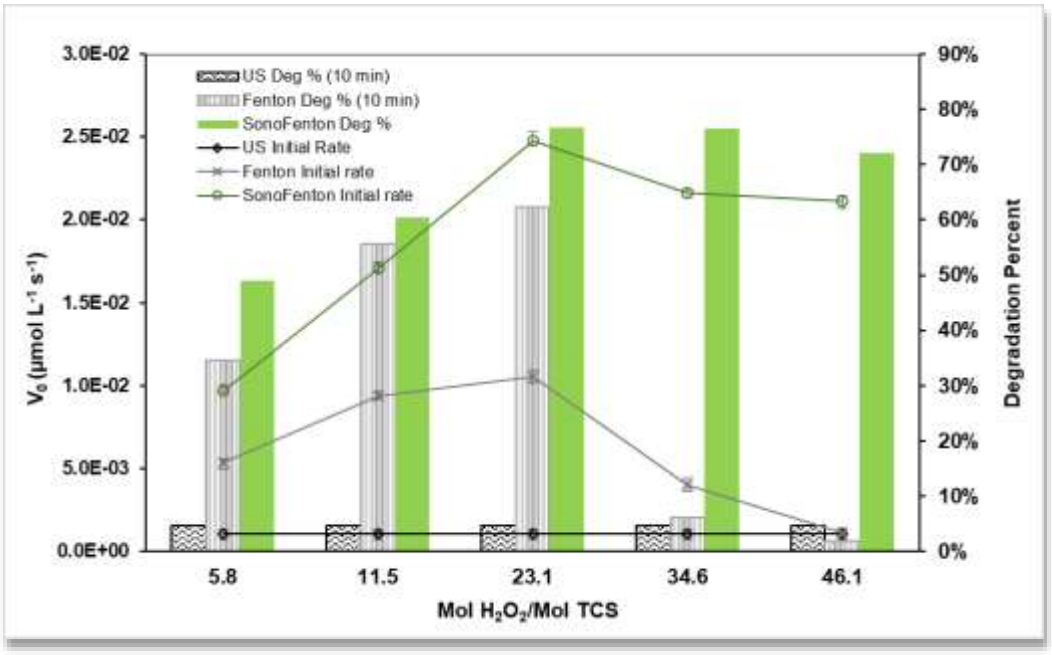


*Figure 48. TCS degradation results varying $H_2O_2$/TCS ratio. Reaction vol: 300 mL, $[TCS]_0$: 4.5 µmol/L, Mol $Fe^{2+}$:Mol TCS: 1.15, pH: 3, Temp: 25±2$_o$C, US frequency: 40 kHz, US power density: 36.9 W/L*

For Fenton and sonoFenton process the initial degradation rate and degradation percent after 10 minutes of reaction achieved maximum values at a $H_2O_2$: TCS ratio of 23.1. Moving forward, initial rates dropped considerably as shown Figure 48. In the same way, after this ratio, degradation percent after 10 minutes dropped in a dramatic way for Fenton process, but slightly for sonoFenton processes. This result confirms the scavenging effect of $H_2O_2$ for the Fenton process for TCS degradation. Babuponnusami and Muthukumar (2011) (Babuponnusami and Muthukumar 2011) studied sonoFenton process for degrading phenol, finding an optimum for

$H_2O_2$:Phenol ratio of 11. After this value, degradation rates diminished considerably, confirming the mentioned scavenging effect. Conversely, Ranjit et al (2008)(Ranjit et al. 2008) studied sonoFenton degradation of 2,4 dichlorophenol (DCP), using a narrow range for the ratio $H_2O_2$:DCP: between 6 and 14. In their research, they found no detrimental effect on degradation percent when increasing this ratio value in the studied range.

Results shown for sonoFenton processes the $H_2O_2$ scavenging effect is much lower than for the Fenton process alone. Thus, it can be concluded the synergic effect of US and Fenton is important compared to the peroxide scavenging effect, managing to counteract its negative effect to a large extent (Figure 49). This synergic effect includes OH radical production by US directly and by decomposition of $H_2O_2$ mainly at the bubble surface.

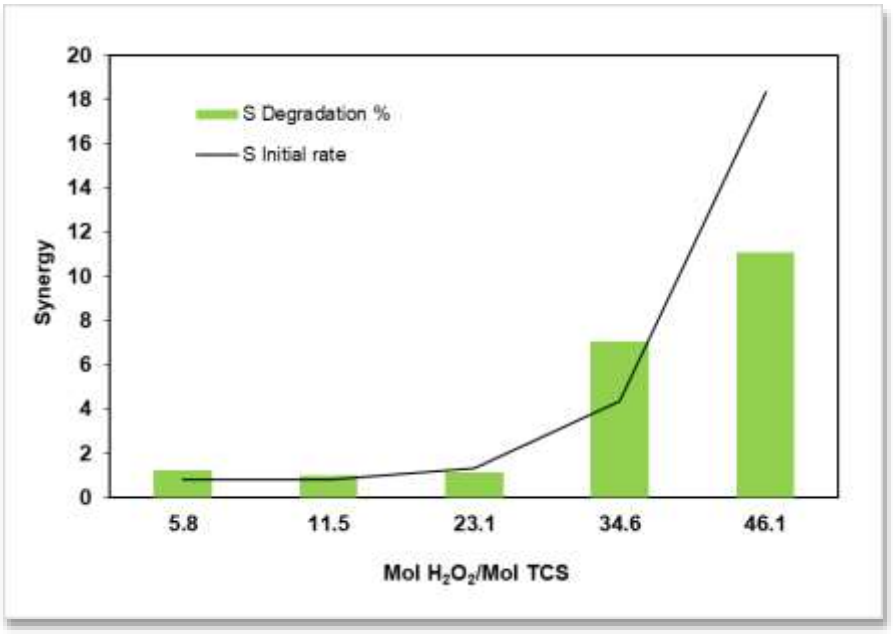


*Figure 49. Synergy varying $H_2O_2$/TCS ratio. Reaction vol: 300 mL, $[TCS]_0$: 4.5 µmol/L, Mol $Fe^{2+}$:Mol TCS: 1.15, pH: 3, Temp: 25±2°C, US frequency: 40 kHz, US power density: 36.9 W/L*

An enhancement of 41% in the degradation percent in the SonoFenton process against Fenton process was found for a $H_2O_2$/TCS ratio of 5.8; and of 23% for a $H_2O_2$/TCS ratio of 23.1 (US frequency: 40 kHz). Ranjit et al (2008)(Ranjit et al. 2008) found a 72% enhancement in DCP degradation for a $H_2O_2$:DCP ratio value of 6. Additionally, a 26% of enhancement in DCP degradation percent for a $H_2O_2$:DCP ratio of 14 (US frequency: 35 kHz) was found. Differences can be related to the US power, but this value was not reported in their study.

This is the reason synergy for this combined process is a better measure to understand the advantages of SonoFenton process versus using the two processes separately. In this case, synergy was positive for degradation percent for all the $H_2O_2$/TCS ratios with a very high value for ratios higher than 23.1. This confirms the advantage of using the combined process and the interesting effect of US when the $H_2O_2$ scavenging is strong.

### 8.3.2 pH effect

An important variable for the Fenton reaction is pH., being the optimal around 3 for most processes (Figure 50). At higher pH, the effectivity of ferrous ion is reduced due to the presence of relatively inactive iron oxohydroxides, and also due to the precipitation of ferric hydroxide. Similarly, at lower pH values, iron complex species are formed and they react more slowly with $H_2O_2$ (Babuponnusami and Muthukumar 2014a).

TCS has a pKa=7.9, and at a pH from 3 to 6.9 is almost completely in its molecular form. For the US degradation, it means molecules migrate easily towards the bubble surface where OH radicals generated by US radiation are in excess and reaction is taking place. No substantial differences in US efficiency are expected varying the pH in this range. Experiments were made at a $Fe^{2+}$/TCS ratio of 1 and $H_2O_2$/TCS ratio of 20 varying the pH between 3 and the neutral pH for TCS aqueous solution. The best initial reaction rate was for SonoFenton process at pH 3: $1.42 \times 10^{-2}$ mol $L^{-1}$ $s^{-1}$.

The best degradation percent after 10 degradation minutes was for pH 4: 80.4 %. For Fenton and SonoFenton, a similar trend was observed. After this, pH degradation efficiency begins to decay slowly for both processes. The most important thing to notice is in sonoFenton processes for a pH of 5, a similar efficiency was found than for the Fenton process at pH 3. Degradation percentages for these processes were 62.5% and 62.9%, respectively. This confirms the results found in other studies in which the use of US results in sonoFenton process with similar efficiencies than Fenton processes at higher pH values. This has obvious advantages related to posterior neutralization and also on the chemicals consumption. Ranjit et al, (2008) (Ranjit et al. 2008) found for 2,4 dichlorophenol degradation, a reduction of 50% in the $Fe^{2+}$ required, of 31% in $H_2O_2$, and similar results at pH 5 with sonoFenton process versus Fenton alone. Siddique et al (2014) (Siddique et al. 2014) also found an improvement when using US for degrading reactive Blue 19, resulting in lower $Fe^{2+}$ and $H_2O_2$ concentrations to achieve the same degradation efficiency. Synergy was between 1.02 and 1.14 for all the pH values analyzed, showing there is not an additional beneficial effect from using combined processes at different pH values under the reaction conditions.

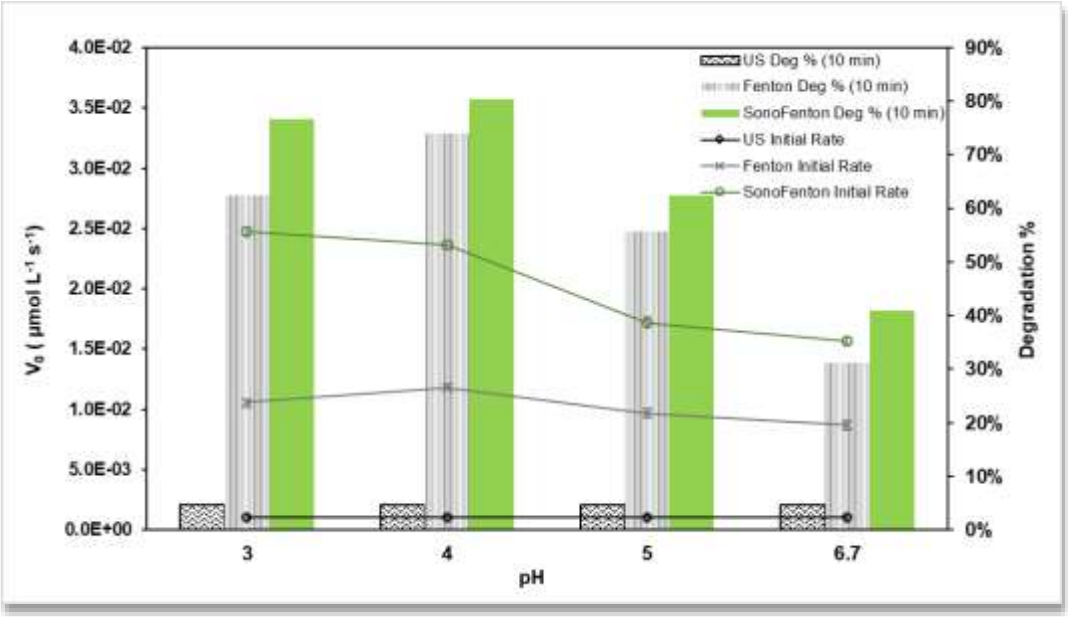


*Figure 50. TCS degradation results varying pH. Reaction vol: 300 mL, $[TCS]_0$: 4.14 µmol/L, Mol $Fe^{2+}$:Mol TCS: 1.25, Mol $H_2O_2$:Mol TCS: 25, Temp: 25±2°C, US frequency: 40 kHz, US power density: 36.9 W/L*

### 8.3.3 Mineralization

Total Organic Carbon was measured to study the degree of conversion of TCS into $CO_2$ and $H_2O$ under the three processes analyzed. Results are shown in Figure 51.

It can be noticed that mineralization rates are very slow compared to those for TCS degradation for all the processes. The best mineralization extent was obtained for the sonoFenton process, in which a 27% of mineralization was achieved after 30 mins of reaction, while TCS was totally depleted in 18 minutes. For US and Fenton mineralization was less than 5% in this time. (Munoz et al. 2012) obtained a 30% of TCS mineralization at 60 reaction minutes for fenton-like reaction, while TCS was totally depleted in 15 minutes by Fenton-like reaction. Other studies have shown SonoFenton processes are much more efficient to mineralize organic compounds such as dichlorophenol (Ranjit et al. 2008), where mineralization of SonoFenton process was between 2.4 and 3.6 times the efficiency for mineralization. Segura et al (2012)(Segura et al. 2012) found that phenol mineralization efficiency was improved more than twice by the use of US on an enhanced Fenton process.

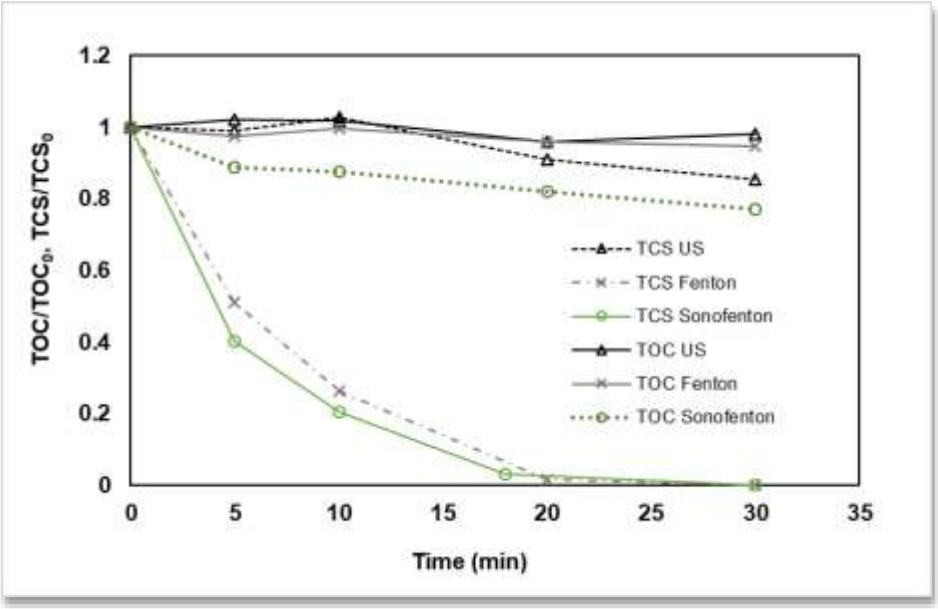


*Figure 51. TCS mineralization and degradation result. Reaction vol: 300 mL, $[TCS]_0$: 25 µmol/L, Mol $Fe^{2+}$:Mol TCS: 1, Mol $H_2O_2$:Mol TCS: 20, Temp: 25±2°C, US frequency: 40 kHz, US power density: 36.9 W/L*

### 8.3.4 Toxicity and byproducts

(Munoz et al. 2012) studied TCS degradation by Fenton-like reaction, finding that it gives rise to aromatic intermediates, mainly p-hydroquinone of TCS and 2,4-dichlorophenol, evolving to short chain organic acids. In their study, eco-toxicity measured by Microtox test had a steep decrease in a short time (more than 95% in 15 min), under the following conditions: $[TCS]_0$ = 10 mg/L, $[H_2O_2]_0$ = 25 mg/L, $[Fe^{3+}]_0$ = 1 mg/L. At this condition, TCS was totally depleted in 15 mins.

In this study, eco-toxicity decreased with TCS concentration showing that less toxic byproducts are being generated in all the processes, as shown in Figure 52.**¡Error! No se encuentra el origen de la referencia.** For a 67% of TCS degradation, $TOX/TOX_0$ had the following values: US: 0.696; Fenton: 0.72; and sonoFenton: 0.684 - very similar values for all of them. The results found in this study are according to those found in the literature for TCS degradation by other Advanced Oxidation Processes. Generated byproducts are less toxic than TCS, and its depletion generates a proportional decrease in eco-toxicity.

Analytes from reaction mixture were extracted in order to concentrate and purify them using Strata Phenyl SPE columns: (55 µm, 70 A, 200mg/3mL, in a process as indicated in Section 3.1.5. Only 2,4 dichlorophenol (DCP) was detected for Fenton

and SonoFenton processes at 50% and 60% of TCS degradation, respectively. This coincides with previous reports in that DCP is one of the main TCS degradation byproducts. In the literature for TCS degradation by both Fenton-like, and US degradation, similar mechanisms have been proposed: (Munoz et al. 2012) suggested that hydroxylation initially occurred over the aromatic ring, followed by ether bound giving rise to 2,4 dichlorophenol or 4-chlorocathecol. Further attack of OH radicals result in dichlorobenzenediols. Afterwards, organic acids are generated by the ring opening of the aromatic intermediates. For US TCS degradation, (Vega et al. 2018) proposed that 2,4 dichlorophenol was produced by reductive chlorination via electron attack and cleavage of the ether bond, followed by the ring opening to generate organic acids such as acetic and oxalic acid. In this study, the presence of DCP as a byproduct from Fenton and sonoFenton evidences the validity of these mechanisms for TCS degradation by OH radicals oxidation.

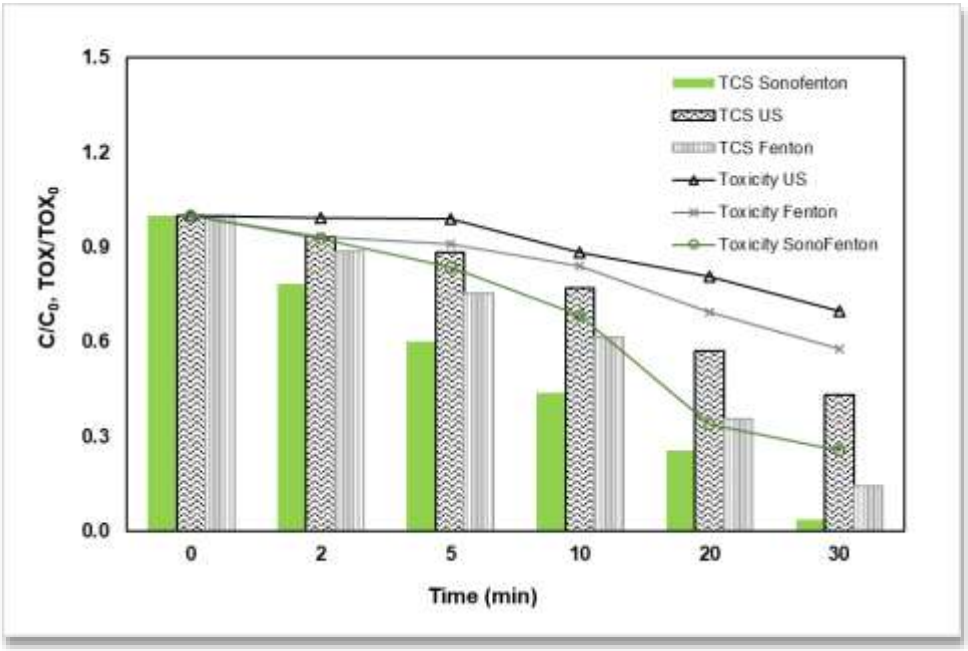


*Figure 52. Toxicity evolution. Reaction vol: 300 mL, [TCS]$_0$: 2.35 µmol/L, Mol $Fe^{2+}$:Mol TCS: 1, Mol $H_2O_2$:Mol TCS: 20, Temp: 25±2°C, US frequency: 40 kHz, US power density: 36.9 W/L*

## 8.4 Conclusions

It was demonstrated that SonoFenton processes is better than Fenton and low frequency US for degrading TCS under a wide set of conditions studied. $Fe^{2+}$ concentration had a positive effect over all the processes up to a $Fe^{2+}$/TCS ratio of 0.856, in which it doesn't further increase because of an inhibitory effect. $H_2O_2$

concentration also had a positive effect up to a $H_2O_2$/TCS ratio of 23.1. After this concentration, efficiency started decreasing because of a scavenging effect. This effect was much more important for Fenton than for sonoFenton process. Optimum Fenton process pH was 4. Additionally, under the same conditions, the same efficiency was obtained for sonoFenton process made at pH of 5 than Fenton process at a pH of 3. A synergic effect of US + Fenton was observed under almost all conditions analyzed, being more important at low $Fe^{2+}$ concentrations and high $H_2O_2$ concentrations. The highest synergy value found was 1.68 for a $Fe^{2+}$/TCS ratio of 0,058 and $H_2O_2$/TCS of 11.5. This means the US and Fenton process together was up to 68% more efficient than the sum of both efficiencies separately. Best reaction conditions analyzed in terms of degradation percent after 10 reaction minutes were $Fe^{2+}$/TCS: 1.25; $H_2O_2$/TCS: 25, pH:4; giving as a result a Fenton degradation percent after 10 minutes of reaction of 73.9% and for sonoFenton of 80.4%. An enhancement of 8.7% for the sonoFenton process versus Fenton processes; and a synergic effect of 4% were found for these conditions. Mineralization was better for sonoFenton process; being 27% at 30 reaction minutes, and of less than 5% for US and Fenton processes under the same conditions. Toxicity decreased proportionally with TCS depletion, being sonoFenton toxicity the 44%of toxicity for Fenton process after 30 reaction minutes. This shows as previously shown in other Fenton and US studies for TCS degradation, its degradation products are less toxic.

# Chapter 9

# 9 OPTIMIZATION OF BP3 ULTRASOUND DEGRADATION IN A MULTIFREQUENCY REACTOR USING RESPONSE SURFACE METHODOLOGY

## 9.1 Abstract

Response Surface Methodology was used for optimizing operating variables for a multi-frequency ultrasound reactor using BP-3 as a model compound (Figure 53). The response variable was the BP-3 degradation percent after 10 sonication minutes. Frequency at levels from 574, 856 and 1134 kHz were used. Power density, pulse time (PT), silent time (ST) and PT/ST ratio effects were also analyzed. $2^2$ and $2^3$ experimental designs were used for screening purposes and a central composite design was used for optimization. An optimum value of 79.2% was obtained for a frequency of 574 kHz, a power density of 200 W/L, and a PT/ST ratio of 10. Significant variables were frequency and power level, the first having an optimum value after which degradation decreases while power density level had a strong positive effect on the whole operational range. PT, ST, and PT/ST ratio were not significant variables although it was shown that pulsed mode ultrasound has better degradation rates than continuous mode ultrasound; the effect less significant at higher power levels.

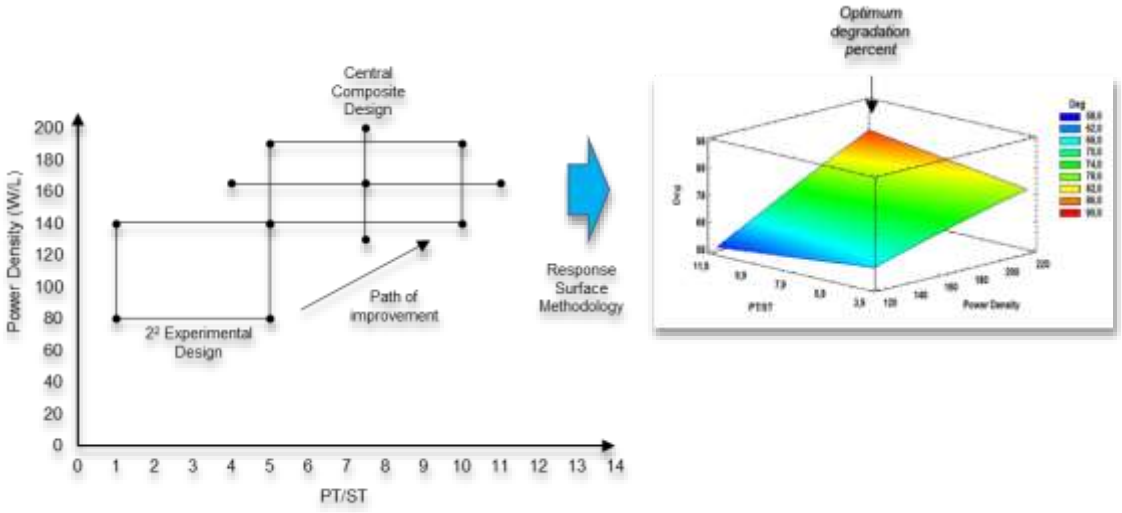


*Figure 53. Graphical Abstract. Chapter 9*

## 9.2 Introduction

Ultrasound (US) is one of the promising advanced oxidation treatments having an advantage over other treatments in that it does not use chemicals to achieve oxidation. At the same time it has good degradation and mineralization rates. Zuñiga & Peñuela (Zúñiga-Benítez et al. 2016) used ultrasound for degrading BP-3 in a probe-tip reactor obtaining 91.4% degradation at 60 minutes of reaction, for low frequency level of 20 kHz, and power level of 80.1 W, showing the ultrasound potential for degrading this compound. However, optimization of ultrasound degradation variables, and its degradation at high frequency levels is necessary in order to achieve compound degradation and/or mineralization in the shortest possible times, with the lowest energy consumption. Previous studies in ultrasound degradation for other compounds other than BP-3 have analyzed the effect of variables such as ultrasonic frequency, ultrasonic power/intensity, gas, and pH on water pollutant's ultrasound degradation, leaving one variable constant and changing the others. Only one paper reports an analysis considering the interactions for variables affecting the ultrasound degradation of carbon disulfide (Adewuyi and Oyenekan 2007). The factors analyzed in that study were ultrasonic frequency and intensity, solution temperature, and gas. It used a Taguchi statistical experimental methodology, which compared to a full factorial design, diminished considerably the number of experiments to be made. This kind of analysis must be done in order to take into account the simultaneous effects of the variables and their interactions.

Response Surface Methodology (RSM), is a collection of mathematic and statistic tools useful for modelling and analyzing systems in which a response variable is influenced by several variables. The goal of this methodology is optimizing the response variable. Initially, it has a screening step in which a $2^k$ design is used in search of the variables that have effect on the response variable using few experiments. Adding central points to this design allows checking if there is some surface curvature. Finally, an approach as the central composite design is used for characterizing the area of optimal response. In this design, axial points are added to adjust a quadratic model (Montgomery 2012).

In the present study, the analysis using RSM was applied for the optimization of ultrasound degradation for BP-3 including the pulsed mode ultrasound variables and its interaction with power and frequency for a multi-frequency ultrasound reactor. Variables analyzed were: power density (P), frequency, PT, ST, and PT/ST ratio. With RSM, we modeled and analyzed the response of interest (BP-3 degradation) due to changes in these variables looking for interactions that could be being ignored in previous studies. This approach let us understand these variable's

relationships in the search for optimum degradation rate. In this paper, we present a straightforward path for optimizing operational variables in a multi-frequency ultrasound reactor.

## 9.3 Variables for optimization

According to the hot spot theory, ultrasound degradation of pollutants is caused by the acoustic cavitation, that is, creation, expansion, and implosive collapse of gas bubbles in liquid by the effect of ultrasound irradiation (Apfel 1981). Thermal decomposition of water in the compression of the oscillating bubbles produces mainly hydroxyl free radicals (Henglein 1987). These radicals react with hydrogen molecules, oxygen peroxide, pollutants, or can recombine forming hydrogen peroxide (Henglein 1987). Solute degradation processes can take place in different sites: inside the collapsing bubbles, in the bubble/liquid interphase, and in the bulk solution (Okitsu et al. 2006).

Operation variables such as power density, frequency, and pulsed mode for US radiation have influence on pollutant degradation. When power intensity of ultrasound radiation increases, acoustic amplitude increases generating more violent collapse of the bubbles (Adewuyi and Oyenekan 2007). It is well known that power intensity could have an optimum value in which maximum pressure and temperature during collapse will give an optimal degradation rate. Higher intensities could generate bubble shielding, in which a dense cloud of bubbles attenuate the effect of the ultrasound radiation, generating higher decrease in wave intensity along the reactor length compared to that one in the optimum power (Cheng et al. 2012).

Frequency is an important variable influencing the kind of processes occurring in the solution. At low frequencies, physical effects predominate and the number of cavitation events are less than at higher frequencies (Thangavadivel et al. 2012). Also, higher bubble volumes make collapsing bubbles have higher vapor content. This effect generates less energetic implosion of bubbles resulting in lower OH radical generation. On the other hand, at high frequencies, bubble lives and sizes are smaller, resulting in a lower vapor presence at the collapsing moment, generating a more energetic bubble implosion. However, at higher frequencies, shorter rarefaction cycles could generate molecules that are not sufficiently stretched to generate the bubble. Also, at higher frequencies, overall bubble surfaces are lower, and mass transfer of the pollutants towards the bubble could dominate the overall rate. It has been shown that optimal frequency is mainly a function of the substance properties (Adewuyi and Oyenekan 2007).

Pulsed wave mode ultrasound also has an important effect in ultrasound effectiveness. This effect is related with the effectiveness of the formation, growing and imploding of the bubbles (cavitation effect), and with the ability of the pollutant molecules to diffuse to the bubble surface where degradation mainly occurs for some pollutants (kinetic-adsorption effect). During continuous wave ultrasound, bubble clusters could appear. These bubbles do not absorb enough energy to be active and the proximity of the bubbles could also increase bubble coalescence. Pulsed wave mode ultrasound makes these effects diminish (Deojay et al. 2011). It has been demonstrated for non-volatile hydrophobic compounds, that there is a dependence of the degradation rates on the pulse length, and on the interval for ultrasound radiation(Yang et al. 2005). In that study, short pulses generated insufficient activation of cavitation bubbles and longer pulses favored the surfactant accumulation over the bubble surface in a kinetic-diffusion controlled degradation mechanism. In the same way, (Neppolian et al. 2009) showed a positive effect of pulsed mode ultrasound on the oxidation of Arsenic (III) to Arsenic (IV). For mixtures of surfactants with non-surfactants, Yang et al (Yang et al. 2006) showed surfactant degradation rate significantly enhanced with pulsed ultrasound, being the concentration of reactants - and pulse interval, the principal factors affecting degradation rates.

In general, it has been shown the ability of ultrasound to generate chemically active bubbles could be dependent on the ratio of the US pulse length and pulse interval (Deojay et al. 2011) and enhancement of ultrasound during pulsed ultrasound depends on the frequency (Yang et al. 2008). However, these studies were made under a limited range of pulsing conditions and a straightforward relationship was not established. Therefore, the same authors conducted a study varying conditions for pulse length and pulse interval in a wide range (Deojay et al. 2011) for octyl benzene sulfonate ultrasound degradation. In their study, they did not find a clear trend for the degradation rate as a function of ultrasound frequency and pulse mode, despite having found there was an effect of these two variables.

## 9.4 Results

### 9.4.1 Screening Experiments

Factors in the design of experiments are independent variables that can affect the variable of analysis, in this case, BP-3 degradation percent. Compound properties influencing US degradation rates include hydrophobicity, volatility, diffusivity, and reactivity with OH radicals. BP-3 has a molecular weight of 228.1, a high Log ($K_{OW}$) of 3.8, low volatility - $K_H$ of $1.5*10^{-8}$ Atm-$m^3$/mol, and a molar volume of 190 ml/mol, so it is expected that it diffuses towards bubble interphase (Xiao et al. 2014).

Because of this, BP-3 probably is degrading in the bubble surface and could have a degradation rate improvement using pulsed mode ultrasound.

Therefore, variables analyzed were frequency level US power density (P), pulse Time, and silent time. An initial screening analysis was made for detecting variables influencing degradation percentage. Frequency values studied were 373, 574 and 856 kHz; P was set at 80 and 140 W/L, PT and ST were both set at 20 and 100 ms (Table 8). This experimental design required $2^3$ experiments, and four central point experiments were added. Experiments were made by duplicate for a total of 18 experiments for each frequency level. In total, 54 experiments were conducted at this stage. Results and ANOVA tables for these designs and all the designs in this paper can be found in Appendix 2

*Table 8. Factors and Levels for the $2^3$ factorial experimental design*

| Factor | Level Values | | |
|---|---|---|---|
| | -1 | 1 | Central point |
| P (W/L) - $X_1$ | 80 | 140 | 110 |
| PT (ms) - $X_2$ | 20 | 100 | 60 |
| ST (ms) - $X_3$ | 20 | 100 | 60 |

For making a comparison between pulsed and continuous mode ultrasound, Pulse Enhancement (PE*) was analyzed. PE is defined as (Xiao et al. 2013c):

$$PE^*(\%) = \frac{(Deg)_{PW} - (Deg)_{CW}}{(Deg)_{CW}} \times 100\% \quad (68)$$

Where $(Deg)_{PW}$ is degradation percent for pulsed mode ultrasound, $(Deg)_{CW}$ is degradation percent for pulsed mode ultrasound after 10 minutes of sonication and for the corresponding frequency and power density levels. Results for this combination of variable values are shown in Figure 54.

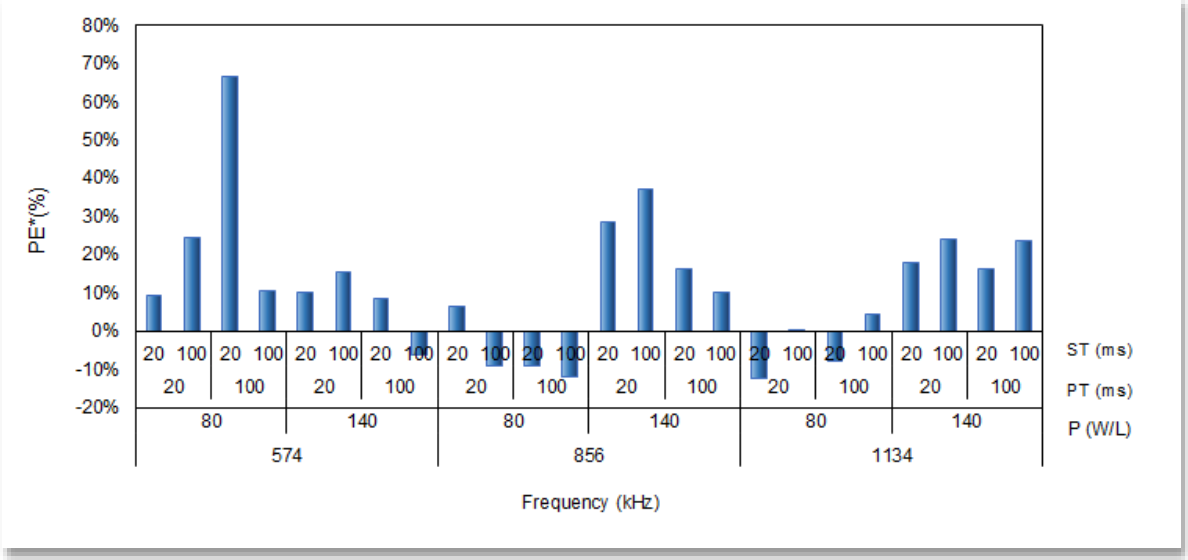


*Figure 54. Pulse Enhancement (PE*) for combination of variables Frequency, Power Density, PT and ST. Reaction Volume: 300 mL, T: 20 ±2°C, Initial BP-3 Concentration: 1 mg/L, Sonication Time: 10 min*

Response variable analyzed was degradation percent after 10 minutes of degradation under these treatments. ANOVA analysis was made in STATGRAPHICS Centurion XVI.I. For this screening analysis at a frequency of 574 kHz following conclusions were made: Power density was a significant variable, having a positive effect on degradation rates. This effect was positive and significant for all frequencies; however, the effect of PT and ST was unclear for all frequencies.

In Figure 55, maximum degradation values for this set of experiments are shown. They were 68.4% for 574 kHz; 56.2% for 856 kHz; and 51.8% for 1134 kHz. The conditions at which these maximum values were obtained were the same for the three frequency levels: power density: 140 W/L, PT: 100 ms and ST: 20 ms. In this figure it can be seen that degradation values for 574 kHz are higher than those at 856 and 1134 kHz, indicating that 574 kHz or a lower frequency value is the optimum for BP-3 degradation, and that at higher frequencies lower rates are found according to the explanation of frequency effect made in section 3. 856 and 1134 kHz resulted in similar degradation percents, Therefore, from now on only the frequency of 574 kHz was used for optimization.

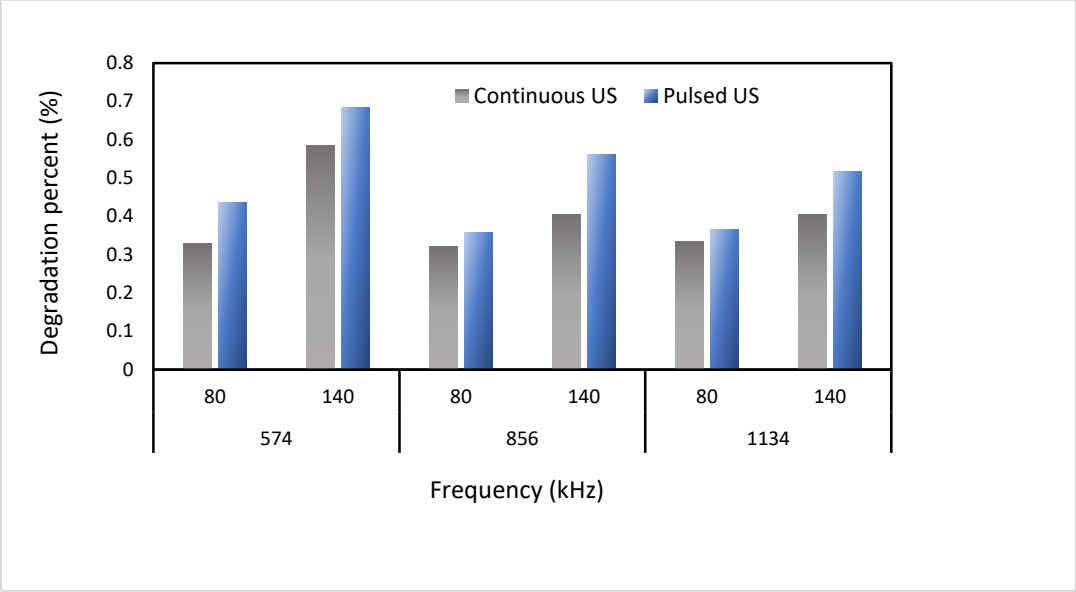


*Figure 55. Maximum degradation percent VS frequency, Power density. Pulsed US, Continuous US*

Another statistical analysis was made for frequency 574 kHz using the variable PT/ST instead of PT and ST separately, for the same results obtained in these experiments. The purpose was exploring a possible relationship with this variable according to that previously reported in literature, as explained in section 3. Variables values are shown in Table 9. Design was a factorial $2^2$, one replicate each, for a total of eight experiments. After lineal model analysis, conclusion by ANOVA results was made that power density and PT/ST were both significant variables and their effects were positive on degradation levels (Table 10). The maximum degradation value obtained (68.4%) in this case corresponded to the highest power density level, and to the highest PT/ST ratio (5).

*Table 9. Factors and levels for the $2^2$ factorial experimental design (574 kHz, BP-3 Initial Concentration: 1 mg/L, T: 25°C±2°C, ST: 20 ms)*

| Factor | Level Values | |
|---|---|---|
| | -1 | 1 |
| P (W/L) - $X_1$ | 80 | 140 |
| PT/ST - $X_2$ | 1 | 5 |

*Table 10. ANOVA for $2^2$ experimental design in Table 7*

| Source | F-Ratio | p-Value |
|---|---|---|
| A: Power Density | 503.41 | 0.0002 |

| | | |
|---|---|---|
| B: Pulse Time/Silent Time | 10.66 | 0.0469 |
| AB | 0.50 | 0.5314 |
| *R-squared* = | | *99.4216* |
| *R-squared (adjusted for d.f.)* = | | *98.6504* |

Therefore, the variables for optimization chosen were power density and PT/ST ratio for the frequency level of 574 kHz.

### 9.4.2 Optimization of Ultrasound Degradation of BP-3

By means of Response Surface Methodology, the response, in this case, degradation level can be optimized changing the variables that influence it. Response as a function of affecting variables must be set as the first step looking forward an optimum (Montgomery 2012). Values for power density and PT/ST ratio were set moving forward on the direction of degradation ascend. It means that higher power density levels and higher PT/ST values were used. ST was kept constant in 20 ms, because the highest degradation was found at this value. This is a sequential procedure, in which variables move forward along the path of response increase. Variables for the next experiment's series were set as shown in Table 11. A factorial design $2^2$ was used, each experiment was made 3 times, for a total of 12 experiments. As previously, variables such as reactor geometry, reaction volume, temperature, and initial concentration were maintained constant along the experiments.

*Table 11. Factors and levels for the $2^2$ factorial experimental design (574 kHz, BP-3 Initial Concentration: 1 mg/L, T: 25°C±2°C, ST: 20 ms)*

| Factor | Level Values | |
|---|---|---|
| | -1 | 1 |
| P (W/L) - $X_1$ | 140 | 200 |
| PT/ST - $X_2$ | 5 | 10 |

The ANOVA analysis showed that power density, PT/ST ratio, and the crossed effect power density-PT/ST were statistically significant. The linear model fits very well within the response at this range. The maximum degradation level for this new set of experiments was higher than previous maximum degradation obtained, being 78.2%. PT/ST optimum value was five and optimum power density level was 200 W/L also being the maximum possible power density level for the reactor. Power effect was positive and, contrary to the previous set of experiments in this series PT/ST ratio had a negative effect on response variable. Consequently, conclusion was made that experiment conditions were around the optimum area. In order to

use a second order model and look for the optimal conditions, a central composite design (Montgomery 2012) was used as shown in Figure 56. Values for power density were set between 130 and 200 W/L while PT/ST ratio was set between 4 and 11. Each experiment was made once, with four central points, for 12 experiments.

ANOVA results showed that only the variable power density was statistically significant. For this set of experiments, a maximum degradation level of 79.2% was obtained for P=200 W/L and a PT/ST ratio of 10. But, very similar degradation values were obtained for P= 200 W/L and PT/ST= 7.5 and for P=190 W/L and PT/ST= 5.

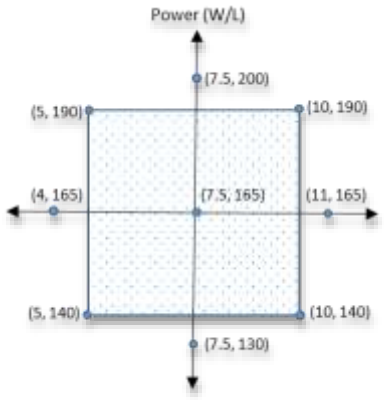


*Figure 56. Central Composite Design. Frequency: 574 kHz*

In Figure 57, it can be seen that for the a constant power level there is a weak dependence of degradation percentage with PT/ST ratio, but conversely, the effect of power density for a constant PT/ST ratio is very important. Therefore, a further analysis for the PT/ST ratio effect was made by means of a series of experiments made at two constant power density values: 140 W/L and 200 W/L, varying PT/ST ratio between 3 and 12. For each power density level, 11 treatments were made - at least - in duplicate. Total BP-3 degradation after 10 minutes of sonication and initial velocity rates obtained are shown in Figure 58**¡Error! No se encuentra el origen de la referencia.**.

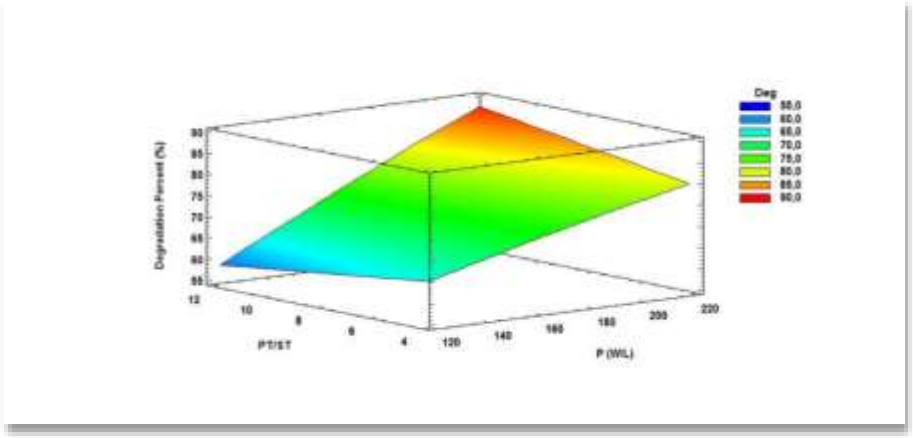


*Figure 57. Surface response for Central Composite Design. Frequency: 574 kHz*

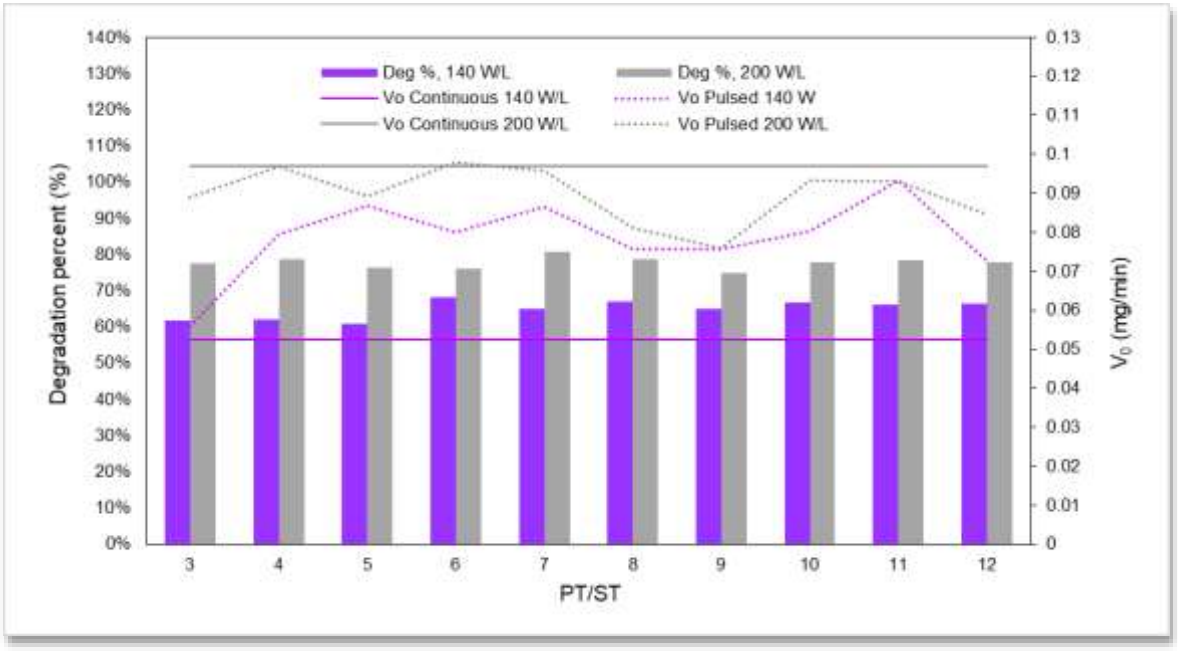


*Figure 58. BP-3 Degradation percent after 10 sonication minutes and $r_0$ vs PS/ST ratio*

A confirmation from this new set of experiments was set. There is no pattern for BP-3 degradation percent or initial degradation rates depending on the PT/ST ratio at any of the power density levels analyzed. The values are all around the same value for the whole range. For 574 kHz at a power density level of 200 W/L, a similar degradation percent was found for all the PT/ST ratios from 3 to 12. Its average value was 77.7%. For the same frequency and a power density level of 140 W/L a similar behavior was found. Degradation was almost the same for all the PT/ST ratios from 3 to 12. The average degradation percent was 64.9%, 16% lower than at 200 W/L.

However, an interesting result for the initial degradation rates for continuous mode and pulsed mode at these two power density levels was found. In Figure 58, it is shown that for P=200 W/L there is little or no difference between initial degradation rates for pulsed and continuous ultrasound.

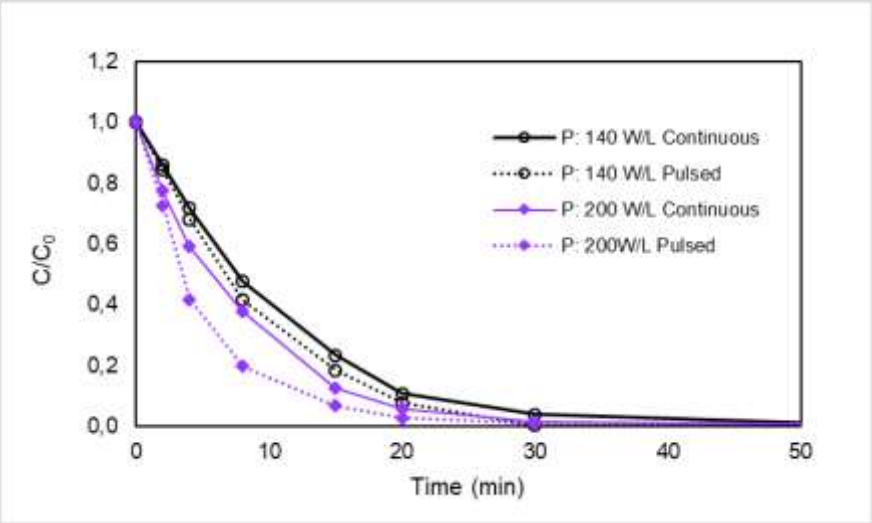


*Figure 59. BP-3 Degradation profile. Power density: 140 and 200 W/L, 574 kHz, V: 300 mL, ST: 20 ms, PT/ST: 7*

However, for P=140 W/L there is a significant increase when pulsed instead of continuous mode US is used. For 200 W/L initial degradation rate at a PT/ST ratio of 7 was 0.09 mg/min, almost the same rate for continuous mode pulse was 0.097 mg/min. However, for the lower power density level of 140 W/L, a bigger difference was found: 0.0525 mg/L for continuous mode, 0.0786 mg/L for pulsed mode (45% higher). The reason for this is that at low power densities, OH radical generation is low and mass transfer of BP-3 molecules towards the bubble surface is determinant for the overall reaction rate. In the silent times, BP-3 molecules can diffuse towards the bubble surface for reacting with OH radicals generated in the next pulse. At higher power density levels, OH radicals generation is higher and OH radicals are more readily available at the bulk fluid for reacting with BP-3 molecules, having the pulsed mode ultrasound less effect than at lower power levels. This effect is low also for higher frequencies and medium power densities but the reason is different: Even when at high frequencies the bubble surfaces are lower, and mass transfer has an important effect over the overall rate, there is also a low OH radical generation due to shorter rarefaction cycles and low power level. Consequently, OH rate generation can be as important as mass transfer in overall degradation rate. That is why pulsed US mode has a moderate effect on rates, as shown in Figure 54 for 856 and 1134 kHz and power level 80 W/L.

In Figure 59, the degradation profile for the optimum conditions found at a PT/ST ratio of 7 (which was arbitrarily chosen) is shown compared to that one for continuous mode degradation profile. Pulsed mode gives faster initial degradation, but total degradation time is 30 minutes in both cases.

## 9.5 Conclusions

Response Surface Methodology was used for optimizing BP-3 degradation in a multi-frequency ultrasound reactor. A $2^3$ experiment with two central points design was used for screening purposes analyzing the BP-3 degradation percent after 10 minutes of sonication varying power density, frequency, pulse time (PT) and silent time (ST). A conclusion was extrapolated the frequency with higher degradation percent was 574 kHz, power density had a strong positive effect on BP-3 degradation percent, PT and ST did not, but PT/ST ratio had a weak positive effect. Sequential procedure was used moving towards the area of ascent and a $2^2$ experimental design used for higher power density levels and higher PT/ST ratio. At this new variable's range, power density continued having a strong positive effect, but PT/ST ratio had a weak negative effect. Consequently, a central composite design was used for using a second order model and looked for an optimum in this area. This analysis showed that PT/ST ratio had no effect on degradation rate. Thus, two series of experiments were made, one for 140W/L and another for 200 W/L, varying the PT/ST ratio in the study area in order to find a pattern. From these experiments, it was found all the analyzed range degradation values were very similar, that is, there was no pattern depending on PT/ST ratio at any power density level. The optimum degradation percent value of 79.2% was obtained for a frequency of 574 kHz, a power density of 200 W/L, and a PT/ST ratio of 10.

Consequently, it was found the only two variables affecting degradation level were frequency and power density and that in the range in which reactor works (0-200 W/L, and 574, 856 and 1134 kHz), the power density effect is always positive. The best results were found at 574 kHz, the lowest frequency level. At higher frequencies, the detrimental effects of shorter rarefaction cycles and the BP-3 mass transfer could be the cause of the lower degradation rates. Conversely, pulsed mode ultrasound, PT, ST, and PT/ST did not affect the whole studied range. However, higher degradation rates were found for pulsed rather than continuous mode ultrasound - this effect being more important at low power densities.

# 10 CONCLUSIONS

Ultrasound radiation at high frequencies is an effective treatment for degrading organic compounds such as triclosan, benzophenone 1 and benzophenone 3 at low concentrations in water. For initial concentrations between 1 and 2 mg/L, total degradation times under the best conditions found in this study were less than 30 minutes for TCS and BP3. For BP1 total degradation time was of 120 minutes.

The effect of US generator variables such as frequency and power on the extent and degradation rate was confirmed, showing that frequency has an optimum depending on the compound properties, and power too. For triclosan and benzophenone 3 the optimum frequency was 574 kHz, and degradation rate increased over the whole operational range of the US generator. For benzophenone 1, optimum frequency was 856 kHz and optimum power density was 40 W/L.

In the literature, nonlinear models for explaining ultrasound processes kinetics are being widely used, under the assumption that an equilibrium is reached over the bubble's surface before collapse, and the reaction occurs as a Langmuir-Hinshelwood mechanism. It consists in the adsorption and desorption of the compound in the bubble surface at a rate determined by the constants of absorption and desorption, compound concentration in the bulk fluid and ratio of the reaction sites in the bubble surface occupied by the solute. In this study, for the three analyzed compounds, and under the best conditions found, high frequencies and high power densities, it was shown that this model is not applicable. Conversely, a mechanism in which rates depend on the characteristics of the US radiation (constant related to OH radicals generation), the rate constant of reaction between OH radicals and compound, depending mainly of the diffusional characteristics of the compound, and the bulk compound rate of recombination for radicals, was found as the appropriate model. Under certain assumptions, this mechanism is represented by a pseudo linear model that fitted statistically well for the three compounds.

Pulsed mode ultrasound was extensively studied looking for filling a gap in the literature in which some research has been made looking for a straightforward relationship between Pulse Enhancement and pulse characteristics, such as pulse time, silent time or the ratio PT/ST. Literature reports this last ratio has an effect over pulse enhancement, but conducted research has not been able to show a clear relationship between them. For the three compounds, pulsed mode was used with

PT and ST values between 20 and 100 ms, finding that there was a statistically initial rate enhancement around 15% for TCS (10-50 ms); 56.7% for BP1 (PT=ST=50 ms); and for BP3 for 140 W/L it was found that there was a positive enhancement in average 33% for 140 W/L varying PT/ST between 1 and 12; but for a higher power density level of 200 W/L the enhancement was slightly negative.

The experimental design applied to BP3 case, in which not only the variables PT, ST and PT/ST were analyzed keeping constant the other variables, but varying power, frequency, PT, ST and PT/ST simultaneously, showed that the enhancement effect of pulsed mode US for molecules degrading over the bubble surface is not always positive, and there is not a relationship with PT/ST variable. In general it was shown that this effect is positive and noticeable at low power density levels. Conclusion can be made that at high frequency levels there is a high probability of OH radicals to be reacting with molecules at the bulk solution, and rates are controlled by OH generation rates and compound-OH reaction rates more than by molecules diffusion.

Consequently, when OH radical generation is low, at low power densities, an interesting way of enhancing degradation rates is using pulsed mode US, taking advantage of the facts that molecules move towards the bubble's surface in the silent times. However, the way for obtaining optimum conditions for pulsed ultrasound is still not clearly understood.

Because of this, further research is needed, to fully understand this effect. It is recommended to compare results for low, medium and high power densities; and use molecules that are highly hydrophobic, and with low molecule sizes (molar vol< 130 mL/mol). The reason is that the effect is high for these compounds, making analysis easier. Once more clear conclusions could be obtained with these compounds, research could be extended to other compounds to prove the veracity of these conclusions. An interesting research possibility is to stablish a relationship between compound properties such as Log $K_{ow}$ and molar volume with Pulse Enhancement. An experimental design covering a range of high and low values for these properties versus Pulse Enhancement values could result in a quantitative relationship that could better explain this phenomenon.

Using radical scavengers such as methanol, isopropyl alcohol, and 2-propanol that scavenge OH radicals in the bulk solution and bubble surface, it could be concluded that OH radicals were mainly responsible for degradation in US processes. And, using sodium acetate as radical scavenger, it was concluded that TCS and BP3 degrade mainly at the bubble surface, while BP1 is partly degraded in the bulk solution.

pH is a variable that could influence US degradation because the deprotonated form of the molecules could be more or less reactive, or could be more hydrophilic limiting the mobility of the molecules towards the bubble surface were OH radicals are in high concentration. However, for TCS and BP3 it was checked that pH does not have any effect on degradation rates. Given the limiting step for degradation with OH radicals is the diffusion, conclusion is made that diffusivity does not change enough when deprotonated for making a difference in degradation rates.

Toxicity analysis by Microtox technique is a useful and reliable way to establish the conversion by US in more or less toxic byproducts. Given mineralization rates are very low for US, this could be an important and limiting aspect to be taken into account for its applicability alone or in combination with other techniques such as biological degradation, where toxicity to microorganisms is an important variable. For TCS, toxicity is a very important variable, if we consider it is am antimicrobial agent, and AOPs has shown to give as byproducts toxic substances such as dioxins and chlorophenols. For TCS, toxicity diminishes proportionally with TCS concentration, but after TCS is being totally depleted, toxicity rises in a steep pattern. For BP3 an interesting effect was found: toxicity diminishes at the beginning, but, after 30% of BP3 depletion, toxicity increases reaching almost twice the initial toxicity. For BP1 toxicity raised initially to be 1.4 the initial toxicity, and its final value was very similar to the initial one. It is worth to note that acute toxicity values for BP3 and BP1 are very low compared to those for TCS. And in general, toxicity has to be considered as an important variable for TCS, and also considering the concentration values found for these compounds in water treatment plants and the environment compared to their $EC_{50}$ values.

For TCS it was shown for the first time, that OH radicals generated by US radiation, attack directly TCS molecule generating 2,7/2,8-dibenzodichloro-p-dioxin. Previous studies have found this byproduct in photolytic TCS degradation, and the consensus along different researchers is that it was generated by the direct effect of UV radiation over TCS molecule. This study shows this conclusion could be partly changed, and this toxic byproduct, of principal interest for AOPs process on TCS, could be generated also by OH radical reaction, even in photolysis processes.

SPE showed to be an interesting method to isolate and concentrate degradation byproducts, and interesting conclusions were found from the possible byproducts detected by this technique. TCS, by the presence of chlorides in their structure, being ring activators, gets hydroxylated before ether bond cleavage, as shown by detection of hydroxylated byproducts such as 4-chloro-3-(4 chlorophenoxy)phenol and 2'-chloro[1,1'-biphenyl]-2,5-diol. Posterior ether bond cleavage and further oxidation by electrophilic OH attack resulted in by products such as 2,4 dichlorophenol, acetic

acid, and oxalic acid. Benzophenone 3 showed a possible reaction mechanism in which aromatic ring without substitutions is opened by OH attack generating a possible by products such as 1-(2-Hydroxy-4-methoyphenyl) propan-1-one. Also, ketone bond cleavage and posterior oxidation of aromatic rings generate benzoic, acetic and formic acids.

Benzophenone 1 also showed a possible reaction mechanism in which there is a cleavage between both aromatic rings, ring opening and further oxidation generating benzoic acid and benzaldehyde. But similarly to BP3, benzene ring containing hydroxyl groups can be oxidized and aromatic ring opened before cleavage of both aromatic rings generating acetophenone, 1 phenyl-2 buten-1-one, and 1 phenyl-2 buten-1-one.

SonoFenton degradation of TCS showed very good results for TCS depletion, but not for mineralization. Synergy between both processes showed that combining both processes is better than making degradation by each separated process or one after the other. Toxicity decreased proportionally with TCS depletion showing this process generates less toxic byproducts than TCS.

Comparative degradation for the three compounds by US, UV and $H_2O_2$ showed that the best degradation results were for $H_2O_2$/UV processes for TCS and BP1, showing a positive synergy value for both. It was showed, that BP1 and BP3 are very stable to UV radiation, and that hydrophobicity plays a very important role in the effectiveness of US degradation for these compounds, more than diffusivity or chemical structure.

# 11 REFERENCES


Adewuyi, Y. G., and Oyenekan, B. a. (2007). "Optimization of a sonochemical process using a novel reactor and Taguchi statistical experimental design methodology." *Industrial and Engineering Chemistry Research*, 46(2), 411–420.

Apfel, R. E. (1981). "7. Acoustic Cavitation." *Methods in experimental Physics*, New York, NY, 355–411.

Aranami, K., and Readman, J. W. (2007). "Photolytic degradation of triclosan in freshwater and seawater." *Chemosphere*, 66(6), 1052–1056.

Babuponnusami, A., and Muthukumar, K. (2011). "Degradation of Phenol in Aqueous Solution by Fenton, Sono-Fenton and Sono-photo-Fenton Methods." *Clean - Soil, Air, Water*, 39(2), 142–147.

Babuponnusami, A., and Muthukumar, K. (2014a). "A review on Fenton and improvements to the Fenton process for wastewater treatment." *Journal of Environmental Chemical Engineering*, Elsevier B.V., 2(1), 557–572.

Babuponnusami, A., and Muthukumar, K. (2014b). "A review on Fenton and improvements to the Fenton process for wastewater treatment." *Journal of Environmental Chemical Engineering*, 2(1), 557–572.

Bagal, M. V., and Gogate, P. R. (2014a). "Wastewater treatment using hybrid treatment schemes based on cavitation and Fenton chemistry: A review." *Ultrasonics Sonochemistry*, Elsevier B.V., 21(1), 1–14.

Bagal, M. V., and Gogate, P. R. (2014b). "Wastewater treatment using hybrid treatment schemes based on cavitation and Fenton chemistry: A review." *Ultrasonics Sonochemistry*, Elsevier B.V., 21, 1–14.

Balmer, M. E., Buser, H. R., Muller, M. D., and Poiger, T. (2005). "Occurrence of Some Organic UV Filters in Wastewater, in Surface Waters, and in Fish from Swiss Lakes." *Environmental science & technology*, 39(4), 953–962.

Basturk, E., and Karatas, M. (2014). "Advanced oxidation of Reactive Blue 181 solution: A comparison between Fenton and Sono-Fenton Process." *Ultrasonics Sonochemistry*, 21(5), 1881–1885.

Beckett, M. a, and Hua, I. (2001). "Impact of Ultrasonic Frequency on Aqueous Sonoluminescence and Sonochemistry." *The Journal of Physical Chemistry A*, 105(15), 3796–3802.

Behera, S. K., Oh, S. Y., and Park, H. S. (2010). "Sorption of triclosan onto activated carbon, kaolinite and montmorillonite: Effects of pH, ionic strength, and humic acid." *Journal of Hazardous Materials*, Elsevier B.V., 179(1–3), 684–691.

De Bel, E., Janssen, C., De Smet, S., Van Langenhove, H., and Dewulf, J. (2011). "Sonolysis of ciprofloxacin in aqueous solution: Influence of operational parameters." *Ultrasonics*

*Sonochemistry*, Elsevier B.V., 18(1), 184–189.

Bianchi, C. L., Pirola, C., Ragaini, V., and Selli, E. (2006). "Mechanism and efficiency of atrazine degradation under combined oxidation processes." *Applied Catalysis B: Environmental*, 64(1–2), 131–138.

Blair, E. (1971). *Chlorodioxins – Origin and Fate*. American Chemical Society, Washington D.C.

Blüthgen, N., Zucchi, S., and Fent, K. (2012). "Effects of the UV filter benzophenone-3 (oxybenzone) at low concentrations in zebrafish (Danio rerio)." *Toxicology and applied pharmacology*, 263(2), 184–94.

Buxton, G. V., Greenstock, C. L., Helman, W. P., and Ross, A. B. (1988). "Critical Review of rate constants for reactions of hydrated electrons, hydrogen atoms and hydroxyl radicals (·OH/·O− in Aqueous Solution." *Journal of Physical and Chemical Reference Data*, 17(2), 513–886.

Calafat, A. M., Wong, L., Ye, X., Reidy, J. A., and Needham, L. L. (2008). "Concentrations of the Sunscreen Agent Benzophenone-3 in Residents of the United States : National Health and Nutrition Examination Survey 2003 – 2004." *Environmental Health Perspectives*, 116(7), 893–897.

Celeiro, M., Vignola Hackbarth, F., Selene, S. M. A. G., Llompart, M., and Vilar, V. J. P. (2018). "Assessment of advanced oxidation processes for the degradation of three UV filters from swimming pool water." *Journal of Photochemistry and Photobiology A: Chemistry*, 351, 95–107.

Chamarro, E., Marco, A., and Esplugas, S. M. (2001). "Use of Fenton reagent to improve organic chemical biodegradability." *Water Research*, 35(4), 1047–1051.

Chen, X., Nielsen, J. L., Furgal, K., Liu, Y., Lolas, I. B., and Bester, K. (2011). "Biodegradation of triclosan and formation of methyl-triclosan in activated sludge under aerobic conditions." *Chemosphere*, 84(4), 452–456.

Chen, X., Richard, J., Liu, Y., Dopp, E., Tuerk, J., and Bester, K. (2012). "Ozonation products of triclosan in advanced wastewater treatment." *Water Research*, 46(7), 2247–2256.

Cheng, D., Sharma, S., and Mudhoo, A. (2012). *Handbook on Applications of Ultrasound Sonochemistry for Sustainability*. Taylor & Francis.

Chiha, M., Hamdaoui, O., Baup, S., and Gondrexon, N. (2011). "Sonolytic degradation of endocrine disrupting chemical 4-cumylphenol in water." *Ultrasonics sonochemistry*, Elsevier B.V., 18(5), 943–50.

Chiha, M., Merouani, S., Hamdaoui, O., Baup, S., Gondrexon, N., and Pétrier, C. (2010). "Modeling of ultrasonic degradation of non-volatile organic compounds by Langmuir-type kinetics." *Ultrasonics sonochemistry*, Elsevier B.V., 17(5), 773–82.

Coronado, M., De Haro, H., Deng, X., Rempel, M. A., Lavado, R., and Schlenk, D. (2008). "Estrogenic activity and reproductive effects of the UV-filter oxybenzone (2-hydroxy-

4-methoxyphenyl-methanone) in fish." *Aquatic Toxicology*, 90(3), 182–187.

Dann, A. B., and Hontela, A. (2011). "Triclosan: Environmental exposure, toxicity and mechanisms of action." *Journal of Applied Toxicology*, 31(4), 285–311.

Dehghani, M. H., Mahvi, A. H., Najafpoor, A. A., and Azam, K. (2007). "Investigating the potential of using acoustic frequency on the degradation of linear alkylbenzen sulfonates from aqueous solution." *Journal of Zhejiang University SCIENCE A*, 8(9), 1462–1468.

Deojay, D. M., Sostaric, J. Z., and Weavers, L. K. (2011). "Exploring the effects of pulsed ultrasound at 205 and 616 kHz on the sonochemical degradation of octylbenzene sulfonate." *Ultrasonics sonochemistry*, Elsevier B.V., 18(3), 801–809.

Doosti, M. R., Kargar, R., and Sayadi, M. H. (2012). "Water treatment using ultrasonic assistance: A review." *Proceedings of the International Academy of Ecology and Environmental Sciences*, 2(2), 96–110.

Du, Y., Wang, W. Q., Pei, Z. T., Ahmad, F., Xu, R. R., Zhang, Y. M., and Sun, L. W. (2017). "Acute toxicity and ecological risk assessment of benzophenone-3 (BP-3) and benzophenone-4 (BP-4) in ultraviolet (UV)-filters." *International Journal of Environmental Research and Public Health*, 14(11), 1–15.

Farré, M., Asperger, D., Kantiani, L., González, S., Petrovic, M., and Barceló, D. (2008). "Assessment of the acute toxicity of triclosan and methyl triclosan in wastewater based on the bioluminescence inhibition of Vibrio fischeri." *Analytical and Bioanalytical Chemistry*, 390(8), 1999–2007.

La Farre, M., Garcia, M.-J., Tirapu, L., Ginebreda, A., and Barcelo, D. (2001). "Wastewater toxicity screening of non-ionic surfactants by Toxalert(R) and Microtox(R) bioluminescence inhibition assays." *Analytica Chimica Acta*, 427(2), 181–189.

Fent, K., Kunz, P. Y., and Gomez, E. (2008). "UV Filters in the Aquatic Environment Induce Hormonal Effects and Affect Fertility and Reproduction in Fish." *CHIMIA International Journal for Chemistry*, 62(5), 368–375.

Fent, K., Kunz, P. Y., Zenker, A., and Rapp, M. (2010a). "A tentative environmental risk assessment of the UV-filters 3-(4-methylbenzylidene-camphor), 2-ethyl-hexyl-4-trimethoxycinnamate, benzophenone-3, benzophenone-4 and 3-benzylidene camphor." *Marine Environmental Research*, Elsevier Ltd, 69, S4–S6.

Fent, K., Kunz, P. Y., Zenker, A., and Rapp, M. (2010b). "A tentative environmental risk assessment of the UV-filters 3-(4-methylbenzylidene-camphor), 2-ethyl-hexyl-4-trimethoxycinnamate, benzophenone-3, benzophenone-4 and 3-benzylidene camphor." *Marine environmental research*, 69(Supplement 1), S4-6.

Fent, K., Zenker, A., and Rapp, M. (2010c). "Widespread occurrence of estrogenic UV-filters in aquatic ecosystems in Switzerland." *Environmental pollution (Barking, Essex : 1987)*, 158(5), 1817–24.

Fitzgerald, M. E., Griffing, V., and Sullivan, J. (1956). "Chemical Effects of Ultrasonics—

``Hot Spot'' Chemistry." *The Journal of Chemical Physics*, 25(1956), 926.

Frontistis, Z., and Mantzavinos, D. (2012). "Sonodegradation of 17 a -ethynylestradiol in environmentally relevant matrices : Laboratory-scale kinetic studies." *Ultrasonics - Sonochemistry*, 19(1), 77–84.

Gago-Ferrero, P., Badia-Fabregat, M., Olivares, A., Piña, B., Blánquez, P., Vicent, T., Caminal, G., Díaz-Cruz, M. S., and Barceló, D. (2012). "Evaluation of fungal- and photo-degradation as potential treatments for the removal of sunscreens BP3 and BP1." *The Science of the total environment*, 427–428, 355–63.

Gago-ferrero, P., Demeestere, K., Díaz-Cruz, M. S., and Barceló, D. (2013). "Ozonation and peroxone oxidation of benzophenone-3 in water : Effect of operational parameters and identification of intermediate products." *Science of the Total Environment*, 443, 209–217.

García, F., Braun, A., and Oliveros, E. (2015). "Fundamentals and Applications of the Photo-Fenton Process to Water Treatment." *Environmental Photochemistry Part III*, Springer Berlin Heidelberg.

Goel, M., Hongqiang, H., Mujumdar, A. S., and Ray, M. B. (2004). "Sonochemical decomposition of volatile and non-volatile organic compounds--a comparative study." *Water research*, 38(19), 4247–61.

Gogoi, A., Mazumder, P., Tyagi, V. K., Tushara Chaminda, G. G., An, A. K., and Kumar, M. (2018). "Occurrence and Fate of Emerging Contaminants in Water Environment: A Review." *Groundwater for Sustainable Development*, 6, 169–180.

Greenberg, M. M. (Ed.). (2009). *Radical and Radical Ion Reactivity in Nucleic Acid Chemistry*. John Wiley & Sons, Hoboken, New Jersey, USA.

Hartmann, J., Bartels, P., Mau, U., Witter, M., Tümpling, W. V., Hofmann, J., and Nietzschmann, E. (2008). "Degradation of the drug diclofenac in water by sonolysis in presence of catalysts." *Chemosphere*, 70, 453–461.

Hayduk, W., and Laudie, H. (2015). "Prediction of diffusion coefficients for nonelectrolytes in dilute aqueous solutions." *Journal of Toxicology and Environmental Health, Part A*, 78(8), 492–505.

Henglein, A. (1987). "Sonochemistry: Historical developments and modern aspects." *Ultrasonics*, 25, 6–16.

Hernández-Leal, L., Temmink, H., Zeeman, G., and Buisman, C. J. N. (2011). "Removal of micropollutants from aerobically treated grey water via ozone and activated carbon." *Water Research*, 45(9), 2887–2896.

Hites, R. A. (2011). "Dioxins: An Overview and History †." *Environmental Science & Technology*, 45(1), 16–20.

Holsapple, M. P., McCay, J. A., and Barnes, D. W. (1986). "Immunosuppression without liver induction by subchronic exposure to 2,7-dichlorodibenzo-p-dioxin in adult female B6C3F1 mice." *Toxicology and Applied Pharmacology*, 83(3), 445–455.

Hua, I., and Hoffmann, M. R. (1997). "Optimization of ultrasonic irradiation as an advanced oxidation technology." *Environmental Science and Technology*, 31(8), 2237–2243.

Hua, I., Hua, I., Hoechemer, R. H., Hoechemer, R. H., Hoffmann, M. R., and Hoffmann, M. R. (1995). "Sonolytic Hydrolysis of p-Nitrophenyl Acetate: The Role of Supercritical Water." *The Journal of Physical Chemistry*, 99, 2335–2342.

van Iersel, M. M., Benes, N. E., and Keurentjes, J. T. F. (2008). "Importance of acoustic shielding in sonochemistry." *Ultrasonics Sonochemistry*, 15(4), 294–300.

Im, J., Son, H., Kim, S., Khim, J., and Zoh, K. (2011). "Effect of Frequency on the Sonolytic Degradation of Carbon Tetrachloride." *Sustainable Environment Research*, 21(2), 167–172.

In, S. ., Kim, S. H., Go, R. E., Hwang, K. A., and Choi, K. C. (2015). "Benzophenone-1 and Nonylphenol Stimulated MCF-7 Breast Cancer Growth by Regulating Cell Cycle and Metastasis-Related Genes Via an Estrogen Receptor α-Dependent Pathway." *Journal of Toxicology and Environmental Health, Part A*, 78(8), 492–505.

Ince, N. H., Gültekin, I., and Tezcanli-Güyer, G. (2009). "Sonochemical destruction of nonylphenol: effects of pH and hydroxyl radical scavengers." *Journal of hazardous materials*, 172(2–3), 739–43.

Ince, N. H., and Ziylan, A. (2015). "Single and Hybrid Applications of Ultrasound for Decolorization and degradation of textile dye residuals in water." *Green Chemistry for Dyes Removal from Waste Water*, Scrivener Publishing. Wiley., 261–294.

Jennings, V. L. K., Rayner-Brandes, M. H., and Bird, D. J. (2001). "Assessing chemical toxicity with the bioluminescent photobacterium (Vibrio fischeri): A comparison of three commercial systems." *Water Research*, 35(14), 3448–3456.

Jeon, H.-K., Chung, Y., and Ryu, J.-C. (2006). "Simultaneous determination of benzophenone-type UV filters in water and soil by gas chromatography-mass spectrometry." *Journal of chromatography. A*, 1131, 192–202.

Jeon, H.-K., Sarma, S., Kim, Y.-J., and Ryu, J.-C. (2008). "Toxicokinetics and metabolisms of benzophenone-type UV filters in rats." *Toxicology*, Elsevier, 248(2–3), 89–95.

Kasprzyk-Hordern, B., Dinsdale, R. M., and Guwy, A. J. (2008). "Multiresidue methods for the analysis of pharmaceuticals, personal care products and illicit drugs in surface water and wastewater by solid-phase extraction and ultra performance liquid chromatography–electrospray tandem mass spectrometry." *Analytical and Bioanalytical Chemistry*, 391(4), 1293–1308.

Khanna, S., Chakma, S., and Moholkar, V. S. (2013). "Phase diagrams for dual frequency sonic processors using organic liquid medium." *Chemical Engineering Science*, Elsevier, 100, 137–144.

Kidak, R., and Dogan, S. (2015). "Degradation of trace concentrations of alachlor by medium frequency ultrasound." *Chemical Engineering and Processing: Process Intensification*, 89, 19–27.

Kidak, R., and Ince, N. H. (2006). "Effects of operating parameters on sonochemical decomposition of phenol." *Journal of Hazardous Materials*, 137, 1453–1457.

Kim, S. H., Hwang, K. A., Shim, S. M., and Choi, K. C. (2015). "Growth and migration of LNCaP prostate cancer cells are promoted by triclosan and benzophenone-1 via an androgen receptor signaling pathway." *Environmental Toxicology and Pharmacology*, 39(2), 568–576.

Kimura, T., Sakamoto, T., Leveque, J., Sohmiya, H., Fujita, M., Ikeda, S., and Ando, T. (1996). "Standardization of ultrasonic power for sonochemical reaction." *Ultrasonics Sonochemistry*, 3(3), S157–S161.

Koda, S., Kimura, T., Kondo, T., and Mitome, H. (2003). "A standard method to calibrate sonochemical efficiency of an individual reaction system." *Ultrasonics sonochemistry*, 10(3), 149–56.

Kolpin, D. W., Kolpin, D. W., Furlong, E. T., Furlong, E. T., Meyer, M. T., and Meyer, M. T. (2002). "Pharmaceuticals, Hormones, and Other Organic Wastewater Contaminants in U.S. Streams, 1999-2000: A National Recoinnaissance." *Environmental Science & Technology*, 36(6), 1202–1211.

Latch, D. E., Packer, J. . J. L., Stender, B. L. B. ., VanOverbeke, J., Arnold, W. A. W. A., and McNeill, K. (2005a). "Aqueous photochemistry of triclosan: Formation of 2,4-dichlorophenol, 2,8-dichlorodibenzo-p-dioxin, and oligomerization products." *Environmental Toxicology and Chemistry*, 24(3), 517–525.

Latch, D. E., Packer, J. L., Arnold, W. A., and McNeill, K. (2003). "Photochemical conversion of triclosan to 2,8-dichlorodibenzo-p-dioxin in aqueous solution." *Journal of Photochemistry and Photobiology A: Chemistry*, 158(1), 63–66.

Latch, D. E., Packer, J. L., Stender, B. L., VanOverbeke, J., Arnold, W. A., and McNeill, K. (2005b). "Aqueous photochemistry of Triclosan: Formation of 2,4-dichlorophenol, 2,8-dichlorodibenzo-p-dioxin, and oligomerization products." *Environmental Toxicology and Chemistry*, 24(3), 517.

Latch, D. E., Packer, J. L., Stender, B. L., VanOverbeke, J., Arnold, W. a, and McNeill, K. (2005c). "Aqueous photochemistry of triclosan: formation of 2,4-dichlorophenol, 2,8-dichlorodibenzo-p-dioxin, and oligomerization products." *Environmental toxicology and chemistry / SETAC*, 24(3), 517–525.

Legrini, O., Oliveros, E., and Braun, A. M. (1993). "Photochemical processes for water treatment." *Chemical Reviews*, 93, 671–698.

Li, W., Ma, Y., Guo, C., Hu, W., Liu, K., Wang, Y., and Zhu, T. (2007). "Occurrence and behavior of four of the most used sunscreen UV filters in a wastewater reclamation plant." *Water research*, 41(15), 3506–12.

Liu, Y. S., Ying, G. G., Shareef, A., and Kookana, R. S. (2011). "Photostability of the UV filter benzophenone-3 and its effect on the photodegradation of benzotriazole in water." *Environmental Chemistry*, 8(6), 581–588.

Lores, M., Llompart, M., Sanchez-Prado, L., Garcia-Jares, C., and Cela, R. (2005). "Confirmation of the formation of dichlorodibenzo-p-dioxin in the photodegradation of triclosan by photo-SPME." *Analytical and Bioanalytical Chemistry*, 381, 1294–1298.

Ma, Y.-S., Sung, C.-F., and Lin, J.-G. (2010). "Degradation of carbofuran in aqueous solution by ultrasound and Fenton processes: Effect of system parameters and kinetic study." *Journal of hazardous materials*, 178(1–3), 320–5.

Machulek Jr., A., Oliveira, S. C., Osugi, M. E., Ferreira, V. S., Quina, F. H., Dantas, R. F., Oliveira, S. L., Casagrande, G. a, Anaissi, F. J., Silva, V. O., Cavalcante, R. P., Gozzi, F., Ramos, D. D., Rosa, A. P. P. Da, Santos, A. P. F., Castro, D. C. De, and Nogueira, J. a. (2013). "Chapter 6. Application of Different Advanced Oxidation Processes for the Degradation of Organic Pollutants." *Organic Pollutants - Monitoring, Risk and Treatment*.

Mahamuni, N. N., and Adewuyi, Y. G. (2010). "Advanced oxidation processes (AOPs) involving ultrasound for waste water treatment: a review with emphasis on cost estimation." *Ultrasonics sonochemistry*, 17(6), 990–1003.

Mahvi, A. (2009). "Application of Ultrasonic Technology for Water and Wastewater Treatment." *Iranian Journal of public Health*, 38(2), 1–17.

Makino, K., Mossoba, M. M., and Riesz, P. (1983). "Chemical effects of ultrasound on aqueous solutions. Formation of hydroxyl radicals and hydrogen atoms." *The Journal of Physical Chemistry*, 87(24), 1369–1377.

Malato, S., Fernández-Ibáñez, P., Maldonado, M. I., Blanco, J., and Gernjak, W. (2009). "Decontamination and disinfection of water by solar photocatalysis: Recent overview and trends." *Catalysis Today*, 147(1), 1–59.

Marcelino, R. B. P., Queiroz, M. T., Amorim, C. C., Leão, M. M. D., and Brites-Nóbrega, F. F. (2015). "Solar energy for wastewater treatment: review of international technologies and their applicability in Brazil." *Environmental science and pollution research international*, 22(2), 762–773.

Martinez, M., and Peñuela, G. a. (2012). "Analysis of triclosan and 4n-nonylphenol in Colombian reservoir water by gas chromatography-mass spectrometry." *Water and Environment Journal*, n/a-n/a.

Mezcua, M., Gómez, M. J., Ferrer, I., Aguera, A., Hernando, M. D., and Fernández-Alba, A. R. (2004). "Evidence of 2,7/2,8-dibenzodichloro-p-dioxin as a photodegradation product of triclosan in water and wastewater samples." *Analytica Chimica Acta*, 524, 241–247.

Montgomery, D. C. (2012). *Design and Analysis of Experiments*. John Wiley & Sons, Inc.

Munoz, M., de Pedro, Z. M., Casas, J. A., and Rodriguez, J. J. (2012). "Triclosan breakdown by Fenton-like oxidation." *Chemical Engineering Journal*, 198–199, 275–281.

Muruganandham, M., Suri, R. P. S., Jafari, S., Sillanpää, M., Lee, G., Wu, J. J., and Swaminathan, M. (2014). "Recent Developments in Homogeneous Advanced Oxidation Processes for Water and Wastewater Treatment." *International Journal of*

*Photoenergy*, 2014, 1–21.

Naddeo, V., Landi, M., Scannapieco, D., and Belgiorno, V. (2013). "Sonochemical degradation of twenty-three emerging contaminants in urban wastewater." *Desalination and Water Treatment*, 51(34–36), 6601–6608.

Nanzai, B., Okitsu, K., Takenaka, N., Bandow, H., and Maeda, Y. (2008). "Sonochemical degradation of various monocyclic aromatic compounds: Relation between hydrophobicities of organic compounds and the decomposition rates." *Ultrasonics Sonochemistry*, 15(4), 478–483.

Navarro, N. M., Chave, T., Pochon, P., Bisel, I., and Nikitenko, S. I. (2011). "Effect of ultrasonic frequency on the mechanism of formic acid sonolysis." *Journal of Physical Chemistry B*, 115, 2024–2029.

Negreira, N., Canosa, P., Rodríguez, I., Ramil, M., Rubí, E., and Cela, R. (2008). "Study of some UV filters stability in chlorinated water and identification of halogenated by-products by gas chromatography-mass spectrometry." *Journal of Chromatography A*, 1178(1–2), 206–214.

Negreira, N., Rodríguez, I., Ramil, M., Rubí, E., and Cela, R. (2009). "Sensitive determination of salicylate and benzophenone type UV filters in water samples using solid-phase microextraction, derivatization and gas chromatography tandem mass spectrometry." *Analytica Chimica Acta*, 638(1), 36–44.

Neppolian, B., Doronila, A., Grieser, F., and Ashokkumar, M. (2009). "Simple and efficient sonochemical method for the oxidation of arsenic(III) to arsenic(V)." *Environmental Science and Technology*, 43(17), 6793–6798.

Okitsu, K., Iwasaki, K., Yobiko, Y., Bandow, H., Nishimura, R., and Maeda, Y. (2005). "Sonochemical degradation of azo dyes in aqueous solution: A new heterogeneous kinetics model taking into account the local concentration of OH radicals and azo dyes." *Ultrasonics Sonochemistry*, 12, 255–262.

Okitsu, K., Suzuki, T., Takenaka, N., Bandow, H., Nishimura, R., and Maeda, Y. (2006). "Acoustic multibubble cavitation in water: A new aspect of the effect of a rare gas atmosphere on bubble temperature and its relevance to sonochemistry." *Journal of Physical Chemistry B*, 110(41), 20081–20084.

Onorati, F., and Mecozzi, M. (2004). "Effects of two diluents in the Microtox toxicity bioassay with marine sediments." *Chemosphere*, 54(5), 679–687.

Orvos, D. R., Versteeg, D. J., Inauen, J., Capdevielle, M., Rothenstein, A., and Cunningham, V. (2002). "Aquatic toxicity of triclosan." *Environmental toxicology and chemistry / SETAC*, 21(7), 1338–1349.

Oturan, M. a., and Aaron, J.-J. (2014). "Advanced Oxidation Processes in Water/Wastewater Treatment: Principles and Applications. A Review." *Critical Reviews in Environmental Science and Technology*, 44(23), 2577–2641.

Palenske, N. M., Nallani, G. C., and Dzialowski, E. M. (2010). "Physiological effects and

bioconcentration of triclosan on amphibian larvae." *Comparative Biochemistry and Physiology - C Toxicology and Pharmacology*, 152(2), 232–240.

Park, M. A., Hwang, K. A., Lee, H. R., Yi, B. R., Jeung, E. B., and Choi, K. C. (2013). "Benzophenone-1 stimulated the growth of BG-1 ovarian cancer cells by cell cycle regulation via an estrogen receptor alpha-mediated signaling pathway in cellular and xenograft mouse models." *Toxicology*, 8(305), 41–48.

Petrie, B., Barden, R., and Kasprzyk-Hordern, B. (2014). "A review on emerging contaminants in wastewaters and the environment: Current knowledge, understudied areas and recommendations for future monitoring." *Water Research*, Elsevier Ltd, 72(0), 3–27.

Petrie, B., Barden, R., and Kasprzyk-Hordern, B. (2015). "A review on emerging contaminants in wastewaters and the environment: Current knowledge, understudied areas and recommendations for future monitoring." *Water Research*, 72, 3–27.

Pétrier, C. (2015a). "The use of power ultrasound for water treatment." *Power Ultrasonics*, Elsevier, 939–972.

Pétrier, C. (2015b). "The use of power ultrasound for water treatment." *Power Ultrasonics. Applications of High-Intensity Ultrasound*, J. A. Gallego and K. F. Graff, eds., Woodhead Publishing, Elsevier Inc, 939–972.

Petrier, C., David, B., and Laguian, S. (1996). "Ultrasonic degradation at 29 kHz and 500 kHz of atrazine and pentachlorophenol in aqueous solution: preliminary results." *Chemosphere*, 32(9), 1709–1718.

Pétrier, C., and Francony, a. (1997). "Ultrasonic waste-water treatment: incidence of ultrasonic frequency on the rate of phenol and carbon tetrachloride degradation." *Ultrasonics sonochemistry*, 4, 295–300.

Petrier, C., Jiang, Y., and Lamy, M. F. (1998). "Ultrasound and environment: Sonochemical destruction of chloroaromatic derivatives." *Environmental Science and Technology*, 32(9), 1316–1318.

Petrier, C., Lamy, M., Francony, A., Benahcene, A., and Bernard, D. (1994). "Sonochemical Degradation of Phenol in Dilute Aqueous Solutions: Comparison of the Reaction Rates at 20 and 487 kHz." *Journal of Physical Chemistry*, 98, 10514–10520.

Petrovic, M. (2003). "Analysis and removal of emerging contaminants in wastewater and drinking water." *TrAC Trends in Analytical Chemistry*, 22(10), 685–696.

Pryor, W. A. (1986). "Oxy-radicals and related species: Their formation, lifetimes, and reactions." *Annual Review of Phsysiology*, 48, 657–667.

Ramos, S., Homem, V., Alves, A., and Santos, L. (2016). "A review of organic UV-filters in wastewater treatment plants." *Environment International*, 86, 24–44.

Ranjit, P. J. D., Palanivelu, K., and Lee, C. S. (2008). "Degradation of 2,4-dichlorophenol in aqueous solution by sono-Fenton method." *Korean Journal of Chemical Engineering*,

25(1), 112–117.

Rayaroth, M. P., Aravind, U. K., and Aravindakumar, C. T. (2015a). "Sonochemical degradation of Coomassie Brilliant Blue : Effect of frequency , power density , pH and various additives." *Chemosphere*, 119, 848–855.

Rayaroth, M. P., Aravind, U. K., and Aravindakumar, C. T. (2015b). "Sonochemical degradation of Coomassie Brilliant Blue: Effect of frequency, power density, pH and various additives." *Chemosphere*, 119, 848–855.

Ren, Y. Z., Franke, M., Anschuetz, F., Ondruschka, B., Ignaszak, A., and Braeutigam, P. (2014). "Sonoelectrochemical degradation of triclosan in water." *Ultrasonics Sonochemistry*, 21(6), 2020–2025.

Riesz, P., Berdahl, D., and Christman, C. L. (1985). "Free radical generation by ultrasound in aqueous and nonaqueous solutions." *Environmental Health Perspectives*, 64, 233–252.

Rooze, J., Rebrov, E. V, Schouten, J. C., and Keurentjes, J. T. F. (2013). "Ultrasonics Sonochemistry Dissolved gas and ultrasonic cavitation – A review." *Ultrasonics sonochemistry*, 20, 1–11.

Rozas, O., Vidal, C., Baeza, C., Jardim, W. F., Rossner, A., and Mansilla, H. D. (2016). "Organic micropollutants (OMPs) in natural waters: Oxidation by UV/H2O2treatment and toxicity assessment." *Water Research*, 98(December), 109–118.

Rule, K. L., Ebbett, V. R., and Vikesland, P. J. (2005). "Formation of Chloroform and Chlorinated Organics by Free-Chlorine-Mediated Oxidation of Triclosan." *Environmental Science & Technology*, 39(9), 3176–3185.

Sabaliunas, D., Webb, S. F., Hauk, A., Jacob, M., and Eckhoff, W. S. (2003). "Environmental fate of Triclosan in the River Aire Basin, UK." *Water research*, 37(13), 3145–54.

Sanchez-Prado, L., Barro, R., Garcia-Jares, C., Llompart, M., Lores, M., Petrakis, C., Kalogerakis, N., Mantzavinos, D., and Psillakis, E. (2008). "Sonochemical degradation of triclosan in water and wastewater." *Ultrasonics sonochemistry*, 15(5), 689–94.

Sanchez-Prado, L., Llompart, M., Lores, M., Garc??a-Jares, C., Bayona, J. M., and Cela, R. (2006). "Monitoring the photochemical degradation of triclosan in wastewater by UV light and sunlight using solid-phase microextraction." *Chemosphere*, 65(8), 1338–1347.

Santos, A. J. M., Miranda, M. S., and Esteves da Silva, J. C. G. (2012). "The degradation products of UV filters in aqueous and chlorinated aqueous solutions." *Water Research*, 46(10), 3167–3176.

Sathishkumar, P., Mangalaraja, R. V., and Anandan, S. (2016). "Review on the recent improvements in sonochemical and combined sonochemical oxidation processes - A powerful tool for destruction of environmental contaminants." *Renewable and Sustainable Energy Reviews*, 55, 426–454.

Schlumpf, M., Cotton, B., Conscience, M., Haller, V., Steinmann, B., and Lichtensteiger, W. (2001). "In vitro and in vivo estrogenicity of UV screens." *Environmental Health*

*Perspectives*, 109(3), 239–244.

Schlumpf, M., Schmid, P., Durrer, S., Conscience, M., Maerkel, K., Henseler, M., Gruetter, M., Herzog, I., Reolon, S., Ceccatelli, R., Faass, O., Stutz, E., Jarry, H., Wuttke, W., and Lichtensteiger, W. (2004). "Endocrine activity and developmental toxicity of cosmetic UV filters - An update." *Toxicology*, 205, 113–122.

Segura, Y., Martínez, F., Melero, J. A., Molina, R., Chand, R., and Bremner, D. H. (2012). "Enhancement of the advanced Fenton process (Fe 0/H 2O 2) by ultrasound for the mineralization of phenol." *Applied Catalysis B: Environmental*, Elsevier B.V., 113–114, 100–106.

Semones, M. C., Sharpless, C. M., MacKay, A. A., and Chin, Y. P. (2017). "Photodegradation of UV filters oxybenzone and sulisobenzone in wastewater effluent and by dissolved organic matter." *Applied Geochemistry*, Elsevier Ltd, 83, 150–157.

Serna-Galvis, E. A., Silva-Agredo, J., Giraldo-Aguirre, A. L., and Torres-Palma, R. A. (2015). "Sonochemical degradation of the pharmaceutical fluoxetine: Effect of parameters, organic and inorganic additives and combination with a biological system." *Science of the Total Environment*, Elsevier B.V., 524–525, 354–360.

Serpone, N., Terzian, R., Hidaka, H., and Pelizzetti, E. (1994). "Ultrasonic Induced Dehalogenation and Oxidation of 2-, 3-, and 4-Chlorophenol in Air-Equilibrated Aqueous Media. Similarities with Irradiated Semiconductor Particulates." *The Journal of Physical Chemistry*, 98(10), 2634–2640.

Sharma, S., and Sanghi, R. (Eds.). (2012). *Advances in Water Treatment and Pollution*. Springer.

Siddique, M., Farooq, R., and Price, G. J. (2014). "Synergistic effects of combining ultrasound with the Fenton process in the degradation of Reactive Blue 19." *Ultrasonics Sonochemistry*, Elsevier B.V., 21(3), 1206–1212.

Siedlecka, E. M., and Stepnowski, P. (2005). "Phenols Degradation by Fenton Reaction in the Presence of Chlorides and Sulfates." *Polish Journal of Environmental Studies*, 14(6), 823–828.

Sirés, I., Oturan, N., Oturan, M. a., Rodríguez, R. M., Garrido, J. A., and Brillas, E. (2007). "Electro-Fenton degradation of antimicrobials triclosan and triclocarban." *Electrochimica Acta*, 52(17), 5493–5503.

Sivakumar, M., and Pandit, A. B. (2001). "Ultrasound enhanced degradation of Rhodamine B: Optimization with power density." *Ultrasonics Sonochemistry*, 8, 233–240.

Son, H. S., Ko, G., and Zoh, K. D. (2009). "Kinetics and mechanism of photolysis and TiO2 photocatalysis of triclosan." *Journal of Hazardous Materials*, 166(2–3), 954–960.

Song, Z., Wang, N., Zhu, L., Huang, A., Zhao, X., and Tang, H. (2012). "Efficient oxidative degradation of triclosan by using an enhanced Fenton-like process." *Chemical Engineering Journal*, Elsevier B.V., 198–199, 379–387.

Stamatis, N., Antonopoulou, M., Hela, D., and Konstantinou, I. (2014). "Photocatalytic

degradation kinetics and mechanisms of antibacterial triclosan in aqueous TiO 2 suspensions under simulated solar irradiation." *Journal of Chemical Technology & Biotechnology*, 89(8), 1145–1154.

Suarez, S., Dodd, M. C., Omil, F., and von Gunten, U. (2007). "Kinetics of triclosan oxidation by aqueous ozone and consequent loss of antibacterial activity: Relevance to municipal wastewater ozonation." *Water Research*, 41(12), 2481–2490.

Summoogum, S. L., Altarawneh, M., Mackie, J. C., Kennedy, E. M., and Dlugogorski, B. Z. (2012). "Oxidation of dibenzo-p-dioxin: Formation of initial products, 2-methylbenzofuran and 3-hydro-2-methylenebenzofuran." *Combustion and Flame*, The Combustion Institute., 159(10), 3056–3065.

Suslick, K. S., Didenko, Y., Fang, M. M., Hyeon, T., Kolbeck, K. J., McNamara, W. B., Mdleleni, M. M., and Wong, M. (1999). "Acoustic cavitation and its chemical consequences." *Philosophical Transactions of the Royal Society A: Mathematical, Physical and Engineering Sciences*, 357, 335–353.

Sutkar, V. S., and Gogate, P. R. (2009). "Design aspects of sonochemical reactors: Techniques for understanding cavitational activity distribution and effect of operating parameters." *Chemical Engineering Journal*, 155, 26–36.

Teledyne Tekmar Co. (2003). *Apollo 9000™ TOC Combustion Analyzer. User Manual*. Mason, Ohio USA.

Thangavadivel, K., Megharaj, M., Mudhoo, A., and Naidu, R. (2012). "Degradation of organic pollutants using ultrasound." *Handbook on Applications of Ultrasound: Sonochemistry for Sustainability*, CRC Press, 447–474.

Thompson, A., Griffin, P., Stuetz, R., and Cartmell, E. (2014). "The Fate and Removal of Triclosan during Wastewater Treatment." *Water Environment Research*, 77(1), 63–67.

Tijani, J. O., Fatoba, O. O., Madzivire, G., and Petrik, L. F. (2014). "A Review of Combined Advanced Oxidation Technologies for the Removal of Organic Pollutants from Water." *Water, Air, & Soil Pollution*, 225(9).

Tohidi, F., and Cai, Z. (2015). "GC/MS analysis of triclosan and its degradation by-products in wastewater and sludge samples from different treatments." *Environmental science and pollution research international*, 22(15), 11387–11400.

Torres, R., Pétrier, C., Combet, E., Carrier, M., and Pulgarin, C. (2008). "Ultrasonic cavitation applied to the treatment of bisphenol A. Effect of sonochemical parameters and analysis of BPA by-products." *Ultrasonics sonochemistry*, 15(4), 605–11.

Tsui, M. M. P., Leung, H. W., Lam, P. K. S., and Murphy, M. B. (2014a). "Seasonal occurrence, removal efficiencies and preliminary risk assessment of multiple classes of organic UV filters in wastewater treatment plants." *Water Research*, Elsevier Ltd, 53(i), 58–67.

Tsui, M. M. P., Leung, H. W., Wai, T. C., Yamashita, N., Taniyasu, S., Liu, W., Lam, P. K. S., and Murphy, M. B. (2014b). "Occurrence, distribution and ecological risk assessment of multiple classes of UV filters in surface waters from different countries." *Water*

*Research*, 67, 55–65.

Vega, L. P., Soltan, J., and Peñuela, G. A. (2018). "Sonochemical degradation of triclosan in water in a multifrequency reactor." *Environmental Science and Pollution Research*, Environmental Science and Pollution Research, 1–12.

Vione, D., Caringella, R., De Laurentiis, E., Pazzi, M., and Minero, C. (2013). "Phototransformation of the sunlight filter benzophenone-3 (2-hydroxy-4-methoxybenzophenone) under conditions relevant to surface waters." *The Science of the total environment*, 463–464, 243–51.

Waltman, E. L., Venables, B. J., and Waller, W. T. (2006). "Triclosan in a North Texas wastewater treatment plant and the influent and effluent of an experimental constructed wetland." *Environmental Toxicology and Chemistry*, 25(2), 367–372.

Wong-Wah-Chung, P., Rafqah, S., Voyard, G., and Sarakha, M. (2007). "Photochemical behaviour of triclosan in aqueous solutions: Kinetic and analytical studies." *Journal of Photochemistry and Photobiology A: Chemistry*, 191(2–3), 201–208.

Wu, C. H., Andy Hong, P. K., and Jian, M. Y. (2012a). "Decolorization of Reactive Red 2 in Fenton and Fenton-like systems: Effects of ultrasound and ultraviolet irradiation." *Reaction Kinetics, Mechanisms and Catalysis*, 106(1), 11–24.

Wu, M., Li, J., Xu, G., Ma, L., Li, J., Li, J., and Tang, L. (2018). "Pollution patterns and underlying relationships of benzophenone-type UV-filters in wastewater treatment plants and their receiving surface water." *Ecotoxicology and Environmental Safety*, 152, 98–103.

Wu, Q., Shi, H., Adams, C. D., Timmons, T., and Ma, Y. (2012b). "Oxidative removal of selected endocrine-disruptors and pharmaceuticals in drinking water treatment systems, and identification of degradation products of triclosan." *The Science of the total environment*, 439, 18–25.

Xiao, R., Diaz-rivera, D., He, Z., and Weavers, L. K. (2013a). "Using pulsed wave ultrasound to evaluate the suitability of hydroxyl radical scavengers in sonochemical systems." *Ultrasonics sonochemistry*, 20, 990–996.

Xiao, R., Diaz-Rivera, D., He, Z., and Weavers, L. K. (2013b). "Using pulsed wave ultrasound to evaluate the suitability of hydroxyl radical scavengers in sonochemical systems." *Ultrasonics Sonochemistry*, Elsevier B.V., 20(3), 990–996.

Xiao, R., Diaz-Rivera, D., and Weavers, L. K. (2013c). "Factors influencing pharmaceutical and personal care product degradation in aqueous solution using pulsed wave ultrasound." *Industrial and Engineering Chemistry Research*, 52(8), 2824–2831.

Xiao, R., Wei, Z., Chen, D., and Weavers, L. K. (2014). "Kinetics and Mechanism of Sonochemical Degradation of Pharmaceuticals in Municipal Wastewater." *Environmental Science and Technology*, 48, 9675–9683.

Yang, B., and Ying, G.-G. (2014). "Removal of Personal Care Products Through Ferrate(VI) Oxidation Treatment." *Personal Care Products in the Aquatic Environment. Handbook of*

*Environmental Chemistry*, M. S. Dìaz-Cruz and D. Barceló, eds., Springer International Publishing Switzerland, Switzerland.

Yang, B., Ying, G. G., Zhao, J. L., Zhang, L. J., Fang, Y. X., and Nghiem, L. D. (2011). "Oxidation of triclosan by ferrate: Reaction kinetics, products identification and toxicity evaluation." *Journal of Hazardous Materials*, Elsevier B.V., 186(1), 227–235.

Yang, L., Rathman, J. F., and Weavers, L. K. (2005). "Degradation of alkylbenzene sulfonate surfactants by pulsed ultrasound." *J Phys Chem B*, 109(33), 16203–16209.

Yang, L., Rathman, J. F., and Weavers, L. K. (2006). "Sonochemical degradation of alkylbenzene sulfonate surfactants in aqueous mixtures." *Journal of Physical Chemistry B*, 110, 18385–18391.

Yang, L., Sostaric, J. Z., Rathman, J. F., and Weavers, L. K. (2008). "Effect of ultrasound frequency on pulsed sonolytic degradation of octylbenzene sulfonic acid." *Journal of Physical Chemistry B*, 112(3), 852–858.

Yang, W., Zhou, H., and Cicek, N. (2014). "Treatment of Organic Micropollutants in Water and Wastewater by UV-Based Processes: A Literature Review." *Critical Reviews in Environmental Science and Technology*, 44(13), 1443–1476.

Yu, J. C., Kwong, T. Y., Luo, Q., and Cai, Z. (2006). "Photocatalytic oxidation of triclosan." *Chemosphere*, 65(3), 390–399.

Zhang, Y., Xie, Q., Chen, J., Li, Y., and Fu, Z. (2015). "Insights into the photochemical transformation pathways of triclosan and 2'-HO-BDE-28." *Journal of Hazardous Materials*, Elsevier B.V., 300, 354–358.

Zhao, Y. H., Ji, G. D., Cronin, M. T. D., and Dearden, J. C. (1998). "QSAR study of the toxicity of benzoic acids to Vibrio fischeri, Daphnia magna and carp." *Science of the Total Environment*, 216(3), 205–215.

Zúñiga-Benítez, H., Soltan, J., and Peñuela, G. A. (2016). "Application of ultrasound for degradation of benzophenone-3 in aqueous solutions." *International Journal of Environmental Science and Technology*, Springer Berlin Heidelberg, 13(1), 77–86.

# 12 APPENDICES

## 12.1 Appendix 1. GC MS Spectrums for degradation by products

### 12.1.1 Triclosan

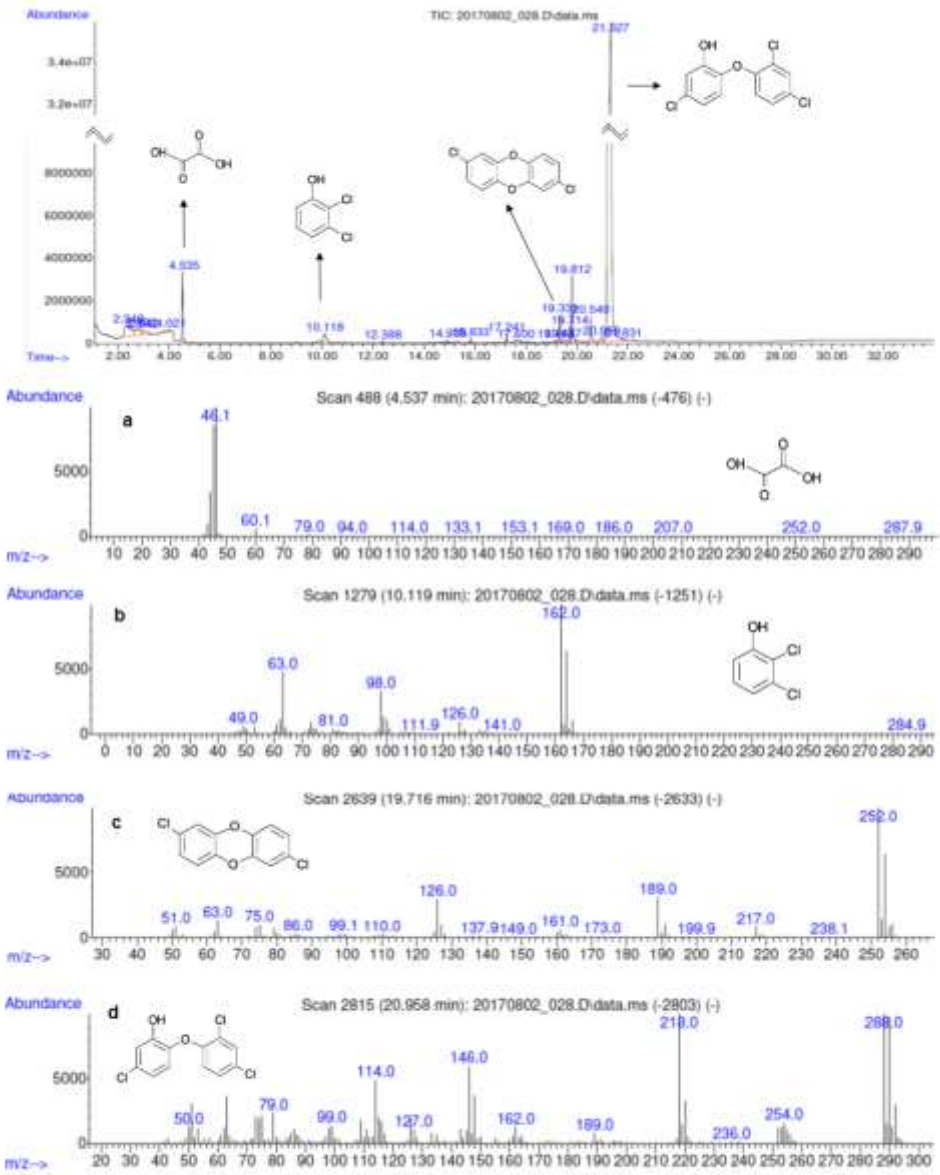


*Figure 60. GC-MS Spectrums. Extract made with Strata Phenyl (55 µm, 70 A, 200mg/3mL) column. 40% TCS degradation. a. Oxalic acid, b. 2,4 dichlorophenol, c. 2,7/2,8-dibenzodichloro-p-dioxin, d. Triclosan*

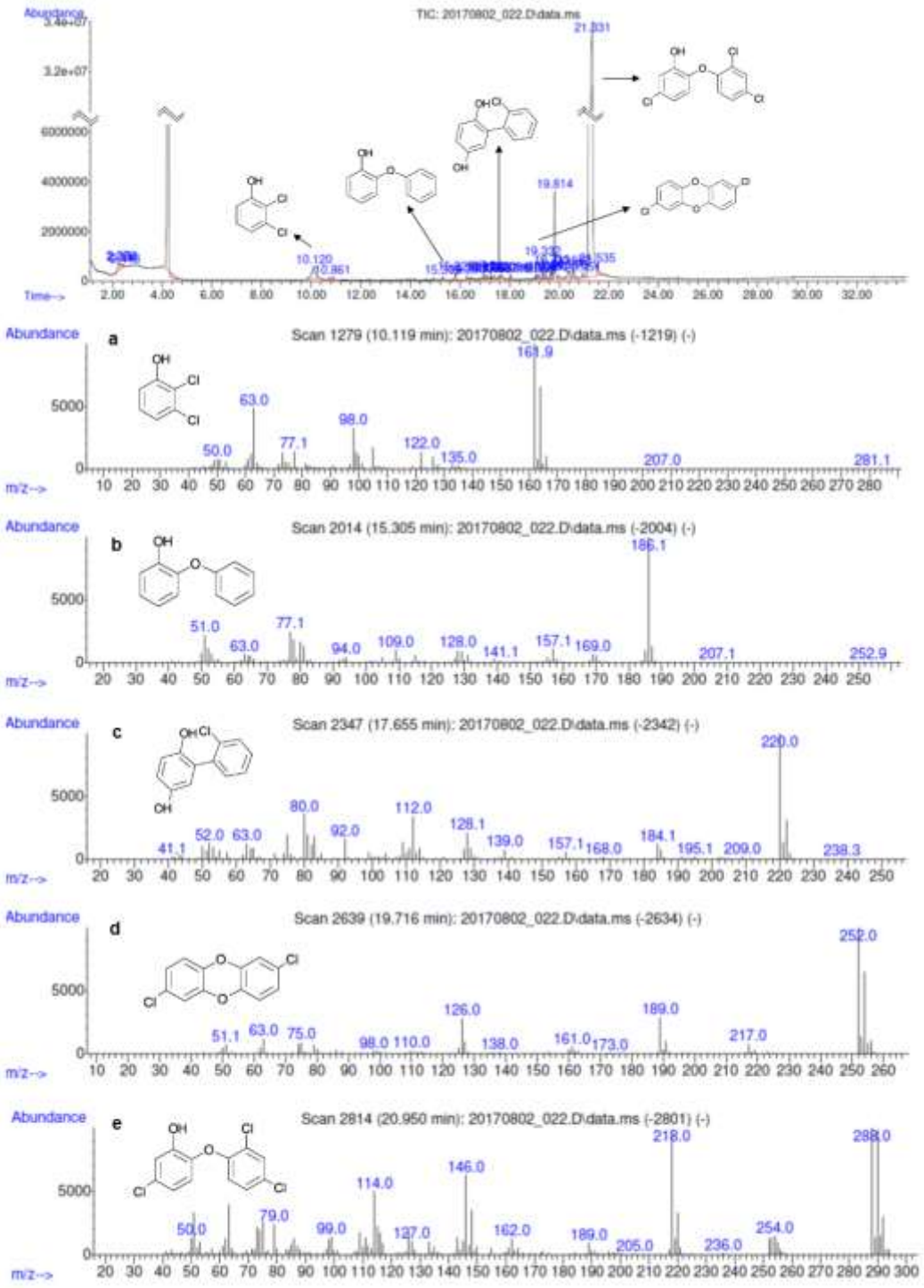


*Figure 61. GC-MS Spectrums. Extract made with Strata X-C (33 µm, 200 mg/3 mL) column. 40% TCS degradation. a. 2,4 dichlorophenol, b. 2-phenoxyphenol, c. 2'-chloro[1,1'-biphenyl]-2,5-diol, d. 2,7/2,8-dibenzodichloro-p-dioxin, e. Triclosan*

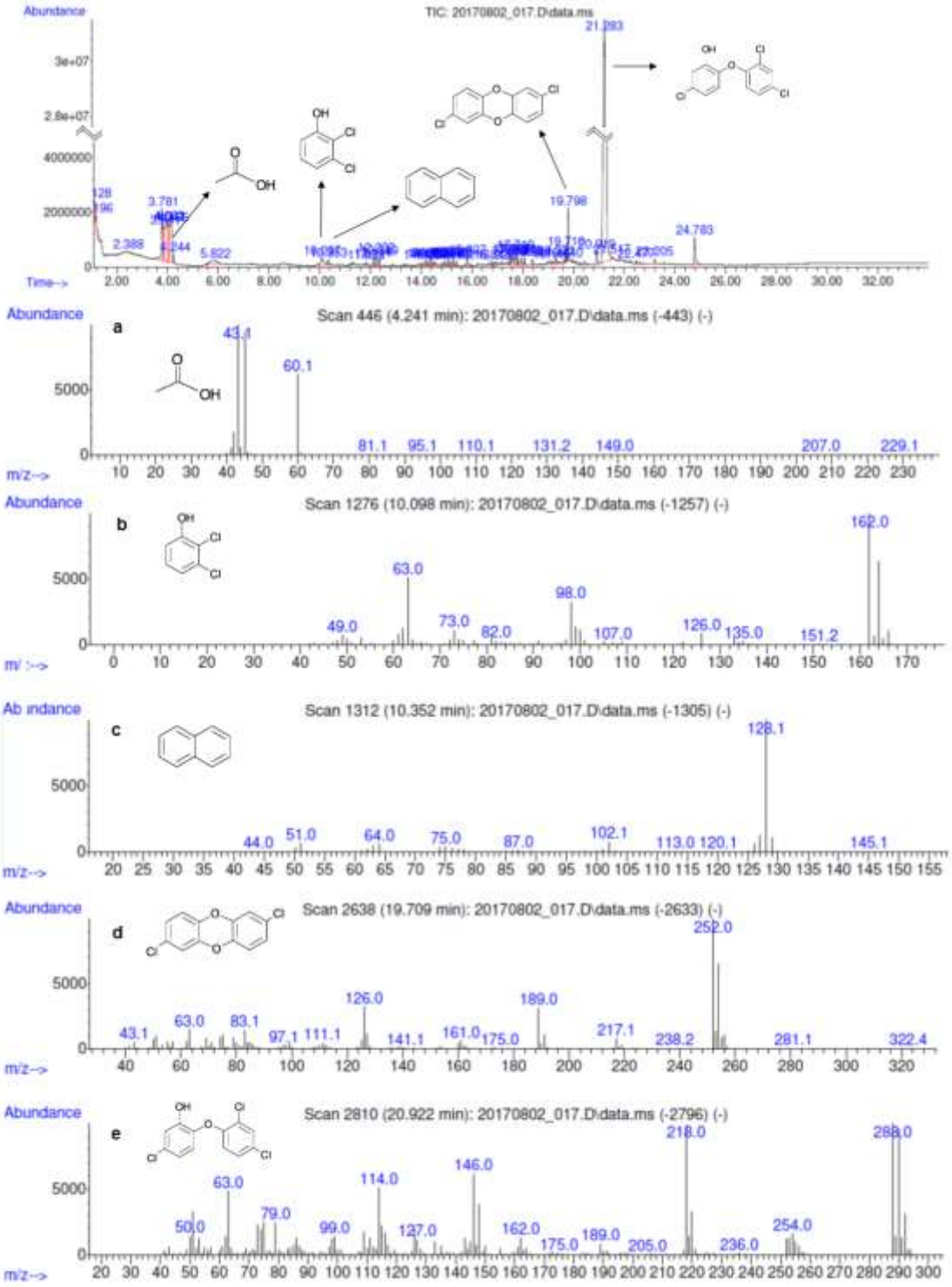


*Figure 62. GC-MS Spectrums. Extract made with Agilent PS DVB (500mg/6 mL) column. 90% TCS degradation. a. Acetic acid, b. 2,4 dichlorophenol, c. Naphthalene, d. 2,7/2,8-dibenzodichloro-p-dioxin, e. Triclosan*

## 12.1.2 Benzophenone 3

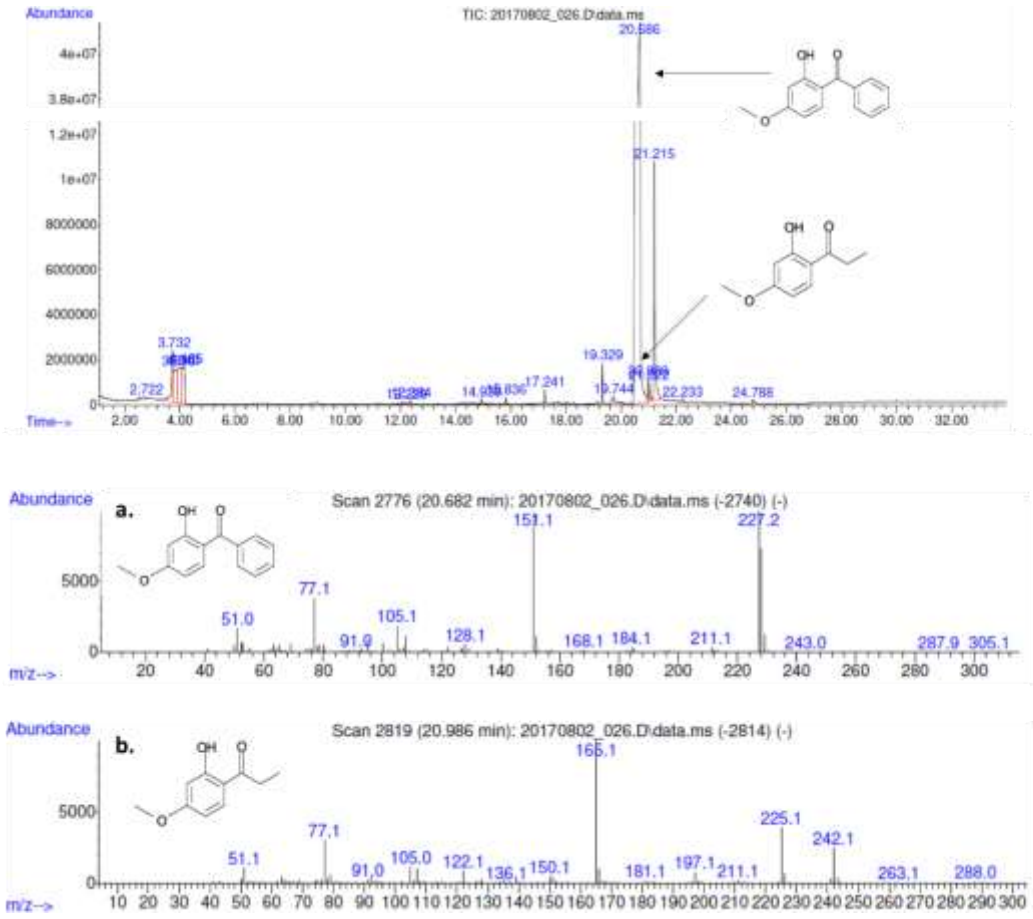


*Figure 63. GC-MS Spectrums. Extract made with Strata Phenyl (55 µm, 70 A, 200mg/3mL) column. 40% BP-3 degradation. a. 1-(2-Hydroxy-4-methoyphenyl)propan-1-one, b. Benzophenone-3*

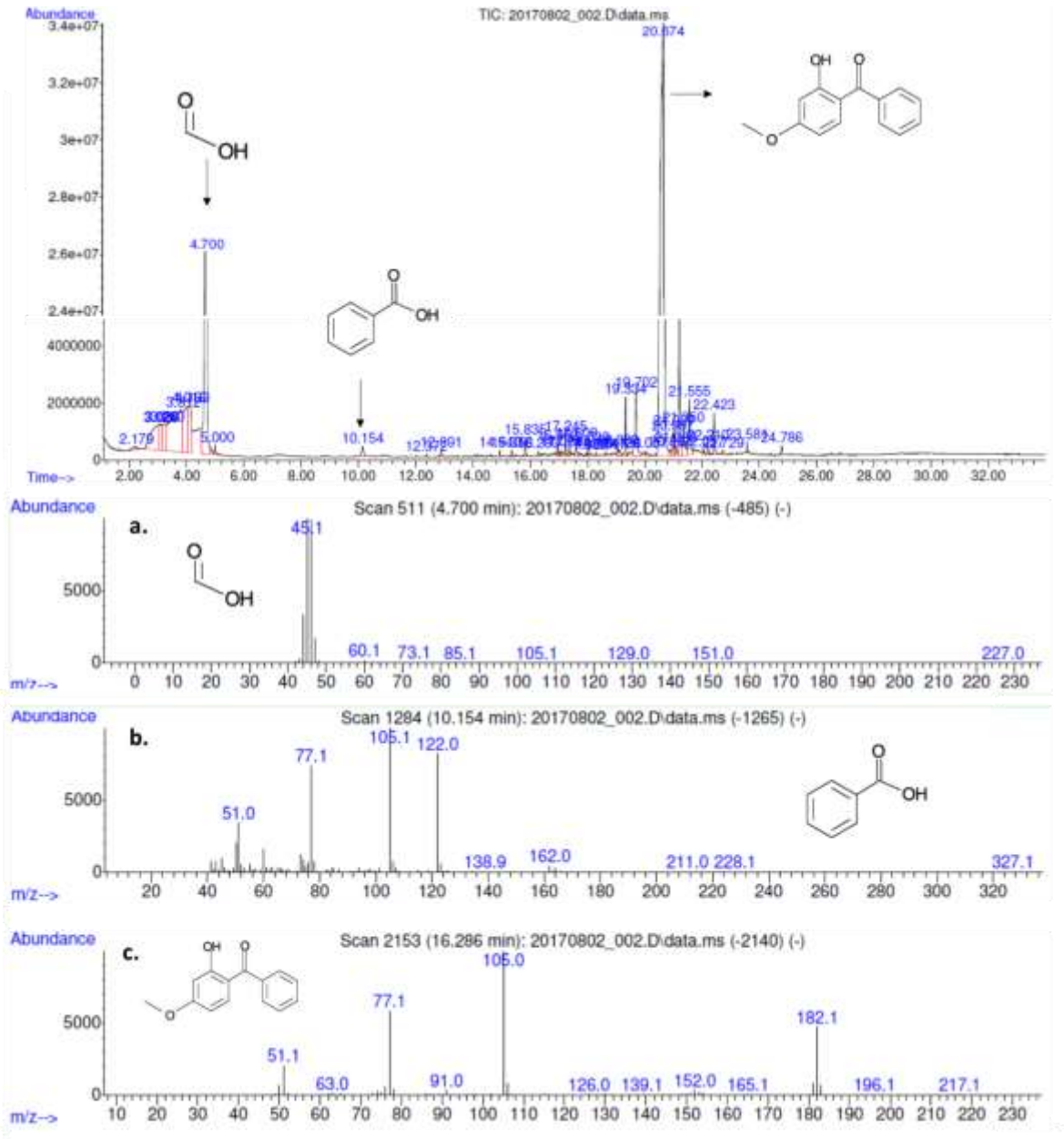


*Figure 64. GC-MS Spectrums. Extract made with Strata X-C (33 µm, 200 mg/3 mL) column. 40% BP-3 degradation. a. Formic acid, b. Benzoic acid, c. Benzophenone-3*

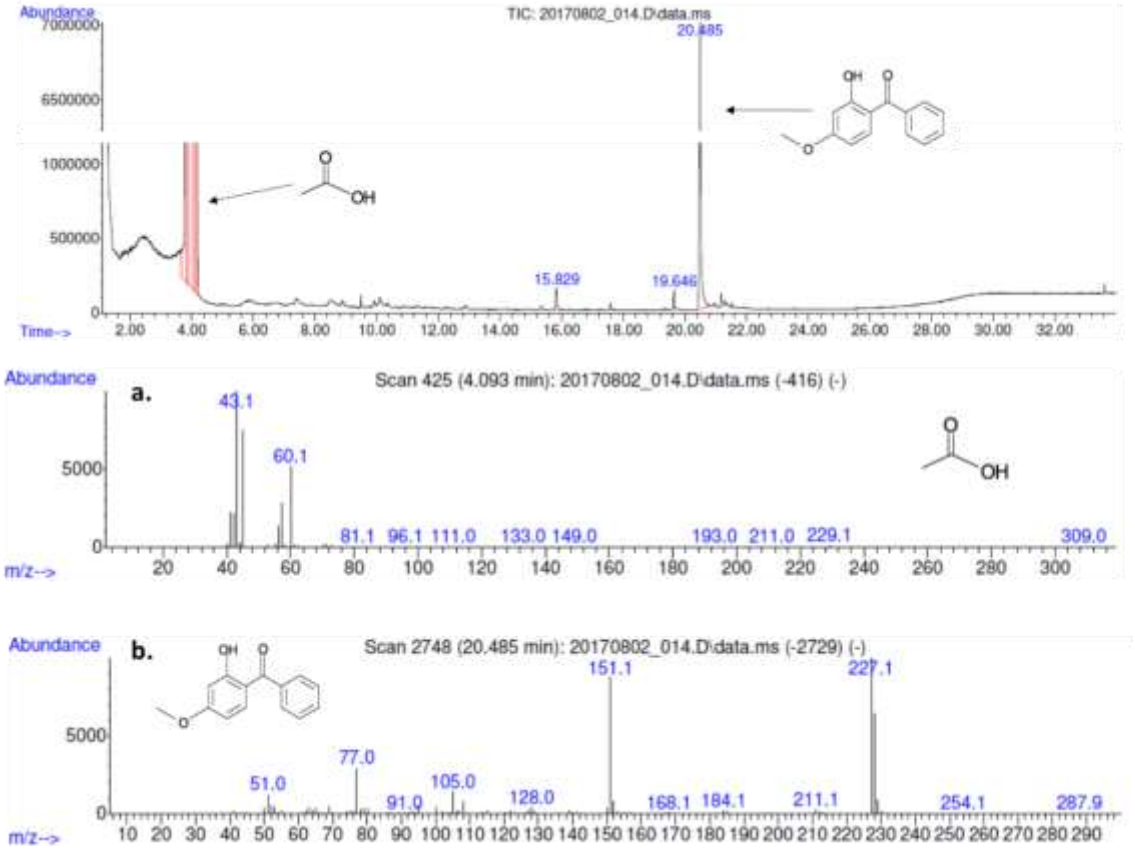


*Figure 65. GC-MS Spectrums. Extract made with Agilent PS DVB (500mg/6 mL) column. 90% BP-3 degradation. a. Acetic acid, b. Benzophenone-3*

### 12.1.3 Benzophenone 1

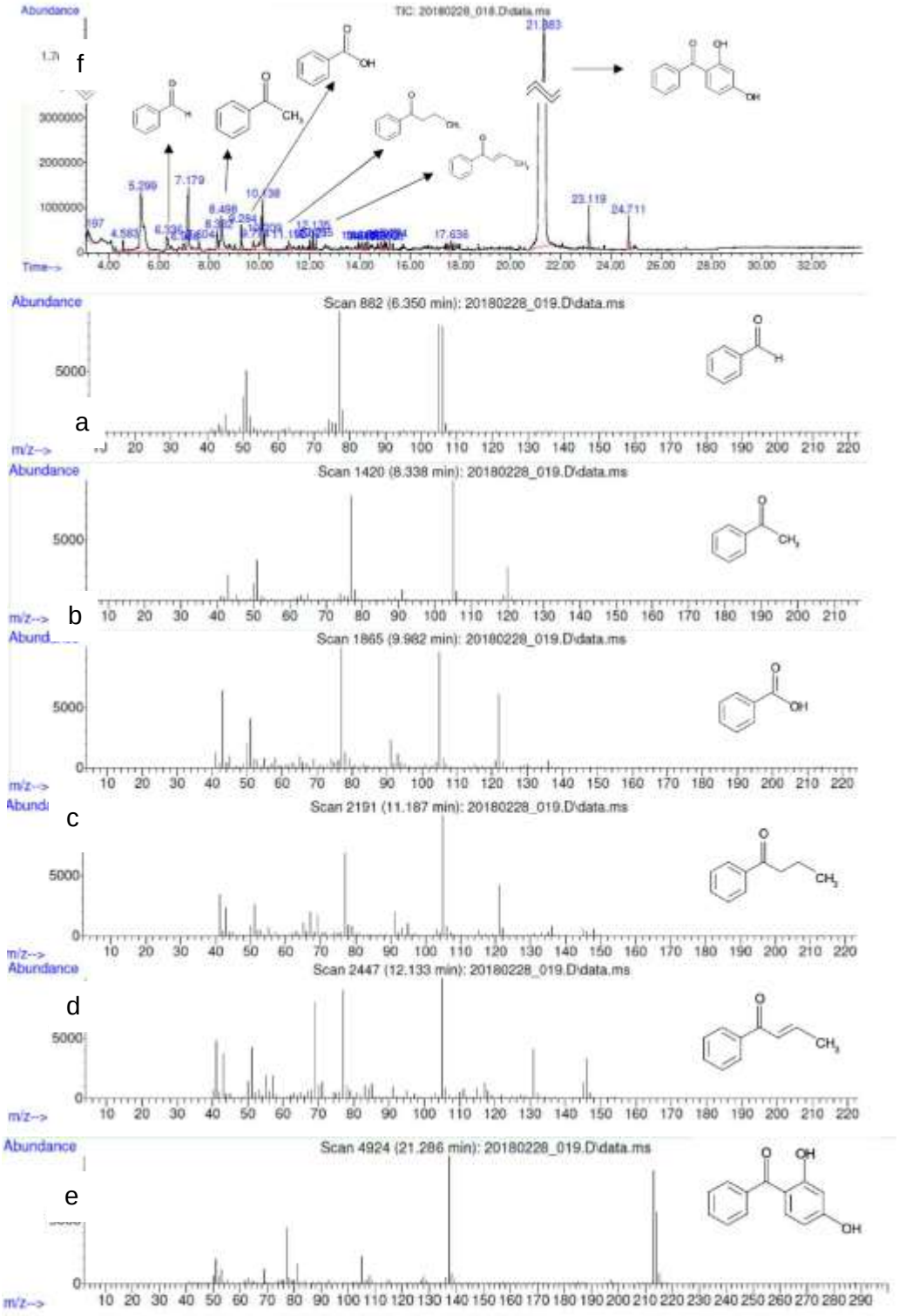


*Figure 66. GC-MS Spectrums. Extract made with Strata Phenyl (55 µm, 70 A, 200mg/3mL) column. a. Benzaldehyde, b. Acetophenone, c. Benzoic acid, d.1 phenyl, 1-butanone, e. 1 phenyl-2-buten-1-one, f. Benzophenone 1*

## 12.2 Appendix 2. Results and ANOVA Tables for Chapter 9

*Table 12. Results for the $2^3$ experimental design in duplicate with 4 central points. Frequency: 574 kHz*

| Power W/L | Pulse Time ms | Silent Time ms | Deg |
|---|---|---|---|
| 80 | 20 | 20 | 0.38254 |
| 140 | 20 | 20 | 0.64014 |
| 80 | 100 | 20 | 0.40692 |
| 140 | 100 | 20 | 0.68407 |
| 80 | 20 | 100 | 0.37679 |
| 140 | 20 | 100 | 0.62887 |
| 80 | 100 | 100 | 0.3577 |
| 140 | 100 | 100 | 0.54745 |
| 110 | 60 | 60 | 0.59483 |
| 110 | 60 | 60 | 0.57505 |
| 80 | 20 | 20 | 0.33631 |
| 140 | 20 | 20 | 0.64842 |
| 80 | 100 | 20 | 0.40968 |
| 140 | 100 | 20 | 0.66751 |
| 80 | 20 | 100 | 0.43636 |
| 140 | 20 | 100 | 0.6383 |
| 80 | 100 | 100 | 0.36943 |
| 140 | 100 | 100 | 0.54837 |
| 110 | 60 | 60 | 0.57758 |
| 110 | 60 | 60 | 0.59023 |

*Table 13. Results for the 23 experimental design with 4 central points. Frequency: 856 kHz*

| **Power** | **Pulse Time** | **Silent Time** | **Deg** |
|---|---|---|---|
| **W/L** | ms | ms | |
| 80 | **20** | **20** | **0.35103** |
| 140 | 20 | 20 | 0.53526 |
| 80 | 100 | 20 | 0.29974 |
| 140 | 100 | 20 | 0.55205 |
| 80 | 20 | 100 | 0.35908 |
| 140 | 20 | 100 | 0.46212 |
| 80 | 100 | 100 | 0.24155 |
| 140 | 100 | 100 | 0.45982 |
| 110 | 60 | 60 | 0.4359 |
| 110 | 60 | 60 | 0.44165 |
| 80 | 20 | 20 | 0.33079 |
| 140 | 20 | 20 | 0.51019 |
| 80 | 100 | 20 | 0.28226 |
| 140 | 100 | 20 | 0.56194 |
| 80 | 20 | 100 | 0.32297 |
| 140 | 20 | 100 | 0.4819 |
| 80 | 100 | 100 | 0.32366 |
| 140 | 100 | 100 | 0.4336 |
| 110 | 60 | 60 | 0.44717 |
| 110 | 60 | 60 | 0.43912 |

*Table 14. Results for the $2^3$ experimental design in duplicate with 4 central points. Frequency: 1134 kHz*

| Power W/L | Pulse Time ms | Silent Time ms | Deg |
|---|---|---|---|
| 80 | 20 | 20 | 0.30181 |
| 140 | 20 | 20 | 0.44142 |
| 80 | 100 | 20 | 0.35816 |
| 140 | 100 | 20 | 0.48558 |
| 80 | 20 | 100 | 0.31584 |
| 140 | 20 | 100 | 0.47523 |
| 80 | 100 | 100 | 0.33286 |
| 140 | 100 | 100 | 0.50053 |
| 110 | 60 | 60 | 0.39726 |
| 110 | 60 | 60 | 0.41313 |
| 80 | 20 | 20 | 0.28525 |
| 140 | 20 | 20 | 0.51111 |
| 80 | 100 | 20 | 0.31377 |
| 140 | 100 | 20 | 0.51824 |
| 80 | 20 | 100 | 0.30066 |
| 140 | 20 | 100 | 0.46534 |
| 80 | 100 | 100 | 0.36598 |
| 140 | 100 | 100 | 0.50053 |
| 110 | 60 | 60 | 0.39289 |
| 110 | 60 | 60 | 0.40945 |

*Table 15. ANOVA for $2^3$ with central point experimental design in table 10*

| Source | F-Ratio | p-Value |
|---|---|---|
| A: P (W/L) | 117.30 | 0.0000 |
| B: PT | 0.29 | 0.5972 |
| C: ST | 2.34 | 0.1519 |
| AB | 0.46 | 0.5127 |
| AC | 2.51 | 0.1391 |
| BC | 5.52 | 0.0367 |
| *R-squared =* | | *91.4559* |
| *R-squared (adjusted for d.f.) =* | | *86.4718* |

*Table 16. ANOVA for $2^3$ with central point experimental design in table 11*

| Source | F-Ratio | p-Value |
|---|---|---|
| A: P (W/L) | 169,86 | 0,0000 |
| B: PT | 3,04 | 0,1069 |
| C: ST | 8,82 | 0,0117 |
| AB | 4,23 | 0,0620 |
| AC | 7,18 | 0,0201 |
| BC | 1,43 | 0,2554 |
| *R-squared =* | | *94,1905* |
| *R-squared (adjusted for d.f.) =* | | *90,8016* |

*Table 17. ANOVA for $2^3$ with central point experimental design in table 12*

| Source | F-Ratio | p-Value |
|---|---|---|
| A: P (W/L) | 188,30 | 0,0000 |
| B: PT | 8,37 | 0,0201 |
| C: ST | 0,19 | 0,6774 |
| AB | 0,33 | 0,5813 |
| AC | 0,54 | 0,4823 |
| BC | 0,00 | 0,9466 |
| *R-squared =* | | *96,1163* |
| *R-squared (adjusted for d.f.) =* | | *92,718* |

*Table 18. Results for the 22 factorial experimental design. (574kHz, BP-3 Initial Concentration: 1 mg/L, T: 25°C±2°C, ST: 20 ms)*

| Power W/L | PT/ST | Deg |
|---|---|---|
| 80 | 1 | 0.38254 |
| 140 | 1 | 0.64014 |
| 80 | 5 | 0.40692 |
| 140 | 5 | 0.68407 |
| 80 | 1 | 0.33631 |
| 140 | 1 | 0.64842 |
| 80 | 5 | 0.40968 |
| 140 | 5 | 0.66751 |

*Table 19. ANOVA for $2^2$ experimental design in Table 7*

| Source | F-Ratio | p-Value |
|---|---|---|
| A: Power Density | 503.41 | 0.0002 |
| B: Pulse Time/Silent Time | 10.66 | 0.0469 |
| AB | 0.50 | 0.5314 |
| *R-squared =* | | *99.4216* |
| *R-squared (adjusted for d.f.) =* | | *98.6504* |

*Table 20. Results for the $2^2$ factorial experimental design (574kHz, BP-3 Initial Concentration: 1 mg/L, T: 25°C±2°C, ST: 20 ms)*

| Power W/L | PT/ST | Deg |
|---|---|---|
| 140 | 5 | 0,662 |
| 200 | 5 | 0,782 |
| 140 | 10 | 0,651 |
| 200 | 10 | 0,769 |
| 140 | 5 | 0,684 |
| 200 | 5 | 0,765 |
| 140 | 10 | 0,637 |
| 200 | 10 | 0,774 |

*Table 21. ANOVA for the $2^2$ factorial experimental design in table 18*

| Source | F-Ratio | p-Value |
|---|---|---|
| A: Power Density | 457.23 | 0 |
| B: Pulse Time/Silent Time | 6.88 | 0.0394 |
| AB | 7.21 | 0.0363 |
| *R-squared =* | | *98.74* |
| *R-squared (adjusted for d.f.) =* | | *97.70* |

*Table 22. Estimated effects for the $2^2$ factorial experimental design in table 18*

| Effect | Estimate | Stnd. Error |
|---|---|---|
| average | 71,475 | 0,270074 |
| A:Power | 11,55 | 0,540147 |
| B:PT/ST | -1,41667 | 0,540147 |
| AB | 1,45 | 0,540147 |

Standard errors are based on total error with 6 d.f.

*Table 23. Results for the CCD factorial experimental design (574 kHz, BP-3 Initial Concentration: 1 mg/L, T: 25°C±2°C, ST: 20 ms)*

| Power W/L | PT/ST | Deg |
|---|---|---|
| 140 | 5 | 0.67 |
| 190 | 5 | 0.78 |
| 140 | 10 | 0.637 |
| 190 | 10 | 0.792 |
| 130 | 7,5 | 0.665 |
| 200 | 7,5 | 0.782 |
| 165 | 4 | 0.715 |
| 165 | 11 | 0.738 |
| 165 | 7,5 | 0.705 |
| 165 | 7,5 | 0.736 |
| 165 | 7,5 | 0.746 |
| 165 | 7,5 | 0.707 |

*Table 24. ANOVA for the CCD in Table 21*

| Source | F-Ratio | p-Value |
|---|---|---|
| A: Power Density | 47.45 | 0.0005 |
| B: Pulse Time/Silent Time | 0.03 | 0.8597 |
| AA | 0.02 | 0.8855 |
| AB | 1.04 | 0.3478 |
| BB | 0.00 | 0.9836 |
| *R-squared =* | | *89.00 %* |
| *R-squared (adjusted for d.f.) =* | | *79.83 %* |

*Table 25. Regression Coefficients for the CCD in Table 21*

| Cofficient | Estimate |
|---|---|
| constant | 53,1305 |
| A:Power Density | 0,149536 |
| B:PT/ST | -2,95735 |
| AA | -0,00021001 |
| AB | 0,018 |
| BB | 0,00299899 |

Standard errors are based on total error with 6 d.f.

## 12.3 Appendix 3. Associated Products

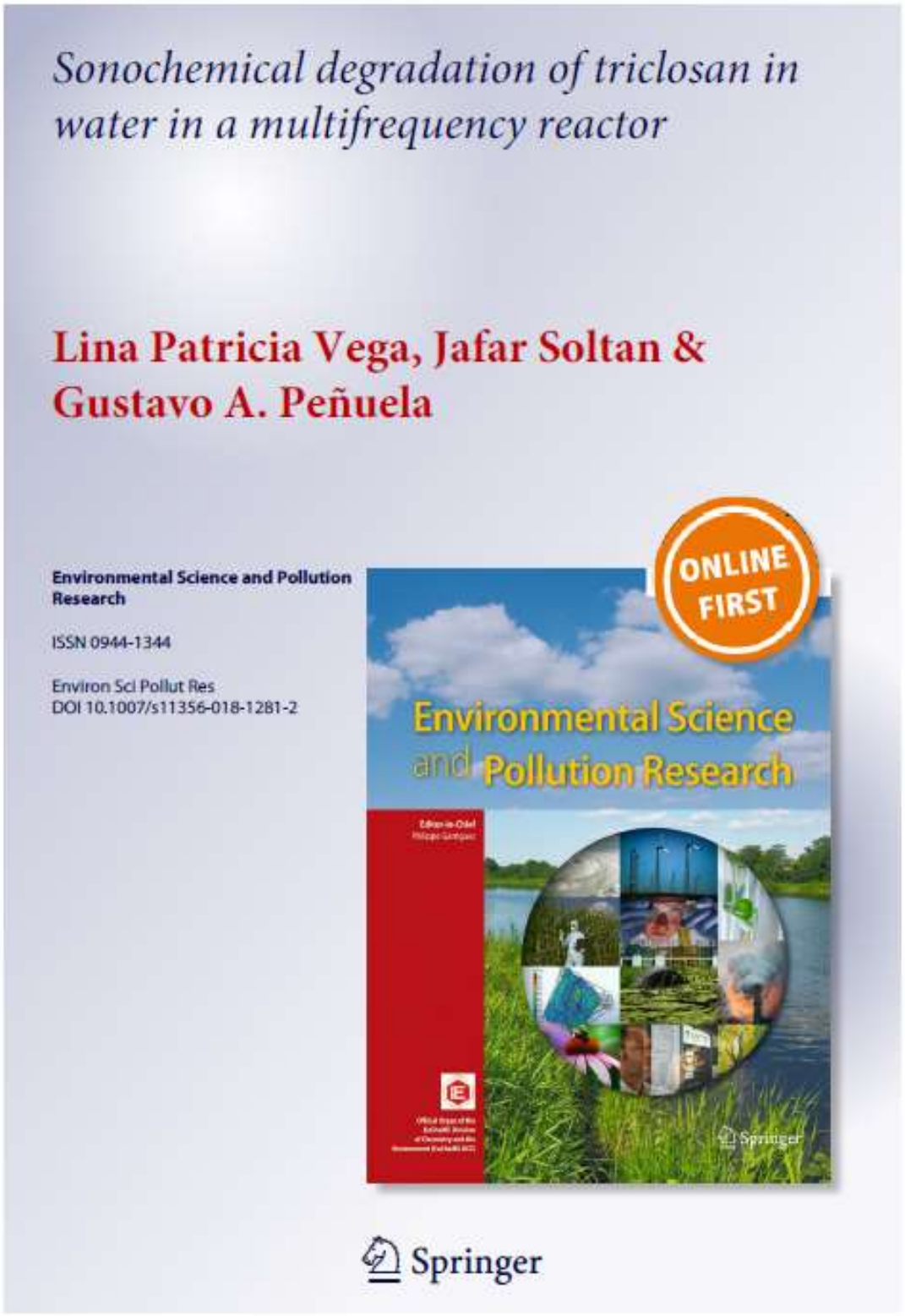

Environmental Science and Pollution Research
https://doi.org/10.1007/s11356-018-1281-2

ADVANCED OXIDATION TECHNOLOGIES: STATE-OF-THE-ART IN IBERO-AMERICAN COUNTRIES

# Sonochemical degradation of triclosan in water in a multifrequency reactor

Lina Patricia Vega [1,2] · Jafar Soltan [1] · Gustavo A. Peñuela [2]

Received: 27 September 2017 / Accepted: 11 January 2018


**Abstract**
Degradation of triclosan (TCS) by multifrequency ultrasound (US) was studied at high and low frequencies. Frequency effect on initial degradation rates was analyzed, and an optimum frequency was found. Power density always has a positive effect on degradation rates over the whole equipment work range. A reaction mechanism similar to that proposed by Serpone resulted in a pseudo-linear model that fitted statistically better than the nonlinear model proposed by Okitsu. Pulsed US showed a positive effect on degradation rates; however, simultaneous analysis of the effect of power, frequency, pulse time, and silent time did not show a clear trend for degradation as a function of pulse US variables. According to these results and those for degradation in the presence of radical scavengers, it was concluded that US TCS degradation was taking place in the bubble/liquid interface. A toxicity test was conducted by Microtox®, showing a decrease in toxicity as TCS concentration decreased and increase in toxicity after total depletion of TCS. Eight possible degradation by-products were identified by GC-MS analysis, and a degradation pathway was proposed.

**Keywords** Advanced oxidation processes · Kinetic models · Sonochemistry · Triclosan · High-frequency ultrasound · Triclosan toxicity

## Introduction

Triclosan (5-chloro-2-{2,4-dichlorophenoxy}phenol) is commonly used as an antiseptic agent in personal care and consumer products (Petrovic 2003). Detection frequency of triclosan (TCS) has been as high as 57.6% in the US surface waters where it had an average concentration of 0.14 μg/L between 1999 and 2000 (Kolpin et al., 2002). In spite of TCS being a nonpersistent chemical and not being toxic for humans and some mammals, it has negative effects on aquatic ecosystems, such as changes in capacity of nutrient assimilation and in the structure of the food chain in water bodies (Sabaliunas et al. 2003). But, the most important aspect in environmental pollution caused by TCS is the generation of toxic compounds such as clorodioxins, chlorinated phenols, polychlorinated biphenyl ethers, dihydroxy derivatives, and bioaccumulative species such as polychlorinated dibenzodioxins and methyltriclosan (Rule et al. 2005; Sirés et al. 2007; Wu et al. 2012; Song et al. 2012; Munoz et al. 2012).

A number of reports about TCS degradation by common oxidation processes have been published. These methods include chlorination (Rule et al. 2005) and oxidation with permanganate (Wu et al. 2012). Advanced oxidation processes have also been applied for degradation of TCS. Those include electrofenton (Sirés et al. 2007), fenton like (Munoz et al. 2012; Song et al. 2012), and photocatalytic processes (Son et al. 2009; Stamatis et al. 2014).

Sonochemical degradation is an advanced oxidation process extensively studied for removal of recalcitrant organic pollutants at low concentrations (Son et al. 2009; Stamatis et al. 2014). Sonochemical degradation is caused by acoustic

Responsible editor: Vitor Pais Vilar

**Electronic supplementary material** The online version of this article (https://doi.org/10.1007/s11356-018-1281-2) contains supplementary material, which is available to authorized users.

✉ Lina Patricia Vega
patricia.vega@udea.edu.co

[1] Department of Chemical and Biological Engineering, University of Saskatchewan, 57 Campus Drive, Saskatoon, SK S7N 5A9, Canada

[2] Grupo GDCON, Facultad de Ingeniería, Sede de Investigación Universitaria (SIU), Universidad de Antioquia, Calle 70 No. 52-21, Medellín, Colombia

Published online: 29 January 2018

cavitation, that is, the creation, expansion, and implosive collapse of gas bubbles in liquids irradiated by US waves (Apfel 1981). Thermal decomposition of water in the compression of oscillating bubbles produces mainly hydroxyl free radicals (Henglein 1987). These radicals react with hydrogen molecules, oxygen peroxide, and pollutants, or they can recombine forming hydrogen peroxide, mainly in the bubble interface (Henglein 1987). Solute degradation processes can take place in different sites: inside collapsing bubbles, in the bubble/liquid interface, and in bulk solution (Okitsu et al. 2006).

Ultrasound has the advantage over other advanced oxidation processes in that it can be used in very complex matrices. It does not need visible light radiation, does not use additional reactants, does not need to change solution pH, does not generate sludge, and does not require catalysts. However, it is a high-cost process due to the high amount of energy needed for operation (Mahamuni and Adewuyi 2010). Understanding of the mechanism of the reaction and the effect of ultrasound system is useful in the search for process optimization. Many variables such as US power, frequency, reactor geometry, mode of US (pulsed or continuous), and pH, among others, influence the extent of a pollutant degradation by US. Two studies have reported on low-frequency sonochemical degradation of TCS exploring the extent, rate of degradation, general rate values (Naddeo et al. 2013), and the effect of solution matrix on the rate of degradation (Sanchez-Prado et al. 2008). However, these studies besides being made at low–medium frequencies (20 and 80 kHz) (Pétrier 2015) did not analyze the effect of variables such as frequency, US mode, pH, and radical scavengers, the same as toxicity evolution and generated by-products. Those variables are analyzed in this study looking for a broader understanding of this process. Some interesting effects such as the use of dual frequencies for further augmentation of ultrasound intensity (Khanna et al. 2013) and of solution toxicity after TCS depletion should be considered for future studies.

## Methods

### Chemicals

Solutions were prepared using Millipore water (18 MΩ cm). Triclosan (> 99%), from Sigma-Aldrich (St. Louis, MO, USA), was used in liquid chromatography and in ultrasonic degradation experiments. HPLC grade acetonitrile was obtained from Fisher Chemicals (NJ, USA).

The pH adjustment was carried out with 1.0 M sodium hydroxide from Sigma-Aldrich (St. Louis, MO, USA). As radical scavengers, methanol, pure ethyl alcohol HPLC/spectrophotometric grade from Sigma-Aldrich (St. Louis, MO, USA), and 2-propanol USP grade from Panreac (99.5%) (Barcelona, Spain) were used. Microtox acute reagent, reconstitution solution, diluent, and adjusting osmotic solution, from Modern Water (New Castle, DE, USA) were used for toxicity assays. Dichloromethane for analysis EMSURE (> 99.8%) from Merck KGaA (Darmstadt, Germany), methanol Baker analyzed LC-MS reagent (99.9%) from Avantor (PA, USA), and Nitrogen 5.0 (> 99.9999%) from Linde were used for solid-phase extraction (SPE). Strata Phenyl (200 mg/3 mL), Strata-X-C (200 mg/3 mL), and Agilent PS DVB (500 mg/6 mL) cartridges were used for SPE. He 5.0 (> 99.9999%) from Linde was used for GC-MS.

### Experimental setup and procedures

#### Ultrasonic reactors

Triclosan degradation experiments at high frequencies were conducted in a cylindrical reactor with a capacity of 500 mL. A Meinhardt Ultrasonics with a Power Multifrequency Generator MG was used. Two transducers were used to generate ultrasonic wave: one for frequencies 215 and 373 kHz and another one for frequencies 574, 856, and 1134 kHz. Solution temperature was kept at 25 ± 2 °C using a water cooling bath. A schematic of the reactors used is shown in Fig. 1 in supplemental material. Ultrasonic energy density for this reactor calculated by the calorimetric method (Kimura et al. 1996) is showed in Fig. 2 in the supplemental material. Reactor was half filled using a solution volume of 300 mL in each experiment. Different sample volumes were withdrawn at different time intervals depending on the variable to be measured.

For kinetic modeling, experiments were also conducted at low frequency (20 kHz) in a cylindrical glass reactor. An Ultrasonic VCX-500 (Sonics and Materials, USA) with probe tip system was used as an US generator. A solid probe (tip diameter 13 mm, length 136 mm, material: titanium alloy) was used to generate ultrasonic waves. The probe was immersed in the reaction solution, leaving a distance of 4 cm from the reactor bottom. Solution temperature was maintained at 25 ± 2 °C using a water cooling bath. Ultrasonic energy density calculated by the calorimetric method was 76 W/L (amplitude 40%). A volume of 250 mL of reaction solution was used in every experiment, and samples of 1.5 mL were withdrawn at different time intervals for TCS analysis. Runs were repeated at least three times. The average value is reported in most cases; standard deviations were below 5%.

### Chemical and microbiologic analysis

#### High-performance liquid chromatography

TCS concentration in water for kinetic analysis in the probe-type reactor was determined by reverse phase

chromatography using a Thermo Scientific Dionex UltiMate 3000 Series HPLC system, with autosampler, an Acclaim 120 C18 column (silica with a 120 A° pore diameter, 5 μm, 4.6 × 250 mm), and a diode array detector set at 254 nm. The mobile phase was a mixture of acetonitrile and Milli-Q water (70:30, *v/v*); flow rate was 1.0 mL/min; injection volume was 80 μL, and column temperature was 40 °C. This analytical procedure showed good linearity in the range of 0.1 to 10 ppm ($R^2 = 0.9997$). For other experiments, TCS concentration was determined using Agilent 1200 Series HPLC system with autosampler, a Zorbax SB-C18 column (porous silica with 80 A° pore diameter, 3.5 μm, 4.6 × 150 mm), and a diode array detector set to 205 nm. The mobile phase was a mixture of acetonitrile/Milli-Q water (55:45, *v/v*); flow rate was 1.2 mL/min; injection volume was 80 μL, and column temperature was 30 °C. This analytical procedure showed good linearity in the range of 0.02 to 2 ppm ($R^2 = 0.999$). The detection limit was 0.0028 ppm, and quantification limit was 0.009 ppm. Repeatability was 1.6% for the measurement range.

### Solid-phase extraction

Analytes from reaction mixture were extracted in order to concentrate and purify them using three different SPE columns: Strata Phenyl (55 μm, 70 A, 200 mg/3 mL), Strata X-C (33 μm, 200 mg/3 mL), and PS DVB (500 mg/6 mL). Conditioning of the column was conducted with methanol, followed by Milli-Q water. Then, 100 mL of reaction solution was passed through the columns at a rate of 5 mL/min. After that, analytes were eluted with a mix of dichloromethane-methanol, and the resulting extract was dried with nitrogen to a volume of 700 μL. The extract was washed from the walls of the recipient and transferred in a total volume of 1 mL to vials for analysis by GC-MS.

### Gas chromatography-mass spectrometry

Analytes from degraded solution extracted by SPE as described in "Solid-phase extraction" section were analyzed in a gas chromatograph (Agilent 7890A) coupled to a mass spectrometer (Agilent 5975C). This system has a temperature programmed and vaporizing multimode inlet (MMI), in pulsed splitless mode. An Agilent 19091S-433UI HP-5ms Ultra Inert 30 m × 250 μm × 0.25 μm column was used for separation. Oven temperature was set at 50 °C for 3 min, and then, it was ramped at 10 °C/min to 310 °C, and hold for 5 min. Injector temperature was set at 150 °C for 0.1 min, ramped at 600 °C/min to 325 °C, hold by 5 min, then ramped at 5 °C/min to 290 °C and hold for 10 min. Interface temperature was 250 °C. Mass spectrum was obtained by electronic impact at 70 eV using full-scan mode. Injection volume was 5 μL. MassHunter software was used for quantification, detection, and identification of degradation by-products using NIST 14 Mass Spectral Library.

### Toxicity test

Toxicity was measured using a Microtox Model 500 Analyzer. This assay used the reduction in the bioluminescence of marine bacteria, *Vibrio fischeri*, when exposed to the pollutants. Toxicity was expressed as $EC_{50}$, the pollutant concentration reducing 50% of the initial luminescence. 81.9% Basic Test was used for determining $EC_{50}$, and 81.9% screening test for determining luminescence reduction throughout the treatment.

## Results and discussion

### Effect of frequency

Ultrasound frequency is an important variable that influences the kind of processes occurring in solution. At low frequencies, physical effects predominate and the number of cavitation events is less than those at higher frequencies (Thangavadivel et al. 2012). Also, higher bubble volumes make leads to higher vapor content in collapsing bubbles. This effect generates less energetic implosion of bubbles resulting in lower OH radical generation. On the other hand, at high frequencies, bubble lives and sizes are smaller, resulting in a lower vapor content at the collapse moment, generating more energetic bubble implosion. It has been shown that optimal frequency is mainly a function of properties of the substance (Adewuyi and Oyenekan 2007). For analyzing this effect on US degradation of TCS, experiments at the same power density were conducted, and degradation pattern was established for different frequencies. In Fig. 1, TCS degradation profiles for frequencies from 215 to 1134 kHz at power density of 40 W/L are shown. In Fig. 2, profiles are shown for 574, 856, and 1134 kHz and a power density of 140 W/L.

For both power density levels, the frequency of 574 kHz had the highest degradation rates. At 40 W/L, 88% of TCS was degraded in 60 min, while at 140 W/L, TCS was completely degraded in less than 25 min. This time is equal to or less than 20% of those found in previous studies for US degradation of TCS (Sanchez-Prado et al. 2008) used 80 kHz US, nominal power = 135 W ($C_0 = 5$ μg/L) obtaining almost 100% TCS degradation in 120 min. Conversely, Naddeo et al. (2013) used 45 kHz US, power density = 100 W/L ($C_0 = 1$ μg/L) and obtained 95% TCS degradation at 180 min, in a mixture of 23 contaminants. At higher frequencies of 856 and 1134 kHz, shorter rarefaction cycles generate molecules that could not be sufficiently stretched to generate the bubble.

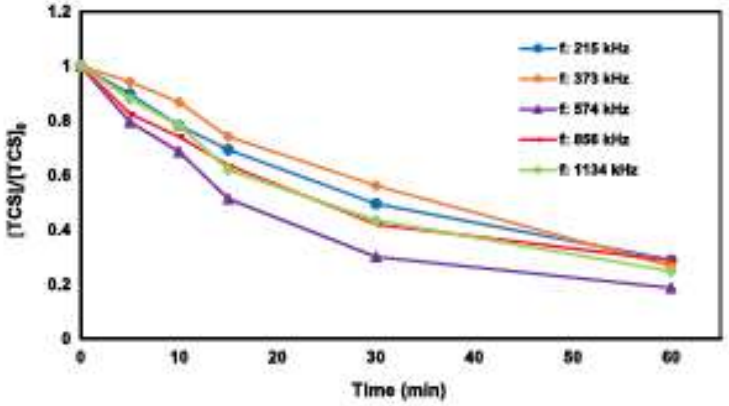


Fig. 1 Effect of frequency on TCS degradation. Power density 40 W/L, solution volume 300 mL, initial TCS concentration 1 mg/L, T 25 ± 2 °C

Also, overall bubble surfaces are smaller, and mass transfer of the pollutants towards the bubble surface dominates the overall rate, resulting in lower degradation rates.

## Effect of power density

Power density has an important impact on ultrasound degradation rates. As power density of US radiation increases, acoustic amplitude increases generating more violent collapse of the bubbles (Adewuyi and Oyenekan 2007). It has been widely demonstrated that power density has an optimum value in which maximum pressure and temperature during collapse generate an optimal degradation rate. This occurs because at high densities, bubble shielding occurs attenuating the effect of the US radiation. At power intensities higher than the optimum, a dense cloud of bubbles forms close to the transducer. This cloud prevents the ultrasound wave propagation due to scattering and absorption. Although some studies report that electrical energy loss is higher as power increases due to decoupling effect (van Iersel et al. 2008), at the conditions used in this study (reactor geometry, liquid height, frequency level), this effect is not occurring.

Experiments were conducted at the optimum frequency of 574 kHz varying power densities. Figure 3 shows the profile of concentration with reaction time.

As can be seen in this figure, for this reactor and under the conditions mentioned, the highest TCS degradation rate was obtained at the highest power density level of the equipment, 200 W/L. There was no optimum power value after which degradation rates started to decrease. Although some studies report that electrical energy loss is higher as power increases due to decoupling effect (van Iersel et al. 2008), at the conditions (reactor geometry, liquid height, frequency level), this effect is not occurring.

## Pulsed ultrasound effect

Pulsed wave (PW) is US radiation in intermittent pulses of specific duration. Various studies have found that under certain optimal conditions, PW US enhances the degradation of the compound when a reaction is taking place in the bubble interface. Pulsed wave US allows time for diffusion of the molecules to the interface, where the reaction is taking place (Xiao et al. 2013b). Xiao et al.

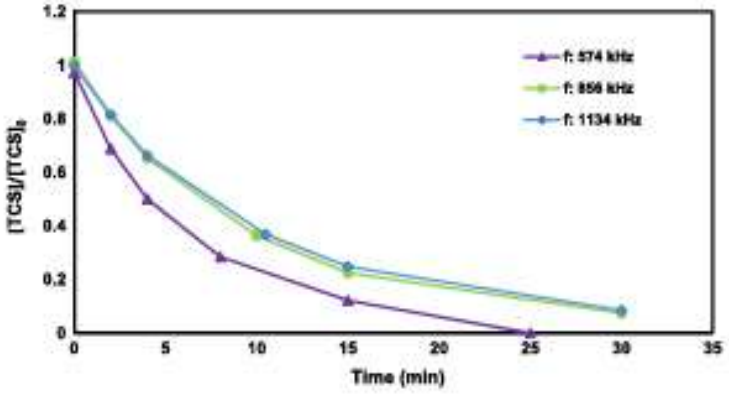


Fig. 2 Effect of frequency on TCS degradation. Power density 140 W/L, solution volume 300 mL, initial TCS concentration 1 mg/L, T 25 ± 2 °C

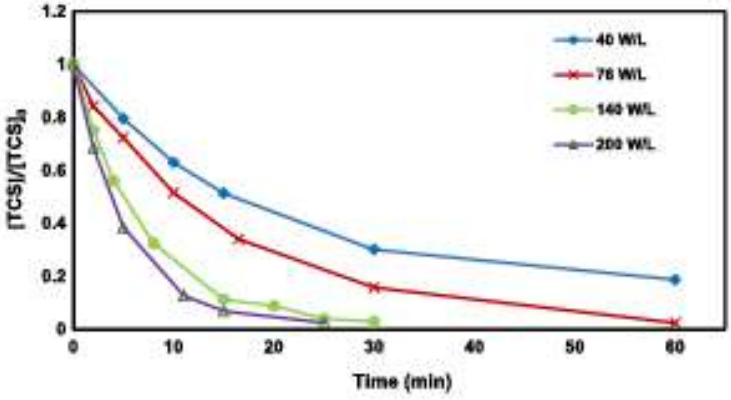


Fig. 3 Effect of power density on TCS degradation. Frequency 574 kHz, solution volume 300 mL, initial concentration 1 mg/L, T 25 ± 2 °C

(2014) showed that in PW mode US, small-sized and highly diffusing molecules diffuse more quickly to the cavitation bubbles, contrary to the effect for large molecules. This effect is more important for small compounds with molar volumes less than 130 mL/mol that can diffuse more readily to bubble interface. The authors also concluded that PW enhancement is higher for compounds with high diffusivity and high octanol/water partition coefficient ($K_{ow}$). TCS is expected to degrade at bubble surface, because of its hydrophobic and nonvolatile character (log $K_{ow} = 4.76$, $K_H = 4.99 \times 10^{-9}$ atm m$^3$/mol). Thus, a PW mode US enhancement was expected for its US degradation.

In Fig. 4, results are shown for pulse enhancement (PE*). PE is defined as

$$PE^*(\%) = \frac{(Deg)_{PW} - (Deg)_{CW}}{(Deg)_{CW}} \times 100\% \quad (1)$$

where $(Deg)_{PW}$ is degradation percent for PW mode US and $(Deg)_{CW}$ is degradation percent for PW mode US, after 10 min of sonication, and for the corresponding frequency and power density levels. Total reaction time for PW mode US was calculated according to the following equation (Yang et al. 2005):

$$t_{total} = t_{sonication}\left(1 + \frac{ST}{PT}\right) \quad (2)$$

where $t_{total}$ is the total reaction time, $t_{sonication}$ is the real sonication time (10 min), $ST$ is the time between pulses (silent time), and $PT$ is the pulse time. For this equipment, $ST$ and $PT$ could be varied in a range from 0 to 10,000 ms continuously. Pulse time and silent times of 10 and 50 ms were used.

From this set of experiments, an experimental design $2^3$ with four central points was devised along with an ANOVA analysis. This showed that the only variable that had a statistical significance and effect over degradation after 10 min of degradation was the power density. That is, there was not a clear trend for degradation percent as a response to variations in PT, ST, or PT/ST. However, from Fig. 4, it could be seen that PW enhancement was positive in almost all the experiments, and its values were higher

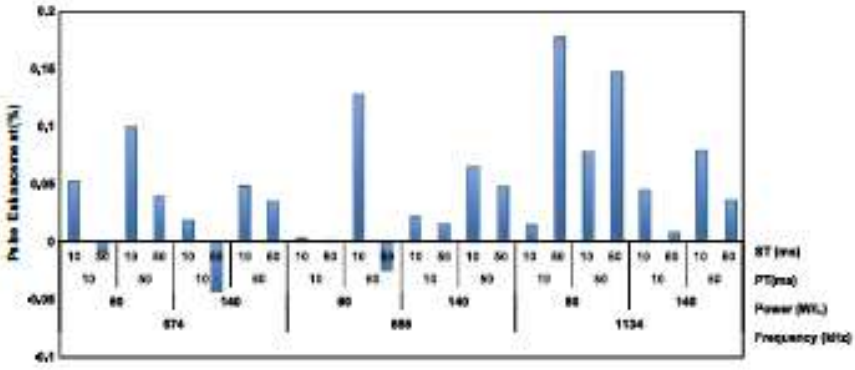


Fig. 4 Pulse enhancement for PW mode US. Reaction vol 300 mL, T 25 ± 2 °C

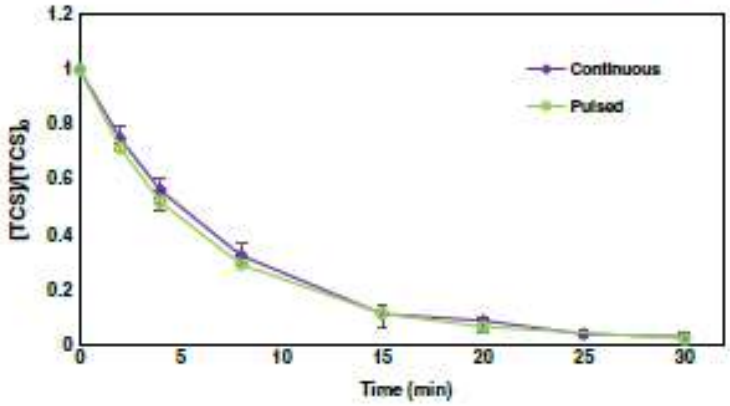


Fig. 5 TCS degradation profiles for continuous and PW mode US. Frequency 574 kHz, power density 140 W/L, initial TCS concentration 1 mg/L, solution volume 300 mL, T 25 ± 2 °C

for the low power density level used (80 W/L). Figure 5 shows the degradation profiles for continuous and PW mode US. It shows that degradation is slightly faster for PW mode US. In order to compare the initial degradation rates for the reaction using pulsed wave ultrasound with those using continuous wave ultrasound, an ANOVA analysis was conducted. Models without the effect of pulsed wave mode and those taking into account the effect of the pulsed ultrasound mode as a dummy variable were compared. Because of the low Pr value for the $F$ statistic in the ANOVA analysis, it was concluded that pulsed wave mode has a positive effect on the initial degradation rate of triclosan. Initial reaction rates for PW US were 15.3% higher for the batch reactor, 574 kHz, initial concentration 1 mg/L, and power density 140 W/L. For the probe-type reactor at a lower frequency (20 kHz), initial concentration 1.9 mg/L, power density 76 W/L, and volume 250 mL, initial reaction rate was 17% higher for PW US.

Higher initial reaction rates for PW US mode for low and high frequencies and for different reactor types confirm that TCS is degraded at the interfacial region. For periods without US radiation, TCS molecules diffuse from the bulk solution to the bubble interface. However, enhancement was not high because of TCS molar volume (194.3 mL/mol) and diffusivity ($5.9 \times 10^{-6}$) as calculated according to Hayduk and Laudie (1974).

## Effect of radical scavengers

Recent studies recognize that sonochemical decomposition of organic compounds in water can proceed in three regions (Okitsu et al. 2005):

1. Inside bubbles.
2. At the interface between the cavitation bubbles and the bulk solution.
3. In the bulk solution.

In regions 1 and 2, mainly pyrolysis and radical reactions occur, and in region 3, reactions with OH radicals are the most prevalent.

Xiao et al. (2013a) studied the ability of various radical scavengers to interact with cavitation bubbles reporting that acetic acid/acetate appears to scavenge OH free radicals only in the solution, without any interaction with the bubble interface. Other studies have found that some alcohols such as terthutanol, ethanol, methanol, and isopropyl alcohol (Ince et al. 2009; Serna-Galvis et al. 2015; Zúñiga-Benítez et al. 2016; Latch et al. 2005; De Bel et al. 2011) scavenge OH radicals in the bubble surface and bulk solution. Since TCS is not a volatile compound and is hydrophobic (log $K_{ow}$ = 4.76), it is expected that it tends to accumulate mostly in the interface region of the cavitation bubbles.

Experiments were made using methanol, ethanol, and 2-propanol as radical scavengers using a radical scavenger: TCS molar ratio of 500:1. The resulting degradation profiles are shown in Fig. 6.

Comparing the initial TCS degradation rates for US degradation at 574 kHz, with scavenger, inhibition was 51.4% for methanol, 47.4% for ethanol, and 42.0% for 2-propanol. Henry's law constant for TCS ($K_{H\text{-}TCS}$ is $4.99 \times 10^{-9}$ atm m$^3$/mol) is much lower than those for radical scavengers used ($K_{H\text{-methanol}}$ is $4.55 \times 10^{-6}$ atm m$^3$/mol, $K_{H\text{-ethanol}}$ is $5 \times 10^{-6}$ atm m$^3$/mol, and $K_{H\text{-propanol}}$ is $7.5 \times 10^{-6}$ atm m$^3$/mol). Thus, TCS degradation inhibition in the presence of the scavengers is explained by the scavenger's accumulation at bubble interface due to their higher volatility. This generates higher reaction rates of scavengers with OH radicals than those of TCS.

## Kinetics of sonochemical degradation

US degradation reactions are modeled usually as a pseudo-first-order kinetic expression. However, Okitsu et al. (2006) proposed a nonheterogeneous kinetic model similar

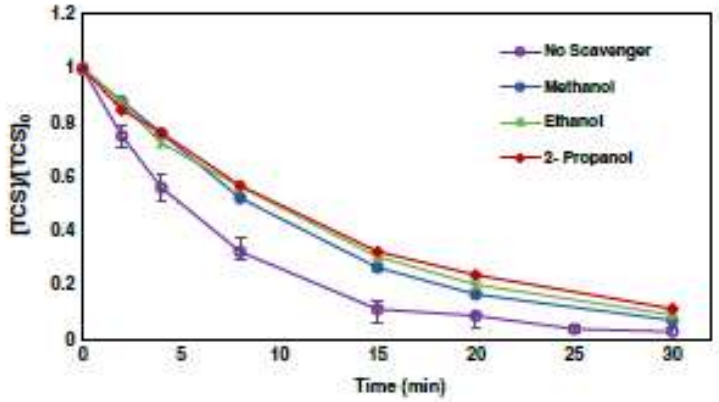


Fig. 6 Effect of radical scavengers ethanol, methanol, and 2-propanol in TCS degradation by US in bath reactor. Frequency 574 kHz, power density 140 W/L, initial TCS concentration 1 mg/L, solution volume 300 mL, T 25 ± 2 °C

to a Langmuir–Hinshelwood or Eley–Rideal mechanism occurring in the bubble–solution interface. This model is based on the assumption that before collapsing of the bubble, a pseudo-equilibrium of adsorption and desorption of pollutant at the gas/liquid interface exists. This results in the general model (Eq. 3):

$$r = k\theta = \frac{kK[TCS]}{1 + K[TCS]} \tag{3}$$

where $K = {}^{k_1}/_{k_{-1}}$, $k_1$ and $k_{-1}$ are the sorption and desorption rate constants in the bubble surface, and $k$ is the pseudo-first-order rate constant for the reaction of TCS with OH radicals.

On the other hand, Serpone et al. (1994) proposed a general reaction mechanism for chlorophenol degradation by US where reactions can occur in the bulk solution or in the interface, reaching a general expression similar to that of Okitsu. However, in this model, considering that the reaction is taking place in the bubble interface, where OH concentration is high and pollutant concentration is low, the rate expression becomes of first order in the concentration of TCS. Details of these models applied to TCS degradation are provided in the supplemental material (ref)

$$\left(\frac{d[TCS]}{dt}\right) = k_g[TCS] \tag{4}$$

Equations (3) and (4) were evaluated to determine the goodness of fit of the experimental data to the expressions. Several experiments were conducted measuring initial TCS degradation rates for various TCS initial concentrations. Two different conditions were used for this purpose: one, using the probe tip reactor for low frequency 20 kHz, power density 76 W/L, pH 6.9, volume 250 mL, and temperature 25 ± 2 °C and the other, with the ultrasonic bath with planar transducer, high frequencies 574 kHz, power density 140 W/L, pH 6.9, volume 300 mL, and temperature 25 ± 2 °C. Concentrations varied from 1.7 to 11 μM. Data for 25 min of reaction for probe tip reactor and 2 min of reaction for reactor with planar transducer was used. In this time, less than 20% of TCS degradation was achieved in both cases. The use of these initial rates avoids the interference of the reaction by-products.

Nonlinear regression analysis was used for testing the goodness of the fit of the model for Eq. (3) by an algorithm in R software version 3.1.3 using the instruction nls. This approach generated nonlinear (weighted) least-squares estimates of the parameters. On the other hand, ordinary least squares analysis was used for testing the pseudo-first-order model (Eq. 4). Results for regression parameters, $t$ statistic probabilities ($p$), coefficient of determination ($R^2$), and sum of squared errors (SSE) are showed in supplemental material Tables 1 and 2. Experimental values and predicted curves by the two models are shown in Fig. 7.

According to the squared sum of residues (SSE) with similar values, a good fit for both models was achieved. Pseudo-first-order model (Eq. 2) had a good correlation coefficient, a good $p$ value for $t$ statistics for equation parameters, and an $F$ statistic values of 339.3 and 680.3 for the probe tip reactor and bath reactor, respectively. This proves the goodness of fit for this model. However, the model in Eq. (1) gives a low value for the $t$ value of the parameter $K$ in the denominator, for both reactors. There is no statistical evidence for the validity of this parameter, and consequently of this model.

Based on this analysis, pseudo-first-order model better explained TCS degradation for both reactors and at low and high frequencies. Conditions used to obtain Eq. (2) are applicable and match with the fact that TCS degrades mainly at bubble surface, according to the proposed mechanism by Serpone et al. (1994). Rate constant for the batch reactor was 20.4 times higher than for probe tip reactor. Many variables may explain this, but especially, frequency and power density values that were higher for the batch reactor can be mentioned. Sanchez-Prado et al. (2008) found a rate constant of 0.0272 $min^{-1}$ for the linear model for TCS degradation in deionized water, for a frequency of

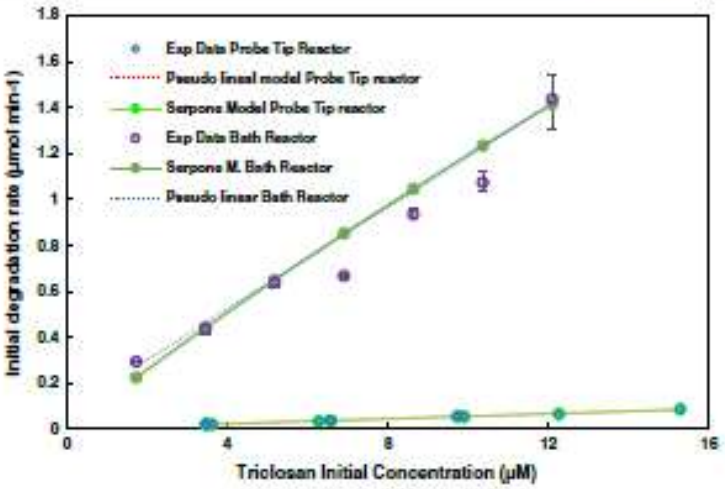


**Fig. 7** Initial degradation rate vs TCS initial concentration. Probe tip reactor: frequency 20 kHz, power density 76 W/L, pH 6.9, volume 250 mL, temperature 25 ± 2 °C. Bath reactor: frequency 574 kHz, power density 140 W/L, pH 6.9, volume 300 mL, temperature 25 ± 2 °C. Predicted curves for the linear model (dotted line), and the Serpone et al. (1994) model (continuous line)

85 kHz and nominal power of 135 W. This value is four times less than that found in this study. In their study, Sanchez-Prado et al. used data for 120-min reaction time. The approach used in this study is a more accurate representation of the initial reaction rates.

## Effect of pH

Depending on its $pK_a$ value, at certain pH levels, a compound can be in its molecular or in its ionic form with different proportions. An ionic form of a compound has different hydrophobicity than its molecular form, and hydrophobic compounds in their molecular form accumulate more readily in the interfacial area than in their ionic form. TCS has a $pK_a = 7.9$, and at a pH of 6.9, it is almost complete in its molecular form. At higher pH values, TCS is in its deprotonated form and tends to accumulate less in the bubble interface where radical OH concentration is higher. US experiments at pH 10 were conducted to examine the effect of pH on initial rate for TCS degradation. At pH 10, about 99% of TCS is in anionic form, according to the following expression (Chiha et al. 2011):

$$\varphi_{ionic} = \frac{1}{1 + 10^{(pK_a - pH)}} \quad (5)$$

Comparing the results for pH 10 with those obtained at natural pH at optimal frequency and high power density level, it can be seen in Fig. 8 that there is no difference in degradation rates. At this pH value, TCS is still highly hydrophobic (log $K_{ow} = 3$) (Behera et al. 2010). Because of this, reducing TCS hydrophobicity at pH 10 could generate a lower mobility of the molecules towards the bubble surface, but also, in the phenolate form, TCS is more reactive with OH radicals than in the phenolic form, because $O^-$ is better in activating the aromatic ring as has been found in studies of chlorine-mediated oxidation (Rule et al. 2005). As can be seen from these experiments, the net effect is null. Therefore, there is no reduction in the total degradation rate at higher pH values.

## Toxicity

An ecotoxicity assay was conducted using Microtox® equipment that measures the decrease in the natural luminescence of the marine bacteria *Vibrio fischeri* in the presence of TCS in aqueous solution. Diminishing bioluminescence indicates diminishing cellular respiration. Toxic substances change the percentage of protein and lipid synthesis, thus changing the light emission level. The toxicity is expressed as effective concentration $EC_{50}$: pollutant concentration producing a 50% reduction in light emission (Onorati and Mecozzi 2004).

The 81.9% Basic Test was used as shown in the Guide to Microtox M500 procedure for acute toxicity. Initial TCS concentration was 0.68 mg/L in deionized water, and response was measured at 5 and 15 min. There was no significant difference in the response for 15 min to that of 5 min. $EC_{50}$ was 0.164 mg/L. This result is similar to that obtained by Farré et al. (2008) who found a $EC_{50}$ value of 0.28 mg/L using Microtox procedure for TCS solutions in water in concentrations ranging from 0.0375 to 2 mg/L.

Toxicity path as US degradation occured was measured for a TCS solution with an initial concentration of 0.68 mg/L, treated at 574 kHz and 140 W/L for 90 min. Three milliliter samples were withdrawn at different times and analyzed using Microtox by the 81.9% screening test. Results are shown in Fig. 9.

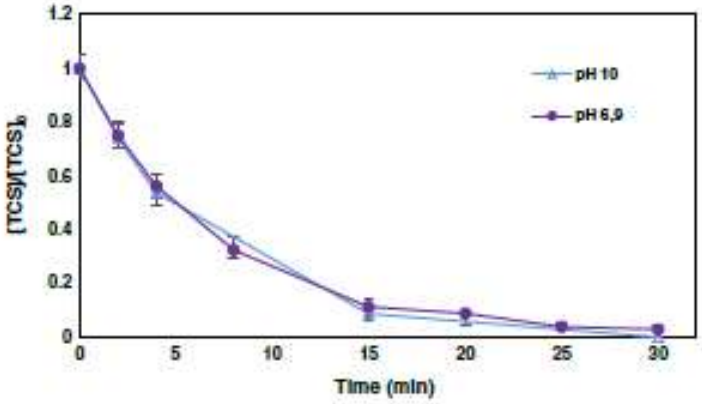


Fig. 8 Effect of pH on TCS degradation by US. Frequency 574 kHz, power density 140 W/L, initial TCS concentration 1 mg/L, solution volume 300 mL, T 25 ± 2 °C

Toxicity profile shows that toxicity decreases as TCS concentration decreases, increasing afterwards. Farré et al. (2008) found that methyl TCS, a possible TCS degradation by-product, had an $EC_{50}$ of 0.21 mg/L (Microtox acute toxicity method), slightly lower than that of TCS. 2,7/2,8-Dichlorodibenzo-p-dioxin (2,8-DCDD) was detected as a US TCS degradation by-product, but it has been reported that its acute toxicity is low (Blair 1971). Further study must be done on biodegradability of by-products as triclosan is depleted, and of the possible by-products generating this toxic effect. This will help to determine if stopping degradation before total mineralization is the best option for US triclosan degradation.

However, it can be expected that other polychlorinated dibenzo-p-dioxins (PCDDs) and polychlorinated dibenzofurans (PCDFs) are being generated. One of them, the tetrachloro dibenzo-p-dioxin has one of the lowest known LD50 (Hites 2011). Trichlorophenol and tetrachlorophenol, possible TCS degradation by-products, could be transformed in this highly toxic chemical, and other similar.

However, further research is needed to fully understand the reason behind toxicity increase after TCS depletion.

## Degradation products

Deionized water spiked at 10 mg/L with TCS was sonicated, and aliquots of the solution were taken at 40 and 90% of TCS degradation. Compounds were isolated from the water samples by solid-phase extraction. Separation and detection of degradation products were accomplished by gas chromatography-mass spectrometry. Eight possible compounds were detected, based on the presence of the molecular ion; interpretation of their fragment ions in the mass spectra was conducted using MassHunter software and NIST 14 Mass Spectral Library.

2,7/2,8-Dibenzodichloro-p-dioxin was identified at 40 and 90% of TCS degradation, for the three SPE columns used. This is a very well-known TCS degradation product. It has been reported as produced by the direct effect of UV radiation at basic and neutral pH (Mezcua et al. 2004;

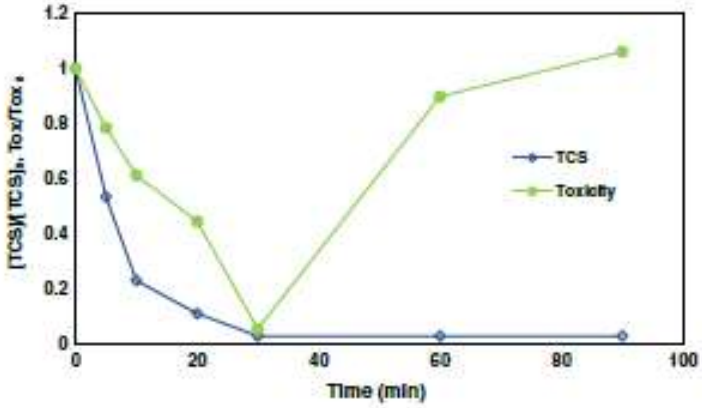


Fig. 9 Toxicity evolution for TCS degradation by US. Initial concentration 0.68 mg/L, frequency 574 kHz, power density 140 W/L, volume 300 mL, T 25 ± 2 °C

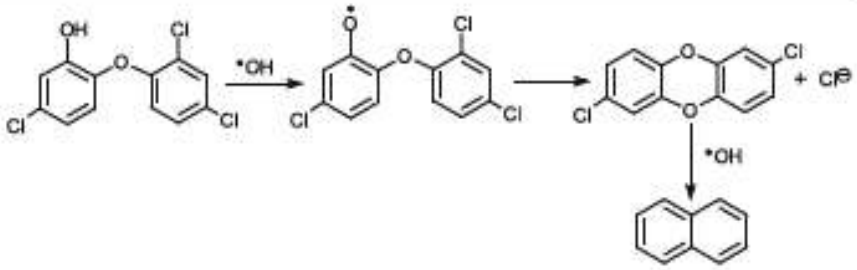


Fig. 10 Reaction mechanism for dibenzodichloro-p-dioxin formation

Latch et al. 2005; Wong-Wah-Chung et al. 2007; Lores et al. 2005; Aranami and Readman 2007), and in municipal wastewater treatment plants (WWTPs) (Tohidi and Cai 2015). The reaction mechanism that we proposed for its production by ultrasound degradation includes hydrogen abstraction from the phenolic moiety by OH radicals and posterior cyclization (Fig. 9). Previous studies of TCS photodegradation have shown that this reaction is caused by the effect of direct UV radiation on TCS and depends on UV wavelength (Aranami and Readman 2007; Stamatis et al. 2014). However, the results obtained in this study show that this reaction can occur due to the direct attack of OH radicals. The peak area found at 40 and 90% of TCS degradation is very similar, showing that this is a persistent by-product.

Naphtalene was detected at 40% of TCS degradation with SPE extraction with PS DVB column. This compound has been reported by Summoogum et al. (2012) in the oxidation of dibenzo-p-dioxin with $O_3/N_2$ mixture at temperatures between 400 and 800 °C. We propose that in US degradation, it is produced by the attack of OH radicals over dibenzo-p-dioxin as shown in Fig. 10.

2,4-Dichlorophenol was also identified at both reaction times, for the three SPE columns. This compound has been previously reported as a TCS photolysis (Latch et al. 2003, 2005), photocatalytic (Yu et al. 2006), and permanganate oxidation by-product (Wu et al. 2012). For US treatment, we propose that it is produced by reductive chlorination via electron attack and cleavage of the ether bond.

4-Chloro-3-(4 chlorophenoxy)phenol was detected at both reaction times with Phenyl and XC columns. 2-Phenoxyphenol and 2′-chloro[1,1′-biphenyl]-2,5-diol were also detected as possible degradation products at both reaction times, and were extracted by XC column. These are hydroxyl-TCS derivatives formed by the electrophilic attack of OH radicals over dichlorobenzene or chlorophenol rings of TCS molecule or its hydroxylated derivatives, followed by dechlorination.

Acetic acid was detected in samples at 60 and 90 min of reaction extracted by SP DVB column. Oxalic acid was also detected in sample at 60 min of reaction extracted by Strata Phenyl column. After cleavage of the benzene ring, further oxidation of intermediates could lead to ring opening generating these carboxylic acids before mineralization. Carboxylic acids such as oxalic, formic, and acetic have been previously detected as final products of TCS degradation (Sirés et al. 2007). The total mechanism proposed is shown in Fig. 11.

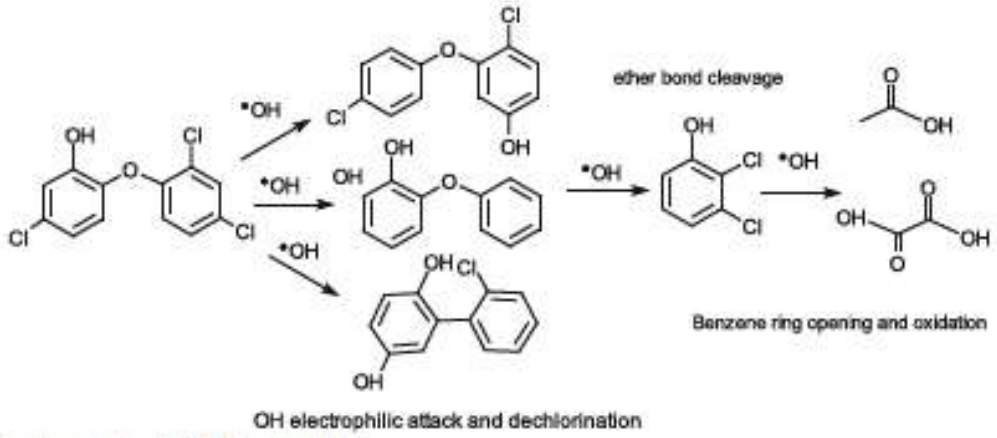


Fig. 11 Reaction mechanism for TCS degradation by US

## Conclusions

Optimum frequency for TCS degradation was 574 kHz, and optimum power value was 200 W/L—the highest achievable power value for US reactor. For these values, total TCS degradation was achieved in 25 min. Two different kinetic models for TCS degradation at natural pH were proposed based on the models found in other studies for US degradation of organic pollutants. These models considered that reaction with OH radicals takes place at the bubble's surface. But their reaction mechanisms were different. One was based on a saturation-type reaction over the bubble surface, while the other took into account that radical reactions could take place over the bubble surface or in the bulk solution. A pseudo-linear kinetic model resulting from the application of the second mechanism had the best statistical fit for this system. The kinetic constant had a value of 0.110441 $min^{-1}$, (574 kHz, 140 W/L), four times higher than those found in other studies for US TCS degradation at lower frequencies. TCS degradation at natural pH takes place over the bubble surface, and its degradation rate depends on TCS bulk concentration, the rate of generation and recombination of radicals, and the rate of reaction between TCS and OH radicals.

Initial reaction rates for PW US were 15.3% higher than those for continuous US, and inhibition was between 42.0 and 51.4% for different alcohols as radical scavengers in the bulk fluid and bubble surface. These results confirmed that TCS is being degraded at the bubble's surface. Toxicity $EC_{50}$ value measured in the Microtox® toxicity test was 0.164 mg/L. Toxicity decreased continuously with TCS depletion. After TCS total degradation, toxicity increased showing that toxic by-products are being generated.

Eight possible degradation by-products were found, among them 2,7/2,8-dibenzodichloro-p-dioxin and 2,4-dichlorophenol, showing that OH radicals could generate this toxic by-products at neutral pH and that further research is needed to understand their fate in US processes.

**Acknowledgments** The authors wish to thank NSERC, the Canadian Bureau for International Education (CBIE), and the ELAP program; the Colombian Administrative Department of Science, Technology and Innovation (COLCIENCIAS); the University of Saskatchewan; and the University of Antioquia for the support of this work.

## References

Adewuyi YG, Oyenekan BA (2007) Optimization of a sonochemical process using a novel reactor and Taguchi statistical experimental design methodology. Ind Eng Chem Res 46:411–420. https://doi.org/10.1021/ie060844c

Apfel RE (1981) 7. Acoustic cavitation. In: Ultrasonics. Series: Methods in experimental physics. Elsevier, New York, pp 355–411

Arnsami K, Readman JW (2007) Photolytic degradation of triclosan in freshwater and seawater. Chemosphere 66:1052–1056. https://doi.org/10.1016/j.chemosphere.2006.07.010

Behera SK, Oh SY, Park HS (2010) Sorption of triclosan onto activated carbon, kaolinite and montmorillonite: effects of pH, ionic strength, and humic acid. J Hazard Mater 179:684–691. https://doi.org/10.1016/j.jhazmat.2010.03.056

Blair E (1971) Chlorodioxins—origin and fate. American Chemical Society, Washington D.C

Chiha M, Hamdaoui O, Baup S, Gondrexon N (2011) Sonolytic degradation of endocrine disrupting chemical 4-cumylphenol in water. Ultrason Sonochem 18:943–950. https://doi.org/10.1016/j.ultsonch.2010.12.014

De Bel E, Janssen C, De Smet S et al (2011) Sonolysis of ciprofloxacin in aqueous solution: influence of operational parameters. Ultrason Sonochem 18:184–189. https://doi.org/10.1016/j.ultsonch.2010.05.003

Farré M, Asperger D, Kantiani L et al (2008) Assessment of the acute toxicity of triclosan and methyl triclosan in wastewater based on the bioluminescence inhibition of Vibrio fischeri. Anal Bioanal Chem 390:1999–2007. https://doi.org/10.1007/s00216-007-1779-9

Hayduk W, Laudie H (1974) Prediction of diffusion coefficients for non-electrolytes in dilute aqueous solutions. AICHE J 20:611–615. https://doi.org/10.1002/aic.690200329

Henglein A (1987) Sonochemistry: historical developments and modern aspects. Ultrasonics 25:6–16. https://doi.org/10.1016/0041-624X(87)90003-5

Hites RA (2011) Dioxins: an overview and history†. Environ Sci Technol 45:16–20. https://doi.org/10.1021/es1013664

Ince NH, Gültekin I, Tezcanli-Güyer G (2009) Sonochemical destruction of nonylphenol: effects of pH and hydroxyl radical scavengers. J Hazard Mater 172:739–743. https://doi.org/10.1016/j.jhazmat.2009.07.058

Khanna S, Chakma S, Moholkar VS (2013) Phase diagrams for dual frequency sonic processors using organic liquid medium. Chem Eng Sci 100:137–144. https://doi.org/10.1016/j.ces.2013.02.016

Kimura T, Sakamoto T, Leveque J et al (1996) Standardization of ultrasonic power for sonochemical reaction. Ultrason Sonochem 3:S157–S161. https://doi.org/10.1016/S1350-4177(96)00021-1

Kolpin DW, Kolpin DW, Furlong ET et al (2002) Pharmaceuticals, hormones, and other organic wastewater contaminants in U.S. streams, 1999-2000: A national Reconnaissance. Environ Sci Technol 36:1202–1211. https://doi.org/10.1021/es011055j

Latch DE, Packer JL, Arnold WA, McNeill K (2003) Photochemical conversion of triclosan to 2,8-dichlorodibenzo-p-dioxin in aqueous solution. J Photochem Photobiol A Chem 158:63–66. https://doi.org/10.1016/S1010-6030(03)00303-5

Latch DE, Packer JL, Stender BLB et al (2005) Aqueous photochemistry of triclosan: formation of 2,4-dichlorophenol, 2,8-dichlorodibenzo-p-dioxin, and oligomerization products. Environ Toxicol Chem 24:517–525. https://doi.org/10.1897/04-243R.1

Lores M, Llompart M, Sanchez-Prado L et al (2005) Confirmation of the formation of dichlorodibenzo-p-dioxin in the photodegradation of triclosan by photo-SPME. Anal Bioanal Chem 381:1294–1298. https://doi.org/10.1007/s00216-004-3047-6

Mahamuni NN, Adewuyi YG (2010) Advanced oxidation processes (AOPs) involving ultrasound for waste water treatment: a review with emphasis on cost estimation. Ultrason Sonochem 17:990–1003. https://doi.org/10.1016/j.ultsonch.2009.09.005

Mezcua M, Gómez MJ, Ferrer I et al (2004) Evidence of 2,7/2,8-dibenzodichloro-p-dioxin as a photodegradation product of triclosan in water and wastewater samples. Anal Chim Acta 524:241–247. https://doi.org/10.1016/j.aca.2004.05.050

Munoz M, de Pedro ZM, Casas JA, Rodriguez JJ (2012) Triclosan breakdown by Fenton-like oxidation. Chem Eng J 198–199:275–281. https://doi.org/10.1016/j.cej.2012.05.097

Naddeo V, Landi M, Scannapieco D, Belgiorno V (2013) Sonochemical degradation of twenty-three emerging contaminants in urban wastewater. Desalin Water Treat 51:6601–6608. https://doi.org/10.1080/19443994.2013.769696

Okitsu K, Iwasaki K, Yobiko Y et al (2005) Sonochemical degradation of azo dyes in aqueous solution: a new heterogeneous kinetics model taking into account the local concentration of OH radicals and azo dyes. Ultrason Sonochem 12:255–262. https://doi.org/10.1016/j.ultsonch.2004.01.038

Okitsu K, Suzuki T, Takenaka N et al (2006) Acoustic multibubble cavitation in water: a new aspect of the effect of a rare gas atmosphere on bubble temperature and its relevance to sonochemistry. J Phys Chem B 110:20081–20084. https://doi.org/10.1021/jp064598u

Onorati F, Mecozzi M (2004) Effects of two diluents in the Microtox toxicity bioassay with marine sediments. Chemosphere 54:679–687. https://doi.org/10.1016/j.chemosphere.2003.09.010

Pétrier C (2015) The use of power ultrasound for water treatment. In: Power ultrasonics. Applications of high-intensity ultrasound. Woodhead Publishing, Elsevier, pp 939–972. https://doi.org/10.1016/B978-1-78242-028-6.00031-4

Petrovic M (2003) Analysis and removal of emerging contaminants in wastewater and drinking water. TrAC Trends Anal Chem 22:685–696. https://doi.org/10.1016/S0165-9936(03)01105-1

Rule KL, Ebbett VR, Vikesland PJ (2005) Formation of chloroform and chlorinated organics by free-chlorine-mediated oxidation of triclosan. Environ Sci Technol 39:3176–3185. https://doi.org/10.1021/es048943+

Sabaliunas D, Webb SF, Hauk A et al (2003) Environmental fate of triclosan in the River Aire Basin, UK. Water Res 37:3145–3154. https://doi.org/10.1016/S0043-1354(03)00164-7

Sanchez-Prado L, Barro R, Garcia-Jares C et al (2008) Sonochemical degradation of triclosan in water and wastewater. Ultrason Sonochem 15:689–694. https://doi.org/10.1016/j.ultsonch.2008.01.007

Serna-Galvis EA, Silva-Agredo J, Giraldo-Aguirre AL, Torres-Palma RA (2015) Sonochemical degradation of the pharmaceutical fluoxetine: effect of parameters, organic and inorganic additives and combination with a biological system. Sci Total Environ 524-525:354–360. https://doi.org/10.1016/j.scitotenv.2015.04.053

Serpone N, Terzian R, Hidaka H, Pelizzetti E (1994) Ultrasonic induced dehalogenation and oxidation of 2-, 3-, and 4-chlorophenol in air-equilibrated aqueous media. Similarities with irradiated semiconductor particulates. J Phys Chem 98:2634–2640. https://doi.org/10.1021/j100061a021

Sirés I, Oturan N, Oturan MA et al (2007) Electro-Fenton degradation of antimicrobials triclosan and triclocarban. Electrochim Acta 52:5493–5503. https://doi.org/10.1016/j.electacta.2007.03.011

Son HS, Ko G, Zoh KD (2009) Kinetics and mechanism of photolysis and TiO2 photocatalysis of triclosan. J Hazard Mater 166:954–960. https://doi.org/10.1016/j.jhazmat.2008.11.107

Song Z, Wang N, Zhu L et al (2012) Efficient oxidative degradation of triclosan by using an enhanced Fenton-like process. Chem Eng J 198–199:379–387. https://doi.org/10.1016/j.cej.2012.05.067

Stamatis N, Antonopoulou M, Hela D, Konstantinou I (2014) Photocatalytic degradation kinetics and mechanisms of antibacterial triclosan in aqueous TiO 2 suspensions under simulated solar irradiation. J Chem Technol Biotechnol 89:1145–1154. https://doi.org/10.1002/jctb.4387

Summoogum SL, Altarawneh M, Mackie JC et al (2012) Oxidation of dibenzo-p-dioxin: formation of initial products, 2-methylbenzofuran and 3-hydro-2-methylenebenzofuran. Combust Flame 159:3056–3065. https://doi.org/10.1016/j.combustflame.2012.05.004

Thanavadivel K, Meghanj M, Madhoo A, Naidu R (2012) Degradation of organic pollutants using ultrasound. Handb Appl Ultrason Sonochem Sustain 447–474. doi:https://doi.org/10.1201/b11012-19

Tohidi F, Cai Z (2015) GC/MS analysis of triclosan and its degradation by-products in wastewater and sludge samples from different treatments. Environ Sci Pollut Res Int. https://doi.org/10.1007/s11356-015-4289-x

van Iersel MM, Benes NE, Keurentjes JTF (2008) Importance of acoustic shielding in sonochemistry. Ultrason Sonochem 15:294–300. https://doi.org/10.1016/j.ultsonch.2007.09.015

Wong-Wah-Chung P, Rafqah S, Voyard G, Sarakha M (2007) Photochemical behaviour of triclosan in aqueous solutions: kinetic and analytical studies. J Photochem Photobiol A Chem 191:201–208. https://doi.org/10.1016/j.jphotochem.2007.04.024

Wu Q, Shi H, Adams CD et al (2012) Oxidative removal of selected endocrine-disruptors and pharmaceuticals in drinking water treatment systems, and identification of degradation products of triclosan. Sci Total Environ 439:18–25. https://doi.org/10.1016/j.scitotenv.2012.08.090

Xiao R, Diaz-rivera D, He Z, Weavers LK (2013a) Using pulsed wave ultrasound to evaluate the suitability of hydroxyl radical scavengers in sonochemical systems. Ultrason Sonochem 20:990–996. https://doi.org/10.1016/j.ultsonch.2012.11.012

Xiao R, Diaz-Rivera D, Weavers LK (2013b) Factors influencing pharmaceutical and personal care product degradation in aqueous solution using pulsed wave ultrasound. Ind Eng Chem Res 52:2834–2831. https://doi.org/10.1021/ie303052a

Xiao R, Wei Z, Chen D, Weavers LK (2014) Kinetics and mechanism of sonochemical degradation of pharmaceuticals in municipal wastewater. Environ Sci Technol 48:9675–9683. https://doi.org/10.1021/es5016197

Yang L, Rathman JF, Weavers LK (2005) Degradation of alkylbenzene sulfonate surfactants by pulsed ultrasound. J Phys Chem B 109:16208–16209. https://doi.org/10.1021/jp052322l

Yu JC, Kwong TY, Luo Q, Cai Z (2006) Photocatalytic oxidation of triclosan. Chemosphere 65:390–399. https://doi.org/10.1016/j.chemosphere.2006.02.011

Zúñiga-Benítez H, Soltan J, Peñuela GA (2016) Application of ultrasound for degradation of benzophenone-3 in aqueous solutions. Int J Environ Sci Technol 13:77–86. https://doi.org/10.1007/s13762-015-0842-x

Ultrasonics - Sonochemistry 43 (2018) 201–207

Contents lists available at ScienceDirect

Ultrasonics - Sonochemistry

journal homepage: www.elsevier.com/locate/ultson

# Benzophenone-3 ultrasound degradation in a multifrequency reactor: Response surface methodology approach

Lina Patricia Vega-Garzon*, Ingry Natalia Gomez-Miranda, Gustavo A. Peñuela

*Grupo GDCON, Facultad de Ingeniería, Sede de Investigación Universitaria (SIU), Universidad de Antioquia, Calle 70 No 52-21, Medellín, Colombia*

ARTICLE INFO

*Keywords:*
Benzophenone 3
Advanced oxidation processes
Sonochemistry
Response Surface Methodology
Pulsed mode ultrasound

ABSTRACT

Response Surface Methodology was used for optimizing operating variables for a multi-frequency ultrasound reactor using BP-3 as a model compound. The response variable was the Triclosan degradation percent after 10 sonication min. Frequency at levels from 574, 856 and 1134 kHz were used. Power density, pulse time (PT), silent time (ST) and PT/ST ratio effects were also analyzed. $2^2$ and $2^3$ experimental designs were used for screening purposes and a central composite design was used for optimization. An optimum value of 79.2% was obtained for a frequency of 574 kHz, a power density of 200 W/L, and a PT/ST ratio of 10. Significant variables were frequency and power level, the first having an optimum value after which degradation decreases while power density level had a strong positive effect on the whole operational range. PT, ST, and PT/ST ratio were not significant variables although it was shown that pulsed mode ultrasound has better degradation rates than continuous mode ultrasound, the effect less significant at higher power levels.

## 1. Introduction

Benzophenone-3 (2-hydroxy-4-methoxybenzophenone, or oxybenzone) (BP-3) is an UVA (320–400 nm) filter widely used in personal care products such as sunscreens, creams, shampoos, and hair sprays [1]. It is released into superficial waters by run off or via wastewater [2,3]. Thus, it has been detected in rivers [4], wastewater [5] and lakes [6], in concentrations as high as 7.8 μg/L. Also, it has been detected in human urine in United States population > 6 years of age at levels of 22.9 ng/mL [7] and at levels of 2.09 ng/mL in paired samples of children and adults in China [8]. Its environmental importance comes from its property of being an endocrine disruptor, a persistent and a bioaccumulative compound [9]. BP-3 alters genes related with the production of sexual hormones. This has been established by assays in which it caused alteration of gene expression in both adult fish and eleuthero-embryos of zebrafish [1]. Its estrogenic and anti-androgenic activity also has been demonstrated in rats by [10]. In the same way, it was shown BP-3 causes alterations in liver, kidney, and reproductive organs in rats and mice when dermally and orally administrated [7].

Some advanced oxidation processes have been applied to BP-3 degradation giving different degradation efficiencies. Photodegradation has not shown good effectiveness, but ozonation and oxidation with Fe (VI) has been very effective. Gago Ferrero et al [11] found BP-3 remained unaltered after 24 h of solar radiation treatment. De Vione et al [12] found similar results degrading BP-3 by sunlight at an initial concentration of 20 μM, finding a half-life time of some weeks. On the other hand, Gago-Ferrero et al., [9] achieved more than 95% BP-3 degradation in 40–50 min of ozonation for an initial BP-3 concentration of 5.1 mg/L, an ozone inlet concentration of 85.7 μmol/$L_{gas}$, and gas flow rate of 120 mL/min. Hernandez-Leal et al [13] obtained more than 99% of degradation in 15 min of ozonation of water containing 285 ng/L of BP-3. Yang & Ying [14] treated BP-3 by oxidation with Fe (VI) obtaining a half-life of 167.8 s of Fe(VI) concentration of 10 mg/l, and pH 8.

Ultrasound (US) is one of the promising advanced oxidation treatments having an advantage over other treatments in that it does not use chemicals to achieve oxidation. At the same time it has good degradation and mineralization rates. Zuñiga & Peñuela [15] used ultrasound for degrading BP-3 in a probe-tip reactor obtaining 91.4% degradation at 60 min of reaction, for low frequency level of 20 kHz, and power level of 80.1 W, showing the ultrasound potential for degrading this compound. However, optimization of ultrasound degradation variables, and its degradation at high frequency levels is necessary in order to achieve compound degradation and/or mineralization in the shortest possible times, with the lowest energy consumption. Previous studies in ultrasound degradation for other compounds other than BP-3 have analyzed the effect of variables such as ultrasonic frequency, ultrasonic power/intensity, gas, and pH on water pollutant's ultrasound degradation, leaving one variable constant and changing the others. Only one paper reports an analysis considering the interactions for

* Corresponding author.
*E-mail addresses:* patricia.vega@udea.edu.co (L.P. Vega-Garzon), ingry.gomez@udea.edu.co (I.N. Gomez-Miranda), gustavo.penuela@udea.edu.co (G.A. Peñuela).

https://doi.org/10.1016/j.ultsonch.2017.10.014
Received 13 June 2017; Received in revised form 29 September 2017; Accepted 17 October 2017
Available online 18 October 2017
1350-4177/ 

variables affecting the ultrasound degradation of carbon disulfide [16]. The factors analyzed in that study were ultrasonic frequency and intensity, solution temperature, and gas. It used a Taguchi statistical experimental methodology, which compared to a full factorial design, diminished considerably the number of experiments to be made. This kind of analysis must be done in order to take into account the simultaneous effects of the variables and their interactions.

Response Surface Methodology (RSM), is a collection of mathematic and statistic tools useful for modelling and analyzing systems in which a response variable is influenced by several variables. The goal of this methodology is optimizing the response variable. Initially, it has a screening step in which a $2^k$ design is used in search of the variables that have effect on the response variable using few experiments. Adding central points to this design allows checking if there is some surface curvature. Finally, an approach as the central composite design is used for characterizing the area of optimal response. In this design, axial points are added to adjust a quadratic model [17].

In the present study, the analysis using RSM was applied for the optimization of ultrasound degradation for BP-3 including the pulsed mode ultrasound variables and its interaction with power and frequency for a multi-frequency ultrasound reactor. Variables analyzed were: power density (P), frequency, PT, ST, and PT/ST ratio. With RSM, we modeled and analyzed the response of interest (BP-3 degradation) due to changes in these variables looking for interactions that could be being ignored in previous studies. This approach let us understand these variable's relationships in the search for optimum degradation rate. In this paper, we present a straightforward path for optimizing operational variables in a multi-frequency ultrasound reactor.

## 2. Material and methods

### 2.1. Material

Solutions used in these ultrasonic degradation experiments were prepared using Millipore water (18 MΩ cm) and BP-3 (2-hydroxy-4-methoxy-benzophenone) with a purity of > 98% from Alfa Aesar. HPLC grade acetonitrile was obtained from Merck KGaA; Darmstadt, Germany.

### 2.2. Methods

#### 2.2.1. Experimental set up

Degradation experiments were conducted in a cylindrical glass reactor with a total volume of 500 mL with a cooling jacket. An Ultrasonic Power Multifrequency Generator MG (Meinhardt Ultrasonics, Leipig, Germany) was used. An ultrasonic transducer type E/805/T/M (Meinhardt Ultrasonics, Leipig, Germany) was flanged to the generator for generating frequencies of 574, 856 and 1134 kHz. Reactor was coupled to the top of the transducer having ultrasound waves throughout the transverse area. Fig. 1 shows an squeme of the experimental Set up. Frequency level was changed in the generator depending on the experiment set being conducted. Ultrasonic power density was calculated by the calorimetric method [18] using amplitudes from 50 to 100% for the intensity power of the equipment for each frequency level. Then, power density value was set in the proper value using the corresponding amplitude. Pulse time and silent time was adjusted in the equipment that could change these values continuously from 0 to 10,000 ms.

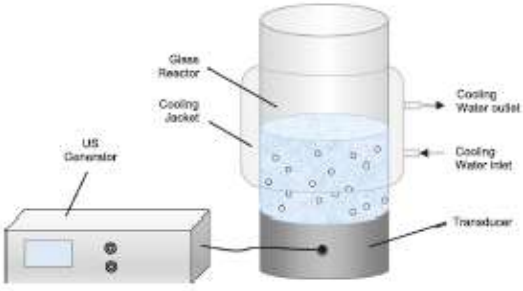


Fig. 1. Experimental set up.

A volume of 300 mL reaction solution was used in every experiment and a sample of 2 mL was withdrawn at the end of the time interval for BP-3 HPLC analysis. Initial BP-3 concentration was 1 mg/L. Solution temperature was maintained at 25 ± 2 °C during reaction time by circulating cooling water in the reactor jacket. Total radiation time was 10 min for each experiment. We chose this reaction time higher than that necessary for measuring initial rates because greater differences between initial and final concentrations were obtained. This minimized the effect of possible experimental or instrumental errors, which could lead to erroneous conclusions. In this time, BP-3 concentration variation was high enough to appreciate the effect of all the variables under analysis. Total reaction time for pulsed mode ultrasound was calculated according to the following equation [19]:

$$t_{total} = t_{sonication}\left(1 + \frac{ST}{PT}\right) \quad (1)$$

where $t_{total}$ is the total reaction time; $t_{sonication}$ is the real sonication time (10 min); $ST$ is the time between pulses (Silent Time); and $PT$ is the Pulse Time.

#### 2.2.2. Chemical analysis

*2.2.2.1. High performance liquid chromatography (HPLC).* BP-3 concentration in water for total degradation analysis was determined by reverse phase chromatography using an Agilent 1200 Series HPLC system with auto sampler, a Zorbax SB-C18 column (porous silica with 80 A° pore diameter, 3.5 µm, 4.6 × 150 mm), and a Diode Array Detector set at 288 nm. The mobile phase was a mixture of acetonitrile and mili Q water (70:30, v/v), flow rate was 0.8 mL/min, injection volume was 100 µL, and column temperature was 30 °C. This analytical procedure showed good linearity in the range of 0.02–2 ppm ($R^2$ = 0.9999). The detection limit was 0.0015 ppm, and quantification limit was 0.005 ppm. Repeatability was 1.3% for the measurement range.

## 3. Theory

According to the hot spot theory, ultrasound degradation of pollutants is caused by the acoustic cavitation, that is, creation, expansion, and implosive collapse of gas bubbles in liquid by the effect of ultrasound irradiation [20]. Thermal decomposition of water in the compression of the oscillating bubbles produces mainly hydroxyl free radicals [21]. These radicals react with hydrogen molecules, oxygen peroxide, pollutants, or can recombine forming hydrogen peroxide [21]. Solute degradation processes can take place in different sites: inside the collapsing bubbles, in the bubble/liquid interphase, and in the bulk solution [22].

Operation variables such as power density, frequency, and pulsed mode for US radiation have influence on pollutant degradation. When power intensity of ultrasound radiation increases, acoustic amplitude increases generating more violent collapse of the bubbles [16]. It is well known that power intensity could have an optimum value in which maximum pressure and temperature during collapse will give an optimal degradation rate. Higher intensities could generate bubble shielding, in which a dense cloud of bubbles attenuate the effect of the ultrasound radiation, generating higher decrease in wave intensity along the reactor length compared to that one in the optimum power [23].

Frequency is an important variable influencing the kind of processes occurring in the solution. At low frequencies, physical effects

predominate and the number of cavitation events are less than at higher frequencies [24]. Also, higher bubble volumes make collapsing bubbles have higher vapor content. This effect generates less energetic implosion of bubbles resulting in lower OH radical generation. On the other hand, at high frequencies, bubble lives and sizes are smaller, resulting in a lower vapor presence at the collapsing moment, generating a more energetic bubble implosion. However, at higher frequencies, shorter rarefaction cycles could generate molecules that are not sufficiently stretched to generate the bubble. Also, at higher frequencies, overall bubble surfaces are lower, and mass transfer of the pollutants towards the bubble could dominate the overall rate. It has been shown that optimal frequency is mainly a function of the substance properties [16].

Pulsed wave mode ultrasound also has an important effect in ultrasound effectiveness. This effect is related with the effectiveness of the formation, growing and imploding of the bubbles (cavitation effect), and with the ability of the pollutant molecules to diffuse to the bubble surface where degradation mainly occurs for some pollutants (kinetic-adsorption effect). During continuous wave ultrasound, bubble clusters could appear. These bubbles do not absorb enough energy to be active and the proximity of the bubbles could also increase bubble coalescence. Pulsed wave mode ultrasound makes these effects diminish [25]. It has been demonstrated for non-volatile hydrophobic compounds, that there is a dependence of the degradation rates on the pulse length, and on the interval for ultrasound radiation [19]. In that study, short pulses generated insufficient activation of cavitation bubbles and longer pulses favored the surfactant accumulation over the bubble surface in a kinetic-diffusion controlled degradation mechanism. In the same way, [26] showed a positive effect of pulsed mode ultrasound on the oxidation of Arsenic (III) to Arsenic (IV). For mixtures of surfactants with non-surfactants, Yang et al [27] showed surfactant degradation rate significantly enhanced with pulsed ultrasound, being the concentration of reactants – and pulse interval, the principal factors affecting degradation rates.

In general, it has been shown the ability of ultrasound to generate chemically active bubbles could be dependent on the ratio of the US pulse length and pulse interval [25] and enhancement of ultrasound during pulsed ultrasound depends on the frequency [28]. However, these studies were made under a limited range of pulsing conditions and a straightforward relationship was not established. Therefore, the same authors conducted a study varying conditions for pulse length and pulse interval in a wide range [25] for octyl benzene sulfonate ultrasound degradation. In their study, they did not find a clear trend for the degradation rate as a function of ultrasound frequency and pulse mode, despite having found there was an effect of these two variables.

## 4. Results

### 4.1. Screening experiments

Factors in the design of experiments are independent variables that can affect the variable of analysis, in this case, BP-3 degradation percent. Compound properties influencing US degradation rates include hydrophobicity, volatility, diffusivity, and reactivity with OH radicals. BP-3 has a molecular weight of 228.1, a high Log ($K_{OW}$) of 3.8, low volatility – $K_H$: of $1.5 * 10^{-8}$ Atm-$m^3$/mol, and a molar volume of 190 ml/mol, so it is expected that it diffuses towards bubble interphase [29]. Because of this, BP-3 probably is degrading in the bubble surface and could have a degradation rate improvement using pulsed mode ultrasound.

Therefore, variables analyzed were frequency level US power density (P), pulse Time, and silent time. An initial screening analysis was made for detecting variables influencing degradation percentage. Frequency values studied were 373, 574 and 856 kHz; P was set at 100 and 140 W/L, PT and ST were both set at 20 and 100 ms (Table 1). This experimental design required $2^3$ experiments, and four central point experiments were added. Experiments were made by duplicate for a total of 18 experiments for each frequency level. In total, 54 experiments were conducted at this stage. Treatments for $2^3$ design are shown in Table 2. Results and ANOVA tables for these designs and all the designs in this paper can be found in the supplemental material (Mendeley Data, v1https://doi.org/10.17632/2kycsjmkj3.1 DOI is reserved but not active).

**Table 1**
Factors and levels for the $2^2$ factorial experimental design.

| Factor | Level Values | | |
|---|---|---|---|
| | −1 | 1 | Central point |
| P (W/L) – $X_1$ | 100 | 140 | 110 |
| PT (ms) – $X_2$ | 20 | 100 | 60 |
| ST (ms) – $X_3$ | 20 | 100 | 60 |

**Table 2**
Factors and levels for the $2^2$ factorial experimental design (574 kHz, BP-3 initial concentration: 1 mg/L, T: 25 °C ± 2°C, ST: 20 ms).

| Factor | Level values | |
|---|---|---|
| | −1 | 1 |
| P (W/L) – $X_1$ | 80 | 140 |
| PT/ST – $X_2$ | 1 | 5 |

For making a comparison between pulsed and continuous mode ultrasound, Pulse Enhancement (PE*) was analyzed. PE is defined as [30]

$$PE^*(\%) = \frac{(Deg)_{PW} - (Deg)_{CW}}{(Deg)_{CW}} \times 100\% \quad (2)$$

where $(Deg)_{PW}$ is degradation percent for pulsed mode ultrasound, $(Deg)_{CW}$ is degradation percent for pulsed mode ultrasound after 10 min. of sonication and for the corresponding frequency and power density levels. Results for this combination of variable values are shown in Fig. 2.

Response variable analyzed was degradation percent after 10 min of degradation under these treatments. ANOVA analysis was made in STATGRAPHICS Centurion XVI.I. For this screening analysis at a frequency of 574 kHz following conclusions were made: Power density was a significant variable, having a positive effect on degradation rates. This effect was positive and significant for all frequencies; however, the effect of PT and ST was unclear for all frequencies. In Fig. 3, maximum degradation values for this set of experiments are shown. They were 68.4% for 574 kHz; 56.2% for 856 kHz; and 51.8% for 1134 kHz. The conditions at which these maximum values were obtained were the same for the three frequency levels: power density: 140 W/L, PT: 100 ms and ST: 20 ms. In this figure it can be seen that degradation values for 574 kHz are higher than those at 856 and 1134 kHz, indicating that 574 kHz or a lower frequency value is the optimum for BP-3 degradation, and that at higher frequencies lower rates are found according to the explanation of frequency effect made in section 3. 856 and 1134 kHz resulted in similar degradation percents, Therefore, from now on only the frequency of 574 kHz was used for optimization.

Another statistical analysis was made for frequency 574 kHz using the variable PT/ST instead of PT and ST separately, for the same results obtained in these experiments. The purpose was exploring a possible relationship with this variable according to that previously reported in literature, as explained in Section 3. Variables values are shown in Table 2. Design was a factorial $2^2$, one replicate each, for a total of eight experiments. After lineal model analysis, conclusion by ANOVA results was made that power density and PT/ST were both significant variables and their effects were positive on degradation levels. The maximum degradation value obtained (68.4%) in this case corresponded to the highest power density level, and to the highest PT/ST ratio (5).

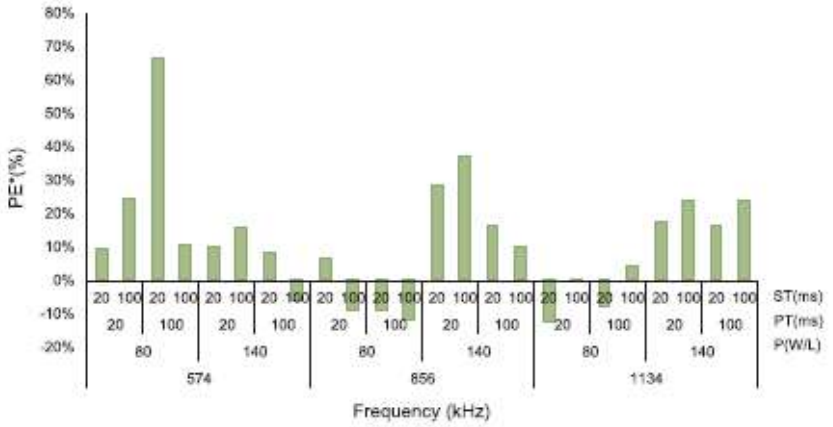


Fig. 2. Pulse Enhancement (PE*) for combination of variables frequency, power density, PT and ST. Reaction volume: 300 mL, T: 20 ± 2 °C, initial BP-3 concentration: 1 mg/L, sonication time: 10 min.

Therefore, the variables for optimization chosen were power density and PT/ST ratio for the frequency level of 574 kHz.

### 4.2. Optimization of ultrasound degradation of BP-3

By means of Response Surface Methodology, the response, in this case, degradation level can be optimized changing the variables that influence it. Response as a function of affecting variables must be set as the first step looking forward an optimum [17]. Values for power density and PT/ST ratio were set moving forward on the direction of degradation ascend. It means that higher power density levels and higher PT/ST values were used. ST was kept constant in 20 ms, because the highest degradation was found at this value. This is a sequential procedure, in which variables move forward along the path of response increase. Variables for the next experiment's series were set as shown in Table 3. A factorial design $2^2$ was used, each experiment was made three times, for a total of twelve experiments. As previously, variables such as reactor geometry, reaction volume, temperature, and initial concentration were maintained constant along the experiments.

The ANOVA analysis showed that power density, PT/ST ratio, and the crossed effect power density-PT/ST were statistically significant. The linear model fits very well within the response at this range. The maximum degradation level for this new set of experiments was higher than previous maximum degradation obtained, being 78.2%. PT/ST optimum value was five and optimum power density level was 200 W/L also being the maximum possible power density level for the reactor. Power effect was positive and, contrary to the previous set of experiments in this series PT/ST ratio had a negative effect on response variable. Consequently, conclusion was made that experiment

Table 3
Factors and levels for the $2^2$ factorial experimental design (574 kHz, BP-3 Initial Concentration: 1 mg/L, T: 25°C ± 2°C, ST: 20 ms).

| Factor | level values | |
|---|---|---|
| | −1 | 1 |
| P (W/L) – $X_1$ | 140 | 200 |
| PT/ST – $X_2$ | 5 | 10 |

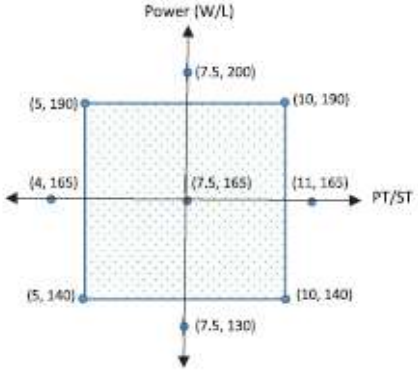


Fig. 4. Central composite design. Frequency: 574 kHz.

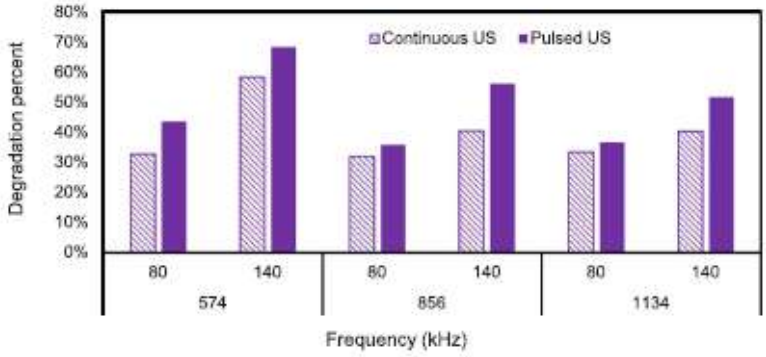


Fig. 3. Maximum degradation percent VS frequency, power density. Pulsed US, continuous US.

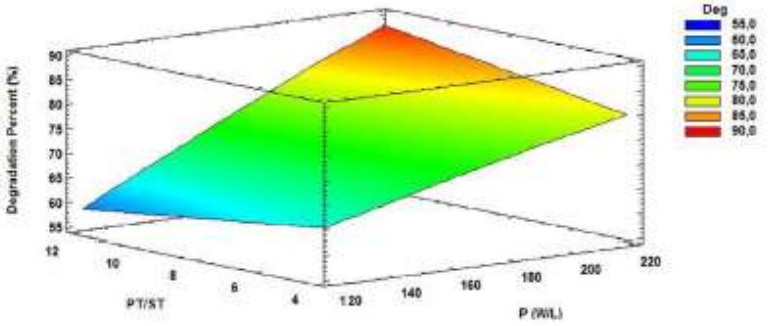


Fig. 5. Surface response for central composite design. Frequency: 574 kHz.

conditions were around the optimum area. In order to use a second order model and look for the optimal conditions, a central composite design [17] was used as shown in Fig. 4. Values for power density were set between 130 and 200 W/L while PT/ST ratio was set between 4 and 11. Each experiment was made once, with four central points, for a total of 12 experiments.

ANOVA results showed that only the variable power density was statistically significant. For this set of experiments, a maximum degradation level of 79.2% was obtained for P = 200 W/L and a PT/ST ratio of 10. But, very similar degradation values were obtained for P = 200 W/L and PT/ST = 7.5 and for P = 190 W/L and PT/ST = 5.

In Fig. 5, it can be seen that for the a constant power level there is a weak dependence of degradation percentage with PT/ST ratio, but conversely, the effect of power density for a constant PT/ST ratio is very important. Therefore, a further analysis for the PT/ST ratio effect was made by means of a series of experiments made at two constant power density values: 140 W/L and 200 W/L, varying PT/ST ratio between 3 and 12. For each power density level, 11 treatments were made – at least – in duplicate. Total BP-3 degradation after 10 min of sonication and initial velocity rates obtained are shown in Fig. 7.

A confirmation from this new set of experiments was set. There is no pattern for BP-3 degradation percent or initial degradation rates depending on the PT/ST ratio at any of the power density levels analyzed. The values are all around the same value for the whole range. For 574 kHz at a power density level of 200 W/L, a similar degradation percent was found for all the PT/ST ratios from 3 to 12. Its average value was 77.7%. For the same frequency and a power density level of 140 W/L a similar behavior was found. Degradation was almost the same for all the PT/ST ratios from 3 to 12. The average degradation percent was 64.9%, 16% lower than at 200 W/L.

However, an interesting result for the initial degradation rates for continuous mode and pulsed mode at these two power density levels was found. In Fig. 6, it is shown that for P = 200 W/L there is little or no difference between initial degradation rates for pulsed and continuous ultrasound. However, for P = 140 W/L there is a significant increase when pulsed instead of continuous mode US is used. For 200 W/L initial degradation rate at a PT/ST ratio of 7 was 0.09 mg/min, almost the same rate for continuous mode pulse was 0.097 mg/min. However, for the lower power density level of 140 W/L, a bigger difference was found: 0.0525 mg/L for continuous mode, 0.0786 mg/L for pulsed mode (45% higher). The reason for this is that at low power densities, OH radical generation is low and mass transfer of BP-3 molecules towards the bubble surface is determinant for the overall reaction rate. In the silent times, BP-3 molecules can diffuse towards the bubble surface for reacting with OH radicals generated in the next pulse. At higher power density levels, OH radicals generation is higher and OH radicals are more readily available at the bulk fluid for reacting with BP-3 molecules, having the pulsed mode ultrasound less effect than at lower power levels. This effect is low also for higher frequencies and medium power densities but the reason is different: Even when at high frequencies the bubble surfaces are lower, and mass transfer has an important effect over the overall rate, there is also a low OH radical generation due to shorter rarefaction cycles and low power level. Consequently, OH rate generation can be as important as mass transfer in overall degradation rate. That is why pulsed US mode has a moderate effect on rates, as shown in Fig. 3 for 856 and 1134 kHz and power level 80 W/L.

In Fig. 7, the degradation profile for the optimum conditions found at a PT/ST ratio of 7 (which was arbitrarily chosen) is shown compared to that one for continuous mode degradation profile. Pulsed mode gives faster initial degradation, but total degradation time is 30 min in both cases.

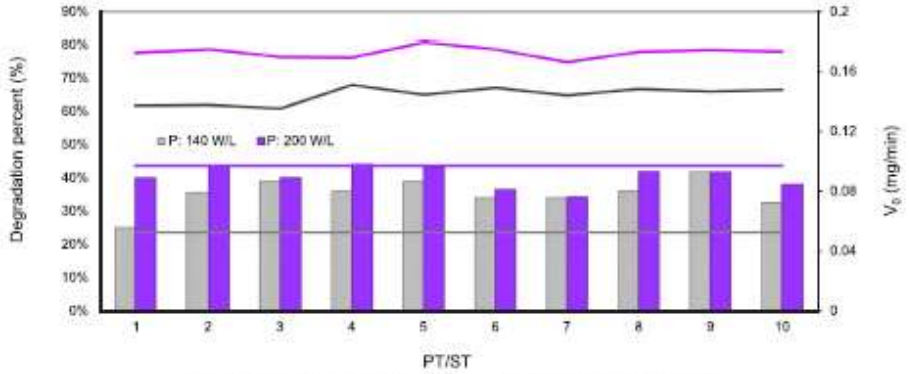


Fig. 6. BP-3 Degradation percent after 10 sonication minutes and $r_0$ vs PS/ST ratio.

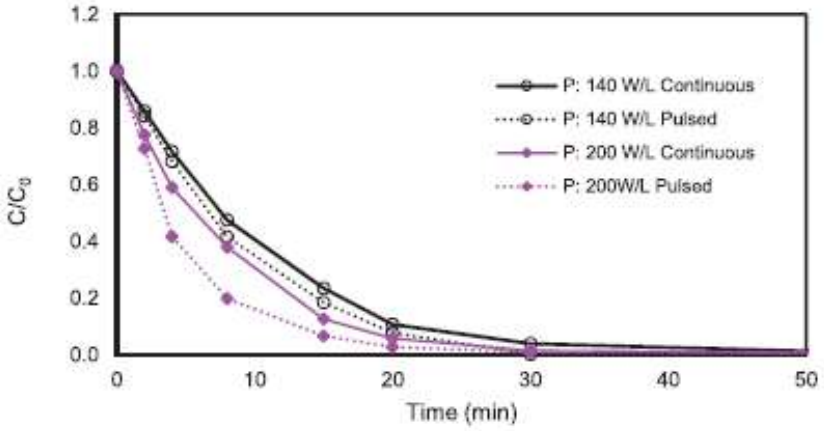


Fig. 7. BP-3 Degradation profile. Power density: 200 W/L, 574 kHz, V: 300 mL, ST: 20 ms, PT/ST: 7.

## 5. Conclusions

Response Surface Methodology was used for optimizing BP-3 degradation in a multi-frequency ultrasound reactor. A $2^3$ experiment with two central points design was used for screening purposes analyzing the BP-3 degradation percent after 10 min of sonication varying power density, frequency, pulse time (PT) and silent time (ST). A conclusion was extrapolated the frequency with higher degradation percent was 574 kHz, power density had a strong positive effect on BP-3 degradation percent, PT and ST did not, but PT/ST ratio had a weak positive effect. Sequential procedure was used moving towards the area of ascent and a $2^2$ experimental design used for higher power density levels and higher PT/ST ratio. At this new variable's range, power density continued having a strong positive effect, but PT/ST ratio had a weak negative effect. Consequently, a central composite design was used for using a second order model and looked for an optimum in this area. This analysis showed that PT/ST ratio had no effect on degradation rate. Thus, two series of experiments were made, one for 140 W/L and another for 200 W/L, varying the PT/ST ratio in the study area in order to find a pattern. From these experiments, it was found all the analyzed range degradation values were very similar, that is, there was no pattern depending on PT/ST ratio at any power density level. The optimum degradation percent value of 79.2% was obtained for a frequency of 574 kHz, a power density of 200 W/L, and a PT/ST ratio of 10.

Consequently, it was found the only two variables affecting degradation level were frequency and power density and that in the range in which reactor works (0–200 W/L, and 574, 856 and 1134 kHz), the power density effect is always positive. The best results were found at 574 kHz, the lowest frequency level. At higher frequencies, the detrimental effects of shorter rarefaction cycles and the BP-3 mass transfer could be the cause of the lower degradation rates. Conversely, pulsed mode ultrasound, PT, ST, and PT/ST did not affect the whole studied range. However, higher degradation rates were found for pulsed rather than continuous mode ultrasound - this effect being more important at low power densities.

## Acknowledgements

The authors wish to thank the Colombian Administrative Department of Science, Technology and Innovation (COLCIENCIAS); and the University of Antioquia for the support of this work.

## Funding

This work was supported by University of Antioquia and the Colombian Administrative Department of Science, Technology and Innovation (COLCIENCIAS).

## Appendix A. Supplementary data

Supplementary data associated with this article can be found, in the online version, at http://dx.doi.org/10.1016/j.ultsonch.2017.10.014.

## References

[1] N. Blüthgen, S. Zucchi, K. Fent, Effects of the UV filter benzophenone-3 (oxybenzone) at low concentrations in zebrafish (Danio rerio), Toxicol. Appl. Pharmacol. 263 (2012) 184–194, http://dx.doi.org/10.1016/j.taap.2012.06.008.
[2] K. Fent, A. Zenker, M. Rapp, Widespread occurrence of estrogenic UV-filters in aquatic ecosystems in Switzerland, Environ. Pollut. 158 (2010) 1817–1824, http://dx.doi.org/10.1016/j.envpol.2009.11.005.
[3] W. Li, Y. Ma, C. Guo, W. Hu, K. Liu, Y. Wang, T. Zhu, Occurrence and behavior of four of the most used sunscreen UV filters in a wastewater reclamation plant, Water Res. 41 (2007) 3506–3512, http://dx.doi.org/10.1016/j.watres.2007.05.039.
[4] B. Kasprzyk-Hordern, R.M. Dinsdale, A.J. Guwy, Multiresidue methods for the analysis of pharmaceuticals, personal care products and illicit drugs in surface water and wastewater by solid-phase extraction and ultra performance liquid chromatography-electrospray tandem mass spectrometry, Anal. Bioanal. Chem. 391 (2008) 1293–1308, http://dx.doi.org/10.1007/s00216-008-1854-x.
[5] M.E. Balmer, H.R. Buser, M.D. Müller, T. Poiger, Occurrence of some organic UV filters in wastewater, in surface waters, and in fish from Swiss lakes, Environ. Sci. Technol. 39 (2005) 953–962, http://dx.doi.org/10.1021/es040055r.
[6] T. Poiger, H.R. Buser, M.E. Balmer, P.A. Bergqvist, M.D. Müller, Occurrence of UV filter compounds from sunscreens in surface waters: regional mass balance in two Swiss lakes, Chemosphere. 55 (2004) 951–963, http://dx.doi.org/10.1016/j.chemosphere.2004.01.012.
[7] A.M. Calafat, L. Wong, X. Ye, J.A. Reidy, L.L. Needham, Concentrations of the sunscreen agent benzophenone-3 in residents of the United States : National Health and Nutrition Examination Survey 2003-2004, Environ. Health Perspect. 116 (2008) 893–897, http://dx.doi.org/10.1289/ehp.11269.
[8] T. Zhang, H. Sun, X. Qin, Q. Wu, Y. Zhang, J. Ma, K. Kannan, Benzophenone-type UV filters in urine and blood from children, adults, and pregnant women in China: partitioning between blood and urine as well as maternal and fetal cord blood, Sci. Total Environ. 461–462 (2013) 49–55, http://dx.doi.org/10.1016/j.scitotenv.2013.04.074.
[9] P. Gago-ferrero, K. Demeestere, M.S. Díaz-cruz, D. Barceló, Ozonation and peroxone oxidation of benzophenone-3 in water: effect of operational parameters and identification of intermediate products, Sci. Total Environ. 443 (2013) 209–217, http://dx.doi.org/10.1016/j.scitotenv.2012.10.006.
[10] M. Schlumpf, P. Schmid, S. Durrer, M. Conscience, K. Maerkel, M. Henseler, M. Gruetter, I. Herzog, S. Reolon, R. Ceccatelli, O. Faass, E. Stutz, H. Jarry, W. Wuttke, W. Lichtensteiger, Endocrine activity and developmental toxicity of cosmetic UV filters – an update, Toxicology. 205 (2004) 113–122, http://dx.doi.org/10.1016/j.tox.2004.06.043.
[11] P. Gago-Ferrero, M. Badia-Fabregat, A. Olivares, B. Piña, P. Blánquez, T. Vicent, G. Caminal, M.S. Díaz-Cruz, D. Barceló, Evaluation of fungal- and photo-degradation as potential treatments for the removal of sunscreens BP3 and BP1, Sci. Total Environ. 427–428 (2012) 355–363, http://dx.doi.org/10.1016/j.scitotenv.2012.03.089.
[12] D. Vione, R. Caringella, F. De laurentiis, M. Pazzi, C. Minero, Phototransformation of the sunlight filter benzophenone-3 (2-hydroxy-4-methoxybenzophenone) under conditions relevant to surface waters, Sci. Total Environ. 463–464 (2013) 243–251, http://dx.doi.org/10.1016/j.scitotenv.2013.05.090.
[13] L. Hernández-leal, H. Temmink, G. Zeeman, G.J.N. Buisman, Removal of

micropollutants from aerobically treated grey water via ozone and activated carbon, Water Res. 45 (2011) 2887–2896, http://dx.doi.org/10.1016/j.watres.2011.03.009.
[14] B. Yang, G.-G. Ying, Removal of personal care products through ferrate(VI) oxidation treatment, in: M.S. Díaz-Cruz, D. Barceló (Eds.), Pers. Care Prod. Aquat. Environ. Handb. Environ. Chem. Springer International Publishing Switzerland, Switzerland, 2014, , http://dx.doi.org/10.1007/698_2014_285.
[15] H. Zúñiga-Benítez, J. Soltan, G.A. Peñuela, Application of ultrasound for degradation of benzophenone-3 in aqueous solutions, Int. J. Environ. Sci. Technol. 13 (2016) 77–86, http://dx.doi.org/10.1007/s13762-015-0842-x.
[16] Y.G. Adewuyi, B.A. Oyenekan, Optimization of a sonochemical process using a novel reactor and Taguchi statistical experimental design methodology, Ind. Eng. Chem. Res. 46 (2007) 411–420, http://dx.doi.org/10.1021/ie060844c.
[17] D.C. Montgomery, Design and Analysis of Experiments, eighth ed., John Wiley & Sons, Inc, 2012, , http://dx.doi.org/10.1198/tech.2006.s372.
[18] T. Kimura, T. Sakamoto, J. Leveque, H. Sohmiya, M. Fujita, S. Ikeda, T. Ando, Standardization of ultrasonic power for sonochemical reaction, Ultrason. Sonochem. 3 (1996) S157–S161, http://dx.doi.org/10.1016/S1350-4177(96)00021-1.
[19] L. Yang, J.F. Rathman, L.K. Weavers, Degradation of alkylbenzene sulfonate surfactants by pulsed ultrasound, J Phys Chem B. 109 (2005) 16203–16209, http://dx.doi.org/10.1021/jp0523221.
[20] R.E. Apfel, 7. Acoustic Cavitation, Methods Exp. Phys. Academic Press, New York, NY, 1981, , http://dx.doi.org/10.1016/S0076-695X(08)60338-5.
[21] A. Henglein, Sonochemistry: Historical developments and modern aspects, Ultrasonics. 25 (1987) 6–16, http://dx.doi.org/10.1016/0041-624X(87)90003-5.
[22] K. Okitsu, T. Suzuki, N. Takenaka, H. Bandow, R. Nishimura, Y. Maeda, Acoustic multibubble cavitation in water: a new aspect of the effect of a rare gas atmosphere on bubble temperature and its relevance to sonochemistry, J. Phys. Chem. B. 110 (2006) 20081–20084, http://dx.doi.org/10.1021/jp064598u.
[23] D. Cheng, S. Sharma, A. Madhoo, Handbook on Applications of Ultrasound Sonochemistry for Sustainability, Taylor & Francis, 2012.
[24] K. Thangavadivel, M. Megharaj, A. Madhoo, R. Naidu, Degradation of organic pollutants using ultrasound, Handb. Appl. Ultrasound Sonochemistry Sustain. 2012, http://dx.doi.org/10.1201/b11012-19.
[25] D.M. Deojay, J.Z. Sostaric, L.K. Weavers, Exploring the effects of pulsed ultrasound at 205 and 616 kHz on the sonochemical degradation of octylbenzene sulfonate, Ultrason. Sonochem. 18 (2011) 801–809, http://dx.doi.org/10.1016/j.ultsonch.2010.10.005.
[26] R. Neppolian, A. Doronila, F. Grieser, M. Ashokkumar, Simple and efficient sonochemical method for the oxidation of arsenic(III) to arsenic(V), Environ. Sci. Technol. 43 (2009) 6793–6798, http://dx.doi.org/10.1021/es900878g.
[27] L. Yang, J.F. Rathman, L.K. Weavers, Sonochemical degradation of alkylbenzene sulfonate surfactants in aqueous mixtures, J. Phys. Chem. B. 110 (2006) 18385–18391, http://dx.doi.org/10.1021/jp062327d.
[28] L. Yang, J.Z. Sostaric, J.F. Rathman, L.K. Weavers, Effect of ultrasound frequency on pulsed sonolytic degradation of octylbenzene sulfonic acid, J. Phys. Chem. B. 112 (2008) 852–858, http://dx.doi.org/10.1021/jp077482m.
[29] R. Xiao, Z. Wei, D. Chen, L.K. Weavers, Kinetics and mechanism of sonochemical degradation of pharmaceuticals in municipal wastewater, Environ. Sci. Technol. 48 (2014) 9675–9683 abs/10.1021/es5016197.
[30] R. Xiao, D. Diaz-Rivera, L.K. Weavers, Factors influencing pharmaceutical and personal care product degradation in aqueous solution using pulsed wave ultrasound, Ind. Eng. Chem. Res. 52 (2013) 2824–2831, http://dx.doi.org/10.1021/ie303052a.

# High Frequency Sonochemical Degradation of Benzophenone-3 in Water

Lina Patricia Vega[1] and Gustavo A. Peñuela, Ph.D.[2]

**Abstract:** Degradation by high frequency ultrasound (US) of the endocrine disruptor, benzophenone-3 (BP-3) is a promising treatment process as it does not need additives and does not generate waste. In this paper the variables affecting this process were studied. The frequency effect on initial degradation rates was analyzed for various frequencies between 215 and 1,134 kHz, and an optimum frequency of 574 kHz was found in this range. Power density had a positive effect on degradation rates over the whole work range. Kinetics adjusted statistically well to a pseudolinear kinetic model. According to these results and those for degradation in presence of radical scavengers, a conclusion was made that US BP-3 degradation was taking place in the bubble/liquid interphase. Toxicity test was conducted by Microtox methods, finding an $EC_{50}$ for 5 min of 1.7 mg/L, and for 15 min of 2.07 mg/L. Toxicity profile along degradation path showed a decrease at the beginning growing after 30% of BP-3 degradation. Four possible degradation byproducts were found by gas chromatography–mass spectrometry (GC-MS) analysis, and a degradation path was proposed. **DOI: 10.1061/(ASCE)EE.1943-7870.0001406.** © *2018 American Society of Civil Engineers.*

**Author keywords:** Advanced oxidation processes; Kinetic models; Sonochemistry; Benzophenone-3.

## Introduction

Benzophenone-3 (2-hydroxy-4-methoxybenzophenone, or oxybenzone) (BP-3) is a UVA filter used in personal care products (Blüthgen et al. 2012). This emergent pollutant reaches superficial waters by run off or via wastewater (Fent et al. 2010b; Li et al. 2007). In the environment it is a persistent and bioaccumulative compound (Gago-Ferrero et al. 2013). It has been demonstrated that it is an endocrine disruptor. It alters genes responsible for the production of sexual hormones, an effect that has been probed in fish and rats (Blüthgen et al. 2012; Schlumpf et al. 2004). Also, alterations in kidney, liver, and reproductive organs have been demonstrated in rats when dermally and orally administrated (Calafat et al. 2008).

Advanced oxidation processes (AOPs) have been used for BP-3 degradation including, ozonation, oxidation with Fe(VI), photodegradation, and ultrasound (US) degradation at low frequencies. Gago-Ferrero et al. (2013) achieved more than 95% of BP-3 degradation in 40–50 min using ozonation for an initial BP-3 concentration of 5.1 mg/L, and an ozone inlet concentration of 85.7 $\mu$mol/$L_{gas}$, and gas flow rate of 120 mL/min. Hernández-Leal et al. (2011) obtained more than 99% of degradation in 15 min of ozonation of water containing 285 ng/L of BP-3. Yang and Ying (2014) treated BP-3 by oxidation with Fe (VI) obtaining a half-life of 167.8 s of Fe(VI) concentration of 10 mg/l, and pH 8. However, photodegradation has not resulted in good degradation efficiencies. Gago-Ferrero et al. (2012) found that BP-3 remained unaltered after 24 h of solar radiation treatment. Vione et al. (2013) found similar results degrading BP-3 by sunlight at an initial concentration of 20 $\mu$M, finding a half-life time of some weeks.

High frequency ultrasound (US) degradation of compounds in water is caused by the creation, expansion, and implosive collapse of gas bubbles in liquids irradiated by US waves (Apfel 1981). Thermal decomposition of water by the compression of oscillating bubbles produces hydroxyl free radicals responsible for degradation (Henglein 1987). US has advantages over other AOPs the absence of added chemicals, of visible light radiation, of change of solution pH, of generated sludge, and of catalysts.

Zúñiga-Benítez et al. (2016) analyzed ultrasound for degrading BP-3 in a probe-tip reactor for low frequency US (20 kHz). The authors studied the effect of ultrasonic applied power, pollutant initial concentration, solution pH, presence of gases, and of radical scavengers. However, it has been shown that US degradation at high frequency levels generally results in higher degradation rates mainly for hydrophobic compounds (Navarro et al. 2011; Kidak and Ince 2006). This study analyzes BP-3 degradation at frequencies between 215 and 1,134 kHz and the primary variables affecting this process. This includes power, frequency, initial concentration, scavenger's presence, and pH. Toxicity evolution and some degradation products were also analyzed.

## Material and Methods

### Chemicals

Millipore water (18 MΩ cm) was used for preparing solutions. Benzophenone-3 (2-hydroxy-4-methoxy-benzophenone) with a purity >98% from (high-performance liquid chromatography) Alfa Aesar was used in ultrasonic degradation experiments. High-performance liquid chromatography (HPLC) grade acetonitrile was obtained from Fisher Chemicals (New Jersey). The pH adjustment was carried out with 1.0 M sodium hydroxide from Sigma Aldrich (St. Louis, Missouri). As radical scavengers pure

[1]Ph.D. Student, Environmental Engineering, Grupo GDCON, Facultad de Ingeniería, Sede de Investigación Universitaria, Universidad de Antioquia, Calle 70 No 52-21, Medellín, Colombia (corresponding author). Email: patricia.vega@udea.edu.co

[2]Associate Professor, Escuela Ambiental, Grupo GDCON, Facultad de Ingeniería, Sede de Investigación Universitaria, Universidad de Antioquia, Calle 70 No 52-21, Medellín, Colombia. Email: gustavo.penuela@udea.edu.co

Note. This manuscript was submitted on December 2, 2017; approved on February 14, 2018 No Epub Date. Discussion period open until 0, 0; separate discussions must be submitted for individual papers. This paper is part of the *Journal of Environmental Engineering*, © ASCE, ISSN 0733-9372.

ethyl alcohol HPLC/spectrophotometric grade from Sigma Aldrich (St. Louis, Missouri), 2-propanol USP grade from Panreac (99.5%) (Barcelona, Spain), and sodium acetate anhydrous from analysis from Carlo Erba reagents (Val-de-Reuil, France) were used. Microtox acute reagent, reconstitution solution, diluent, and adjusting osmotic solution from Modern Water (New Castle, Delaware) were used for toxicity assays.

Dichloromethane for analysis EMSURE (>99.8%) from Merck KGaA (Darmstadt, Germany), methanol Baker Analyzed LC-MS reagent (>99.9%) from Avantor (Center Valley, Pennsylvania), and nitrogen 5.0 (>99.9999%) from Linde were used for solid phase extraction (SPE). Strata phenyl (200 mg/3 mL), Strata-X-C (200 mg/3 mL) and Agilent polystyrene/divinylbenzene (PS DVB) (500 mg/6 mL) cartridges were used for solid phase extraction. The He 5.0 (>99.9999%) from Linde was used for gas chromatography–mass spectrometry (GC-MS).

## Experimental Setup and Procedures

All experiments were conducted in a cylindrical glass reactor with a capacity of 500 mL. A Meinhardt Ultrasonics multifrequency generator MG was used. A scheme is shown in Fig. S1 in the Supplemental Data. Two transducers were used to generate ultrasonic waves: one for frequencies 215 and 373 kHz, and another for frequencies 574, 856, and 1,134 kHz. Solution temperature was kept at 25 ± 2°C using a water cooling bath. Ultrasonic energy density calculated by the calorimetric method (Kimura et al. 1996) is shown in Fig. S2 in the Supplemental Data. Reactor was filled to half, using a solution volume of 300 mL in every experiment. Different sample volumes were withdrawn at different time intervals depending on the variable to be measured. For BP-3 concentration 2 mL samples were withdrawn, and for toxicity 3 mL samples were withdrawn. For byproducts determination reaction stopped at the degradation time analyzed, and 100 mL of this solution were used for SPE. Runs were repeated at least three times. The average value is reported in most cases, and standard deviations were below 5%.

## Chemical Analysis

### High-Performance Liquid Chromatography

BP-3 concentration in water for total degradation analysis was determined by reverse phase chromatography using an Agilent 1,200 Series HPLC system with auto sampler, a Zorbax SB-C18 column (porous silica with 80 Å pore diameter, 3.5 μm, 4.6 × 150 mm), and a diode array detector set at 288 nm. The mobile phase was a mixture of acetonitrile and Milli-Q water (70:30, v/v), flow rate was 0.8 mL/min, injection volume was 100 μL, and column temperature was 30°C. This analytical procedure showed good linearity in the range of 0.02–2 ppm ($R^2 = 0.9999$). The detection limit was 0.0015 ppm, and quantification limit was 0.005 ppm. Repeatability was 1.3% for the measurement range.

### Solid Phase Extraction

Analytes from degraded solution were extracted in order to concentrate and purify them using three different SPE columns: Strata phenyl (55 μm, 70 A, 200 mg/3 mL), Strata X-C (33 μm, 200 mg/3 mL), and PS DVB (500 mg/6 mL). Conditioning of the column was made with methanol, followed of Milli-Q water. Then, 100 mL of reaction solution was passed through the columns at a rate of 5 mL/min. After that, analytes were eluted with a mix of dichloromethane-methanol, and the resulting extract was dried with nitrogen to a volume of 700 μL. The extract was washed from the walls of the recipient and transferred in a total volume of 1 mL to vials for being analyzed by GC-MS.

### Gas Chromatography–Mass Spectrometry

Analytes from degraded solution extracted by SPE as described in section "Solid Phase Extraction" were analyzed in a gas chromatograph Agilent 7890A coupled to a mass spectrometer Agilent 5975C. This has a programmed temperature vaporizing multimode inlet (MMI), in mode pulsed splitless. An Agilent 19091S-433UI HP-5ms Ultra Inert 30 m × 250 μm × 0.25 μm column was used for compounds separation. Oven temperature was set at 50°C for 3 min, and then it was rated at 10°C/min to 310°C, and hold for 5 min. Injector temperature was set at 150°C for 0.1 min, rated at 600°C/min to 325°C, hold by 5 min, then rated 5°C/min to 290°C, and hold for 10 min. Interphase temperature was 250°C. Mass spectrum was obtained by electronic impact at 70 eV using full scan mode. Injection volume was 5 μL. Masshunter software was used for quantification, detection, and identification of degradation byproducts using NIST 14 Mass Spectral Library.

### Toxicity Test

A Microtox Model 500 Analyzer was used for measuring toxicity. Reduction in the bioluminescence of marine bacteria *Vibrio fischeri* when exposed to the pollutants was measured. Toxicity was expressed as $EC_{50}$, the pollutant concentration reducing 50% of the initial luminescence. The 81.9% basic test was used for determining $EC_{50}$, and 81.9% screening test for determining luminescence reduction throughout the treatment.

## Results and Discussion

### Effect of Frequency

One of the most important variables influencing ultrasound degradation processes is frequency. At low frequencies higher temperatures (5,000 K) and pressures (1,000 atm) are obtained, predominating the physical effects on reaction (Thangavadivel et al. 2012). At low frequencies higher bubble volumes are obtained. This produces a high vapor content inside the bubble. Consequently the energetic implode of bubbles generates a lower number of OH radicals. Also, at low frequencies the number of cavitation events is less than at higher frequencies.

High frequencies give smaller bubble lives and sizes, and in consequence, there is a lower vapor content within. This generates a more energetic bubble implosion and a high OH radicals production. However, a detrimental effect at higher frequencies can be caused because the shorter rarefaction cycles could generate molecules that do not get sufficiently stretched to generate a bubble (Rayaroth et al. 2015). This is, the cavitation efficiency decreases, but occurs more frequently (Pétrier and Francony 1997). Also, overall rates can be dominated by mass transfer due to lower bubble surfaces at higher frequencies (Adewuyi and Oyenekan 2007). Because of this, an optimum frequency exists. This optimum depends on the substance properties related to the vapor pressure that influences the energy of bubbles implosion, the hydrophobicity and volatility that determines the place were reaction is taking place, and the mass transfer toward the bubble that depends primarily on the molecule size (Pétrier and Francony 1997). Several studies have found that US degradation of nonvolatile–hydrophobic compounds occur at higher rates at high frequencies, or have an optimum in the high frequency range (Yang et al. 2008). Petrier et al. (1998) showed that chlorobenzene degrades more readily at an US frequency of 500 kHz than at one of 20 kHz. The same effect was found for atrazine and pentachlorophenol degradation at 20 and 500 kHz (Petrier et al. 1996). Pétrier and Francony (1997) degraded phenol and carbon tetrachloride at 20, 200, 500, and 800 kHz, finding that 200 kHz was the optimum frequency. The

4-cumylphenol was degraded by US at 80, 300, and 600 kHz, with 300 kHz being the optimum frequency (Chiha et al. 2011). In Figs. 1 and 2, BP-3 degradation profiles for frequencies from 215 to 1,134 kHz at power densities of 40 and 140 W/L are shown.

In this study, for both power density levels analyzed, the optimum frequency was 574 kHz. At this frequency the highest degradation rates were obtained. At a power density of 40 W/L, 77% of BP-3 ($C_0 = 1$ mg/L), was degraded in 60 min, and at a higher value of 140 W/L, BP-3 was completely degraded in 40 min. In Zúñiga-Benítez et al. (2016) for a higher value of power density (200 W/L), but for a low frequency of 20 kHz, only 50% of degradation was achieved in 60 min of reaction. This shows that for the same levels of power intensity, high ultrasound frequencies are better until an optimum after which degradation rates start declining.

### Effect of Power Density

In Fig. 3, the effect of power density on BP-3 degradation is shown. Power intensity has an important influence in ultrasound degradation rates. As power intensity of ultrasound radiation increases, acoustic wave amplitude increases generating more violent collapse of the bubbles and high OH radicals generation (Adewuyi and Oyenekan 2007). It has been widely demonstrated that power intensity has an optimum value in which pressure and temperature during collapse generates an optimal degradation rate. At higher intensities bubble shielding occurs attenuating the effect of the ultrasound radiation (Cheng et al. 2012). In this study, the shielding effect is observed in that an increase in the power density does not result in a proportional increase in the degradation rate (van Iersel et al. 2008). In Fig. 3, degradation curves for 140 and 200 W/L are closer than those for 40 and 90 W/L. However, degradation rates continue being higher for higher power densities. Degradation rates grew continuously with power density, having their maximum value at 200 W/L, the maximum allowable power for the equipment. At this level 98% degradation was achieved in 30 min. This is half the time obtained in the previous study made in a probe-tip reactor at the same power density level, but at low frequency (20 kHz) and higher BP-3 initial concentration (3.9 mg/L) (Zúñiga-Benítez et al. 2016).

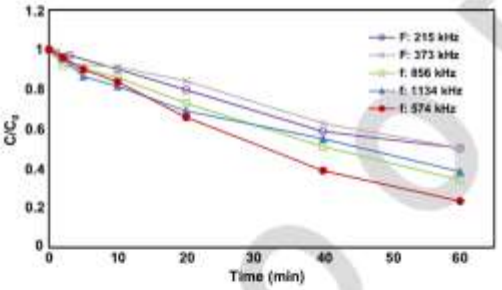


F1:1 F1:2 **Fig. 1.** Effect of frequency on BP-3 degradation. Power density = 40 W/L; solution volume = 300 mL; $C_0 = 1$ mg/L; and $T = 25 \pm 2$°C.

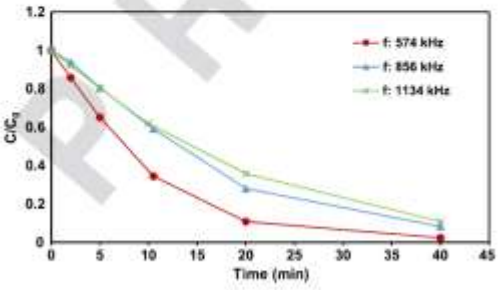


F2:1 F2:2 **Fig. 2.** Effect of frequency on BP-3 degradation. Power density = 140 W/L; solution volume = 300 mL; $C_0 = 1$ mg/L; and $T = 25 \pm 2$°C.

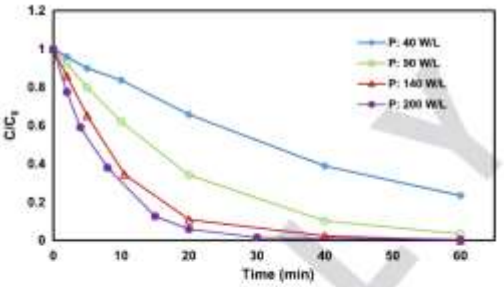


F3:1 F3:2 **Fig. 3.** Effect of power density on BP-3 degradation. Frequency = 574 kHz; solution volume = 300 mL; $C_0 = 1$ mg/L; and $T = 25 \pm 2$°C.

### Radical Scavengers Effect

Sonochemical decomposition of organic compounds in water can proceed inside the bubbles, at the interphase between the cavitation bubbles and the bulk solution, and at the bulk solution (Okitsu et al. 2005). Inside the bubbles and at the bubble surface pyrolysis and radical reactions primarily occur, and at bulk solution reactions with OH radicals are the most important.

Volatility is measured by Henry's law constant ($K_H$), which relates partial pressure of BP-3 above the liquid, with its concentration in the solution. Because BP-3 is not a volatile compound, it is expected that it does not pyrolyze in cavitation bubbles because the effect of volatility on degradation rates becomes pronounced at $K_H$ values above $2.4 \times 10^{-5}$ atm · m$^3$/mol (Nanzai et al. 2008). The BP-3 $K_{H\text{-}BP\text{-}3}$ is $1.5 \times 10^{-8}$ atm · m$^3$/mol. Conversely, as BP-3 is hydrophobic ($\log K_{ow} = 3.8$), it is expected that it tends to accumulate mostly in the interphase region of the cavitation bubbles.

Studies made by Ince et al. (2009), Serna-Galvis et al. (2015), Zúñiga-Benítez et al. (2016), Latch et al. (2005), and De Bel et al. (2011) show that some alcohols like tertbutanol, ethanol, methanol, and isopropyl alcohol scavenge OH radicals at bubble surface and bulk solution. Conversely, acetic acid/acetate appears to scavenge OH radicals only in the solution, without any interaction with the bubble interphase (Xiao et al. 2013).

To check where reaction of BP-3 is taking place, and to probe OH radicals that are the responsible for its degradation, experiments were made using ethanol, 2-propanol, and sodium acetate as radical scavengers. Radical scavenger concentration of 4.3 mM was used. The BP-3 initial concentration was 4.3 $\mu$M, so radical scavenger was always in excess. Resulting degradation profiles are shown in Fig. 4.

Comparing initial BP-3 degradation rates for US degradation at 574 kHz with scavenger, inhibition was 11.5% for ethanol, 28.5%

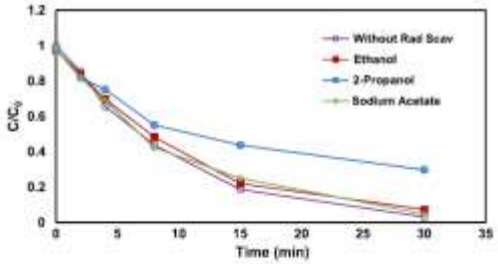


F4:1 F4:2 F4:3 **Fig. 4.** Effect of radical scavengers on BP-3 degradation. Frequency = 574 kHz; power density = 200 W/L; solution volume = 300 mL; $C_0$ = 1 mg/L; and $T = 25 \pm 2$°C.

for 2-propanol, and it has no statistical difference for sodium acetate. Henry's law constant for BP-3 ($K_{H\text{-}BP\text{-}3}$ is $1.5 \times 10^{-8}$ atm · m$^3$/mol) is much lower than those for radical scavengers used ($K_{H\text{-ethanol}}$ is $5 \times 10^{-6}$ atm · m$^3$/mol, and $K_{H\text{-}2\text{-propanol}}$ is $7.5 \times 10^{-6}$ atm · m$^3$/mol). Thus, BP-3 degradation inhibition in presence of the scavengers is explained by the scavengers' quenching of OH radicals in the bubble, interphase, and bulk solution, and to a diminished available energy for $H_2O$ thermolysis (Xiao et al. 2013). This generates higher reaction rates of scavengers with OH radicals than those of BP-3. Conversely, sodium acetate did not have any effect on initial degradation rates because it scavenge OH radicals in the bulk solution, showing that under these conditions BP-3 degradation is taking place only at the bubble surface.

### Kinetics of Sonochemical Degradation

Different models have been proposed for explaining ultrasound reactions kinetics. Okitsu et al. (2006) proposed a nonheterogeneous kinetic model similar to a Langmuir–Hinshelwood or Eley–Rideal mechanism. In this approach the assumption is made that the reaction is occurring in the bubble–solution interphase. There, a pseudoequilibrium of adsorption and desorption of pollutant exists before collapsing of the bubble at the gas/liquid interphase. This results in a general model that is summarized in Eq. (1)

$$r = k\theta = \frac{kK[\text{BP3}]}{1 + K[\text{BP3}]} \quad (1)$$

where $K = (k_1/k_{-1})$, $k_1$, and $k_{-1}$ are the sorption and desorption rate constants in the bubble surface, and $k$ is the pseudo-first-order rate constant for the reaction of BP-3 with OH radicals.

The general reaction mechanism for chlorophenol degradation by ultrasound by Serpone et al. (1994) proposed reactions could take place in the bulk solution or in the interphase. The resulting general expression was similar to that of Okitsu et al. But in this model, when the reaction is taking place in the bubble interphase, where OH concentration is high and pollutant concentration is low, the rate expression becomes of first order in the concentration of benzophenone 3

$$\left(\frac{d[\text{BP3}]}{dt}\right) = -k_B[\text{BP3}] \quad (2)$$

Detailed explanation of these models applied to BP-3 degradation is in the Supplemental Data. Rate Eqs. (1) and (2) were evaluated to check the goodness of fit of the experimental data to these expressions. Statistical methods were used for correlating BP-3 initial concentration and initial degradation rates for various initial BP-3 initial concentration levels. Degradation rates were calculated for the first two reaction minutes. In this time, less than 20% of BP-3 degradation was achieved. Thus the interaction of reaction products with OH radicals was minimized and primarily the interaction of BP-3 and these radicals was analyzed. Experiments were made at 574 kHz and 140 W/L. The BP-3 initial concentrations were in the range from 2.3 to 21.6 $\mu$M.

The goodness of fit of the model for Eq. (1) was analyzed by nonlinear regression by an algorithm in R using the instruction nls. Nonlinear (weighted) least-squares estimates of the parameters were found. The pseudo-first-order model [Eq. (2)] was analyzed by ordinary least-squares analysis by an algorithm in R for linear regressions. Regression parameters, t-statistic probabilities ($p$), coefficient of determination ($R^2$), and sum of squared errors (SSE) for both are shown in Table 1. Fig. 5 presents the experimental values and predicted curves for both models.

The squared sum of residues (SSE) had similar values for both models showing a goof fit of the data. Pseudo-first-order model [Eq. (2)] had a good correlation coefficient and a good $p$-value for t-statistics for equation parameter. The nonlinear model presented in Eq. (1) gives a low value for the $t$-value of the parameter $K$ in the denominator. Consequently there is no statistical evidence for the validity of this parameter and consequently of this model.

Conversely, pseudo-first-order model explained adequately BP-3 degradation having good $p$-values for t-statistic, a good $R^2$, and a good SSE. Therefore the conclusion can be made that BP-3 degrades primarily at the bubble surface according to the approach proposed by Serpone et al. (1994). Rate constant was 0.0404 min$^{-1}$. The linear model does not go through the origin, having a slight deviation that could be attributed to a small part of the reaction taking place on the bulk solution and experimental errors. This result was different to

**Table 1.** Parameters of the kinetic models for BP-3 degradation

| Model | Parameters | $R^2$ | SSE |
|---|---|---|---|
| Eq. (1) | $k_1K$: 0.0402448 ($t$-value: 5.599, $p = 1.48 \times 10^{-08}$) | — | 0.05038 |
| | K: −0.0001664 ($t$-value: −0.022, $p = 0.982$) | | |
| Eq. (2) | $k_B$: 0.040402 ($t$-value: 25.353, $p = 2 \times 10^{-18}$) | 0.9669 | 0.04922 |

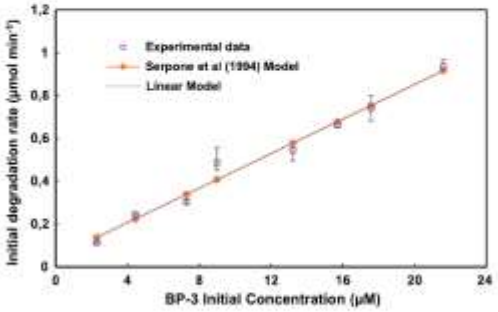


F5:1 F5:2 F5:3 **Fig. 5.** Initial degradation rate versus BP-3 initial concentration. Frequency = 574 kHz; power density by calorimetric method = 200 W/L; pH = 6.9; volume = 300 mL; and $T = 25 \pm 2$°C).

that of Zúñiga-Benítez et al. (2016) who obtained that kinetics followed a nonlinear model as that presented in Eq. (1). The difference can be attributed to the fact that this kinetic analysis was made at a higher frequency level (574 kHz). At this frequency there are different conditions for OH radical concentrations and for the diffusivity could have a different effect, affecting overall degradation rates in a different way.

### Effect of pH

A compound can be in its molecular or in its ionic form with different proportions depending on its $pK_a$ value. Hydrophobic compounds in their molecular form accumulate more readily in the interfacial area than in their ionic form. BP-3 has a $pK_a = 7.56$, and at a natural pH of 6.9 it is almost completely in its molecular form. At higher pH values than 7.56, BP-3 is in its deprotonated or phenolate form, and tends to accumulate less in the bubble interphase where radical OH concentration is higher. Ultrasound experiments at pH 10 were conducted to examine this effect on initial rate for BP-3 degradation. At this pH value more than 99% of BP-3 is in anionic form, according to the following expression (Chiha et al. 2011):

$$\varphi_{ions} = \frac{1}{1 + 10^{(pK_a - pH)}} \tag{3}$$

Comparing degradation for pH 10 with those obtained at natural pH, it is shown in Fig. 6 that there is no difference in degradation rates. However, it is known that for phenolic compounds, the deprotonated form, or phenolate, is more reactive with OH radicals because it undergoes one-electron oxidation much more readily than phenolic form (Greenberg 2009). However, OH radical reaction rates are usually limited by mass transfer. Therefore, a possible reason for the nule effect of the pH over degradation rates is that both species have similar diffusivities in water.

### Toxicity

A Microtox equipment was used for conducting ecotoxicity essays. It measures the decrease in the natural luminescence of the marine bacteria *Vibrio fischeri* in the presence of BP-3 in aqueous solution. A diminishing in the bioluminescence indicates the diminishing in their cellular respiration. When exposed to the toxic substances, there is a change in the percentage of protein and lipid synthesis, and this changes the light emission level. Toxicity is expressed as effective concentration, $EC_{50}$, with pollutant concentration generating a 50% reduction in light emission (Onorati and Mecozzi 2004).

For determining BP-3 acute toxicity, 81.9% basic test was used according to the Guide to Microtox M500 procedure. A BP-3 solution in deionized water with a concentration of 4.93 mg/L was used, and response was measured for several dilutions at 5 and 15 min. Resulting $EC_{50}$ for 5 min was 1.7 mg/L, and for 15 min was 2.07 mg/L. Microtox procedures are widely used because its results are generally correlated with those for acute toxicity analysis made on *Daphnia magna* (La Farre et al. 2001). For BP-3, Fent et al. (2010a) reported a value for acute toxicity $LC_{50}$ value on *Daphnia magnia* of 1.9 g/L, very close to this result found using *Vibrio fischeri* bacteria.

Toxicity path as US degradation occurred was measured for a treated BP-3 solution with an initial concentration of 1 mg/L, irradiated at 574 kHz and 200 W/L for 90 min. The 3 mL samples were withdrawn at different times, and analyzed in Microtox equipment by the 81.9% screening test. Results are shown in Fig. 7.

There are few reports about BP-3 byproducts by OH reaction. (Gago-Ferrero et al. 2012) found dihydroxybenzophenone (BP-1) as one of the byproducts of BP-3 photodegradation, this being 200 times more strogenic than BP-3. Another possible compound such as 2,2'-dihydroxy-4-methoxybenzophenone found in BP-3 ozonation (Gago-ferrero et al. 2013) and other similar possible hydroxylated byproducts could have more harmful effects than BP-3 (Jeon et al. 2008). However, further research beyond the scope of this study is needed to understand the reason of this toxicity increase as BP-3 is degrated.

### Degradation Byproducts

Four possible degradation byproducts were found. Deionized water spiked at 10 mg/L with BP-3 was sonicated and aliquots of the solution were taken when 30% of degradation was achieved. Compounds were isolated from the water samples by SPE according to procedure described in the "Solid Phase Extraction" section. Separation and detection of degradation products was accomplished by gas chromatography–mass spectrometry (see section "Gas Chromatography–Mass Spectrometry"). Possible compounds were detected, based on the presence of the molecular ion, and interpretation of their fragment ions in the mass spectra was conducted using an identification program of NIST 14 Mass Spectral Library. Spectrums are shown in Figs. S3, S4, and S5 in the Supplemental Data.

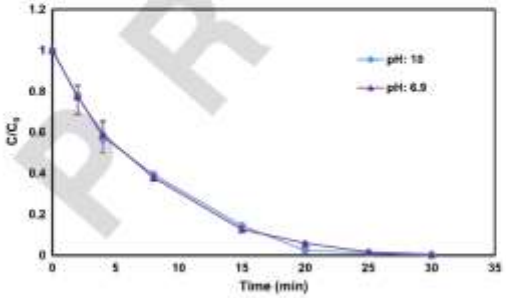


**Fig. 6.** Effect of pH on BP-3 degradation by ultrasound. Power density = 200 W/L; frequency = 574 kHz; solution volume = 300 mL; $C_0 = 1$ mg/L; and $T = 25 \pm 2$°C.

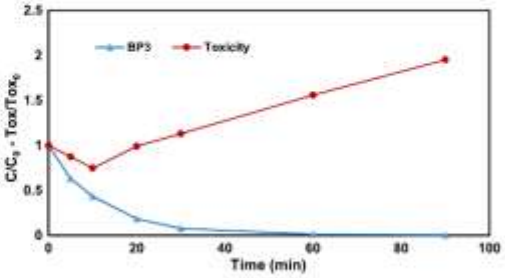


**Fig. 7.** Toxicity evolution for benzophenone-3 degradation by ultrasound. Power density = 140 W/L; frequency = 574 kHz; solution volume = 300 mL; $C_0 = 4.93$ mg/L; and $T = 25 \pm 2$°C.

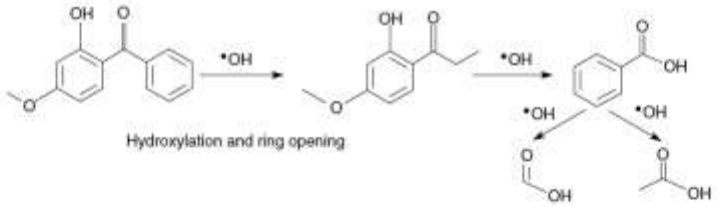


F8:1 **Fig. 8.** BP-3 proposed degradation mechanism.

The 1-(2-hydroxy-4-methoyphenyl) propan-1-one was identified in the extract made with phenyl column, at 22.235 min. The mechanism proposed for its generation is the hydroxylation by OH radicals attack over the nonsubstituted benzene moiety, leading to posterior ring opening.

Benzoic acid was identified in the extract made with XC Column at 10.154 min. This compound was found by Vione et al. (2013) in their study of BP-3 photo transformation. This byproduct can be generated after bond cleavage between the carbonyl group and the aromatic ring with hydroxyl and methoxy functions (Vione et al. 2013). Other similarly generated byproducts found in this study were acetic acid and formic acid obtained in the extract made with DVB (4.093 min) and XC columns (3.26 min). These acids can be generated by nonspecific OH attack over oxidized BP-3 intermediates after bond cleavage between the two benzene rings and its opening. A general proposed mechanism is shown in Fig. 8.

## Conclusions

Optimum frequency for benzophenone-3 degradation was 574 kHz and optimum power value was 200 W/L. For these values, 98% BP-3 degradation was achieved in 30 min. Two different kinetic models for BP-3 degradation at natural pH were proposed. One was based on a saturation type reaction over the bubble surface while the other took into account radical reactions could take place over the bubble surface or in the bulk solution. A pseudolinear kinetic model resulting from the application of the second mechanism had the best fit for this system. The kinetic constant had a value of 0.040402 $min^{-1}$, (574 kHz, 140 W/L), four times higher than those found in other studies for US TCS degradation at lower frequencies. Triclosan degradation at natural pH takes place over the bubble surface and its degradation rate depends on triclosan bulk concentration, the rate of generation and recombination of radicals, and the rate of reaction between triclosan and OH radicals.

Inhibition with radical scavengers was 11.5% for ethanol, 28.5% for 2-propanol, and it has no statistical difference for sodium acetate. These results confirmed BP-3 is being degraded only at the bubble's surface. Toxicity $EC_{50}$ value measured in the Microtox toxicity test was 1.7 mg/L after 5 min. Toxicity decreased with BP-3 depletion until 30% degradation and increased afterward, showing that more toxic by-products are being generated. Four possible degradation byproducts were found: 1-(2-hydroxy-4-methoyphenyl) propan-1-one, benzoic acid, acetic acid, and formic acid.

## Supplemental Data

Figs. S1–S5 and a detailed model for kinetic Eqs. (S1)–(S12) are available online in the ASCE Library (www.ascelibrary.org).

## References


Adewuyi, Y. G., and B. A. Oyenekan. 2007. "Optimization of a sonochemical process using a novel reactor and Taguchi statistical experimental design methodology." *Ind. Eng. Chem. Res.* 46 (2): 411–420. https://doi.org/10.1021/ie060844c.

Apfel, R. E. 1981. "7. Acoustic cavitation." In *Methods in experimental physics*. 355–411. New York, NY: Academic Press.

Blüthgen, N., S. Zucchi, and K. Fent. 2012. "Effects of the UV filter benzophenone-3 (oxybenzone) at low concentrations in zebrafish (Danio rerio)." *Toxicol. Appl. Pharmacol.* 263 (2): 184–194. https://doi.org/10.1016/j.taap.2012.06.008.

Calafat, A. M., L. Wong, X. Ye, J. A. Reidy, and L. L. Needham. 2008. "Concentrations of the sunscreen agent benzophenone-3 in residents of the United States: National health and nutrition examination survey 2003–2004." *Environ. Health Perspect.* 116 (7): 893–897. https://doi.org/10.1289/ehp.11269.

Cheng, D., S. Sharma, and A. Mudhoo. 2012. *Handbook on applications of ultrasound sonochemistry for sustainability*. Boca Raton, FL: Taylor & Francis.

Chiha, M., O. Hamdaoui, S. Baup, and N. Gondrexon. 2011. "Sonolytic degradation of endocrine disrupting chemical 4-cumylphenol in water." *Ultrason. Sonochem.* 18 (5): 943–950. https://doi.org/10.1016/j.ultsonch.2010.12.014.

De Bel, E., C. Janssen, S. De Smet, H. Van Langenhove, and J. Dewulf. 2011. "Sonolysis of ciprofloxacin in aqueous solution: Influence of operational parameters." *Ultrason. Sonochem.* 18 (1): 184–189. https://doi.org/10.1016/j.ultsonch.2010.05.003.

Fent, K., P. Y. Kunz, A. Zenker, and M. Rapp. 2010a. "A tentative environmental risk assessment of the UV-filters 3-(4-methylbenzylidene-camphor), 2-ethyl-hexyl-4-trimethoxycinnamate, benzophenone-3, benzophenone-4 and 3-benzylidene camphor." Supplement, *Mar. Environ. Res.* 69: S4–S6. https://doi.org/10.1016/j.marenvres.2009.10.010.

Fent, K., A. Zenker, and M. Rapp. 2010b. "Widespread occurrence of estrogenic UV-filters in aquatic ecosystems in Switzerland." *Environ. Pollut.* 158 (5): 1817–1824. https://doi.org/10.1016/j.envpol.2009.11.005.

Gago-Ferrero, P., M. Badia-Fabregat, A. Olivares, B. Piña, P. Blánquez, T. Vicent, G. Caminal, M. S. Díaz-Cruz, and D. Barceló. 2012. "Evaluation of fungal- and photo-degradation as potential treatments for the removal of sunscreens BP3 and BP1." *Sci. Total Environ.* 427–428: 355–363. https://doi.org/10.1016/j.scitotenv.2012.03.089.

Gago-Ferrero, P., K. Demeestere, M. S. Díaz-Cruz, and D. Barceló. 2013. "Ozonation and peroxone oxidation of benzophenone-3 in water: Effect of operational parameters and identification of intermediate products." *Sci. Total Environ.* 443: 209–217. https://doi.org/10.1016/j.scitotenv.2012.10.006.

Greenberg, M. M., ed. 2009. *Radical and radical ion reactivity in nucleic acid chemistry*. Hoboken, NJ: Wiley.

Henglein, A. 1987. "Sonochemistry: Historical developments and modern aspects." *Ultrasonics* 25 (1): 6–16. https://doi.org/10.1016/0041-624X(87)90003-5.

Hernández-Leal, L., H. Temmink, G. Zeeman, and C. J. N. Buisman. 2011. "Removal of micropollutants from aerobically treated grey water via ozone and activated carbon." *Water Res.* 45 (9): 2887–2896. https://doi.org/10.1016/j.watres.2011.03.009.

Ince, N. H., I. Gültekin, and G. Tezcanli-Güyer. 2009. "Sonochemical destruction of nonylphenol: Effects of pH and hydroxyl radical scavengers." *J. Hazard. Mater.* 172 (2–3): 739–743. https://doi.org/10.1016/j.jhazmat.2009.07.058.

Jeon, H. K., S. Sarma, Y. J. Kim, and J. C. Ryu. 2008. "Toxicokinetics and metabolisms of benzophenone-type UV filters in rats." *Toxicology* 248 (2–3): 89–95. https://doi.org/10.1016/j.tox.2008.02.009.

Kidak, R., and N. H. Ince. 2006. "Effects of operating parameters on sonochemical decomposition of phenol." *J. Hazard. Mater.* 137 (3): 1453–1457. https://doi.org/10.1016/j.jhazmat.2006.04.021.

Kimura, T., T. Sakamoto, J. Leveque, H. Sohmiya, M. Fujita, S. Ikeda, and T. Ando. 1996. "Standardization of ultrasonic power for sonochemical reaction." *Ultrason. Sonochem.* 3 (3): S157–S161. https://doi.org/10.1016/S1350-4177(96)00021-1.

La Farre, M., M.-J. Garcia, L. Tirapu, A. Ginebreda, and D. Barcelo. 2001. "Wastewater toxicity screening of non-ionic surfactants by Toxalert and Microtox bioluminescence inhibition assays." *Anal. Chim. Acta* 427 (2): 181–189.

Latch, D. E., J. L. Packer, B. L. Stender, J. VanOverbeke, W. A. Arnold, and K. McNeill. 2005. "Aqueous photochemistry of triclosan: Formation of 2, 4-dichlorophenol, 2, 8-dichlorodibenzo-p-dioxin, and oligomerization products." *Environ. Toxicol. Chem.* 24 (3): 517–525. https://doi.org/10.1897/04-243R.1.

Li, W., Y. Ma, C. Guo, W. Hu, K. Liu, Y. Wang, and T. Zhu. 2007. "Occurrence and behavior of four of the most used sunscreen UV filters in a wastewater reclamation plant." *Water Res.* 41 (15): 3506–3512. https://doi.org/10.1016/j.watres.2007.05.039.

Nanzai, B., K. Okitsu, N. Takenaka, H. Bandow, and Y. Maeda. 2008. "Sonochemical degradation of various monocyclic aromatic compounds: Relation between hydrophobicities of organic compounds and the decomposition rates." *Ultrason. Sonochem.* 15 (4): 478–483. https://doi.org/10.1016/j.ultsonch.2007.06.010.

Navarro, N. M., T. Chave, P. Pochon, I. Bisel, and S. I. Nikitenko. 2011. "Effect of ultrasonic frequency on the mechanism of formic acid sonolysis." *J. Phys. Chem. B* 115 (9): 2024–2029. https://doi.org/10.1021/jp109444h.

Okitsu, K., K. Iwasaki, Y. Yobiko, H. Bandow, R. Nishimura, and Y. Maeda. 2005. "Sonochemical degradation of azo dyes in aqueous solution: A new heterogeneous kinetics model taking into account the local concentration of OH radicals and azo dyes." *Ultrason. Sonochem.* 12 (4): 255–262. https://doi.org/10.1016/j.ultsonch.2004.01.038.

Okitsu, K., T. Suzuki, N. Takenaka, H. Bandow, R. Nishimura, and Y. Maeda. 2006. "Acoustic multibubble cavitation in water: A new aspect of the effect of a rare gas atmosphere on bubble temperature and its relevance to sonochemistry." *J. Phys. Chem. B* 110 (41): 20081–20084. https://doi.org/10.1021/jp064598u.

Onorati, F., and M. Mecozzi. 2004. "Effects of two diluents in the Microtox toxicity bioassay with marine sediments." *Chemosphere* 54 (5): 679–687. https://doi.org/10.1016/j.chemosphere.2003.09.010.

Petrier, C., B. David, and S. Laguian. 1996. "Ultrasonic degradation at 29 kHz and 500 kHz of atrazine and pentachlorophenol in aqueous solution: Preliminary results." *Chemosphere* 32 (9): 1709–1718. https://doi.org/10.1016/0045-6535(96)00088-4.

Pétrier, C., and A. Francony. 1997. "Ultrasonic waste-water treatment: Incidence of ultrasonic frequency on the rate of phenol and carbon tetrachloride degradation." *Ultrason. Sonochem.* 4 (4): 295–300. https://doi.org/10.1016/S1350-4177(97)00036-9.

Petrier, C., Y. Jiang, and M. F. Lamy. 1998. "Ultrasound and environment: Sonochemical destruction of chloroaromatic derivatives." *Environ. Sci. Technol.* 32 (9): 1316–1318. https://doi.org/10.1021/es970662x.

Rayaroth, M. P., U. K. Aravind, and C. T. Aravindakumar. 2015. "Chemosphere sonochemical degradation of coomassie brilliant blue: Effect of frequency, power density, pH and various additives." 119: 848–855.

Schlumpf, M., et al. 2004. "Endocrine activity and developmental toxicity of cosmetic UV filters—An update." *Toxicology* 205 (1–2): 113–122. https://doi.org/10.1016/j.tox.2004.06.043.

Sema-Galvis, E. A., J. Silva-Agredo, A. L. Giraldo-Aguirre, and R. A. Torres-Palma. 2015. "Sonochemical degradation of the pharmaceutical fluoxetine: Effect of parameters, organic and inorganic additives and combination with a biological system." *Sci. Total Environ.* 524–525: 354–360. https://doi.org/10.1016/j.scitotenv.2015.04.053.

Serpone, N., R. Terzian, H. Hidaka, and E. Pelizzetti. 1994. "Ultrasonic induced dehalogenation and oxidation of 2-, 3-, and 4-chlorophenol in air-equilibrated aqueous media. Similarities with irradiated semiconductor particulates." *J. Phys. Chem.* 98 (10): 2634–2640. https://doi.org/10.1021/j100061a021.

Thangavadivel, K., M. Megharaj, A. Mudhoo, and R. Naidu. 2012. "Degradation of organic pollutants using ultrasound." In *Handbook on applications of ultrasound: Sonochemistry for sustainability*, 447–474. Boca Raton, FL: CRC Press.

Torres, R., C. Pétrier, E. Combet, M. Carrier, and C. Pulgarin. 2008. "Ultrasonic cavitation applied to the treatment of bisphenol A. Effect of sonochemical parameters and analysis of BPA by-products." *Ultrason. Sonochem.* 15 (4): 605–611. https://doi.org/10.1016/j.ultsonch.2007.07.003.

van Iersel, M. M., N. E. Benes, and J. T. F. Keurentjes. 2008. "Importance of acoustic shielding in sonochemistry." *Ultrason. Sonochem.* 15 (4): 294–300. https://doi.org/10.1016/j.ultsonch.2007.09.015.

Vione, D., R. Caringella, E. De Laurentiis, M. Pazzi, and C. Minero. 2013. "Phototransformation of the sunlight filter benzophenone-3 (2-hydroxy-4-methoxybenzophenone) under conditions relevant to surface waters." *Sci. Total Environ.* 463–464: 243–251. https://doi.org/10.1016/j.scitotenv.2013.05.090.

Xiao, R., D. Diaz-Rivera, Z. He, and L. K. Weavers. 2013. "Using pulsed wave ultrasound to evaluate the suitability of hydroxyl radical scavengers in sonochemical systems." *Ultrason. Sonochem.* 20 (3): 990–996. https://doi.org/10.1016/j.ultsonch.2012.11.012.

Yang, B., and G.-G. Ying. 2014. "Removal of personal care products through ferrate(VI) oxidation treatment." In *Personal care products in the aquatic environment. Handbook of environmental chemistry*, edited by M. S. Diaz-Cruz and D. Barceló. Cham, Switzerland: Springer International Publishing.

Yang, L., J. Z. Sostaric, J. F. Rathman, and L. K. Weavers. 2008. "Effect of ultrasound frequency on pulsed sonolytic degradation of octylbenzene sulfonic acid." *J. Phys. Chem. B* 112 (3): 852–858. https://doi.org/10.1021/jp077482m.

Zúñiga-Benítez, H., J. Soltan, and G. A. Peñuela. 2016. "Application of ultrasound for degradation of benzophenone-3 in aqueous solutions." *Int. J. Environ. Sci. Technol.* 13 (1): 77–86. https://doi.org/10.1007/s13762-015-0842-x.

UNIVERSIDAD DE ANTIOQUIA

Facultad de Ciencias Exactas y Naturales

CIPOA 2017

The Faculty of Exact and Natural Sciences of the University of Antioquia

**Certifies that**

**LINA PATRICIA VEGA GARZON**

**as**

**PRESENTER**

Participated in the 3rd Iberoamerican Conference on Advanced Oxidation Technologies (III Cipoa) and 2nd Colombian Conference on Advanced Oxidation Processes (II Ccpaox), which took place in Guatapé, Colombia during November 14, 15, 16 and 17 of 2017, corresponding to 33 hours

**Nora Restrepo**

Dean of the Faculty of Exact and Natural Sciences of the University of Antioquia

**Ricardo Antonio Torres**

Congress Coordinator CIPOA 2017